Pre-Clinical Evaluation of a Vaccination Strategy to Induce Liver Resident Memory T Cells against Hepatitis C Virus

Zelalem Addis Mekonnen

The Virology Laboratory

The Basil Hetzel Institute of Medical Research

Discipline of Surgery

School of Medicine

Faculty of Health and Medical Sciences

The University of Adelaide

January 2019

Contents

Abstract

Hepatitis C virus (HCV) is a significant contributor to the global burden of disease with at least 71 million individuals persistently infected with the virus. Although effective anti-viral therapies are available, they are prohibitive in cost and at least 80% of infected individuals are undiagnosed for HCV making the development of an effective vaccine a crucial requirement to eliminate HCV infections. There is much conjecture about how to design an effective HCV vaccine, nonetheless, there is evidence to suggest that a vaccine which can elicit T cell immunity in the liver will be protective. Firstly, tissue-resident memory $CD8^+$ T (T_{RM}) cells have been reported to patrol the liver sinusoids for the lifespan of the individual and play vital roles in the elimination of malaria parasites (*Plasmodium berghei*) following invasion of hepatocytes. Secondly, $CD4^+$ and $CD8^+$ T cell-mediated immunity against non-structural (NS) proteins of HCV correlate with recovery from acute infections in patients. DNA and adeno-associated virus (AAV) have an excellent safety profile and have been effective in gene therapy and vaccinations in humans. Our laboratory has also shown that a DNA vaccine encoding HCV NS proteins and a cytolytic protein, perforin (PRF), is more effective than a canonical DNA vaccine in eliciting HCV-specific T cell responses against NS proteins of HCV. Thus, using a DNA vaccine encoding NS5B from HCV genotype 3a and PRF (pVAX-NS5B-PRF) and recombinant AAV (rAAV) encoding the vaccine antigen (rAAV-NS5B-2A-eGFP) vaccination regimens designed to elicit HCV-specific T cell mediated immunity in the liver were developed and evaluated in this thesis. The vaccination strategy involved intradermal (ID) vaccination of mice with pVAX-NS5B-PRF to prime T cells followed by intravenous (IV) vaccination with rAAV-NS5B-2A-eGFP to trap the primed cells.

To achieve the aims of this thesis, an established fluorescent target array (FTA) technology was modified to identify immunodominant $CD4^+$ T cell and $CD8^+$ T cell epitopes of NS5B *in vivo* to thoroughly analyse NS5B-specific T cell responses in vaccinated mice *in vivo*. Based on the *in vivo* epitope mapping analysis, a $NS5B_{451\text{-}459}$ tetramer was developed that was crucial for isolating

NS5B-specific $CD8^+$ T cells in vaccinated BALB/c mice and determining whether cells had differentiated into T_{RM} (i.e. $CD69^+$ $CD62L^-$) cells in the liver. rAAV-NS5B-2A-eGFP capable of transducing hepatocytes *in vivo* was also developed and used in vaccination studies.

The vaccination regimen described in this thesis elicited robust NS5B-specific killing responses by $CD8^+$ T cells and helper $CD4^+$ T cell responses. Importantly, the heightened immunogenicity of the vaccination regimen also correlated with the formation of NS5B-specific $CD8^+$ T_{RM} cells in the liver. Although, the protective efficacy of this regimen still needs to be evaluated following an authentic HCV challenge, this study highlights that the prime/trap regimen is a promising strategy that can be used to develop a protective vaccination regimen against HCV in the future. Moreover, the results bridge an important gap in the HCV vaccine development especially for vaccines that aim to elicit protective T cell responses in the liver to eliminate the virus shortly after infection and before a divergent quasi-species emerges.

Declaration

I certify that this work contains no material which has been accepted for the award of any other degree or diploma in my name, in any university or other tertiary institution and, to the best of my knowledge and belief, contains no material previously published or written by another person, except where due reference has been made in the text. In addition, I certify that no part of this work will, in the future, be used in a submission in my name, for any other degree or diploma in any university or other tertiary institution without the prior approval of the University of Adelaide and where applicable, any partner institution responsible for the joint-award of this degree.

I give permission for the digital version of my thesis to be made available on the web, via the University's digital research repository, the Library Search and also through web search engines, unless permission has been granted by the University to restrict access for a period of time.

I acknowledge the support I have received for my research through the provision of an Australian Government Research Training Program Scholarship.

Zelalem Addis Mekonnen

Acknowledgments

I would like to begin by sincerely thanking my principal supervisor, Prof. Eric Gowans for giving me this wonderful opportunity of coming to Australia to complete a PhD. I would like to thank Eric not only for the huge support academically, but also for his understanding and kindness over the four years. I would also like to thank my co-supervisors, Dr. Branka Grubor-Bauk and Dr. Danushka Wijesundara for their support and assistance in designing the experiments and analyzing the data presented in this thesis.

I would like to thank the entire Gowans' laboratory, past and present, for all the help and friendship I have received throughout my PhD. In particular, Judy, Jason, Khamis, Mak and Harsh for their assistance with my initial laboratory work and Ashish for his moral support during the final year of my PhD.

My sincere thanks to Dr. David Bowen and members of his group, particularly Dr. Kieran English, for conducting *in vivo* transduction studies of rAAV-NS5B-2A-eGFP in mice. I would also like to thank Preston Leung for his bioinformatics expertise to identify the immunodominant peptide sequence used for tetramer synthesis.

To my friend and brother Dr. Legesse and my sister Alem thank you very much for all the time you listened to my complaints and walked the ups and downs with me.

To my wife, Bell, your love and support have got me to where I am today. To my kids Abiy and Tsion, you mean the world to me. My little angel Tibebeselassie you managed to be part of this journey. I dedicate this thesis to all of you because without your unconditional support I would not fulfill this dream.

Abbreviations

AAP	Assembly activating protein
AAV	Adeno associated virus
AAVS1	Adeno associated virus integration site-1
Ad	Adenovirus
ALT	Alanine aminotransferase
AST	Aspartate aminotransferase
BSA	Bovine serum albumin
HLA	Human leucocyte antigen
ART	Antiretroviral therapy
BGHpolyA	Bovine growth hormone poly adenylation
CARD	Caspase recruitment domain
CAT	Chloramphenicol acetyl transferase
CFSE	Carboxy fluorescein succinimidyl ester
ChAd	Chimpanzee adenovirus
CLA	Cutaneous lymphocyte associated antigen
CLDN1	Claudin 1
CMV	Cytomegalovirus
CPD	Cell proliferation dye
CTV	Cell trace violet
DAA	Directly acting antivirals
DAPI	Diamidino phenylindole

DMEM	Dulbecco's modified Eagle medium
DMSO	Dimethyl sulfoxide
DNA	Deoxyribonucleic acid
ECMV	Encephalomyocarditis virus
EDTA	Ethylene diamine tetra acetic acid
eGFP	Enhanced green fluorescent protein
EGFR	Epidermal growth factor receptor
eIF	Eukaryotic initiation factor
ELISpot	Enzyme-linked immunosorbent spot
EphA2	Ephrin receptor A2
ER	Endoplasmic reticulum
FCS	Foetal calf serum
FMDV2A	Foot-and-mouth disease virus 2A protease
FTA	Fluorescent target array
FV620	Fixable viability dye
GAG	Glycosaminoglycans
GMFI	Geometric mean fluorescent intensity
gt	Genotype
hAAT	Human α-1 anti-trypsin
HBSS	Hanks balanced salt solution
HBV	Hepatitis B virus

HCC	Hepatocellular carcinoma
HCV	Hepatitis C virus
HCVcc	Cell culture derived HCV
HCVpp	HCV pseudo-particle
HDL	High density lipoprotein
HEPES	N-2-hydroxyethylenepiperazine-N'-2ethanesulphonic acid
HEK293	Human embryonic kidney cells
hFIX	Human coagulation factor IX
HIV	Human immunodeficiency virus
HPV	human papilloma virus
HSC	Hepatic stellate cells
HSPG	Heparan sulfate proteoglycan
Huh-7	Human hepatoma cells
ICS	Intracellular cytokine staining
ID	Intradermal
IF	immunofluorescence
IFN	Interferon
IL	Interleukin
IRES	Internal ribosomal entry site
IRF	Interferon regulatory factor
ISG	Interferon stimulated gene

ITR	Inverted terminal repeat
IV	Intravenous
JAK/STAT	Janus kinase/signal transducer and activator transcription
JFH	Japanese fulminant hepatitis
KC	Kupffer cells
LamR	Laminin receptor
LAV	Live attenuated vaccine
LB	Luria broth
LDL	Low density lipoprotein
LRR	Leucocyte rich repeat
LSEC	Liver sinusoid endothelial cells
MAb	Monoclonal antibody
MAD	Melanoma differentiation antigen
MAVS	Mitochondrial antiviral signaling
MCM	Minichromosomal maintenance complex
MCS	Multiple cloning site
MHC	Major histocompatibility complex
miRNA	Micro RNA
MLTF	Major late transcription factor
MOI	Multiplicity of infection
MVA	Modified vaccinia Ankara

MyD88	Myeloid differentiation primary response gene 88
NAb	Neutralising antibodies
NBD	Nucleotide binding domain
NF-κB	Nuclear factor kappa B
NI	Nucleotide inhibitors
NK	Natural killer cells
NLT	Non-lymphoid tissue
NNI	Non-nucleotide inhibitor
NOD	Nucleotide oligomerisation domain
NPC1L1	Cholesterol transporter Niemann-pick C-1 like 1
NS	Non-structural proteins
OCLN	Occludin
ORF	Open reading frame
PAGE	Polyacrylamide gel electrophoresis
PAMP	Pathogen associated molecular pattern
PBMC	Peripheral blood mononuclear cells
PBS	Phosphate buffered saline
PCR	Polymerase chain reaction
PEG	polyethylene glycol
PEI	Polyethyleneimine
PfSPZ	Radiation-attenuated *P. faliciparum* sporozoites

PI	Protease inhibitors
PKR	Protein kinase R
PRF	Perforin
PRR	Pattern recognition receptor
rAAV	Recombinant adeno associated virus
Rag2	Recombination activating gene
RAS	resistance-associated substitution
RBE	Rep binding element
RBS	Rep binding site
RDRP	RNA dependent RNA polymerase
RIG-I	Retinoic acid inducible gene-I
RNA	Ribonucleic acid
ROS	Reactive oxygen species
rpm	Revolution per minute
RSV	Respiratory syncytial virus
RT	Reverse transcriptase
S1PR-1	Sphingosine-1 phosphate receptor-1
scAAV	Self-complementary AAV
SC	Subcutaneous
SCID	Severe combined immunodeficient
SDS	Sodium dodecyl sulfate

SEAP	Secreted alkaline phosphatase
SEM	Standard error of the mean
siRNA	Short interfering RNA
SLO	Secondary lymphoid organ
SR-BI	Scavenger receptor class B type 1
HSV	Herpes simplex virus
STING	Stimulators of interferon gene
STAT	Signal transducer and activator transcription
SURE	Stop unwanted rearrangement event
SVR	Sustained virologic response
TBE	Tis borate EDTA
Tbet	Transcription factor T-bet
T_{CM}	Central memory T cells
TCR	T cell receptor
T_{EM}	Effector memory T cell
Tfr1	Transferrin receptor 1
TGF-β	Transforming growth factor β
TNF	Tumour necrosis factor
Treg	Regulatory T cell
TRIF	Toll IL-1 receptor domain containing adaptor inducing-β
T_{RM}	Tissue resident memory T cell

trs	Terminal resolution site
UTR	Untranslated region
VARNA	Virus associated RNA
vgc	Viral genome copies
VLP	Virus like protein
VP	Viral protein
WPRE	Woodchuck hepatitis virus post transcriptional element

1 Chapter 1: Literature Review

1.1 Hepatitis C virus (HCV)

1.1.1 Biology and Epidemiology of HCV

HCV is one of the leading causes of mortality and morbidity in the world. It was initially identified as the causative agent of non-A, non-B hepatitis. HCV is a RNA virus classified in the genus Hepacivirus in the *Flaviviridae* family [1-3] and is transmitted *via* different routes including exposure to infected blood, injection drug use, sexual contact and as a result of occupational exposure [4, 5].

An estimated 100 million people are serologically positive for HCV and at least 71 million people are persistently infected with the virus [6, 7]. The most recent estimates suggest that nearly 400, 000 HCV-related deaths occur every year, which is an increase by 22% compared to the number of deaths reported annually since the year 2000 [7, 8]. In the next 20 years, though incidence rates are decreasing in developing countries, deaths from HCV-related liver disease will continue to increase [2].

In Australia, 233,490 people were estimated to be persistently infected with HCV in 2013 and 530 people died from HCV-related liver disease. In Australia, costs related to HCV are estimated to increase from $224 million/year in 2013 to $305 million/year in 2030 [9]. Approximately 10,000 new HCV infections occur in Australia per year [10]. However, as a result of AUD$ 1 billion commitment from the Australian government all HCV infected individuals have access to treatment [11].

HCV is classified into different genotypes based on phylogenetic and sequence analysis of the viral genome. Until the recent discovery of a novel HCV genotype, genotype 8 [12], HCV strains were classified into seven genotypes (1-7) and 67 confirmed and 20 provisional subtypes. The different genotypes differ by 30-35% in the nucleotide sequence while the subtypes differ in less

than 15% in the nucleotide sequence [2, 13]. Globally, genotype 1 is the most prevalent, accounting for 46.2% of infections followed by genotype 3 which accounts for 30.1%. Genotypes 2, 4 and 6 account for the remaining cases [2]. Genotype 7 was identified in Canada in four individuals originating from Democratic Republic of Congo [14]. Genotype 8 was also identified in Canada from four patients who were originally from Punjab, India [12].

Acute HCV infection is clinically mild and typically unrecognized as it results in non-specific flu-like symptoms that are commonly observed in most viral infections. Patients who are HCV RNA positive for six months or longer after the acute infection are defined as persistently infected. The transition from acute to chronic hepatitis C is usually sub-clinical and is missed as only 16% of patients are symptomatic [15].

Twenty-five percent of patients will clear the infection spontaneously within a few months of infection, but the virus remains persistent in 75% of the infected individuals [16]. Persistent HCV infection is associated with the development of liver cirrhosis, hepatocellular cancer and liver failure [2].

Several viral and host factors determine the outcome of the infection [15, 17]. A prospective study that assessed clinical, virological, genetic and immunological parameters of individuals with acute HCV infection indicated that multi-specific T-cell responses, raised levels of alanine aminotransferase (ALT) that decline within 4 weeks, jaundice, female gender and > 2.5 log10 HCV-RNA that drops within 8 weeks were associated with spontaneous virus clearance [18]. Genome wide association studies (GWAS) showed a correlation between a single nucleotide polymorphism (SNP) in different alleles and spontaneous- or treatment induced- virus clearance [19, 20]. A SNP (*rs2596542*) in MHC class I poly- peptide related sequence A (MICA) was significantly associated with HCC in 721 HCV-positive cases and 2890 HCV-negative controls from a Japanese population [19]. Kamal, et al also showed that polymorphism in *IL-28B*, a

member of the IFN-λ family, was associated with strong anti-HCV T cells responses. [18]. Similarly, a meta-analysis of host polymorphisms reported that *DQB1*02, DQB1*0301, DRB1*04* and *DRB1*11* were HLA associated polymorphisms correlated with spontaneous- or treatment induced- HCV clearance [21, 22].

1.1.2 HCV genome organisation and replication

1.1.2.1 Genome organisation

The HCV genome (Figure 1.1) contains a single open reading frame (ORF) between untranslated regions (UTR) that are found at the 5' and 3' ends. The internal ribosome entry sites (IRES), that is contained in the 5' end of UTR is responsible for the cap-independent initiation of translation [23].

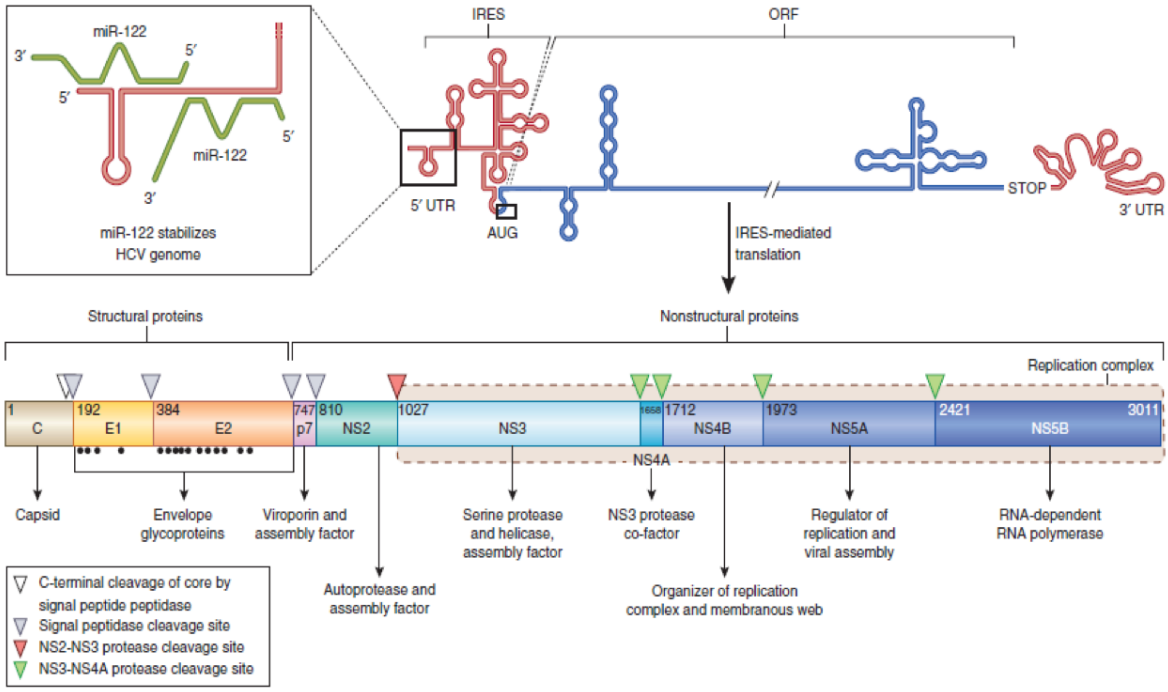

Figure 1.1: The HCV genome and polyprotein processing. The HCV RNA genome (top) contains one long ORF flanked by 5′ and 3′ UTRs. IRES-mediated translation of the ORF leads to a polyprotein (bottom) that is co- and post-translationally processed into ten viral proteins [24].

In cap-independent IRES-mediated translation, viral protein expression is regulated by direct recruitment of ribosomes to the start site of translation. Translation is initiated when a vacant 40S ribosomal subunit binds to the IRES. This binary complex then binds to eukaryotic initiation factor (eIF) 3, as well as the ternary complex eIF-2: Met–tRNAi: GTP to form a 48S-like complex which subsequently leads to the formation of the 80S complex and hence the formation of the first peptide [3]. The HCV RNA 5'UTR contains two conserved microRNA (miR)-122 sites; miR-122 is abundant in human hepatocytes [24]. miR-122 binding has a stimulatory effect on translation, protects degradation of uncapped HCV RNA and inhibits innate immune recognition of the HCV genome [25-27].

1.1.2.2 HCV attachment and entry to the cell

The process that leads to HCV infection of a cell is a complex process that involves attachment then entry and fusion of HCV with its target cells. Glycoproteins on the virus surface and specific receptors on the target cell determine the interaction between HCV and target cells [28].

The binding of HCV E2 to glycosaminoglycans (GAG) on hepatocytes may be the first step in the interaction. This interaction is facilitated by heparan sulfate proteoglycans (HSPG) expressed on hepatocytes. Barth and colleagues showed that degradation of cell surface HSPG with heparinase resulted in a marked reduction in viral envelope protein binding to hepatocytes [1, 29]. In addition to the GAG, lipoprotein receptors and viral lipoprotein structures were shown to play a role in the process of HCV attachment to hepatocytes. ApoE associated with HCV particles is involved in the attachment of HCV to hepatocytes and the addition of HCV to Huh-7 cells in the presence of ApoE-specific monoclonal antibodies (MAb) prevented virus attachment [30]. However, when the anti-ApoE antibodies were added after virus attachment viral protein expression was not inhibited suggesting that ApoE contributes to virus attachment rather than virus entry [30-32]. Low density lipoprotein receptors (LDL) were also shown to act as a

cooperative HCV co-receptor that supports viral entry and infectivity through an interaction with ApoE [33, 34].

Once attached to hepatocytes, HCV is internalized via pH dependent clathrin-mediated endocytosis [1]. The entry process requires different molecules including the tetraspanin, CD81, scavenger receptor class B type I (SR-BI), claudin-1 (CLDN1), occludin (OCLN) and the cholesterol receptor Niemann-Pick C1-like 1 (NPC1L1) [35]. Other factors like epidermal growth factor receptor (EGFR), ephrin receptor A2 (EphA2) and transferrin receptor 1 (TfR1) are also involved in the entry process [36].

CD81 is a member of the tetraspanin membrane protein superfamily, whose members function to organize signaling complexes at the cell surface by association with other tetraspanins, integrins, and signaling proteins in a cell-type-dependent manner [37]. CD81 is a HCV co-receptor that directly binds to HCV E2 [35] and plays a key role in HCV entry process [38]. Zhang *et al*. showed the role of CD81 i) by blocking infection using anti-CD81 MAb and ii) by using short interfering RNA (siRNA) that suppressed expression of CD81 in Huh-7.5 cells [39]. Incubation of target cells in the presence of MAb against CD81 followed by infection with HCV pseudoparticles (HCVpp) inhibited infection of Huh-7.5, Hep3B and PLC/PR5 cells [39]. A greatly reduced level of infection was also observed when siRNA that specifically target CD81 (siCD81) was introduced to Huh-7.5 cells. From both observations, it was concluded that CD81 is important for HCV entry to target cells [39].

SR-BI is a lipoprotein receptor of 509 amino acids (aa) with cytoplasmic N- and C-terminal domains separated by a large extracellular domain. It is expressed primarily in liver and steroid hormone producing (steroidogenic) tissues, where it mediates selective cholesteryl ester uptake from high-density lipoprotein (HDL) and may act as an endocytic receptor [40]. SR-BI was identified as a co-receptor by its ability to bind recombinant HCV E2 on HepG2 cells which lack CD81 expression [41]. Zeisel *et al*. reported that antibody-or siRNA-mediated inhibition of SR-

B1 resulted in reduced susceptibility of human hepatoma cells to cell culture grown HCV (HCVcc) [42]. In another study, it was shown that mutant SR-BI with reduced binding capacity for soluble E2 (sE2) was unable to restore susceptibility of SR-BI knocked down Huh-7.5 cell lines to HCVcc infection [40].

OCLN, an endogenous protein expressed in both HCV-permissive and -non-permissive cells, is another important protein required for HCV entry. Although its over expression failed to change the susceptibility of cells to HCVpp, silencing of OCLN inhibited HCVpp and HCVcc infection of Huh-7 cells [43].

A study that demonstrated the role of CLDN-1 as a viral entry factor used non-permissive cells to confirm its role [44]. In this study, expression of CLDN-1 in HEK-293 cells increased their susceptibility to lentiviral particles expressing HCV glycoproteins, HCVpp and HCVcc. Antibody-mediated blockade of CLDN-1 in these cells prevented viral entry suggesting a role for CLDN-1 in viral entry [44].

The NPC1L1 cholesterol uptake receptor which is expressed on hepatocytes was also recognized as an HCV entry factor. Down regulation or antibody- mediated blocking of NPC1L1 resulted in a reduced susceptibility of Huh-7 cells to HCVcc. In addition the inhibition was HCV-specific as a similar effect was not observed after vesicular stomatitis virus G-protein pseudotyped particle (VSVGpp) infection [45].

The entry processes which involves the above factors eventually lead to release of the HCV genome into the cytoplasm, where primary translation can occur [24, 46].

1.1.2.3 RNA replication and protein translation

Once in the cytoplasm, the HCV RNA functions directly as mRNA, because it is a positive sense RNA, and protein translation is initiated through the IRES in the 5'UTR [23, 47]. Following polyprotein cleavage, the viral RNA and non-structural (NS) proteins form a membrane-associated replication complex [47, 48]. Viral RNA replication occurs in this replication complex

using the positive strand RNA genome as a template for the NS5B polymerase to generate the negative strand replicative intermediate [1]. Nascent positive strand RNA genomes can be further translated to produce new viral proteins, serve as templates for further RNA replication or be assembled into infectious virions [46, 49].

Following RNA replication nascent HCV particles form by budding into the endoplasmic reticulum (ER) where the viral core protein, E1, E2 and the viral genome assemble [35, 49]. Nascent virus particles leave the cells through the secretory pathway [50, 51].

Protein translation results in a poly-protein that is cleaved into mature proteins, structural (Core, E1 and E2) and NS proteins (p7, NS2, NS3, NS4A, NS4B, NS5A and NS5B), by viral and host proteases [1, 3].

HCV core is the first structural protein encoded by the HCV ORF and forms the viral capsid [52]. Host signal peptidase cleaves core from the polyprotein and leaves it embedded in the ER while the host peptide peptidase cleaves it into p21 and p19 releasing p21 from the ER [52, 53]. HCV core has numerous functions involving RNA binding, immune modulation, cell signaling, oncogenic potential and autophagy [1]. Core plays an important role in the pathogenesis of HCV because of its ability to 1) circumvent innate immune response by down regulating signal transducer and activator transcription 1 (STAT1) which is required for the formation of IFN-stimulated gene (ISG) factor 3 (ISGF3) and 2) its ability to inhibit priming of $CD4^+$ and $CD8^+$ T cells [54, 55].

The envelope proteins, E1/E2, are glycosylated envelope glycoproteins that surround the viral particles [1]. These proteins are required for viral entry and hence are the targets for neutralising antibodies (NAb). However, the variability of these proteins means that HCV can escape from NAb [56, 57].

The NS proteins are processed by two viral proteases; the NS3 serine protease and the NS2 cysteine protease [52]. NS3 serine protease mediates autocleavage of NS4A and NS4B, after

which NS4A associates with the N-terminus of NS3. The resulting NS3/4A protease complex can then cleave at the NS4B/5A and NS5A/5B junctions, whereas the cleavage between NS2 and NS3 is mediated by the NS2 cysteine protease [3, 46].

Together, the NS proteins constitute the viral proteins of the replication machinery, which replicates the positive sense RNA genome through a dsRNA replicative form and negative strand intermediate. The roles of each of these NS proteins is summarised in Table 1.1.

1.1.3 Pathogenesis of HCV

HCV primarily infects liver cells and demonstrates high levels of virus production, with a production rate of approximately 10^{12} particles per day in a single infected individual [58], exceeding that of human immunodeficiency virus (HIV) and hepatitis B virus (HBV) [59]. Assuming 10% of hepatocytes from 2x 10^{11} hepatocytes per liver tissue are actively producing HCV virions, each hepatocyte will produce approximately 50 viral particles per day [60, 61].

Initial infection with HCV is characterized by the detection of virus in the blood within 2–14 days of exposure, increases in the levels of liver-associated serum enzymes (*i.e.*, ALT and aspartate aminotransferase (AST)) and the gradual appearance of HCV-specific antibodies within 20–150 days of exposure [62]. Patients who cleared the virus during the acute phase showed higher levels of viral RNA and ALT during the first two months after infection with subsequent decline in the third and fourth months [63, 64]. Patients who present with jaundice (thus indicating more severe liver injury) during primary infection are more likely to clear HCV than the majority who acquire HCV without apparent symptoms [65, 66]. More specific symptoms of viral hepatitis can be encountered in a minority of individuals: jaundice, dark urine, anorexia, aversion to smoking among smokers and abdominal discomfort may occur. Physical findings are usually minimal, apart from jaundice in a third of patients. Chronic hepatitis is the most common outcome, usually characterized by raised serum aminotransferases and may lead to fibrosis and cirrhosis in the liver. Thus chronicity is the major complication of acute hepatitis C [15].

Table 1.1: Function of the NS proteins of HCV

NS protein	Function
p7 viroporin	Essential for the production of infectious virus [67]; increases cell permeability, reduces acidification of intracellular vesicle and impairs glycoprotein trafficking [68, 69]
NS2	NS2 is essential for productive viral infection [70]; immunosuppressive; down regulate IFN [71], cysteine protease that cleaves at NS2/NS3 junction [72]
NS3	Serine protease activity in the N-terminal region and NTPase/RNA helicase activity in the C-terminal region [73]; requires C-terminal portion of NS2 (NS2/3 protease) to cleave at NS2-NS3 junction [74]; requires NS4A (NS3/4A protease) for its protease activity to cleave NS3-4A junction [73]; has an important role in supressing host anti-viral response by acting on Toll-IL-1 receptor domain containing adaptor inducing INF-β (TRIF) and mitochondrial anti-viral signaling protein (MAVS) [75, 76]
NS4B	Alters host cell membrane during HCV replication [77]; inhibits retinoic acid inducible gene-I (RIG-I) mediated IFN-β production [78]
NS5A	Binds to RNA when phosphorylated to stabilise RNA during replication [79]; reduced NS5A phosphorylation impaired viral production in JFH-1 culture system while it enhanced replication in the gt1b replicon system [80]; Impairs cytokine production via its interaction with Myeloid differentiation primary response gene 88 (MyD88) [81]
NS5B	RNA dependent RNA polymerase (RDRP) [82]; mediates replication of HCV genome [83]

Persistent infection with HCV generally results in a slowly progressive disease characterized by chronic hepatic inflammation leading to the development of cirrhosis in approximately 10–20%

of patients over 20–30 years of HCV infection. It is the leading cause of end-stage liver disease, hepatocellular carcinoma (HCC) and liver-related death in the Western world. After the establishment of cirrhosis, the outcome is not predictable; cirrhosis may remain indolent or progress to HCC, hepatic decomposition and death [15]. In the absence of antiviral therapy, 67%-91% of patients with HCV-related liver cirrhosis die due to liver-related causes, including HCC or hepatic failure [84]. The transition from chronic liver disease to cirrhosis involves inflammation, activation of hepatic stellate cells (HSC) with ensuing fibrogenesis, angiogenesis, and parenchymal necrotic lesions caused by vascular occlusion [85]. Cirrhosis can result in major complications of liver failure in patients with chronic HCV infection. However, not all patients with cirrhosis will develop complications [86]. Hepatic decompensation, generally defined as the development of ascites, jaundice, variceal bleeding, and/or hepatic encephalopathy, is another outcome of cirrhosis [84].

HCC is one of the most common malignant tumours, representing more than 5% of all cancers [87]. HCV-associated HCCs develop almost exclusively in patients with liver cirrhosis (> 90%) [88]. The mechanism by which HCV infection causes HCC is not clearly understood. However, HCC may result from chronic necro-inflammatory liver disease or as a consequence of direct oncogenic effect of HCV [87]. Cell damage and chronic inflammation may contribute to the malignant transformation of hepatocytes directly through telomere shortening and inactivation of cell cycle checkpoints, release of reactive oxygen species (ROS), or altering paracrine signaling in the cellular environment [88].

1.1.4 Immune response to HCV

1.1.4.1 Innate immune response to HCV

Innate immune responses are the first line of defence against viral infections. In HCV infection innate immunity is important to control viral dissemination and replication [89, 90]. Pattern recognition receptors (PRRs) within infected cells sense the virus as non-self and induce anti-

viral defences (Figure 1.2) [91]. PRRs include RIG-I, toll-like receptors (TLR), nucleotide oligomerization domain (NOD) like receptors (NLR) and protein kinase R (PKR) [91]. The viral components recognized by these PRRs are specific motifs within the viral products termed pathogen-associated molecular patterns (PAMP) [92]. The interaction between PRRs and PAMPs induces activation of transcriptional pathways that allows rapid activation of the innate immune system [93].

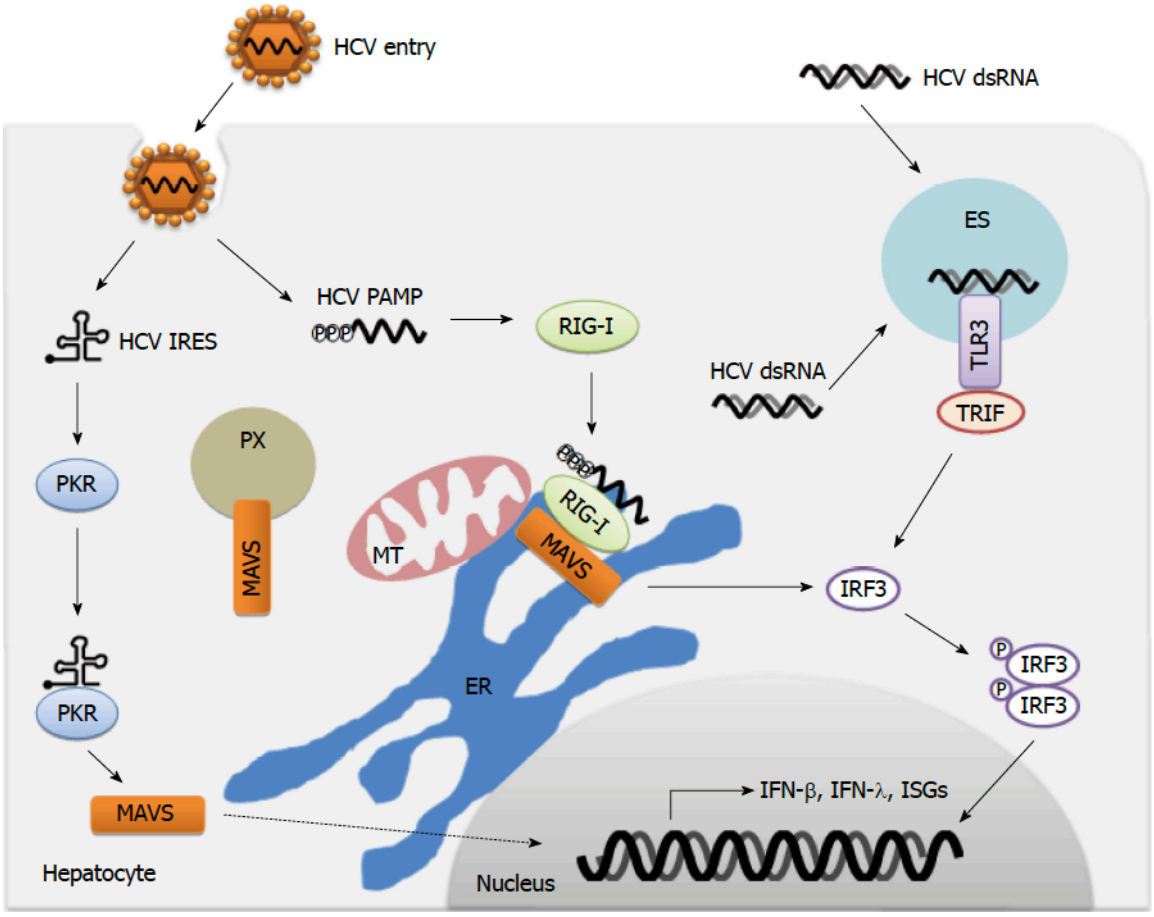

Figure 1.2: Immune sensing of HCV by PRRs [91]. During HCV infection, PKR, RIG-I and TLR-3 recognize dsRNA and become activated. Activation leads to the transduction of signaling through MAVS or TRIF, and subsequent phosphorylation and dimerization of IFN regulatory factor-3 (IRF3) to induce the production of IFN-β, IFN-λ, ISGs and proinflammatory cytokines. MT: Mitochondria; ER: Endoplasmic reticulum; ES: Endosome; PX: Peroxisome

1.1.4.1.1 Innate immune recognition of PAMPs by PRRs

RIG-I belongs to a family of RNA helicases and contains a caspase recruitment domain (CARD) in its N-terminus that allows the recruitment of proteins [94, 95]. RIG-I recognizes blunt or 5′-triphosphorylated (5'ppp) ends of viral genomic RNA segments [94, 96]. Binding of RIG-I to dsRNA leads to signal transmission through the RNA helicase/ATPase domain of the RIG-I. This signaling in turn initiates downstream signaling events that lead to the activation of IRF-3 and nuclear factor kappa B (NF-κB). These signaling cascades induce expression of ISG that control infection [94, 97]. Another RNA helicase that recognises viral RNA is melanoma differentiation antigen 5 (MDA5) [98]. MDA5 mainly recognises long cytoplasmic double stranded (ds) RNAs [99].

TLRs are a family of transmembrane PRR. There are 10 TLRs among which TLR 3, TLR 7 and TLR 9 are associated with virus recognition. TLRs sense virus from within endosomal compartments to signal innate defences. TLR3 recognizes dsRNA, TLR7 detects single stranded (ss) RNA and TLR9 interacts with unmethylated DNA with CpG motifs [98, 100]. TLR3 contains a cytosolic carboxyterminal Toll-IL1 receptor homology (TIR) domain that activates downstream signaling once it recognises dsRNA *via* its amino terminal ectodomain [91]. Signals from TLR 3 are transduced through the adaptor protein Toll-IL 1 receptor homology (TIR) domain containing TRIF while TLR7 and TLR9 signal through MyD88 and the IRAK4-IRAK1-IKKa kinase cascade. Finally, both pathways lead to the activation of NF-κB and IRF3 [91, 98].

NLRs are cytoplasmic receptors that play a crucial role in the innate immune response by recognizing PAMPs [101]. There are five classes of NLR; NLRA (which contain an acidic transactivation domain), NLRB (contains a baculovirus inhibitor of apoptosis protein repeat (BIR)), NLRC (contains a CARD), NLRP (contains a Pyrin domain) and NLRX (contains an unknown domain) [102]. NLRC has been shown to recognize ssRNA derived from respiratory syncytial virus (RSV), influenza A virus, and parainfluenza virus. Upon recognition, NLRC2

associates with IFN promoter stimulator-1 (IPS-1) through an interaction dependent upon the leucine rich repeats (LRR) and nucleotide-binding domains (NBDs) of NLRC. This leads to the production of type I IFN and proinflammatory cytokine release [103].

1.1.4.1.2 Interaction of PRRs with HCV PAMPs

i. RIG-I: RIG-I recognises HCV PAMPs containing a 5'ppp motif in the genomic RNA [91]. Wang *et al*. showed the role of RIG-I signaling in the control of HCV infection. They co-cultured HCV-infected Huh-7 cells with HSC; LX-2 stimulated with or without 5'ppp dsRNA to stimulate the RIG-I ligand and observed significant inhibition of HCV replication. They also demonstrated that IFN-β expression was higher in stimulated cells both at RNA level and protein level [104].

ii. MDA5: siRNA mediated knock down of MDA5 in Huh-7 and HepG2 cells resulted in severely diminished level of IFN production when these cells were transfected with IFN-inducing HCV RNA [105, 106]. Recognition of viral RNA by RIG-I or MDA5 induces a conformational change that exposes the N-terminal CARD domains, which interact with the CARD domain of MAVS that leads to downstream signaling pathways of IFN production [94, 107, 108]. MAVS involvement in the IFN signaling pathway was confirmed in a study that used the NS3/4A protease to deplete endogenous MAVS [107]. According to this study Huh-7 cells over expressing NS3/4A showed increased levels of IFN-λ and activation of IRF 3 when transduced with lentiviral vectors encoding protease resistant MAVS [107].

iii. TLR: HCV structural and non-structural proteins are important PAMPs recognised by TLR2, TLR4, TLR7 and TLR9 [109]. It has been shown that HCV derived immunostimulatory RNA oligonucleotides were recognised by TLR7 leading to the activation of IRF7 and NF-κB in Huh-7 cells [110]. Chloroquine-mediated inhibition of TLR7 signaling in dendritic cells (DC) and peripheral blood mononuclear cells (PBMC) as well as siRNA-mediated knock down of TLR7 expression in Huh-7 cells resulted in reduced production of IFN-α and activation of NF-κB respectively [110]. Another study reported that recognition of HCV NS5A by TLR4 resulted in

secretion of IFN-β and IL-6 from B cells and hepatocytes as noted by the inhibition of HCV-induced cytokine secretion when siRNA against TLR4 was introduced [111]. The role of TLR3 has also been described in suppressing HCV replication through IFN-β and ISGs, in non-parenchymal liver cells, mainly liver sinusoid endothelial cells (LSEC) and Kupffer cells (KC) [112].

iv. NLR: An interaction between NLR and HCV is not well established and to assess the involvement of NLR in innate immune response against HCV, Vegna *et al*. transduced HepaRG cells with a retrovirus vector encoding HCV NS5B and showed high levels of NOD1 expression from these cells. Expression was specific to NS5B as HCV core, NS3, NS4A and NS5A proteins did not alter NOD1 expression [113]. This study also showed that the catalytic activity of NS5B is important for NOD1 mediated downstream signaling of IL-8 and tumour necrosis factor (TNF)-α production. This was evidenced by the use of mutation induced catalytically inactive NS5B which failed to induce with induce NOD1 expression in HepaRG cells [113]. Amina *et al*. showed that exposure of macrophages to HCV induces IL-1β expression through phagocytic virus uptake that activates MyD88, TLR7 and NLRP3 pathways [114].

1.1.4.1.3 HCV and Natural killer (NK) cells

NK cells are important innate immune cells in many viral infections. They recognize and kill virus infected cells and produce antiviral cytokines such as IFN-γ and TNF [115]. When NK cells were cocultured with HCV replicon containing cell lines they were shown to secrete soluble factors which suppress replicon expression and these soluble factors are important in the control of HCV infection [116]. According to this study NK cells did not show a cytolytic effect on ^{51}Cr labelled replicon harbouring cells as no significant release of ^{51}Cr to the medium was observed after 4 hours of incubation [116]. However, this direct lysis inability of NK cell was reversed when NK cells were activated by IL-2 [117]. When constitutively activated IL-2 cDNA transfected NK cells were cocultured with replicon containing hepatoma cell line targets, they

were able to cause lysis of the target cells suggesting that NK cells require IL-2 to be activated [117]. NK cells also showed a positive impact on the clearance of HCV among HIV/HCV co-infected patients [118]. NK cell degranulation was also shown to play role in the cross talk between the innate and adaptive immune response as expression of CD107a, the degranulation marker, correlated with HCV specific T-cell response. However, the correlation was not related to the outcome of HCV infection [119].

1.1.4.1.4 Innate immune evasion by HCV

Although the recognition of HCV PAMPs by PRRs results in immune activation and IFN expression, HCV has the ability to disrupt the PAMP responsive signaling pathways and evade antiviral defences leading to viral persistence [120]. Components of the type I IFN activation pathways including TRIF and MAVS are important host substrates that are targets of HCV NS3/4A protease cleavage [121, 122]. This ultimately blocked the activation of ISG and prevented TLR 3 and RIG-1 signaling [123]. NS4B has also been identified as a strong inhibitor of RIG-I mediated INF-β production as the protein N-terminus was shown to directly bind and inhibit stimulators of IFN genes (STING) activity [124, 125]. NS5A is also among the components of HCV that plays a role in attenuating the innate immune response via its ability to-inhibit ISGs 2'-5' oligonucleotide synthase and induce IL-8 which antagonizes overall ISG expression [126]. Formation of a heterodimer between NS5A and PKR inhibits cyclophilin A activity which in turn blocks IFN effector function [127]. In addition, HCV core protein has been indicated to interfere with Janus kinase/signal transducer and activator transcription (JAK/STAT) signaling to down-regulate ISG expression [128].

HCV has also been shown to inhibit IFN-γ production by NK cells, following cross-linking of CD81 with HCV E2 after exposure to co-stimulatory cytokines [129]. Engagement of CD81 inhibited CD16-mediated tyrosine phosphorylation which is an important signaling pathway to

NK cell activation [130], although this inhibitory activity was not observed when HCV envelope proteins were presented as a component of an infectious HCV particle [131].

1.1.4.2 The adaptive immune response

Unlike the innate immune response that responds within hours or days of infection the adaptive immune response is usually detected 6-8 weeks after infection [89]. The adaptive immune response is associated with recovery from HCV [132].

1.1.4.2.1 Humoral immune response

NAb may directly block attachment of the virus to the host cell and thus inhibit dissemination of infection and may interfere with post-binding steps such as entry of the virus into the host cell. Moreover, NAbs may act as an opsonin in enhancing phagocytosis of virus particles, thereby decreasing viral load [133, 134].

NAb are induced during HCV infection to target epitopes within the HCV envelope glycoproteins E1 and E2, or the E1E2 heterodimer [135]. Pestka *et al.* reported that rapid induction of NAb was associated with clearance of HCV in a single source out-break of HCV [136]. According to the report, among 49 women who were accidentally exposed to HCV contaminated anti-D immunoglobulin, 23 developed persistent infection and they were characterized by the absence or low titre of NAbs during early phase of infection [137]. A study conducted to assess the role of NAb on the clearance of HCV indicated that both the titre and breadth of NAb was higher among subjects who cleared the virus than those among whom the virus persists [136]. This study also showed that the breadth of NAb response decreases after control of viremia and increased during persistent infection [136], as viral persistence in the presence of NAb was still observed.

A study by Zhang and colleagues showed why such viral persistence is common [138]. According to this study the mechanism of viral persistence is due to interfering antibodies that bind to different epitope sites on the E2 glycoprotein which was evidenced by an increased efficacy and

breadth of NAb when the interfering antibodies were removed [138]. However, the concept of interfering antibodies was challenged by other reports that showed the effectiveness of polyclonal antibodies to protect against HCV infection [139] and the additive effect of murine and human immunoglobulins that target different regions of E2 [140, 141].

There are also other mechanisms by which HCV escapes from NAb, among which the most commonly reported mechanism is mutation [142]. Lack of proof reading by the viral polymerase coupled with high replication capacity results in the generation of many variants that have a potential to escape neutralisation [142, 143]. As a result, antibodies generated at certain stage of HCV infection were unable to neutralise HCVpp cloned from the same patient at different time point [56, 144]. Dowd *et al*. tested the neutralisation ability of acute phase sera from HCV patients against HCVpp cloned from the same patient at different time point and showed neutralisation against earlier HCVpp was greater than late stage HCVpp [144]. In another similar report, NAb failed to neutralise HCVpp bearing autologous glycoprotein sequences that were present at a given time [56]. Both studies suggest that HCV is exposed to selection pressure from the humoral immune response which ultimately leads to the emergence of antibody-mediated neutralisation-resistant variants.

Another mechanism of HCV to escape antibody mediated clearance is cell-to-cell transmission [142, 145]. When CD81 negative HepaG2 cells were cocultured with Japanese fulminant hepatitis (JFH)-infected cells in the presence of antibodies that can neutralise cell free virus, HepaG2 cells were infected [145] . This showed that HCV can transfer between cells without the involvement of CD81 via a cell-to-cell contact thus preventing virus neutralisation.

1.1.4.2.2 Cell mediated immune response (CMI)

Studies conducted in patients as well as animal models indicated that strong, multi-specific and long-lasting T-cell immune responses play a vital role in the control of HCV infection [132, 146].

Spontaneous eradication of acute HCV infection is associated with the early induction of broad $CD4^+$ and $CD8^+$ T-cell responses to HCV NS proteins 3, 4, and 5, and to a lesser extent, to the HCV core protein [147]. Antibody-mediated depletion of $CD8^+$ memory T cells resulted in prolonged HCV replication in chimpanzees that were otherwise able to rapidly clear the virus [148] while another study reported that antibody-mediated depletion of $CD4^+$ T cells was also associated with viral persistence [149]. In fact the intrahepatic antiviral $CD4^+$ and $CD8^+$ T cell response is associated with acute control of HCV infection [146] and the decrease of the viral titre coincides precisely with the appearance of HCV-specific T cells and IFN-γ expression in the liver, suggesting that viral clearance is T cell mediated [150]. At the time of clinical presentation and ALT elevation, vigorous proliferation of HCV-specific $CD4^+$ T cells with concomitant IL-2 and IFN-γ production is readily detectable in the blood of patients who recover and clear the infection [151-153]. In contrast, HCV-specific $CD4^+$ T cell responses are absent or weak in those who subsequently develop chronic infection [154]. On the other hand, $CD8^+$ T cells are detectable in the blood of acutely infected patients regardless of virological outcome [154]. In a case-control study that assessed the outcome of acute HCV infection, it was shown that spontaneous clearance of HCV was strongly correlated with high frequency HCV specific $CD8^+$ T cells that are transcription factor T-bet positive ($T\text{-}bet^+$), an important regulator of the production of IFN-γ and cytotoxic molecules by $CD8^+$ T cells [155-157]. Lechner *et al*. also studied immune response in acute HCV infection and showed a higher $CD8^+$ T cell response among individuals who cleared the virus [158]. However, failure to sustain a $CD8^+$ T cell response was shown to be associated with progression to virus persistence [159].

For long term protection from chronic HCV infection memory $CD8^+$ T cells play a vital role in chimpanzees which were serially infected with HCV [148]. Following a second infection these animals were able to clear the infection within 14 days and this was associated with increased cytotoxic activity of liver resident $CD8^+$ T cells and expansion of $CD8^+$ and $CD4^+$ cells in the

blood. Antibody-mediated depletion of $CD8^+$ memory T cells resulted in a failure to resolve a third infection indicating that $CD8^+$ memory T cells were protective against repeated HCV infection [148]. Another study that compared 17 individuals who developed persistent infection and 14 individuals who cleared infection reported that the breadth of $CD8^+$ T cells predicted the outcome of infection as patients who demonstrated CTL responses to at least two HCV peptide pools were statistically more likely to contain HCV infection than patients with responses to ≤1HCV peptide pool [160]. Others also observed that individuals who clear HCV showed significantly broader CTL responses of higher functional avidity and wider variant cross recognition capacity than non-clearers [158, 159, 161].

1.1.5 Model systems for HCV study

1.1.5.1 *In vitro* systems

Several *in vitro* systems for HCV are important in the study of the viral life cycle, pathophysiology and to test efficacy of antivirals [162]. Some of these models are described in the following paragraphs

1.1.5.1.1 Primary hepatocytes

Primary hepatocytes from humans and chimpanzees were the targets of initial attempts to establish HCV infection. It was possible to detect HCV RNA from these cells when they were infected with HCV-containing serum [163]. Human fetal hepatocytes exposed to serum from HCV patients supported replication of HCV gt 1a, 1b, 2a, 2b, and 3. These cells released HCV to the medium for at least 2 months and expressed HCV core protein and negative strand RNA [164]. In another study it was described that normally differentiated human primary hepatocytes supported productive replication of infectious clones of HCV gt 1a, 1b, and 2a, that, when released to the medium, was able to infect naïve hepatocytes [165]. However, the cells had a short passage life and were prone to contamination which pushed scientists to examine better strategies [163].

1.1.5.1.2 HCV Replicon

The HCV replicon was developed in 1999 and allowed the study of the viral RNA replication *in vitro* [166]. This HCV replicon was derived from the consensus Con1 cDNA that was isolated from the liver of a patient chronically infected with a genotype 1b strain and is composed of the HCV 5'-UTR fused to the region encoding the first 12 amino acids of the core , the neomycin phosphotransferase (NeoR) gene as a selectable marker, and the HCV NS3-NS5B regions under the control of the encephalomyocarditis virus (EMCV) IRES, followed by the HCV 3'-UTR. This was constructed after removing coding sequences for C, E1, E2 and p7 of the consensus genome Con-1 (Figure 1.3) [166, 167]. Huh-7 cell were transfected with RNA that was transcribed *in vitro* by T-7 RNA polymerase resulting in the production of cells stably replicating HCV RNA at low levels [5, 163]. HCV replicons have proven to be extremely valuable for studies on the process of HCV replication, as well as for testing of novel antiviral compounds that specifically target the protease activity of NS3 or the polymerase activity of NS5 [168]. The drawback of subgenomic replicons was that even though they express all the NS viral proteins required for viral RNA replication they were unable to produce infectious HCV particles as they are devoid of the coding regions for structural proteins [162].

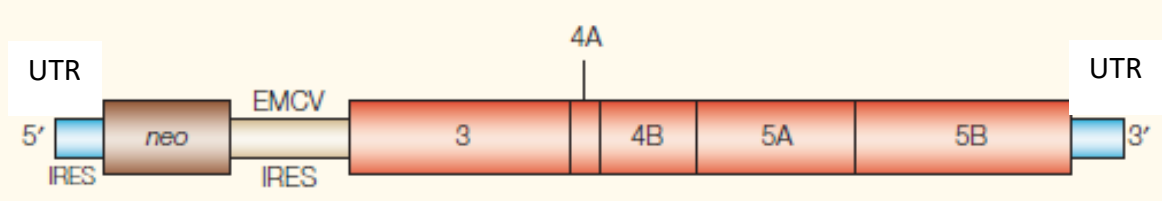

Figure 1.3: HCV sub-genomic replicon: A sub-genomic replicon is derived from the cloned HCV genome by replacing the region that encodes the core protein to the NS2-encoding region of the consensus genome Con-1by the neomycin phosphotransferase gene (neo) and the IRES of EMCV [169].

1.1.5.1.3 Cell culture grown HCV (HCVcc)

The shortcomings of subgenomic replicons were overcome when JFH-1 clone was isolated which replicated 20-fold higher than the Con-1 replicons as determined by colony formation efficiency in Huh7 cells [162, 170]. JFH-1 is a strain of HCV recovered, with its entire genome, from the serum of a Japanese patient with fulminant hepatitis [171]. Based on this isolate a subgenomic replicon was constructed and tested for its replication ability [170]. Unlike its predecessors, JFH-1 replicon did not require adaptive mutation, a reason suggested for the inability of other replicons to release infectious particles, for successful replication *in vitro* [162, 170]. *In vitro* transcribed full length JFH-1 genome or a recombinant chimeric genome with another genotype 2a isolate, secreted infectious virus particles in Huh7 and Huh7.5 cells [172-175]. These cell culture grown virus particles have a spherical shape, have 1.15-1.17g/ml density and are 55nm in diameter [172]. They were infectious in infectious in cultured cells, chimeric mice and chimpanzees [172-175]. The JFH-1 isolate allowed the complete life cycle of HCV to be studied giving greater insight into the underlying mechanisms compared with other available *in vitro* models [174-177].

1.1.5.1.4 HCV Pseudoparticles (HCVpp)

Another cell-based model system that contributed to study HCV viral binding and entry is HCVpps. HCVpps are defective lentiviral particles expressing HCV glycoproteins which are made by assembling HCV glycoproteins E1 and E2 onto retroviral or lentiviral core particles. The HCVpps can mimic the viral entry of HCV [5, 162]. A reporter gene is also packaged in these particles to allow identification of infected cells, thus creating a system to examine virus entry to the cell [178]. HCVpp enabled studies of the entry aspects of the virus life cycle and were used in determining the role of HCV entry factors like CLDN1 and CD81 [44, 178, 179]. They also provided functional assays to screen the effect of neutralising antibodies on virus entry [178].

1.1.5.2 Animal models to study HCV

1.1.5.2.1 Chimpanzees

Chimpanzees are the only non-human primates that can be infected with HCV and hence used to study HCV infection; they can be infected with isolates of the 6 epidemiologically important genotypes [180]. Insights into the characterization of the virus, virus-host interactions and immunopathogenesis were determined by experimental infection of chimpanzees [162] and thus the use of chimpanzees, which have more than 98% genetic similarity with humans has contributed to our understanding of HCV infection [5]. In fact, chimpanzees were used to isolate cDNA from the Non-A, Non-B viral hepatitis genome which finally led to the identification of the virus as HCV [181]. Chimpanzees infected with HCV display elevated aminotransferases and liver biopsies show necro-inflammatory changes after acute infection. However, chimpanzees differ from humans in that their course of infection is milder; persistently infected animals do not develop cirrhosis or fibrosis and only one chimpanzee has been reported to have developed HCV-related hepatocellular carcinoma [182].

Immunological studies in chimpanzees including cellular immune kinetics have been particularly useful [183]. Nascimbeni *et al*. reported that the pattern of the cellular immune response in the blood and liver correlated with virological outcomes in a study that re-challenged chimpanzees which had previously cleared infection [184]. As described in sections 1.1.6.1 and 1.1.6.2, drug and vaccine development studies also largely used chimpanzees [185-187]. Overall chimpanzees are the gold standard animal models for HCV studies, however, their use as a model is banned in most countries primarily due to ethical issues and secondly due to economic reasons [5, 188].

1.1.5.2.2 Tupaia

Tupaia belangeri is a tree shrew native to Southeast Asia. Primary tupaia hepatocytes were shown to be susceptible to serum- or plasma- derived HCV infection [182, 189, 190]. However, these animals are not widely used as a model due to the low and variable HCV infection rates [180].

One study followed tupaia for three years after infection with HCV-positive serum or viral particles reconstituted from full length cDNA. The tupaia developed acute HCV infection and over time they developed chronic hepatitis that worsened progressively. Serum from infected tupaia also infected naïve tupaia. This report indicated that tupaia can be potential model for HCV infection, however, intermittent viremia might be a problem [191]. Moreover, the difficulty to genetically manipulate the animals, and their genetic heterogeneity, as a result of absence of inbred strains of tupaia, represent other limitations with these animal models [182, 192, 193].

1.1.5.2.3 Mouse models for HCV

Mice are not naturally susceptible for HCV infection, but sophisticated genetic manipulations have been used to make them models for HCV infection and pathogenesis. As a result, they have been used with different approaches to bridge between *in vitro* and *in vivo* experiments [192, 194].

In 2001, severe combined immunodeficient (SCID) mice carrying the homozygous plasminogen activator transgene (*Alb-uPA*) with chimeric human livers were developed [195]. The *Alb-uPA* transgene targets urokinase over-production to the liver resulting in a profoundly hypofibrinogenemic state and accelerated hepatocyte death facilitating the transplantation process [196]. It was reported that following transplantation with human liver more than 50% of the liver cross-section was populated with human hepatocytes. These mice showed prolonged HCV infection with high clinically-relevant titres, ranging from $3x10^4$ to $3x10^6$ copies/ml of viral RNA, up to 35 weeks after inoculation with human serum. They support HCV infection with genotypes 1a, 1b, 3a and 6a [195].

In 2012, Ilan *et al*. developed another mouse model, termed the Trimera Mouse model. This model was developed by transplantation of HCV-infected human hepatocytes to lethally irradiated mice reconstituted with bone marrow cells from SCID mice [197]. HCV RNA was

detected in 50% of the transplanted mice on day 12 following transplantation and viral persistence was detected for one month. Treatment of these mice with small molecule antiviral, I70, and anti-HCV MAb, HCV AB^{XTL} 68, reduced the mean viral load in a dose dependent manner [197].

An additional model, the recombination activating gene 2 (Rag2) knockout mouse model was able to support HCV and HBV infection after transplantation with human hepatocytes. Up to 95% chimerism was reported in these models which were evaluated for antiviral drug testing. Consequently, antiviral treatment with pegylated (peg)-IFN alone or peg-IFN with ribavirin (RBV) or peg-IFN with Debio-025, a cyclophilin inhibitor that was shown to reduce HCV viral load in treatment naïve patients when used in combination with peg-INF [198], for two weeks resulted in a $3\log_{10}$ reduction in HCV RNA after two weeks [199]. All of the aforementioned mice models support HCV infection but due to either an immunosuppression or a mismatch in the immune mechanisms they cannot be used in vaccine-related studies [200]. High sensitivity to handling conditions and limited access to fresh human hepatocytes for engraftment are also limitations of these models [201].

The presence of a normal immune system in mice theoretically reflects the natural immune response in humans. Hence immunocompetent mice are vital to study the efficacy of vaccines against HCV [202]. In 2011 an immune deficient Rag2 knockout mice was developed into an immunocompetent model after reconstituting the immune system with human hematopoietic stem cells. This model supported both HCV replication in the transplanted human liver and showed T-cell response against the virus. However, only 50% of the mice were infected with HCV and none of them developed HCV viremia [203].

Another immunocompetent model was developed by using a bicistronic HCV genome expressing CRE recombinase which activates a luciferase reporter molecule. Expression of the reporter signal indicates expression of HCV genome in the liver of the mouse. In this model adenovirus

(Ad) transduction was used to express the human cellular factors (CD81 and OCLN) necessary for HCV entry. All mice expressing CD81 and OCLN were successfully infected with HCV but there was a reduction in the signal 72 hours post infection, which may be related to anti-vector immunity [204]. The model was then modified to stably express all the human factors necessary for HCV entry. Similar to the previous model, reporter activation was observed following HCV CRE infection. Administration of antibodies against the HCV envelope or the host entry factor CD81 resulted in a dose-dependent inhibition of HCV infection. These observations suggested that the model can be used to assess the efficacy of vaccine strategies, at least those passively administered immunizations [205]. None of the above models was used in challenge experiments to examine HCV specific CMI.

The intra-hepatic challenge model developed in the Gowans' laboratory in 2014, showed promising results to test the efficacy of vaccines for HCV [206]. In this model hydrodynamic injection of a HCV gene plus a secreted alkaline phosphatase (SEAP) reporter was used as a "challenge". An effective immune response resulted in a decrease in serum SEAP levels. The co-expression of SEAP allowed a more sensitive method of detecting HCV gene expression in the mouse liver and also enabled longitudinal analysis of the immune response in mice without the need to sacrifice the animals [206]. However, this model has not yet developed in a large animal model.

An immunocompetent, HCV permissive mouse model with evidence of liver disease resulting from HCV infection was reported by Chen *et al*. [207]. The group reported the creation of a transgenic mouse in ICR (CD1) background (C/O^{Tg}) expressing human OCLN and CD81 that were permissive to infection with serum- and cell culture-derived HCV and maintained stable levels of HCV RNA in serum and in liver for over 12 months. *In situ* hybridization of HCV RNA and staining of HCV NS5A protein in the liver cells of mice at different time points confirmed

sustained infection. Moreover, a HCV protease inhibitor cured the infection. The production of infectious viruses was further confirmed by successful infection of Huh7.5.1 cells with mouse sera and successful passage of HCV into naïve C/O^{Tg} mice [207].

1.1.6 Treatment and prevention of HCV infection

1.1.6.1 Treatment

Conventional IFN, recombinant IFN-α, was used as treatment for non-A, non-B hepatitis before the infectious agent was identified as HCV, but response to treatment was not encouraging as a sustained virologic response rate (SVR) was less than 20% [208]. Combination therapies with recombinant PegIFN and RBV, which was the standard therapy for a decade (2001-2011) improved the antiviral efficacy. This combination resulted in 40%-50% SVR in genotype 1 and up to 80% in genotypes 2 and 3 [209]. However, the SVR among treatment-experienced cases was lower compared with treatment-naïve patients [210]. A nationwide study from Germany showed that the SVR in treatment naïve patients was 54.1% while it was 43.5% in retreated cases [211].

The development of directly acting anti-virals (DAA) has changed the history of HCV treatment. Combinations of these specifically targeted drugs and PegIFN and RBV has resulted in an increased rate of SVR, while more recent DAA are PegIFN and RBV free. Based on their target site DAAs can be classified in to three major groups, viz NS3/4A protease inhibitors (PI), NS5A inhibitors and RNA-dependent NS5B polymerase inhibitors [212, 213].

NS3/4A PI: The NS3/4A is a complex bi-functional molecule essential for viral polyprotein processing and RNA replication [3]. The first generation of DAAs included boceprevir (BOC) and telaprevir (TVR) both of which are NS3/4A PI and were approved for use in combination with PegIFN α and RBV in 2011. First generation NS3/4A PIs are largely genotype 1 specific and have an inherent low barrier to viral resistance, but later versions have improved potency and

wider genotypic coverage [214]. A recent report from Sweden showed that triple therapy using a combination of PegIFN, RBV and either BOC or TVR resulted in SVR of 56% [215]. In Brazil the use of these drugs has been discontinued in the clinic due to their high cost and drug related adverse events [216].

Later in 2013 simeprevir (SMV) was approved as a second-generation PI to be used in triple therapy with PegIFN and RBV [168, 213]. In a study that assessed the prevalence and impact of baseline resistance-associated substitution (RAS) in treatment outcome, it has been reported that the presence of baseline SMV RAS was associated with a small reduction in SVR in HCV patients infected with gt1a but had no impact in gt1b infected patients [217].

Grazoprevir is another second-generation NS3/4A PI that demonstrated activity against RAS seen after failed therapy with first generation PI. This drug has been developed to be used in combination with the NS5A inhibitor, elbasvir, for the treatment of chronic HCV gt1 or gt4 infections [218, 219]. Oral elbasvir/grazoprevir 50/100 mg (Zepatier^{TM}) once daily has been approved by the United States Food and Drug Administration in 2016 [220].

NS5A inhibitors*:* The NS5A viral protein is essential for RNA replication and assembly of infectious virions *via* mechanisms that remain poorly understood [214]. Minimal inhibition of NS5A is associated with significant reductions in HCV RNA levels in cell culture-based models, which makes N5A inhibitors among the most potent antiviral molecules yet developed [221]. NS5A inhibitors have pan-genotypic activity, *i.e*., they suppress replication of all HCV genotypes, but their antiviral effectiveness against different genotypes may vary between compounds [222]. Currently approved NS5A inhibitors are ledipasvir (LDV), daclatasvir (DCV), ombitasvir, elbasvir, velpatasvir (VEL) and pibrentasvir (PIB) [223].

Daclatasvir (DAC) was the first NS5A inhibitor to be developed and approved in 2015 for the treatment of HCV gt3 [224, 225]. Ombitasvir is another NS5A inhibitor with picomolar potency

and pan-genotypic activity [168, 225]. LDV was approved to be used in combination with the NS5B nucleotide analogue sofosbuvir (SOF) [226]. Elbasvir showed activity against gt1a, 1b, and 3 *in vitro*, including against some viral variants resistant to other NS5A inhibitors [227]. VEL was assessed for its efficacy in combination with SOF in a double-blinded, placebo controlled phase 3 trial (ASTRAL-1) and a combination of these two anti-viral drugs showed 99% (95% confidence interval, 98 to >99) SVR among patients infected with HCV gt1, 2, 4, 5 and 6 [228]. Likewise, PIB was tested in combination with glecaprevir, a NS3/4A PI, against HCV gt1-6 and results showed higher rates of SVR against these genotypes [229, 230].

NS5B inhibitors: NS5B is RDRP which is necessary for virus RNA replication. The enzyme has a catalytic site and four other sites which are targets for allosteric inhibition [231] and consequently drugs that target the NS5B polymerase are either nucleotide inhibitors (NI) or non-nucleotide inhibitors (NNI) [232]. The binding of these compounds to the NS5B polymerase inhibits conformational changes required for its polymerase activity [233].

SOF, a NI, is a uridine analogue that mimics natural cellular uridine and is incorporated by the HCV RNA polymerase into the elongating RNA strand, resulting in chain termination [168]. Given that the catalytic site of the NS5B protein is highly conserved across HCV genotypes 1–6, this mechanism is believed to account for the broad genotypic activity demonstrated by SOF in HCV replicon cells [234].

Dasabuvir (DVR) is a NNI that is able to mediate viral clearance, mainly HCV gt1, when used in combination with other antiviral agents [235, 236]. DVR is administered in combination with paritaprevir (NS3/4A PI)/ombitasvir (NS5A inhibitor) in the presence of a pharmacokinetic enhancer, ritonavir [237].

Although these DAA are effective, they may induce or select drug resistant mutants due to the high replication capacity of the virus and the low fidelity of the RDRP resulting in numerous

variants which are produced during HCV replication. These may include variants with altered binding sites for DAA that may be selected to become dominant variants. Thus, selection of resistant variants is an intrinsic feature of DAA [238].

Another major problem associated with DAAs is the cost of treatment [239]. According to a study published in 2016, across 26 countries in the Organisation for Economic Co-operation and Development (OECD), the median price for a 12 week course of SOF was US$ 42,017 [240]. A more recent report from the United Kingdom stated that a deal between manufacturers and NHS England has been secured to bring down the treatment cost to about £5000 [241]. When it comes to developing countries with resource limited settings, the use of these drugs is unaffordable which is also the case in several European countries (e.g. Belgium, The Netherlands, Spain, Italy), where DAAs can only be used in patients with advanced fibrosis or cirrhosis [17].

In addition to the limitations noted above, 80% of HCV infected individuals are unaware of their sero-status precluding them from treatment [7, 242, 243]. After lengthy treatment period of 8-24 weeks that involved high cost, treated individuals treated who showed a SVR remain susceptible to reinfection either from a new exposure or a relapse from previously treated HCV, which was observed in patients treated with IFN therapy [244-246].

Considering the global impact of HCV and the limitations associated with HCV treatment there is an urgent need for a vaccine. Vaccines strategies are of great public health importance as they are cost-effective and represent a realistic means to significantly reduce the worldwide mortality and morbidity associated with HCV infection [243].

1.1.6.2 Vaccines

Vaccination is an established method to generate immunity against specific pathogens. There are different methods, described below, to make vaccines [247].

1.1.6.2.1 Live attenuated vaccines (LAV)

LAV have played critical role in controlling many human diseases, among which small pox eradication is one of the successful medical stories [248]. An important goal in vaccine development is to avoid disease from the vaccine itself. To this end, attenuation of viral vaccines is achieved through repeated passaging of the wild type virus in cell cultures [249]. LAV have been successfully used to prevent infections by poliovirus, measles virus, rubella virus and yellow fever virus [248, 250]. Apart from the unpredictable method of attenuation, the main drawback of LAV is the potential of reversion to virulence [251]. Hence this technology is unsuitable for HCV as a consequence of the high mutation rate [252].

1.1.6.2.2 Inactivated virus vaccines

Using either chemical or physical methods, viruses can be inactivated so they will no longer revert to an infectious particle while they are recognized by the immune system [253]. Although inactivated vaccines are safer than LAV, they are weaker in eliciting immune response and hence may require adjuvants and booster dose [248, 254]. Examples of inactivated virus vaccines include vaccines against hepatitis A virus and polio virus [255].

Purified, inactivated HCVcc derived from the J6/JFH-1 chimeric genome, was used to immunize mice [256]. Sera collected from vaccinated mice contained antibodies against the HCV envelope that inhibited infection of cultured cells with HCV genotypes 1a, 1b, and 2a. Moreover, passive transfer of IgG from the immunized mice into uPA-SCID mice with humanized livers prevented infection with the minimum infectious dose of HCV [256]. However regulatory issues and low yield of HCV particle production in cell culture may limit the use of these vaccines [257, 258]

1.1.6.2.3 Subunit vaccines

Subunit vaccines are produced using only part of the virus to raise a protective immune response and because these vaccines cannot replicate in the host, there is no risk of pathogenicity [259]. Immune responses generated as a result of subunit vaccine are typically weak requiring the

incorporation of strong immune-stimulatory components and booster doses [260]. The inactivated subunit influenza virus vaccine and HBV vaccine are licensed vaccines under this technology [261, 262].

As far as HCV is concerned, a recent report showed that soluble HCV E2 (sE2) protein produced in insect cells induced immune responses that prevented infection in a genetically humanised mouse model [263]. Further immunogenicity characterisation in macaques revealed that the vaccine was able to elicit NAbs against HCVcc harbouring structural proteins from multiple genotypes [264].

1.1.6.2.4 Virus like particles (VLP)

VLP are multi-protein supra-molecular structures that mimic the virus particle but do not contain viral genome. VLP-based vaccines are generally considered as safe because they do not replicate [265]. VLPs provide polyvalent structures that can accommodate multiple copies of antigens and are able to stimulate immune cells [266]. The HPV vaccine is an example of a VLP vaccine [266].

Garrone *et al*. reported that VLPs pseudotyped with HCV E2 and/or E1 induced high-titre anti-E2 and/or anti-E1 antibodies, as well as NAbs, in mice and macaques. The NAbs, which were raised against HCV 1a, cross-neutralized five other genotypes tested (1b, 2a, 2b, 4, and 5) [267]. More recently, it has been reported that a quadrivalent gt1a/1b/2a/3a VLP vaccine was able to induce high titre antibodies when adjuvanted with a TLR 2 agonist, although the adjuvant did not change the strength of the NAbs [268]. Further investigations showed that the quadrivalent VLP vaccines was able to induce strong T cell immunity as determined by IFN- γ Enzyme-linked immunosorbent spot (ELISpot) assay [269].

1.1.6.3 HCV vaccines

Vaccines against HCV need not to be protective against infection; rather, prevention of viral persistence will prevent the bulk of HCV associated disease [247]. In the next sections the different approaches used to develop vaccine against HCV are discussed.

1.1.6.3.1 Vaccine approaches to elicit NAbs

Studies in small animal models and non-human primates [270-272] indicated that NAb are important in the prevention of HCV persistence. However the heterogeneity of HCV limits the ability of NAb to be cross protective [257], although cross NAb that recognize conserved regions within E2 have been described [273, 274]. The following text reports the results of a few representative studies.

The use of envelope glycoproteins E1/E2 in vaccine formulations is one of the strategies used to induce NAbs against HCV [257]. A meta-analysis of vaccine efficacy based on chimpanzee models suggested that NAb can play role in protection against HCV. According to the meta-analysis, vaccines with the highest protective efficacy included all or part of the envelope proteins inducing neutralizing antibody, E1E2 T-cell responses or both [185].

Five of seven chimpanzees vaccinated with HCV-1 purified recombinant E1E2 heterodimer in combination with MF59 were protected from IV challenge with homologous virus [275]. Later this vaccine was tested in a heterologous challenge after chimpanzees were reimmunized with recombinant E1E2 [276]. Following vaccination a strong and persistent NAb response was observed although chimpanzees developed acute HCV infection following challenge [276]. Similarly, a vaccine made from the combination of recombinant E1 and E2 from strain HCV-N2 and HRV 1 from isolate HCV-#6, induced high humoral immune response against E1 and E2 and low immune response against HRV1, was reported as non-protective against heterologous challenge with HCV-#6. However, protection was achieved when the anti-HRV 1 titre was increased suggesting that recombinant E1 and E2 vaccination alone is not protective [277].

A DNA vaccine encoding HCV E2 elicited anti-E2 responses but was unable to induce sterilising immunity in chimpanzees after three doses of 2mg of DNA, because both vaccinated and unvaccinated chimpanzees developed infection following homologous challenge. However, vaccinated chimpanzees were able to clear the infection in a shorter time while the unvaccinated chimpanzees developed persistent infection suggesting that the vaccine has modified the infection after challenge and prevented development of persistent infection [278].

Some of the vaccines that contain viral glycoproteins were tested in human clinical trials. A report by Law *et al*. showed that a vaccine comprising E1/E2, adjuvanted with MF59C.1, derived from a single isolate (gt1a) induced broad NAb against all seven major clades [279]. Volunteers were vaccinated intramuscularly with recombinant E1E2/MF59C.1 at 0, 4, 24 and 48 weeks and antibodies were detected by ELISA. [280]. The neutralising ability of these antibodies was shown by their ability to prevent chimeric HCVcc infection of Huh 7.5 cells *in vitro* [279].

Another phase I clinical trial to assess safety and immunogenicity of a recombinant E1 protein vaccine based on vaccinia virus adjuvanted with alum reported that the vaccine was tolerated and had no adverse effects [281]. Immunological assessment showed that all 20 individuals who received three doses of the vaccine plus a booster dose seroconverted and had higher level of antibody than the levels measured 2 weeks after the third dose although the neutralisation capability of these antibodies was not reported [281].

1.1.6.3.2 Vaccine approaches to elicit CMI

There are different approaches to make vaccines that can induce CMI. The use of synthetic peptides is a simple approach to develop a HCV vaccines [247]. IC41, a synthetic peptide vaccine candidate, was shown to be safe in a randomized, placebo-controlled trial among 128 individuals. This vaccine comprised poly L-arginine as a synthetic adjuvant and five synthetic

peptides that harbor HCV T cell epitopes [282]. IFN-γ ELISpot assay showed $CD4^+$ and $CD8^+$ T cell responses in 50% and 40% of the vaccinated individuals, respectively [282].

An Ad-based vaccine against HCV was shown to induce sustained T cell response in humans. HCV gt1b NS proteins encoded by human Ad6 and chimpanzee adenovirus 3 (ChAd3) were used to vaccinate volunteers and the vaccines were shown to be safe [283]. Immunologically, both vaccines primed T cells that targeted 5 peptide pools, though the NS3 peptide pool was the immunodominant, as assessed by IFN-γ ELISpot [283]. Functional analysis of the antiviral response by intracellular cytokine staining (ICS) showed that both $CD4^+$ and $CD8^+$ T cell subsets secreted interleukin-2, IFN-γ and TNF-α. The responses were sustained for at least one year after boosting with the heterologous Ad vector [283]. The response to heterologous strains of HCV showed 50% and 80% lower response to HCV gt1a and HCV gt3a, respectively, as compared to the priming gt1b [283]. Heterologous boosting, ChAd3 followed by ChAd6 or vice versa, failed to result in a significant increase in the magnitude of the immune response and this was speculated to be related to an anti-vector immune response. To overcome this problem the vaccination strategy was later modified by using Modified Virus Ankara (MVA) encoding NS3, NS4, NS5A and NS5B as boosting vector following vaccination with ChAd 3 [284]. This approach resulted in enhanced HCV-specific T cell response with extended duration, greater breadth and poly-functionality [284].

Another approach towards vaccine formulation to induce CMI is the use of DNA vaccines that involve the production of non-viable, non-replicating, non-spreading antigens that can induce $CD4^+$, $CD8^+$ T-cell immunity and B-cell immunity. Furthermore, DNA vaccines are safe as there is no risk of reversion because microorganisms are not directly used [285].

A recent report indicated that a DNA vaccine that encoded the HCV NS3/4/5B polyprotein from gt3a and a cytolytic protein, perforin (PRF), generated HCV-specific IFN-γ responses in mice

[286]. Another cytolytic DNA vaccine encoding HCV NS3 from gt1b was also shown to induce robust CMI in mice and pigs; the immune response was characterized by significantly higher levels of IFN-γ response and NS3 specific $CD8^+$ T cells, although statistical significance in the pig study was not shown due to the small number of pigs [287].

A universal vaccine that can induce CMI against the different genotypes may be necessary to eradicate HCV. To this end, Wijesundara *et al*. tested the immunogenicity of a cytolytic DNA vaccine cocktail encoding NS3, 4A and 5B from HCV gt1a and gt3a [288]. According to this study, *in vivo* T cell responses, as determined by fluorescent target array (FTA), were clearly observed for gt1b and gt3a NS3 and NS5B [288]. Using a combination of NS3/4A, NS4B, NS5A and NS5B in a single vaccine formulation, others also showed that DNA-based HCV vaccines are strongly immunogenic and can induce broad T-cell reactivity in macaques, characterized by high numbers of HCV specific $CD4^+$ and $CD8^+$ T cells that were detectable 6 months post vaccination [242]. Others also reported that DNA vaccines that encode individual non-structural genes are able to induce cellular immunity [289-291].

A DNA vaccine encoding HCV NS3/4A was reported as being safe and well tolerated among individuals chronically infected with HCV [292]. Vaccinated patients showed increased IFN-γ production during the first 6 weeks. Six of eight patients who were under standard of care treatment with PegIFN and RBV showed SVR 1-30 months after vaccination [292].

A recombinant pox virus vaccine (TG-4040) encoding HCV NS3, NS4 and NS5B was able to induce HCV-specific CMI and reduced the viral load in chronic HCV patients [293]. CIGB-230 is a therapeutic DNA vaccine candidate that contains plasmid-encoded HCV core, E1 and E2 polyprotein from HCV genotype 1, a recombinant HCV core protein and pIDKE2 (a plasmid encoding the first 650 amino acids of the HCV polyprotein) [294, 295]. In a phase I clinical trial this vaccine was able to induce a specific T cell proliferative response and a T-cell IFN-γ secretory

response in 73% of the study subjects. Moreover, despite persistent detection of HCV RNA, more than 40% of vaccinated individuals improved or stabilized liver histology, particularly reducing fibrosis [294].

Despite the use of different approaches for the development of vaccines for HCV, there is no licensed vaccine so far. A major obstacle of vaccine development is the genetic diversity of the virus as a result of the error prone RDRP [243] that enables the virus to escape from vaccine induced immune response [296]. The lack of appropriate model systems, ranging from cell culture to animal models, is another factor that impedes the development of an effective vaccine for HCV [252].

1.2 Adeno associated virus (AAV)

1.2.1 Virus structure and genome organization

The adeno-associated virus (AAV) was discovered in 1965 as a contaminant of simian Ad preparations [297]. AAV requires a helper virus for a productive infection and was classified as a *Dependovirus* in the *Parvoviridae* family [298]. The AAV virion is an icosahedral non-enveloped particle which measures 20-25 ηm [299, 300].

AAV serotypes have been isolated from different species including primates, avian and bovine. AAV serotypes 2, 3, 5, and 6 were isolated from human cells, while AAV serotypes 1, 4, and 7–11 have nonhuman primate origins [299]. The general organization of the parvovirus genome is conserved across the different serotypes, with a similar configuration of replication and structural genes [299]. More than 110 primate AAV capsid sequences have been isolated and classified under 12 serotypes [301]. Based on the prevalence of NAb AAV2, 3, and 5 are thought to be of human origin while AAV4 originated from non-human primates [302].

The genome of AAV is a 4.7kb ssDNA that has three open reading frames (ORF), *rep*, *cap* and *aap* (Figure 1.4). The ORFs are enclosed between two inverted terminal repeats (ITR), which are

Cis-acting components of the viral genome that function as the viral origin of replication and packaging signal [303-305]. The gene contains three viral promoters that are identified by their relative map position within the viral genome: p5, p19, and p40 [299]. Each promoter controls the expression of different proteins [306].

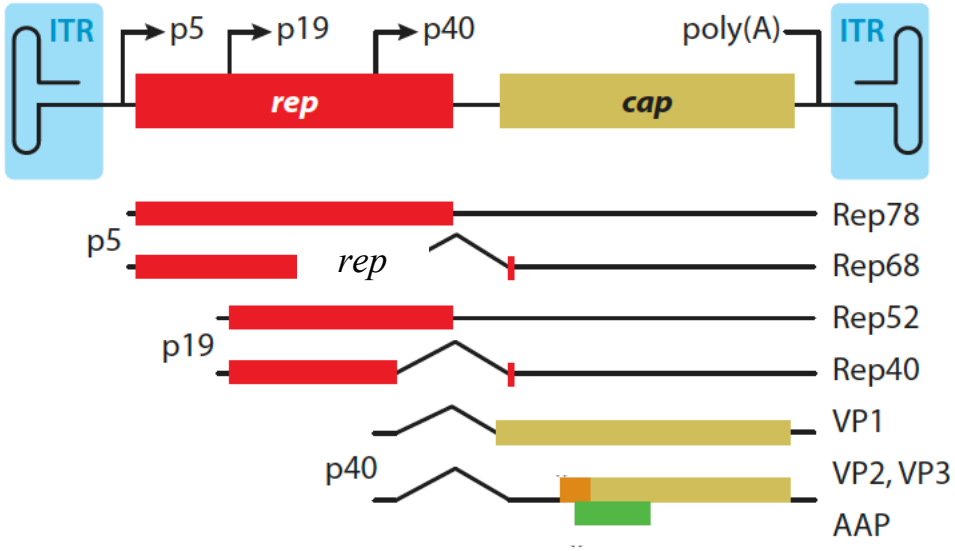

Figure 1.4: The genome of AAV. The AAV genome has three ORFs flanked by ITRs (blue). The rep ORF (red) codes for four Rep proteins (Rep78, Rep68, Rep52, and Rep40) that are synthesized from mRNAs initiated from the p5 and p19 promoters. The cap ORF (yellow) codes for the three capsid proteins (VP1, VP2 and VP3) transcribed from mRNA controlled by p40. The VP2/VP3 mRNA codes for an assembly-activating protein (AAP) (green) AAV [300].

1.2.1.1 Cap gene

Transcription of the cap gene controlled by the p40 promoter leads to the production of VP1, VP2 and VP3 (Figure 1.4) [298]. Together these proteins form the viral capsid which is composed of 60 subunits arranged in an icosahedral symmetry [307]. The different structural proteins are produced following alternate messenger RNA (mRNA) splicing [308]. VP1 is translated from the minor spliced mRNA while VP2 and VP3 are both translated from the more abundant major spliced mRNA [307, 309].

The first step of AAV infection is attachment of the virus to the host cell. This important step is mediated by structures on the capsid of the virus which interact with the cellular receptors found on specific cells (section 1.2.2.1), resulting in the range of tissue tropism seen for the various AAV serotypes [307, 310, 311]. The capsid also determines the transduction activity of rAAV in different organs [312].

VP1, VP2 and VP3 are found in a ratio of 1:1:10 in the capsid. The ratio of VP3 is 10x higher than VP1 and VP2 because VP1 is translated from minor spliced mRNA while VP2 translation is initiated from a less efficient ACG codon, although it is translated from major a spliced mRNA [307]. The N-terminus region of VP1 has a unique phospholipase A2 (PLA2) motif and a putative nuclear localization signal. The phospholipase domain is proposed to play role in virion escape from the endosome. Mutations in the VP1 were shown to decrease infection and impair trafficking suggesting the involvement of this protein in intracellular trafficking of the virus [310, 313]. Serology and receptor usage of AAV is determined by the VP3 which consists of a conserved β-barrel motif of anti-parallel β-sheet [299]. There are controversies around the role of VP2 in virus assembly and packaging. Previous reports state that VP2 is necessary for particle formation in SF9 cells [314]. According to this study, capsid assembly using the three proteins expressed from separate constructs in the absence of viral DNA or helper virus suggested that VP1 plus VP3, VP1 plus VP2, or VP2 alone can form virus-like particles [314]. A similar study with HeLa cells suggested that VP1 or VP2 alone, but not VP3, can form intact particles [315]. This is contrary to a study which reported that the VP2 protein is not essential for assembly or infection [316]. Another study reported that VP2 was not necessary for virus packaging as demonstrated by packaging of rAAV in the absence of VP2. rAAV packaged from two VP was as efficient in transducing cells as the rAAV packaged from all three VP [317].

1.2.1.2 Rep gene

The rep ORF encodes the four NS proteins that are designated by their molecular weight as Rep78, Rep68, Rep52 and Rep40. Transcription of Rep 78 and Rep 68 mRNA is facilitated by the p5 promoter while transcription of Rep52 and Rep40 is mediated by the p19 promoter. Rep78 and Rep68 are involved in the various stages of the AAV life cycle including DNA replication, site-specific DNA integration (section 1.2.3) and regulation of gene expression [310] and have helicase-, strand- and site-specific endonuclease- activities [318, 319]. The Rep52 and Rep40 proteins are DNA helicases essential for the accumulation and packaging of the genome into the capsid [320].

1.2.2 Replication of AAV

1.2.2.1 Viral entry and trafficking

Attachment of AAV to the host cell involves an interaction between the viral proteins and primary- and co-receptors. At least for the best studied serotype, AAV-2, the primary receptor is HSPG determined by a competition assay and mutant cell transduction assay [301].

AAV2 binds directly to cell surface HSPGs *via* an HS-binding motif on the virus capsid. Cultured hepatocytes from mice which lack the *EXT1* gene, which encodes EXT, an enzyme which is involved in the biosynthesis of HSPG, showed low level of transduction with AAV-2 [321]. Immunohistochemical analysis of liver sections from *EXT 1* mutant mice also showed low level of expression of the transgene, indicating that HSPG is important for *in vivo* transduction of mouse liver [321]. Tissue tropism of AAV-2 in a broad range of hosts may be associated with the use of HSPG as the primary attachment receptor [298].

For successful viral entry HSPG-mediated attachment of AAV to the host cell is aided by co-receptors like the hepatocyte growth factor receptor and integrins [301]. C-Met, a receptor for hepatocyte growth factor which is expressed both on epithelial and non-epithelial cells acts as a

co-receptor for AAV-2. Cells constitutively expressing c-Met showed an increased level of GFP expression after transduction with AAV-GFP as compared to cells lacking the protein. However, experiments that assessed the level of attachment failed to show any difference between c-Met expressing and non-expressing cells, but there was increased rate of internalization of AAV to c-Met expressing cells [322].

Integrins also participate in the internalization of AAV 2. The role of $\alpha_v\beta_5$ integrins, molecules involved in cell adhesion and motility was studied by Sanlioglu *et al*. [323]. According to this study antibody-mediated blockage of these integrins inhibited the uptake of AAV2 bound to HSPGs [323]. In another study chemical disruption of integrins using ethylene diamine tetra acetic acid (EDTA)-mediated chelation resulted in a reduced level of infection with AAV, indicating that integrins are also important co-receptor in the infectious process of AAV [324].

The laminin receptor (LamR) is the first receptor described to play role in AAV-8 binding and transduction [325, 326]. Antibody mediated inhibition of LamR or laminin mediated blockage of LamR on HeLa cells significantly inhibited AAV-8 binding to the cells while overexpression of LamR on NIH 3T3 cells resulted in increased transgene expression following transduction with GFP encoding AAV-8 [325].

When it comes to other AAV serotypes sialic acid has been shown to be important in binding and transduction for serotypes 1, 4, 5, and 6 [298, 301]. Binding and transduction studies by including O-linked and N-linked sialic acid glycosylation inhibitors revealed that AAV-4 binding required O-linked sialic acid while AAV-5 needs N-linked sialic acid [327]. Similarly, for AAV-1 and AAV-6, genetic and enzymatic removal of sialic acid markedly reduced binding and transduction of HepG2, Pro-5 and Cos-7 cells by these serotypes. Moreover, proteinase K treatment of cells, but not glycolipid inhibitors, reduced infection of cells by these serotypes suggesting that sialic acid is important for binding of AAV-1 and AAV-6 [298, 301, 328, 329].

More recently, a universal receptor for most of the AAV serotypes has been described by Pilly *et al.* [330]. The receptor is a type I transmembrane protein, KIAA0319L, and was named AAV receptor (AAVR). The authors reported that AAVR was essential for AAV transduction of human cells derived from a broad range of tissues and in an *in vivo* mouse model [330, 331].

Following attachment to the host cell, successful transduction by AAV requires the virion to progress through internalization, cytoplasmic trafficking and finally nuclear entry [332]. AAV is internalized through receptor-mediated endocytosis via clathrin-coated pits or through the clathrin-independent carriers/glycophosphatidylinositol-enriched early endosomal compartments (CLIC/GEEC) pathway [333]. To study the role of dynamin (a cytosolic GTPase), involved in clathrin-dependant endocytosis [334], Stoneham and colleagues used AAV/phage (AAVP) which was generated as a chimera between AAV and a derivative of filamentous M13 bacteriophage [335]. HEK 293 T cells were treated with dynasore prior to- or during- incubation with AAVP. Flow cytometric analysis of transduced cells following inhibition of dynamin activity with dynasore resulted in poor uptake of AAVP as compared to the dimethyl sulfoxide (DMSO)-treated control which had little or no effect on endocytosis. This was also observed when cells were transduced in the presence of a plasmid expressing mutant dynamin II-K44A tagged with GFP. A 57% reduction in GFP expressing cells was noted as compared to the non-transfected cells [335].

Following virus internalisation, the viral genome has to be processed by the host cell for successful gene expression from AAV genome. Gene expression from AAV vectors is characterised by delayed detection. Different reasons are proposed for this; the first one is since the AAV genome is ssDNA, the slow conversion of ssDNA to dsDNA is the primary cause for the delayed expression profile [336, 337]. Intracellular trafficking is the second reason suggested to be a determinant factor in the AAV mediated gene expression [332, 338]. From the studies that

support this hypothesis, Hansen *et al*. claimed that gene expression in NIH 3T3 cells following AAV transduction was not successful due to impaired intracellular trafficking, although these cells have all the necessary receptors and co-receptors required for viral attachment and entry [338]. To show this they performed Southern blot analysis of DNA isolated from AAV infected NIH 3T3 and 293 cells at different time point after infection. Accordingly, within 2 hours, ~76% of the input ssDNA was present in the nucleus of 293 cells while in NIH 3T3 cells essentially all (~99%) of the signal was detected in the cytoplasm. At 48 hours post infection the majority (~82%) of the signal remained in the cytoplasm of NIH 3T3 cells suggesting that AAV vectors attached and internalized successfully but trafficking to the nucleus was impaired [338].

Among the steps in the intracellular trafficking of AAV, endosomal processing represents an important step in the infectious process of the virus [339]. Once in early endosomes, viral particles can be further transported to the late endosomal compartment or released in the cytosol. AAV have been shown to undergo late endosomal processing and utilize microtubules to traffic its genome into the nucleus of infected cells [332].

Douar *et al*. 2001 used brefeldin A to test if AAV is processed further than the early endocytic vesicle [340]. Brefeldin A is a compound that prevents protein transport from the Golgi compartment to the ER and prevent early-to-late endosome transition [340, 341]. According to this study, treatment with brefeldin A led to a decrease of 2 to 3 orders of magnitude in the efficiency of gene transfer, as measured by the level of luciferase activity in 293, HepG2 and HeLa cells transduced by rAAV encoding luciferase (rAAV-Luc) [340].

In another similar study, impaired endosomal processing in NIH 3T3 cells was suggested to be the main reason for the absence of gene expression in these cell types [342]. In the more permissive 293 cells, virions were found in both early and late endosomes or lysosomes, while in NIH 3T3 cells virions were localised only to the early endosome [342]. This was evidenced by

the inhibition of endosomal-lysosomal acidification that decreased transduction of 293 cells while had no effect on NIH 3T3 cells. On the other hand, when NIH 3T3 cells were exposed to hydroxyurea, a compound known to increase AAV-mediated transduction, virions were detected in late endosome of these cells [342].

1.2.2.2 DNA replication, gene expression and virus assembly

AAV DNA replication is initiated by self-priming of the 3' ITR using the host DNA polymerase (pol) δ. The genome is replicated through the 5' ITR to produce a dsDNA intermediate (Figure 1.5A) that is usually closed at one end, termed turnaround form [343]. While copying the 5' ITR a new 3' ITR is generated and serves as a primer for the synthesis of a second strand [300, 304]. Simultaneously, the AAV Rep proteins (Rep78 and Rep68), bind to the Rep-binding element (RBE) on the original 3′ ITR, and cuts the lower strand at the terminal resolution site (trs) (Figures 1. 5 B and C) [344]. This process generates a free 3′ end (Figure 1.5 D), which allows the replication of the original 3′ ITR and the production of a new ssDNA genome as well as another dsDNA intermediate (Figure 1.5 E) which is fed back into the replication cascade [304].

In the case of unsuccessful nicking and terminal resolution (Figure 1.5 F and G) a self-complementary genome that serves as an intermolecular hinge will be formed. This hinge acts to form a duplex genome (dimer-length replicative form of DNA) (Figure 5 H and I) immediately upon uncoating and bypasses the typical need for second-strand synthesis that serves as a bottleneck for ssDNA vectors [304].

Because the two ends are identical, the process occurs equally well from both ends, generating both positive and negative strands for packaging [300, 345]. This replication mechanism results in the production of ssDNA genomes of both polarities, which are then packaged into the capsid [304].

The commonly accepted concept of AAV virion assembly suggests that empty capsids are formed into which single stranded DNA genomes are then introduced [346]. Assembly of the capsid is

facilitated by a protein called AAP. AAP is localized in the nucleolus, where AAV capsid morphogenesis occurs, and transports nascent proteins, mainly VP3 [346]. AAP from AAV-2 was shown to contain nuclear-and nucleolar- localization signals near its C-terminus region. These signals are responsible for the intracellular localization of AAP and are critical to its function in capsid assembly [346, 347].

1.2.2.3 Helper viruses and cellular proteins required for AAV replication

Productive replication of AAV requires helper functions from other viruses mainly Ad or herpes simplex virus (HSV) [298]. Ad helper functions are provided by the E1a, E1b, E4 orf6 and viral associated (VA) RNA. Both E1a and E1b act as transcriptional activators that induce the AAV p5 promoter. Chang *et al.* fused the chloramphenicol acetyltransferase (CAT) gene to a plasmid that contained the AAV p5 transcriptional control region to generate AAVp5-CAT. Transfection of HeLa cells with AAVp5-CAT in the presence of Ad E1a increased CAT expression by 7-fold while transfection in the presence of E1a and E1b proteins caused a 23-fold increase in CAT expression. The increased transcriptional activity of p5 in the presence of E1 is mediated by two elements; the Ad major late transcription factor (MLTF) binding site and a tandemly repeated 10-base pair sequence. These two elements interact to make p5 more responsive to E1a [348]. On the other hand, in the absence of Ad proteins Rep proteins produced from the p5 promoter autorepress the p5 promoter, producing barely detectable levels of Rep protein ensuring AAV genome latency [349]. E1b, E4 orf6, and VA RNA, perform various tasks that include promoting second-strand synthesis of AAV DNA [336], promoting AAV mRNA transport to the cytoplasm, and inhibiting the IFN-induced dsRNA–activated PKR (DAI/PKR) [300]. The product of E2b is a DNA binding protein that is found in the AAV replication complex and enhances *in vitro* replication of AAV DNA [299, 350].

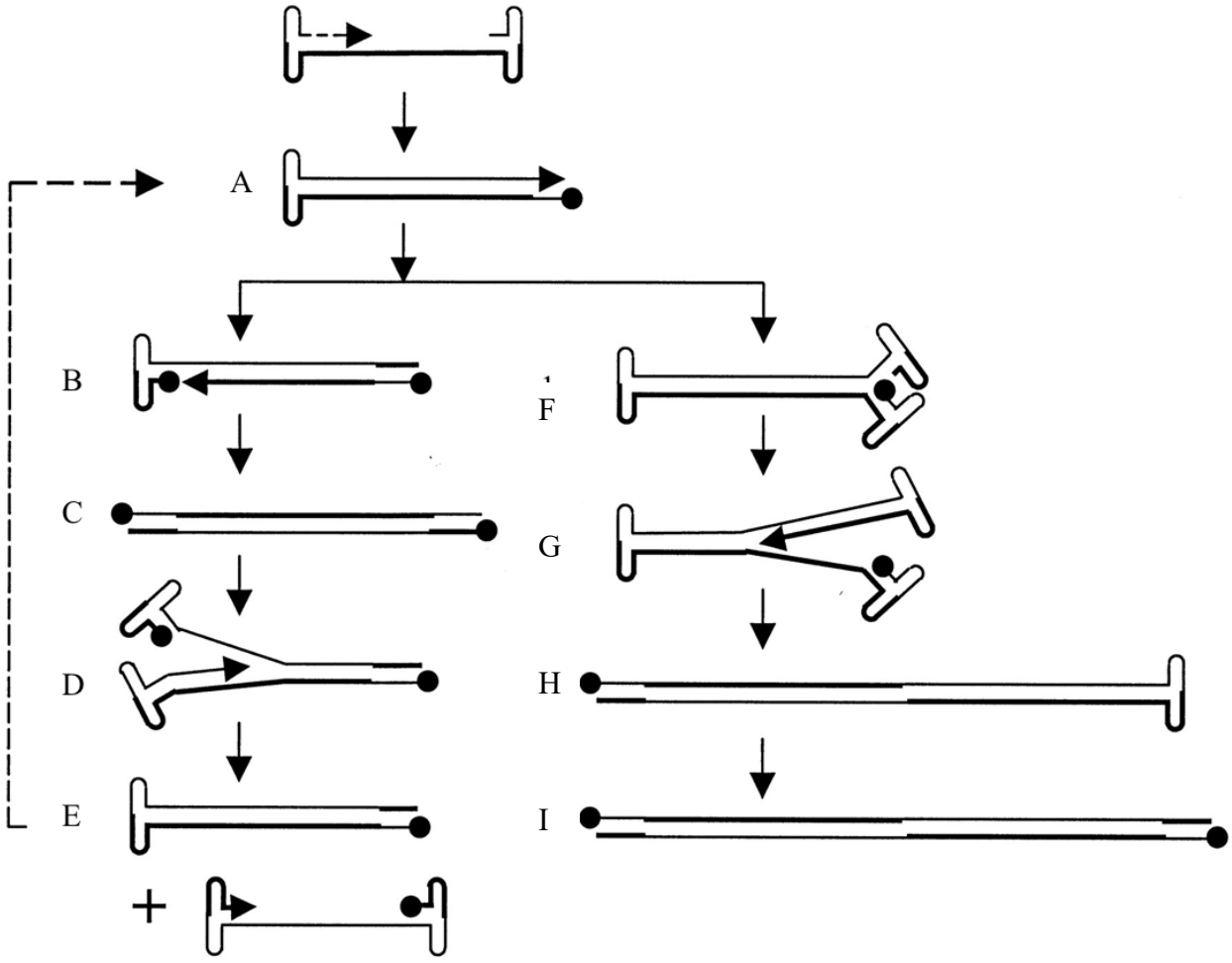

Figure 1.5: AAV genome replication: AAV virions contain a linear ssDNA that replicate through a double strand intermediate turnaround form (A). Turnaround ends are nicked by Rep78 or -68 (closed circle), which becomes covalently attached to the 5' end of the DNA (B). DNA polymerase extends through the terminal repeat to generate replicative form DNA that has two extended ends (C). Steps B and C are often referred to as terminal resolution. Isomerization of the terminal repeat generates a new hairpin, which serves as the primer for DNA synthesis (D) that allows the production of new ssDNA genome and another dsDNA (E) that feeds back to the replication cascade. If DNA synthesis begins prior to resolution of the turnaround end (F and G), the replication complex will proceed through the turnaround end and generate dimer-length replicative-form DNA (H and I).

The helper function of HSV seems to be important during DNA replication unlike that of Ad helper function which mainly is involved in gene regulation. Co-transfection of AAV2 with different HSV genes demonstrated that the HSV helicase primase multienzyme complex composed of UL5, UL8, UL52 and UL29 (major DNA binding protein) were sufficient to mediate helper function [351]. In contrast, by introducing a mutation in UL52 others demonstrated that the primase activity of UL52 is not required for AAV DNA replication as the mutated UL52 had no effect on AAV replication while the UL5 helicase activity was still essential for DNA replication [352].

Cellular factors that that support AAV DNA replication even in the absence of Ad-infection have also been described using an *in vitro* AAV DNA replication assay [353]. The standard *in vitro* AAV DNA replication assay contains linear AAV DNA, HeLa cell extract and Rep78 collected from crude extract of cells infected with a Rep78-expressing baculovirus [354]. In this model it was indicated that cell extract from Ad-infected HeLa cells supported *in vitro* replication of AAV DNA [354]. Later, it was shown that Ad-uninfected cells were able to support AAV DNA replication *in vitro* [353]. Addition of MAb or chemical inhibitors to the standard *in vitro* AAV DNA replication assay, helped to identify cellular factors involved in the *in vitro* AAV DNA replication [353]. Accordingly, antibodies against replication protein A (RPA) and replication factor C (RFC) caused significant inhibition of *in vitro* AAV DNA replication. The addition of aphidicolin, a chemical inhibitor of DNA Pol α, Pol δ and Pol ε, abolished DNA synthesis indicating either one or more of these polymerases is involved in DNA replication [353]. More recent data, based on fractionation assays of extracts from Ad-infected cells, suggested that Pol δ is the only active polymerase required for the replication of AAV DNA [355]. An additional cellular element required for *in vitro* reconstitution of AAV DNA replication was suggested to be minichromosome maintenance complex protein (MCM), which is likely to be a eukaryotic

replicative helicase [356]. This was shown by antibody-mediated blockage of MCM which resulted in the inhibition of AAV DNA replication. Moreover the addition of MCM to a replication assay system that contained purified Rep, proliferating cell nuclear antigen (PCNA), RFC and Pol δ was able to induce AAV DNA replication *in vitro* [356].

1.2.3 Site specific integration of AAV to the human genome

As a result of its defective nature, the AAV will enter a lysogenic pathway if no helper functions are provided by Ad or HSV. This makes AAV the only eukaryotic virus that has a property of establishing latency by integrating its genome into a specific site in the human chromosome 19q13.3-qter [357]. This event shows no effect on expression from the target locus. According to a study by Henckaerts and colleagues, integration of AAV to its target site will cause partial duplication of the target gene, but gene expression was not affected despite these rearrangements [358].

The minimum requirements for site specific integration of AAV DNA are the presence of the large Rep proteins 68 or 78, the viral Rep binding sequence (RBS sequence) and a cellular sequence, present in the AAV integration site 1 (AAVS1), consisting of a trs and RBS signal [344]. AAVS1 was shown to contain a repeated tetra nucleotide sequence of 'GCTC' which is similar to the sequence found in the ITR of the viral DNA. This site was identified as a binding site for Rep78/Rep68 proteins on the viral DNA suggesting that these regulatory proteins are involved in the process of integration [359]. Experiments to assess binding of Rep to the AAVS1 site showed binding of Rep78/Rep68 protein to a 109bp sequence in the AAVS1 site. Further analysis to identify the RBS showed that guanine residues in the GCTC motif was an important binding site [360]. Functional analysis of the AAVS1 sequence showed that a target sequence of 33 nucleotides containing the RBS and trs sequences is necessary and sufficient for AAV site-specific integration [361].

In a study that used transgenic mice carrying the human AAVS1, a 16bp RBE was shown to mediate Rep-dependent integration of the human coagulation factor IX (hFIX) gene. Transgenic mice were hydrodynamically injected with a hFIX expression plasmid (pRBE-CMV-hFIX) containing the 16bp RBE element in the presence of the Rep donor plasmid. Sequence analysis showed site-specific insertion in 4 of 7 animals, but no integration in animals infused with plasmids lacking the 16bp RBE (pN2-CMV-hFIX) or pRBE-CMV-hFIX plasmid alone. As a result, significantly higher levels of hFIX were observed in mice infected with pRBE-CMV-hFIX in the presence of Rep encoding plasmid [362]. The results from this experiment suggested that AAV site specific integration is both RBE- and Rep- dependent [362]. Others also demonstrated that this 16bp RBE is sufficient to mediate Rep-dependent integration into AAVS1 [363].

1.2.4 AAV serotypes and human infection

Approximately 80% of the population is seropositive for anti-AAV antibodies against serotypes 1, 2, 3, and 5. However, there is no observable pathology associated with AAV infection [299]. NAb against the different serotypes of AAV have been reported among different population groups including healthy children, adults and patients with different diseases [364-368]. A limitation to draw conclusion from these studies is that they used different antibody titres to define positive and negative.

A study which examined NAb against AAV-2, AAV-5 and AAV-8 among children with haemophilia reported a prevalence 43.5%, 22.8% and 22.6% respectively [364]. The prevalence of these antibodies showed an increasing trend from early childhood to adolescence [365]. A study which examined 888 samples from four different continents showed that anti-AAV2 seroprevalence ranging from 30% in the US to 60% in Africa. Low antibody titres were observed against AAV-7 and AAV-8 [366]. Another study of a Chinese population reported 92%, 89%, and 69% prevalence of NAb against AAV-2, AAV-3 and AAV-8 respectively [367]. Different groups from around the world reported 59.5% prevalence of NAb against AAV1 among

individuals with heart failure [368] and 37% prevalence of NAb against AAV-5 from HIV positive individuals [369].

1.2.5 Recombinant AAV (rAAV) as a viral vector: Developments and its features

The development of rAAV as a viral vector has resulted from its characteristics such as non-pathogenicity, low immunogenicity and ability to transduce both dividing and non-dividing cells [370, 371]. In addition, the small gene reduces the risk of recombination making it safe for human clinical trials. Moreover, AAV vectors have a broad host and cell tropism range and can transduce *in vitro* and *in vivo* [372].

Following the cloning of a complete AAV-2 genome it was realized that the three ORF are not *cis*-acting genome components for viral replication. This observation led to the suggestion that a transgene could be placed between the ITRs for the production of rAAV provided *cap*, *rep* and *aap* were supplied in *trans* making AAV an important viral vector [304]. The basic design of an AAV vector is relatively simple, in that it consists of an appropriately sized expression cassette flanked by ITRs, which mediate the replication and packaging of the recombinant vector genome by the AAV replication protein Rep and associated factors in producer cells [299].

AAV vectors are feasible and safe vectors in gene-directed therapy. As a result, they have been used to treat diseases like alpha anti-trypsin deficiency, phenylketonuria and neurological disorders [373-376]. The use of rAAV mediated gene therapy has also been examined in the treatment of haemophilia [377]. Phase I/II clinical trials conducted so far showed promising results towards getting treatment for missing coagulation factors; factor VIII (FVIII) for haemophilia A and factor IX (FIX) for haemophilia B [378-380]. Reports from mouse model studies indicated that rAAV encoding sequences of different antigens were able to transduce hepatocytes [381-383].

Although rAAV vectors are gaining popularity in studies involving the introduction of a new gene, as mentioned above, there are also difficulties in the use of these vectors. The first limitation was related to their production, as the use of Ad helper in the production process led to contamination of the AAV vectors, but the replacement of the helper functions with plasmids that encode the necessary helper genes eliminated the problem [304].

A second major limitation is associated with their transgene packaging capacity; rAAV can accept ~4.5 kb of foreign DNA, a vital point if the coding sequence of a therapeutic gene is larger than the packaging capacity [384]. Despite this, studies showed rAAV with inserts ranging from 5.2 kb to 8.9 kb; including a study from, Grieger and Samulski which concluded that serotypes from 1 to 5 can successfully package DNA ranging from 4.4 to 6.0 kb as shown by Southern blotting [317]. A similar study indicated that rAAV packaged an insert of 8.9 kb using a capsid from AAV 5 [385]. In contrast, Wu *et al*. reported that the packaging capacity of AAV cannot exceed 5.2 kb [386]. According to this study, attempts to package 8.6 kb insert size in AAV 2, 5 and 8 resulted in vector genomes that were heterogenous in length and none generated intact 8.6 kb vector genomes. Dot-blot hybridization using DNA isolated from the vector showed no signal after 5.2 kb size revealing that the packaged genome was truncated although the absence 5' ITR was not checked. However, *in vitro* transgene expression from rAAV produced from larger insert size (> 5.2 kb) was observed when HEK293 cells were transduced at high multiplicity of infection (MOI), though the mechanism was not fully understood [386]. One common theme to these studies is that as the genome size increases the transduction efficacy decreases.

One proposed way out to the low level of transduction is the use of self-complementary AAV (scAAV) vectors that is designed as a ss inverted repeat, which folds back upon itself to form a ds genome when entering into infected cells [387]. This strategy is mainly important to bypass the second strand DNA synthesis which is mentioned as a rate limiting step in AAV transduction (Section 2.3.1). McCarty *et al*. reported that the scAAV resulted a 5 to 140-fold increase in

transduction of HeLa cells and resulted significant increase in transgene expression *in vivo* when compared to the conventional rAAV [388]. Others also reported more efficient ocular transduction in mice by scAAV than the ssAAV counterpart [389, 390]. Successful transduction using scAAV was also described in hematopoietic stem cells [391], brain [392] and liver [393]. However, there is one significant limitation associated with scAAV, *i.e.*, its packaging capacity is half the capacity of the ssAAV. This precludes scAAV to be used in the gene therapy of diseases associated with large size gene abnormalities [394] .

1.2.6 Production of rAAV

To overcome the problem of Ad contamination, the standard protocol to generate rAAV involves co-transfection of cells with a vector DNA, *i.e.*, a transgene flanked by the AAV ITRs, a packaging plasmid encoding the *rep* and *cap* genes (without ITRs) and a helper plasmid that provides Ad helper genes [395, 396]. Progress has been made to improve the helper plasmid and pXX6, which contains a mini Ad-genome capable of propagating AAV in the presence of the AAV Rep and Cap protein was developed [397]. pXX6 no longer codes for the hexon, penton, core protein, DNA polymerase, Ad terminal protein and the Ad major late promoter while it contained E21, E4 and VA RNA genes [397]. Combining the AVV vector cassette and the packaging gene cassette into a single plasmid so that both genes can be equally taken by the cells during transfection has also been tried. However, there was no significant difference in the rAAV titre when the two cassettes were used in a single plasmid [397].

Although triple transfection of HEK 293 cells is the standard protocol for AAV production different approaches including the use of i) a baculovirus expression system [398-400], ii) a packaging cell line (HeLa derived cell lines), iii) recombinant Ad encoding the complete rAAV genes in its E1 region [401], iv) a HSV amplicon system [402], v) rAAV packaging cell lines containing inducible Ad helper genes [403] and vi) a two plasmid- (AAV vector and a plasmid that contains AAV Rep and Cap and Ad helper genes) based production [404] have been reported.

1.2.7 Purification of rAAV

Recovery of rAAV from the packaging cell lines involves liberating rAAV from the cells by freeze-thaw cycles, separating rAAV from other cell and media components and concentrating the product. Cellular components can be removed by either centrifugation or filtration [405].

Cesium chloride (CsCl) gradient centrifugation is the commonly employed method of purifying rAAV [406]. Although CsCl purification yields highly pure virus preparations, this yields small scale viral lots suitable for research applications, but the limited availability of ultracentrifuges and a requirement for extensive dialysis of viral preparations due to CsCl toxicity. This results in variable quality of vector preparations, significant loss of infectivity and aggregation in storage [407].

Iodixanol gradient centrifugation is an alternative to CsCl. As it has a much lower toxicity compared to CsCl iodixanol prevents aggregation of rAAV particles and does not reduce infectivity [400, 407].

Chromatographic methods were also developed and used in different studies. These methods increased vector purity, biological potency and throughput [408, 409]. Potter *et al.* developed a simple chromatographic method to purify rAAV 2, 8 and 9 [410]. They utilized flocculation of cell debris under low pH condition for partial purification followed by single step cation exchange chromatography *via* a sulfopropyl column. The flocculation step eliminated the bulk of the contaminating protein and DNA allowing AAV binding to and subsequent elution-from the resin [410]. One step affinity chromatography was also used to purify rAAV produced from insect Sf9 cell lines that contain *rep* and *cap* genes that are induced by baculovirus [398, 399].

1.3 Tissue Resident Memory T (T_{RM}) cells

1.3.1 Introduction to memory T cells

Immunological memory follows the encounter and control of infectious disease by the immune system. When pathogen-specific immune cells are activated they express certain migration

receptors allowing them to home to the site of infection where they contribute to the control of infection [411]. Following successful control of infection, the majority of pathogen specific immune cells will die, but a few of these antigen experienced cells will survive in the host and become memory cells [412].

$CD8^+$ T cells are principal components of this process and protect against pathogens that invade intracellular compartments [413]. Memory $CD8^+$ T cells are present within secondary lymphoid organs (SLO), blood, and the nonlymphoid tissues (NLT), as well as primary lymphoid organs such as thymus and bone marrow [413].

Based on their surveillance pattern, memory $CD8^+$ T cells isolated from human blood are divided into two; central memory T (T_{CM}) cells and effector memory T (T_{EM}) cells [414]. T_{CM} cells express lymph node homing receptors, CD62L and CCR7, but have limited immediate effector function while T_{EM} cells lack lymph node homing receptors but express non-lymphoid tissue target receptors which enable them reach peripheral organs, where they can act against foreign agents [415, 416]. Functionally T_{CM} cells are important for long term protection being involved in secondary responses while T_{EM} cells are immediate responders [417].

Memory T cells can persist for a lifetime in the absence of antigen and even MHC molecules. One example of memory lymphocyte persistence was shown among individuals vaccinated with vaccinia virus vaccine. In these group of volunteers' cellular immunity against vaccinia virus was maintained for decades after the vaccination, with an estimated half-life of 8-15 years [418]. On the other hand, a study in MHC-I deficient mice revealed that $CD8^+$ memory T cells can persist in these mice once they differentiate in to memory T cell subset [419]. Later it was shown that T cell receptor (TCR) expression was not mandatory for the maintenance of memory $CD8^+$ T cells [420].

The mechanism of memory maintenance and lineage relationship between memory T cells is not clearly known. Two models were proposed regarding the development of memory T cells. The first is the linear differentiation model, which predicts that memory cells are the progeny of effector cells that escaped activation induced-cell death [421, 422]. A study by Wherry *et al*. reported T_{CM} cells and T_{EM} cells as a non-distinctive group of cells [423]. According to this report, following pathogen clearance in mice infected with lymphocytic choriomeningitis virus or *Listeria monocytogenes,* T_{EM} cells were converted to T_{CM} cells. In a more continuous manner, following acute infection, $CD8^+$ T cells differentiation follows this path; naïve cells will differentiate into effector cells which then give rise to T_{EM} cells. T_{EM} cells will then differentiate into T_{CM} cells [423].

The second model of memory T cell development suggested that memory T cells directly arise from naïve cells (non-linear differentiation) [421]. In this model T_{EM} cells and T_{CM} cells were described as a completely distinct group of cells [424]. A TCR repertoire study in an adoptive transfer rat model indicated that 75% of T_{CM} cells and T_{EM} cells were derived from a common naïve progenitor cell [424]. Complementing theory, Manjunath and colleagues reported that effector differentiation is not a prerequisite for memory cell differentiation suggesting that the development of memory T cells occurs directly from antigen-activated $CD8^+$ T cells without passing the effector stage [425].

Unlike naïve T cells, memory cells migrate between the blood, the lymph and tissues [414, 426]. The migration pattern of memory T cells and the molecules involved in the process of migration contributed to the heterogeneous phenotype of memory T cells [427]. The migration and distribution of an antigen-specific memory T cell population depends on factors like the site of infection and the type of tissue that is colonized by the antigen [428]. It was shown that pathogen-specific T cells persist in the lungs of mice for over a year after respiratory virus infection; these

cells were present in high number and were distinct from the cell population in the spleen and peripheral lymph nodes [429]. Similarly, HSV type 2 (HSV-2) specific $CD8^+$ T cells express a surface molecule, cutaneous lymphocyte associated antigen (CLA), that enable trafficking to the skin [430]. In contrast, $CD8^+$ T cells specific to non-skin tropic herpesvirus lack CLA [430]. These studies and other similar reports [431, 432] showed the persistent presence of transcriptionally and phenotypically unique memory T cells in specific tissues and these types of memory cells were described as tissue resident memory (T_{RM}) cells which form a third group of memory T cells [433].

1.3.2 Tissue Resident Memory T (T_{RM}) cells

T_{RM} cells are subsets of memory T cells that are maintained in tissues and organs independently of circulating memory T cells (T_{CM-} and T_{EM}- cells) [434]. T_{RM} cells are important in protection against infection in sites where circulating memory T cells are less effective [435]. T_{RM} cells express the integrin subunit CD103, which is not found on their circulating counterparts [436]. However, this is not universal to all T_{RM} cells in all tissues and organs as $CD103^-$ T_{RM} cells are found in the intestinal lamina propria [437, 438]. In addition, CD103 was not upregulated in T_{RM} cells isolated from SLO as compared to T_{RM} cells isolated from the small intestine [439]. T_{RM} cells are phenotypically distinct from other memory T cells; they highly express CD69, an activation marker transiently upregulated in activated T cells, and CD49 (Table 3.1) [433, 434, 440]. Functionally T_{RM} cells are highly cytotoxic and antiviral than other memory T cell subsets which is due to high affinity TCR [441].

The proof of existence of T_{RM} cells is mainly based on parabiosis, a procedure of joining two animals so that they share each-others blood circulation [442], and transplant experiments used to study memory $CD8^+$ T-cell trafficking [443]. To show that T_{RM} cells are non-migratory, Gebhardt *et al.* first transplanted dorsal root ganglia, latently infected with HSV, to under the kidney capsule of a recipient mouse that had circulating HSV-specific $CD8^+$ T cells and this

resulted in the migration of HSV-specific $CD8^+$ T cells from the circulation to the graft [444]. Next the grafted ganglia were extracted and transplanted to a naïve, secondary host. Simultaneously fresh latent ganglia were transplanted into the secondary host at a different site of the kidney capsule. Nine days after the transplantation, grafts were removed and infiltrating cells were analysed; it was found that only recruited $CD8^+$ T cells were found in the fresh graft in contrast to the T_{RM} cells carried by the original graft suggesting that these cells do not egress to the circulation [444]. The presence of T_{RM} cells in the skin was also shown by parabiosis and transplantation studies in mice. These cells remained in the skin and were unable to recirculate [445]. Adoptive transfer of $CD8^+$ T cells from male to female showed that $CD8^+$ T cells with the ability to migrate into the skin survived rejection by the recipient immune system. These cells were those which persisted in the skin following infection, suggesting that these cells escape immune clearance because they were able to enter to the skin rather than entering the circulation [446].

T_{RM} cells exhibit limited motility [446] and they appear non-functional when experimentally returned to the circulation, in contrast to their $CD103^-$ counterparts [447]. Non-recirculating $CD103^+$ T_{RM} cells have now been described in a variety of tissues and organs, including the brain, intestine, skin, and sensory ganglia [444, 447, 448], and CD103 $CD8^+$ T cells in the salivary glands [449] and potentially the lungs [450-452] are likely to belong to this class of resident memory cells.

1.3.2.1 Maintenance of T_{RM} cells

Maintenance of T_{RM} cells within localized tissues depend on their ability to adapt local survival strategies, resist shedding into the lumen at mucosal epithelial surfaces and ignore egress signals [453, 454]. Although the requirements for retention of T_{RM} cells is not universal some of the proposed mechanisms and signals are discussed in the following paragraphs.

Table 1.2. Memory T cell subsets [453]

Subset	Phenotype	Location
T_{CM} cells	$CD44^{high}$, $CD62L^{+}$, $CCR7^{+}$, $CD127^{+}$, $CD69^{-}$, $CD103^{-}$	Lymph nodes, spleen (white pulp > red pulp), blood, and bone marrow
T_{EM} cells	$CD44^{high}$, $CD62L^{-}$, $CCR7^{-}$, $CD127^{+}$, $CD69^{-}$, $CD103^{-}$	Spleen (red pulp > white pulp); fewer in lymph nodes, blood, lung, liver, intestinal tract, reproductive tract, kidney, adipose tissue, and heart
T_{RM} cells	$CD44^{high}$, $CD62L^{-}$, $CCR7^{-}$, $CD11a^{high}$, $CD69^{+}$, $CD103^{+}$	epithelium of the skin, gut, and vagina; salivary glands and lung airways; brain and ganglia (T_{RM} cells isolated from lamina propria, SLO and liver showed a distinct pattern of CD44 and CD103 [439, 455])

The integrin αeβ7, also known as CD103, one marker associated with T_{RM} cells, can bind to E-cadherin, a protein that tethers epithelial cells together *via* a homophilic interaction that forms tight junctions. It is hypothesized that αeβ7 allows $CD8^{+}$ T cells to adhere to the E-cadherin expressed on epithelial cells which supports long term survival [447, 456, 457]. On the other hand, $\alpha e\beta 7^{+}$ $CD8^{+}$ T cells in the brain expressed more B-cell lymphoma-2 protein family (Bcl-2), a family of prosurvival proteins that inhibit cell death [458], early after infection making αeβ7 expression a key protein in $CD8^{+}$ T cell survival [435, 447]. In contrast, others reported that αeβ7 is necessary for $CD8^{+}$ T cell accumulation in the small intestine epithelium following oral infection with *L. monocytogenes* infection, but long-term survival was not dependent on this molecule [459]. Other reports state T_{RM} cells in different organs do not express αeβ7 [439, 460].

From these observations it can be concluded that while αeβ7 expression on antigen specific $CD8^+$ T cells might be strongly indicative of residence, but it is likely that many T_{RM} cells do not depend on, nor even express, αeβ7 [461].

Sphingosine-1 phosphate receptor 1(S1PR1) mediates T cell egress in lymph nodes by inducing chemotaxis to sphingosine-1- phosphate (S1P) present within efferent lymph [462].Thus, downregulation of S1P responsiveness might be one of the mechanisms for the maintenance of TRM cells [461]. S1PR1 downregulation is associated with cell surface expression of the C-type lectin CD69. It has also been shown that CD69 deficient (*$CD69^{-/-}$)* mice had reduced number of T_{RM} cells in the skin epidermis or lungs [450, 463]. In another study it was reported that transcription factor KLF2, that promotes expression of the genes encoding S1PR1, was down regulated in $CD8^+$ T cells in NLTs while forced expression of S1PR1 prevented the establishment of T_{RM} cells [464]. To conclude, the downregulation of S1PR1 and KLF2 and upregulation of CD69 might play important roles in the development and maintenance of T_{RM} cells [461].

Other mechanisms for the retention of T_{RM} cells have also been described. T-box transcription factor (TF) is known to influence the development of innate and adaptive immune system [465]. To assess the impact of T-box TF, Mackay *et al*. used a HSV skin infection model. This study showed that as virus-specific $CD8^+$ T cells progress to the stage of becoming $CD103^+$, T-box TF expression was downregulated and forced expression of T-box TF prevented formation T_{RM} cells in the skin [466]. Observations from this study also showed that there was a reciprocal downregulation of T-box and transforming growth factor (TGF)-β, which has been shown to promote the development of T_{RM} cells [456, 466]. In conclusion, the downregulation of T-box TFs is important for TGF-β mediated cytokine signaling that supports the development and maintenance of T_{RM} cells.

Other factors including $CD4^+$ T cell help, regulatory T cells (Tregs), transcription factor aryl hydrocarbon receptor have also been investigated for their role in the development and maintenance of T_{RM} cells [467-469].

1.3.2.2 Role of T_{RM} cells in bacterial and parasitic infection

Successful elimination of intracellular bacterial and parasitic pathogens requires the generation of a specific T cell response. T_{RM} cells have been reported to be involved in the elimination of these pathogens [459, 470].

It has been shown that an attenuated *Plasmodium falciparum* sporozoite vaccine was protective against controlled human malaria infection at least for 1 year, and studies to assess the immune correlates in non-human primates showed the presence of long-lived INF-γ producing $CD8^+$ T cells in the liver rather than in the blood, and these cells were regarded as T_{RM} cells [471]. An attempt to expand malaria-specific T_{RM} cells in the liver of mice showed a distinct population of $CD8^+$ T cells expressing $CD69^+$ (T_{RM} cells) following vaccination of mice using *Plasmodium berghei* radiation attenuated-sporozoites [455]. These liver T_{RM} cells induced a sterilising immunity against liver stage *P.berghei* sporozoite challenge and protected against malaria infection [455].

Intratracheal vaccination with *Mycobacterium bovis* Bacille Calmette-Guérin (BCG) vaccine resulted in infiltration of airways by T cells that expressed tissue residency markers like CD103 and CD49a. Adoptive transfer of air-way resident T cells into naïve mice confers protection against *Mycobacterium tuberculosis* challenge [472].

The role of T_{RM} cells was also investigated in infections caused by *L. monocytogenes*. CD103-expressing $CD8^+$T cells accumulated in the intestinal mucosa following oral infection of mice by *L. monocytogenes* [459]. To investigate the role of these cells in protection, mice were first treated with anti-$\alpha_4\beta_7$, to prevent migration of cells into intestinal mucosa [473]. Treatment with anti-

$\alpha_4\beta_7$ resulted in a reduced population of T_{RM} cells in the intestinal mucosa while circulating $CD8^+$ T cell population remain unaffected. Subsequent oral *L. monocytogenes* challenge of mice resulted in a high bacterial burden [459].

1.3.2.3 Role of T_{RM} cells in viral infections

The role of T_{RM} cells in viral infections was reported in the context of different viruses including influenza virus, HSV and HPV, and their protective capabilities was demonstrated in the skin, genitourinary tract and the lungs [429, 433, 447, 474-476]. Virus specific T_{RM} cells were shown to possess high affinity TCR making them highly sensitive to antigens which is required for front-line defence [441].

In a HSV skin infection model, following acute cutaneous infection with HSV, virus-specific $CD8^+$ T_{RM} cells were induced [444]. These cells were able to control secondary infection with the virus only in the skin area that was previously infected with virus indicating these cells were non-migratory cells [444]. In an attempt to induce T_{RM} cells in the skin, Mackay *et al*. transferred *in vitro* activated gBT-I T cells into C57BL/6 mice and treated one flank of the mice with the contact-sensitizing agent 2,4-dinitrofluorobenzene (DNFB) to causes non-specific inflammation that can potentially recruit virus specific T cells in to the skin [435]. The results showed a greater number of T_{RM} cells in the DNFB treated flank. Subsequent challenge with HSV showed protection only in the DNFB treated flank, that contained T_{RM} cells, while mice with only circulating $CD8^+$ T cells developed skin lesions and had higher viral titre [435].

In another study, vaccinia virus skin infection has been shown to generate $CD8^+$ T_{RM} cells in the skin [445]. To assess the role of these T_{RM} cells in infection control, a previously infected mouse was parabiotically joined with an uninfected mouse. After separation each mouse was challenged with vaccinia virus. Remarkably, despite the high frequency of T_{CM} cells in the uninfected parabiont these cells were unable to clear the infection until 26 days post infection while the infected parabiont that had T_{RM} cells in their skin completely cleared the virus in 6 days [445].

1.3.2.4 Targeting T_{RM} cells in vaccination

In the next few paragraphs the importance of targeting T_{RM} cells in vaccine development is described in the context of HCV and HIV. Viral infections such as HIV and HCV account for a significant level of morbidity and mortality across the world. As these two viral infections share common transmission routes the comorbidities are also significant and the worldwide prevalence of HIV-HCV co-infection is 2, 278, 400 people [477].

Anti-retroviral therapy (ART) and DAAs have contributed significantly to prolonging the lifespan and curing of HIV- and HCV-infected individuals respectively [478] but the annual incidence of HIV and HCV infections is still rising by millions. Furthermore, only 17 million (< 50%) people have access to ART [359] and only 20% of patients are diagnosed for HCV [7] which make meeting the UN 90-90-90 targets for HIV and WHO Sustainable Development Goals for eliminating HCV extremely challenging. Issues involving drug resistance, reactogenicity associated with life-long ART and the lack of universal access to testing and cost-subsidised therapies minimise the ability of effective anti-viral drugs to end the HIV and HCV epidemics [288]. Thus, there is an urgent need to develop effective vaccines to complement the eradication efforts of ART and DAA.

Vaccines are of great public health importance and the previous success of the smallpox and poliovirus vaccines and the most recent news release on the successful elimination of measles from Singapore and rubella from Australia, Brunei Darussalam and Macao SAR (China) (http://www.who.int/westernpacific/news/detail/31-10-2018-singapore-wipes-out-measles-australia-brunei-darussalam-and-macao-sar-%28china%29-eliminate-rubella) suggest that vaccination is a cost-effective means to eliminate HIV and HCV infections worldwide [243].

Unfortunately, designing a vaccine for these viruses has been particularly challenging because of the mutable nature of the pathogen and complexity of the immune system involved during these

infections [443]. It is known that T cell responses are vital for the control of these viruses in non-human primates and humans [136, 147, 160, 479-484].

The role of circulating memory T cells in protection from systemic infection that result accumulation of pathogens in lymphoid tissues is immense. However, the ability of these cells to contain localised infections in specific organs or tissues is limited [428]. One of the main reasons for this is the delay in T cell recruitment from the circulation providing an advantage to the pathogen to establish infection before the action of the immune system [411]. To overcome this problem vaccines that can induce localised immunity represent a potential strategy. To this T_{RM} cells play the major role in providing protection in localised tissues [485-489]. Vaccines that elicit T_{RM} cells in the liver and the mucosal areas of the genitourinary tract could potentially be the future of vaccine development against HCV and HIV respectively.

From some of the studies [413, 455] discussed in (section 1.3.2.2 and 1.3.2.3) and elsewhere [490] it is clear that T_{RM} cells play important roles in the immune response against hepatotropic pathogens suggesting that T_{RM} cells in the liver against HCV can be potential immune cells to prevent persistent HCV infection.

HIV transmission occurs mainly *via* the genitourinary tissues and intestinal epithelial region. Hence, localised immunity in these regions is necessary to prevent viral entry and transmission. There are also reports showing the induction of antigen specific T_{RM} cells following infection or vaccination with HIV vaccines [491-493]. In human rectosigmoid tissue, abundant $CD8^+$ T_{RM} cells with a robust response against HIV-1 were reported in individuals who controlled HIV-1 infection [493]. On the other hand, a recombinant influenza virus expressing HIV-1 gag protein p24 was able to induce both systemic and mucosal HIV specific $CD8^+$ T cell response in mice following intranasal vaccination [494]. An intravaginal boost with this vaccine resulted in robust and sustained immune response in the vagina [494]. A further study on the intranasal priming

followed by intravaginal boost indicated that immune cells induced by this strategy were $CD103^+$ $CD8^+$ T cells, which are presumably T_{RM} cells [491]. These cells were largely found in the vaginal epithelia and their activation by a cognate antigen in the vagina resulted in the recruitment of both innate and adaptive immune cells [491]. To complement the above studies, Zaric *et al.* reported the establishment of long lived antigen-specific T_{RM} cells in the mucosal tissues of female genitalia and respiratory tract following micro-needle array-mediated vaccination of mice with recombinant Ad5 encoding HIV-1 gag [492]. An intravaginal boost, 150 days after Ad5-gag, with CpG adjuvanted immunodominant HIV-1 CN54 $gag_{308–318}$ epitope increased the frequency of these cells [492]. These reports suggest the possibility of inducing local immunity that can act as a frontline defence against the virus.

1.3.2.5 Prime/Trap vaccination strategy to induce T_{RM} cells

It has been shown that a robust population of antigen-specific $CD8^+$ T cells can be established in the genital tract following a vaccination strategy termed prime-pull [495]. In this strategy transgenic mice were subcutaneously (SC) immunized with attenuated HSV-2 to activate HSV-2 specific $CD8^+$ T cells. Five days later chemokines CXCL9 and CXCL10 were applied topically to the vaginal cavity [495] to mediate recruitment of effector $CD8^+$ T cells to infected tissues via the chemokine receptor CXCR3 [496]. According to this study, SC immunization (prime) with attenuated HSV-2 generates a robust systemic virus-specific $CD8^+$ T-cell response that was comparable to intravaginal immunization. When the CXCL9 and CXCL10 were applied topically to the vagina (pull) robust recruitment of virus-specific $CD8^+$ T cells was observed, and these cells were able to establish a resident population [495]. One important observation from this study was that T_{RM} cells induced by the prime and pull strategy were protective against HSV challenge. This prime and pull strategy or prime-boost strategy [491] or prime-trap strategy [455] used in different studies revealed that the strategy was able to expand T_{RM} cells.

Collectively the above observations indicate that a strategy to prime antigen specific $CD8^+$ T cells and attracting these cells to a specific area of tissue or organ (liver) might be an effective way of generating an effective HCV vaccine.

1.4 Experimental Aims

The main aim of the work described in this thesis is to develop a prime-trap strategy that can result in the appearance of T_{RM} cells in the liver, that are likely to be highly protective, following ID vaccination of mice with a DNA vaccine encoding NS5B of HCV gt3a and the cytolytic protein, PRF, (pVAX-NS5B-SV40-PRF) to prime T cells followed by IV vaccination with rAAV encoding the vaccine antigen (NS5B) and eGFP (rAAV-NS5B-2A-eGFP) to trap primed T cells. The specific aims of the project are

1. To prepare and purify rAAV-NS5B-2A-eGFP
2. To identify immunodominant peptides of NS5B of gt3a HCV that can be recognized by T cells in the liver and spleen for tetramer synthesis
3. To assess CMI following prime/trap vaccination strategy
4. To characterise $CD8^+$ T cells elicited by the prime/trap vaccination strategy

2 Chapter 2: Materials and Methods

A list of reagents, list of equipment and list of kits is provided in Appendix I, II and III respectively. The formulae for bacterial and mammalian cell growth media are provided in Appendix IV and V. A list of labelling dyes and antibodies, buffers and primers is provided in Appendix VI, VII, and VIII respectively.

2.1 Bacterial strains, supplements and storage

2.1.1 Bacterial strains

2.1.1.1 *Escherichia coli* DH5α cells

Genotype: F– Φ80*lac*ZΔM15 Δ (*lac*ZYA-*arg*F) U169 *rec*A1 *end*A1*hsd*R17 (rK–, mK+) *pho*A *sup*E44 λ– *thi*-1 *gyr*A96 *rel*A1. This strain of *E. coli* was used for the propagation of DNA vaccines (pVAX-NS5B-PRF and pVAX-PRF) and p5E1VD2/8 plasmid.

2.1.1.2 SURE-2 super-competent cells

Genotype: e14-(McrA-) Δ *(mcrCB-hsdSMR-mrr) 171 endA1 gyrA96 thi-1 supE44 relA1 lac recB recJ sbcC umuC*::Tn*5* (Kanr) *uvrC* [F′ *proAB lacI*qZΔ*M15* Tn*10* (Tetr) Amy Camr}(Catalogue # 200152, Stratagene, Agilent technologies)

This strain, "Stop Unwanted Rearrangement Events" (SURE), allows the cloning of certain DNA segments that are "unclonable" in conventional *E. coli* strains. The SURE strain lacks components of the pathways that catalyse the rearrangement and deletion of non-standard secondary and tertiary structures, including cruciforms (caused by inverted repeats) and Z-DNA, that occur frequently in eukaryotic DNA and that impede the cloning of the eukaryotic DNA in conventional strains (https://www.agilent.com/cs/library/usermanuals/public/200256.pdf). Cloning of genes into pAM2AA vector and propagation of plasmid pXX6 was performed in these cells.

2.1.2 Preparation of heat competent *E. coli*

Competent DH5α *E. coli* or SURE 2 super-competent cells were produced for bacterial transformations. The bacterial cells were streaked out from a glycerol stock onto a Psi-b agar

plate containing no antibiotics, and incubated for 20 hours at 37°C. The following day a single colony was picked and grown in 10 ml of Psi-a media at 37 °C for 4 hours (until OD_{550} = 0.3). This starter culture was diluted 1:20 in 100 ml Psi-a medium and incubated at 37°C for a further 3 hours (until OD_{550} = 0.48). The bacterial culture was then chilled on ice for 5 minutes and pelleted by centrifugation at 4500 revolution per minute (rpm) for 5 minutes at 4 °C. The supernatant was removed and the bacterial cells were resuspended in 40 ml chilled TfbI solution. The cells were incubated for a further 5 minutes on ice and then centrifuged at 4500 rpm for 5 minutes at 4 °C. The supernatant was removed, the cells were resuspended in 4 ml of chilled TfbII solution and incubated for 15 minutes on ice. The cells were then aliquoted into 50 µl volumes and snap frozen in liquid nitrogen. The aliquots were stored at -80 °C until required.

2.1.3 Supplement

Ampicillin (stock solution of 100 mg/ml) or Kanamycin (stock solution 50 mg/ml) was added to Luria-Broth (LB) media at 1:1000 dilution when necessary. The final concentration of the antibiotics was 0.1 mg/ml and 0.05 mg/ml, respectively.

2.1.4 Glycerol stocks of bacteria

For long term storage of transformed bacteria, glycerol stocks were produced by adding 0.5 ml of an overnight bacterial culture in antibiotic-supplemented LB media to 0.5 ml of sterile 40% glycerol in an eppendorf tube. The glycerol stocks were stored at -80°C.

2.2 *In vitro* techniques

2.2.1 pAM2AA-eGFP plasmid

pAM2AA-eGFP was a gift from Dr. David Bowen (Centenary Institute, Sydney). This plasmid was constructed by inserting eGFP into pAM2AA plasmid which in turn was constructed by removing the *cap* and *rep* genes from the AAV genome leaving only the *cis* acting inverted terminal repeats (ITR). Flanked by the ITRs, the vector contains a liver specific enhancer and promoter region, *viz.* two ApoE enhancers and the human α-1 anti-trypsin promoter (hAAT), a

multiple cloning site (MCS) for restriction enzyme digestion and insertion, the enhanced green fluorescent protein (eGFP) reporter gene, a woodchuck hepatitis virus post-transcriptional regulatory element (WPRE), the Bovine Growth Hormone poly adenylation (BGHPolyA) site that terminates transcription and an ampicillin resistance selectable marker (Figure 2.1). The codon optimised sequence of HCV gt3a NS5B was cloned into the MCS under the control of the AopE/hAAT enhancer and promoter, upstream of the eGFP gene. Protease cleavage between NS5B and eGFP was achieved by introducing the foot and mouse disease virus 2A (FMDV2A) protease.

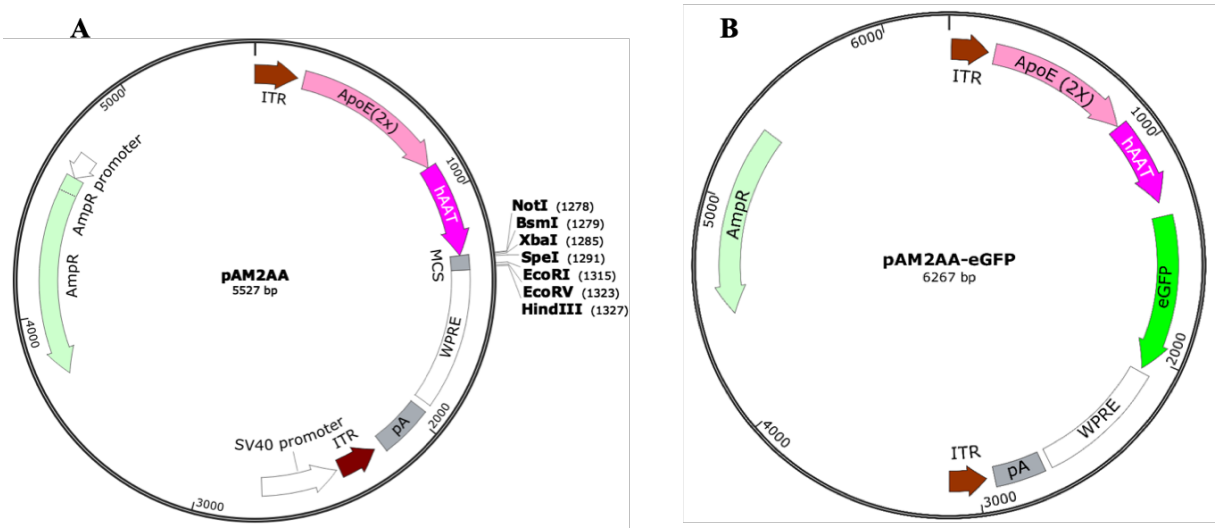

Figure 2.1 A schematic map of pAM2AA (A) and pAM2AA-eGFP (B) showing the AAV-ITRs, ApoE enhancer, hAAT promoter, multiple cloning site (MCS), WPRE, and BGH polyadenylation site (pA) (Generated using SnapGene®)

2.2.2 PCR primer design and gene amplification

Primers were designed to amplify an entire gene of interest and introduce a start codon (ATG), a stop codon and/or a Kozak sequence (GCCACC) when necessary. Primers also introduced restriction enzyme sites to allow subsequent digestion and ligation of the PCR product into a plasmid. See Appendix IX for all primer sequences.

Primer sequences were sent to Geneworks Pty Ltd or Integrated DNA Technologies (IDT) Inc. for synthesis. PCR amplification of genes of interest was performed on a Peltier PTC-200 Thermal Cycler using the Kapa High Fidelity (HiFi) Taq polymerase enzyme kit (Geneworks # KP-KK2102). Each reaction mixture contained 1X KAPA HiFi buffer, 0.3 mM of each of the dNTPs, 0.3 mM forward primer, 0.3 mM reverse primer, 10-50 ηg of template DNA and 0.5 U KAPA HiFi DNA polymerase adjusted to a final volume of 50 µl with MQ H_2O. Each reaction was performed as per the following cycling conditions (Table 2.1).

Table 2.1. Cycling conditions for PCR

Cycling	Initial cycle	x35 cycles			Final cycle
	Denaturation	Denaturation	Annealing	Extension	Extension
Temperature (^{O}C)	98	93	Tm*	72	72
Time	2 minutes	20 seconds	15 seconds	1minute/kb	5 minutes
*Annealing temperature was Tm for KapaTaq Hifi and Tm-5 for KapaTaq					

2.2.3 Gel electrophoresis and DNA purification

PCR products were analysed by gel electrophoresis on 0.8-1% w/v agarose gel in Tris-Borate EDTA (TBE) buffer (0.22M Trizma base, 180mM Boric acid, 5mM EDTA). DNA bands were visualized using GelRed (Biotium #41003) and a BioRad GelDoc imager and compared to a molecular weight standard DNA ladder (New England Biolabs NEB 100bp, 1000bp, or 2500bp) to confirm that the DNA amplicon was the correct size. The correct band size that contained the amplified gene was purified using the PureLink® Quick Gel Extraction and PCR purification

Combo Kit (Life Technologies #K3100-01). Excised gel slices that contained the correct size DNA band were dissolved in solubilisation buffer at a ratio of 1:3 and incubated at 50°C for 15 minutes. The dissolved DNA was then mixed with isopropanol to increase DNA yield. The DNA was then bound to the quick spin column by centrifugation at 13,000 rpm for 1 minute. The column was washed once with 500µl of wash buffer and centrifuged again at 13,000rpm for 1minute. DNA was eluted from the column by adding 30-50µl of elution buffer and centrifuging at 13,000rpm for 1minute.

2.2.4 Digestion and Ligation

The PCR product of the gene of interest and the plasmid backbone were digested by an appropriate restriction endonuclease (NEB) at 37ºC overnight to ensure complete digestion. The digested products were purified using PureLink® Quick Gel Extraction and PCR purification Combo Kit (Life Technologies #K3100-01) as described in section 2.2.3.

The pAM2AA vector was de-phosphorylated using Antarctic phosphatase (NEB #M0289). The phosphatase reaction mix that contained digested, purified vector, 1 U phosphatase and 1X phosphatase buffer was incubated for 20 minutes at 37°C. The phosphatase was heat inactivated at 65 °C for 15 minutes.

To ligate the digested components, the insert and vector were mixed at a ratio of 1:1, 3:1 and 5:1 keeping the final amount of DNA to 100 ηg. The mixture was incubated at 16°C overnight in the presence of T4 ligase (NEB #M0202). The ligated mixture was transformed into SURE 2 super competent *E. coli*, plated on to LB agar containing ampicillin and grown at 37°C overnight.

Colonies from positive plates were screened using colony PCR for the presence of the cloned gene and positive colonies were grown overnight in LB containing ampicillin at 37°C on a shaker. Plasmid DNA mini-prep was prepared (Section 2.2.6) and digested using appropriate restriction enzymes and analysed by agarose gel electrophoresis to confirm the presence of the gene of interest.

2.2.5 DNA Sequencing

The gene of interest in the plasmid was sequenced using a forward primer that anneals to the hAAT promoter region and a reverse primer that anneals to the 5' end of the eGFP gene. Sequencing reactions were performed using Big Dye terminator mix (IMVS) using 1.2ul of 10uM forward or reverse primer and 250ng of DNA. The BLAST nucleotide alignment tool was used to confirm that the sequence in the plasmid DNA matched the sequence of the gene of interest.

2.2.6 Plasmid DNA amplification and purification

Briefly, transformed *E. coli* cells were grown for 16 hours at 37 °C on a shaker in antibiotic-supplemented LB media. The bacteria were pelleted by centrifugation and resuspended, then the bacteria were lysed with lysis buffer. The lysis buffer was neutralised by neutralisation buffer. All the buffers were provided in the kits, described below.

The miniprep was prepared using PureLink® plasmid miniprep kit (ThermoFisher Scientific). Bacterial debris was removed by centrifugation at 12000 rpm for 10 minutes and the supernatant was added to the silica spin column to bind and purify the DNA. The column was washed with the buffer provided and the DNA was eluted in the elution buffer.

The endotoxin-free DNA mega-preparation was prepared using Qiagen® Mega prep kit (Qiagen #12191). In this case bacterial debris was removed using a vacuum by passing the bacterial lysate through a filter provided in the kit. The flow-through was added to a gravity-flow column to bind DNA. The column was washed, the DNA was eluted in elution buffer and then precipitated using isopropanol. The DNA was pelleted by centrifugation at 4000 rpm for 90 minutes and washed with 70 % ethanol. The DNA pellet was then air-dried and dissolved in endotoxin free TE-buffer. The concentration of DNA was determined using Nanodrop2000 spectrophotometer (ThermoFisher Scientific) and DNA was considered as "pure" when the absorbance (A) ratio at A 260/280 was ~ 1.8.

2.2.7 Cell culture and transfection

2.2.7.1 Cell culture

Human Embryonic Kidney (HEK 293T) cells and HT1080 cells were cultured in Dulbecco's modified Eagles medium (DMEM) supplemented with 10% heat inactivated foetal calf serum (FCS) and 1% penicillin/streptomycin and incubated at 37°C in 5% CO_2. Cell cultures were routinely grown in a T75 cell culture flask and passaged at 80-90% confluency.

2.2.7.2 Cell storage and retrieval

For cell storage, cells were trypsinised, pelleted and re-suspended in 1 ml of 10% DMSO in FCS and transferred to a cryovial. The cells were then transferred to a freezing container (Nalgene) and stored at -80°C overnight then transferred to liquid nitrogen. To retrieve cells from liquid nitrogen, vials of cells were thawed in a 37°C water bath and then transferred to a 10 ml falcon tube; 9 ml of pre-warmed media was then added, and the cells were pelleted by centrifugation at 300x *g* for 5 minutes. The supernatant was removed, the cells were re-suspended in fresh media and plated.

2.2.7.3 Transient transfection

Appropriate numbers of cells were seeded on to cell culture plates or flasks and allowed to adhere overnight resulting in approximately 60-70% cell confluency on the day of transfection. Lipofectamine® LTX with Plus™ Reagent from Invitrogen (Thermo Fisher Scientific #15338100) was used to transfect cells in 96, 24 and 6 well cell culture plates. Briefly DNA, diluted with Opti-MEM, was mixed with plus reagent (1µg DNA with 1µl of plus reagent) and incubated for 5 minutes at room temperature. LTX diluted with Opti-MEM was added to the DNA-plus reagent mixture in a 1:1 ratio, incubated for 5 minutes at room temperature and then transferred to the wells. A control well transfected with DNA encoding the reporter gene eGFP was used to confirm transfection efficiency. The transfected cells were incubated for 48-72 hours

at 37°C in 5% CO_2 and protein expression was assessed by flow cytometry, immunofluorescence staining or direct microscopic examination

2.2.8 Immunofluorescence staining

Forty-eight hours post-transfection with DNA, cells were fixed with 4% paraformaldehyde for 20 minutes, permeabilised with methanol at -20°C and then blocked with 2.5% Bovine serum albumin (BSA) (Sigma-Aldrich) containing 0.3% Triton X-100 (Sigma-Aldrich) in phosphate buffered saline (PBS) prior to the addition of the primary antibody. HCV gt3a patient pooled serum, representing the primary antibody, was diluted 1 in 300 in 1% BSA, 0.3% Triton X-100 in PBS, added to the cells and incubated for 3 days at 4°C. After washing, the secondary antibody, goat anti-human Alexa 555 (Life Technologies), was added to the cells and incubated for 2 hours at 37°C then washed. The cells were then stained with diamidino phenylindole (DAPI) (Life Technologies) and examined with a Zeiss LSM-700 fluorescent microscope.

2.2.9 rAAV-NS5B-2A-GFP production

2.2.9.1 Preparation of HEK293 T cells

HEK 293 T cells were seeded in T75 tissue culture flasks at a density of $6x10^6$ cells per flask and allowed to adhere overnight resulting in approximately 80-90% cell confluency on the day of transfection.

2.2.9.2 Preparation of polyethyleneimine (PEI)

Ten mg of linear PEI was dissolved in 1ml of PBS (without Ca^{2+}/Mg^{2+}) by heating at 80°C. Once completely dissolved, it was diluted to 1mg/ml (working solution) with PBS. The working solution was filter sterilized using a 0.2µm filter and used immediately [497, 498]. Fresh PEI was prepared whenever needed for transfection.

2.2.9.3 Triple transfection

rAAV-NS5B-2A-GFP was packaged following triple transfection using PEI as described elsewhere [497]. All plasmid concentrations were adjusted to 1 µg/µl in TE buffer before mixing. The plasmids were mixed at a 3:1:1 ratio of pXX6:pAM2AA-NS5B-2A-eGFP: p5E1VD2/8, *i.e.,* 25.2 µg of pXX6, 8.4 µg of pAM2AA-NS5B-2A-GFP and 8.4 µg of p5E1VD2/8. PEI was added to the DNA mixture at a 3:1 ratio. Accordingly, 126µl of 1mg/ml PEI was added to 42µg total DNA. The transfection mixture was adjusted to a total volume of 1.5 ml DMEM and was vortexed for a few seconds then incubated at room temperature for 15-20 minutes [497, 498]. The mixture was then added to a T75 flask. The flasks were returned to the incubator for 72 hours at 37°C, 5% CO_2.

2.2.9.4 Virus harvest and purification

rAAV was harvested and purified using a modified polyethylene glycol- (PEG) 8000/sodium chloride (NaCl) precipitation method described by Guo *et al.,* 2012 [498]. Briefly, the cells were removed by scraping, and the culture media was centrifuged at 3000 × *g* for 10 minutes to pellet the cells and cell debris. The cells were pooled into one 50 ml conical tube then lysed with 5 ml of lysis buffer (50 mM Tris–Cl; 150 mM NaCl; 2 mM $MgCl_2$, pH 8.0). AAV particles were released from the cells with three freeze/thaw cycles between dry ice-ethanol and a 37°C water bath. Fifty U/ml benzonase and 10 U/ml RNase were added to the solution and incubated for 1hour at 37°C. To remove the cell debris, the cells were centrifuged at 2500 × g for 10 minutes and the supernatant was harvested.

Forty percent PE-8000 (Sigma-Aldrich), 2.5 N NaCl, was added to the supernatant to a final concentration of 8%, 0.5 N respectively. The solution was then incubated overnight at 4°C on a mixer and centrifuged at 12,000 rpm for 1hour. The supernatant was discarded and the pellet containing the virus was resuspended in a minimal volume of 50mM HEPES buffer (pH=8).

The crude rAAV solution was treated with an equal volume of chloroform and vigorously vortexed for 2 minutes at room temperature. The solution was centrifuged at 370 x *g* using a desktop centrifuge for 5 minutes, and the supernatant was allowed to stand at room temperature for 30 minutes to evaporate the chloroform. The virus-containing solution was filtered through a 0.2µm filter, transferred to an Amicon ultra centrifugal filter (100K MWCO, Amicon) device and concentrated by centrifuging at 3000 rpm for 10 minutes. The concentrated virus was dispensed into 100µl aliquots and stored at -80°C until further use.

2.2.9.5 SDS-polyacrylamide gel electrophoresis (SDS-PAGE)

The purity of rAAV-NS5B-GFP was evaluated by electrophoresis in 10% SDS-PAGE as described elsewhere [499, 500]. Five µl of the virus stock was mixed with an equal volume of 2x loading buffer and incubated at 95°C for 5 minutes. The sample was loaded to the gel and electrophoresed at 200 V. The gel was immersed and incubated twice in a pre-staining solution (50% methanol and 10% acetic acid) and stained with 0.25% (*w*/*v*) Coomassie Brilliant Blue R250 dissolved in a solution containing 50% methanol (*v*/*v*) and 10% glacial acid (*v*/*v*), and de-stained (40% methanol and 8% acetic acid) until clear bands with low background were shown.

2.2.9.6 Titration of rAAV-NS5B-2A-GFP using quantitative real time-PCR

The yield of virus following purification was determined by quantitative real time PCR using the AAVpro® titration kit for real time PCR version 2 (TaKaRa, Catalogue # 6233). In this method, PCR amplification is monitored in real time using a fluorescent DNA intercalator. The reagent in this kit, SYBR® Premix Ex Taq ™ II, includes a hot start PCR enzyme and SYBR Green I for fluorescent detection. The quantification was based on the virus ITRs.

Briefly 2µl of the purified virus was treated with DNase at 37°C for 20 minutes in a 20 µl final volume. The DNase was inactivated by incubating at 95°C for 10 minutes. Then, 20 µl of AAV lysis buffer (provided with the kit) was added to the sample and incubated at 70°C for 15 minutes

to release the viral genome. The released viral genome was diluted 50-fold using EASY dilution buffer (provided with the kit) and 5 µl of the diluted sample was used as a template for real time PCR.

The reaction mixture was prepared as follows in a final volume of 25µl; 5 µl of template, 12.5 µl of SYBR® Premix Ex Taq II (2X conc.), 0.5 µl 50X Primer mix (provided with the kit) and 7 µl of dH_2O. The PCR was run in a 3-step cycling condition with one cycle of initial denaturation at 95°C for 2 minutes followed by annealing for 5 seconds at 95°C (35 cycles) and elongation for 30 seconds at 60°C. A positive control (a plasmid DNA that contained the AAV ITR, provided with the kit) at different concentration ranges ($2x10^2$ to $2x10^7$copies/µl) was run with the samples to generate a standard curve.

2.2.9.7 *In vitro* transduction of HT1080 Cells with rAAV-NS5B-2A-GFP

HT1080 cells were seeded on to a 96 well cell culture plate at a density of $2.5x10^4$ cells per well in 100 µl of DMEM (10% FCS and 1% P/S). On the next day the virus was thawed from -80°C, mixed with DMEM (2% FCS and 1% P/S) and the virus-containing medium was used to replace the growth medium. A final concentration of 5 µM Hoechst 33342 (Invitrogen) was used as a transduction inducing agent [501, 502].

2.2.9.8 RT-PCR for the detection of packaged viral genome

2.2.9.8.1 RNA extraction

HT1080 cells were transduced with rAAV-NS5B-2A-GFP as described above and RNA was extracted using QIAGEN RNeasy mini kit as per the manufacturer's instructions. Briefly, cells were homogenized with a lysis buffer followed by ethanol (70%) precipitation. The sample was passed through a RNeasy spin column after which it was washed and eluted using RNase free water. The concentration of the RNA was measured using a Nano-drop spectrophotometer and used for cDNA synthesis.

2.2.9.8.2 cDNA synthesis

RNA was converted to cDNA using the SuperScript™ IV VILO™ Master Mix (Invitrogen) following the manufacturer's instructions. Briefly, 500 ηg of RNA template was digested with Genomic DNA wipeout at 42°C for 2 minutes in a final volume of 10 µl. Next, 4µl of SuperScript™ IV VILO™ Master Mix were added and the final volume was adjusted to 20µl using nuclease free water. The master mix contained reverse transcriptase (RT), a proprietary recombinant RNase inhibitor, helper proteins, stabilizer proteins, oligo (dT)18, random hexamer primers, $MgCl_2$ and dNTPs. The mixture was transferred to a thermal cycler and reverse transcription was performed under the following conditions; annealing at 25°C for 10 minutes, reverse transcription at 50°C for 10 minutes and enzyme inactivation at 85°C for 5 minutes. Controls of no RNA and no RT were included.

2.2.9.8.3 PCR

Using the cDNA as a template, the PCR was performed to detect NS5B and eGFP sequences. Multiple primers that can amplify a sequence of not more than 400bp long were designed. These primers encompass the region of NS5B and eGFP in the rAAV genome sequence. A house keeping gene GAPDH was included as a positive control for transcription. The reaction mix (total volume of 20 µl with RNase-free MilliQ water, 2.5 mM $MgCl_2$, 1X QuantiFast SYBR Green PCR Master mix, 1 µl cDNA, 1 µM of the forward primer and 1 µM reverse primers) was subjected to a 3-step cycling program with initial denaturation at 95°C for 2 minutes, followed by annealing at 95 °C for 5 seconds and elongation (fluorescent detection) at 60 °C for 30 seconds.

2.2.9.9 Fluorescent Target Array (FTA)

2.2.9.9.1 FTA cell preparation

The use of FTA, a technology where autologous spleenocytes from naïve mice are fluorescently bar coded and transferred to vaccinated mice, to assess T cell functionality *in vivo* was previously described elsewhere [503, 504]. Briefly, splenocytes from age and sex matched naïve mice were

collected and pooled. The cells were counted and evenly distributed into 2 ml aliquots in R-5 (RPMI-1640 (Invitrogen), 5% FCS, 25 mM HEPES, 1 mM Sodium Pyruvate, 1x 2mE, 1% Pen Strep). The cells were then stained with different concentrations, ranging from 0.97 mM-10 mM, of cell trace violet (CTV, Lot # 1753289, Eugene) for 5 minutes at room temperature and washed once in 10 ml of R-5. Cells from each tube were then equally split into up to 4 aliquots and labelled with 0.08 mM-2.7 mM of carboxy fluorescein succinimidyl ester (CFSE, Cat # C34554, Life Technologies) in a final volume of 1 ml of R-5 for 5 minutes at room temperature. After washing the cells once, the cells were pulsed with 0.001-10 μg/ml of MHC-I or MHC-II binding peptide epitopes for 4 hours at 37°C. The cells were sedimented and washed with R-5 and pooled into two 2 ml aliquots. Pooled cells were labelled with either 2.7 mM or10 mM cell proliferation dye (CPD, Lot # E15450-106, eBioscience Inc.).

2.2.9.9.2 Peptide formulations

To assess NS5B-specific T cell responses NS5B peptides were used to stimulate splenocytes collected from naïve mice. The peptides were obtained through BEI Resources, NIAID, NIH: Peptide Array, Hepatitis C virus, K3a/650, NS5B protein. The peptides were 14- to 19-mer with 11 or 12 amino acid overlaps. Individual peptides were dissolved in 50μL 100% DMSO to a stock concentration of 20 mg/ml. Individual peptides were then mixed into pools of 30 peptides and diluted with RPMI (1% Pen/Strep) to a final concentration of 100ug/ml.

2.2.10 Epitope prediction and selection

Peptide prediction and selection was performed by Dr. Preston Leung, at the Viral Immunology Systems Program (VISP), The Kirby Institute, UNSW Sydney. Peptide sequences ranging from 14 to 19 amino acids from the HCV gt3a NS5B protein were used as input data for epitope prediction using IEDB MHC Class I epitope prediction algorithm (available at www.iedb.org). H2-kD was selected as the parameter for HLA type and epitope prediction length was restricted to 9 amino acids. *IEDB Recommended* approach was the algorithm selected to perform the

prediction. The result of this prediction was downloaded in *.csv* format. These data were then put through an in-house script to match with epitopes that were experimentally validated with strong immune response. The epitopes which matched the experimentally validated epitopes and had high prediction score (scores closer to 0.0 indicates a better predicted epitope) were selected for tetramer synthesis.

2.2.10.1 Antibody labelling of cells

Murine lymphocytes isolated from the liver and spleen were stained with a cocktail of different antibodies. First the cells were stained with fixable viability dye (FV620, Cat # 564996, BD Bioscience) diluted 1:500 for 20 minutes at room temperature in the dark. Cells were then washed and stained with a NS5B tetramer-APC (Bimolecular Research Facility, The John Curtin School of Medical Research, Canberra) diluted 1:50 for 45 minutes in the dark. The cells were then washed twice with PBS and labelled with a cocktail of antibodies including anti-CD44 FITC (Cat # 103006, Biologened) diluted 1:50, ant-CD11a BV510 (Cat # 563669, BD Bioscience) diluted 1:50, anti-CXCR3 BV421 (Cat # 562937, BD Bioscience) diluted 1:100, anti-CD8a AF780 (Lot # 4299472, eBioscience Inc.) diluted, anti-CD69 PE-Cy7 (Cat # 552879, BD Bioscience) diluted 1:100 and anti-CD62L PE (Cat # 553151, BD Bioscience) diluted 1:100. The fluorochromes conjugated to the antibodies in the cocktail include: phycoerythrin (PE) Cyanine (Cy) 7 or PE-Cy7 (CD69), APC-efluor® 780 (CD8), PE (CD62L), Brilliant Violet 421 (CXCR3) and Brilliant Violet 510 (CD11a).

2.2.10.2 Flow cytometry

Following staining of lymphocytes isolated from the liver and spleen, cells were analysed immediately on a BD FACSCanto II Flow Cytometer and the results were analysed using FlowJo software. Autofluorescence from cells was controlled by including unstained cell control and dead cells were discriminated from live cells using a FV620 staining. Compensation controls were run for each of the fluorochromes to correct for spectral overlap. When necessary,

Fluorescence minus one (FMO) controls were run to control data spread due to multiple fluorochromes.

2.3 *In vivo* techniques

2.3.1 Mice

Mice used in vaccination experiments, described in Chapters 4 and 5, were female BALB/c mice bred in specific pathogen free conditions at the University of Adelaide Laboratory Animal Services and housed at the Queen Elizabeth Hospital animal facility in PC2 compliant conditions. The mice were aged 6-8 weeks and weighed at least 16 grams at the start of experiments. The number of mice in each group was 7. Mice were weighed once weekly and clinical records were taken every day. C57BL/6 mice were used to titrate rAAV-NS5B-2A-eGFP.

2.3.2 Anaesthetic

For all procedures, mice were anesthetized by isofluorane provided by the animal facility.

2.3.3 Intradermal (ID) vaccination

Intradermal (ID) injection was used to deliver plasmid DNA vaccines to the dermis of the mice. Mice were anaesthetized, and the ear was swabbed with alcohol. An insulin syringe was used to inject the vaccine in a volume of 40 µl PBS; 20µl was delivered to each ear. The needle was inserted bevel side up so that the needle head was visible beneath the skin and vaccine was injected to form a bleb. The ears were observed for any inflammation or tissue damage post vaccination.

2.3.4 Intravenous (IV) tail vein injection

The mice were restrained and the tail vein was dilated by warming the tail with a heat lamp. The mice were injected with rAAV-NS5B-2A-GFP or PBS (in case of control groups) or FTA cells in a final volume of 200ul using an insulin syringe.

2.3.5 *In vivo* transduction of mouse hepatocytes

In vivo transduction of mouse hepatocytes with rAAV-NS5B-2A-eGFP was conducted by Dr. Kieran English at David Bowen's laboratory, the Centenary Institute Sydney. Briefly, 8 weeks old male C57BL/6 mice were IV injected with different doses of rAAV-NS5B-2A-GFP or PBS. Seven days post injection hepatocytes were isolated by retrograde perfusion of the liver through the inferior vena cava using 25mL Hank's balanced salt solution (HBSS). Infusion was started using HBSS supplemented with 0.5 mM EDTA followed by HBSS and completed using HBSS supplemented with 5mM CaCl and 0.05% Collagenase IV.

Following perfusion, the gall bladder was removed and discarded, the liver was removed and placed in a petri dish containing RPMI supplemented with 2% FCS where hepatocytes were separated from the liver by scraping with the back of a scalpel blade. The hepatocyte solution was then placed into a 50 ml falcon tube, then centrifuged at 500rpm for 5 minutes to pellet the cells and the supernatant was discarded. The hepatocytes were resuspended in 10 ml PBS and 6 ml of isotonic Percoll was added. The Percoll/hepatocyte solution was then centrifuged at 2000rpm for 10 minutes (Percoll allows live hepatocytes to form a pellet while dead hepatocytes float). The supernatant was discarded, and the hepatocyte pellet was resuspended in 10 ml FACS wash and stained with DAPI for flow cytometry.

Flow cytometry was carried out using the FACS Canto II (Becton Dickinson, North Ryde, NSW, Australia), and data were acquired using BD FACSDiva software (Becton Dickinson, North Ryde, NSW, Australia). Flow cytometry data were analysed using Flowjo software (Tree Star Incorporates, Ashland, OR, USA) version 9.8.3 for Mac OSX 10.10.2.

2.3.6 Spleen and Liver collection

2.3.6.1 Spleen collection

The spleen was removed from the left side of the abdomen using forceps and passed through a 70 μm cell strainer (BD #352350) using a 2 ml syringe plunger as a pestle. The cells were washed in 20 ml R-5 media and resuspended in 500 μl red blood cell lysis buffer (Sigma #R7757) for 45 seconds at room temperature to deplete red blood cells. The cells were then washed twice in 20 ml of R-5, resuspended in 2 ml of R-10 and cell numbers and viability assessed by trypan blue staining. The cells were then stained and analysed by flow cytometry.

2.3.6.2 Liver collection

The liver was harvested for the analysis of lymphocytes, but the abundant hepatocytes needed to be removed. The liver was perfused with 20 ml of PBS via the portal vein before it was removed from the animals. After removal it was homogenized by chopping in HBSS (3% FCS, 1% Pen/strep) using surgical scissors and passed through 70 μm cell strainer. The cells were then pelleted by centrifugation at 400 *x g* for 10 minutes. The cells were resuspended in 30% isotonic Percoll in HBSS and centrifuged at 500 *x g* for 20 minutes with no brake to allow the hepatocytes to float while lymphocytes and red blood cells were sedimented. The top layer was carefully removed using a Pasteur pipette and the lymphocytes in the pellet were washed twice with HBSS (3% FCS). One ml of RBC lysis buffer was added to the lymphocytes and incubated for 5 minutes at room temperature. Following RBC depletion, the lymphocytes were washed in HBSS (3% FCS) and resuspended in R-10. The cells were counted and stained for flow cytometry analysis.

2.4 Sample size

Based on earlier works [286-288], the study is powered to detect a difference in groups of 135 units at the 5% alpha level with 80% statistical power. Assuming unequal variance –standards deviations were found to be 38 and 100 units –a sample of 7 animals per group is required.

2.5 Statistical analyses

GraphPad Prism 6 software was used to construct the graphs presented in this study. All statistical analyses were performed using the IBM SPSS Statistics software (version 24). Data distribution were checked for normality using the Shapiro-Wilk test and normally distributed data were subjected to a parametric Levene's test to test for homogeneity of variance. For normally distributed and homoscedastic data, one-way ANOVA with Tukey's multiple comparison test was used to determine the statistical significance between comparisons. For all heteroscedastic data sets, Welch ANOVA with Games-Howell post-hoc was used to determine the statistical significance between comparisons. For non-normally distributed data a Kruskal-Wallis H test was used to determine the statistical significance of the data.

3 Chapter 3: Production of rAAV encoding HCV NS5B and GFP

3.1 Introduction

rAAV vectors have gained increased popularity in the field of gene therapy and vaccine development. Safe clinical outcomes and availability of different viral serotypes coupled with relatively sustained gene expression made them efficient options [304, 505]. AAV-based vaccines were tested against different infectious diseases [506], including HIV [507, 508], HPV [509, 510] and influenza virus [511]. Previously, an AAV-based malaria vaccine was shown to induce long-term antigen-specific antibody responses but was not protective from *P. yoelii* infection [512]. However, more recently a rAAV-based vaccine boosted the immune response from radiation-attenuated sporozoites and resulted in effective immune clearance of *P. berghei* following sporozoite challenge [455]. As both malaria parasites and HCV affect the liver, this chapter aimed to investigate the role of rAAV-based vaccines against HCV. To achieve this aim, rAAV encoding HCV gt3a NS5B and GFP (rAAV-NS5B-2A-eGFP) was required.

Several different approaches can be used to produce rAAV including the development of HEK 293 suspension cell lines that can grow in serum-free conditions, the baculovirus expression vector system (BEVS) utilizing *Spodoptera frugiperda* (*Sf9*) cells and the dual recombinant HSV (rHSV) infection system [513]. These different approaches share common factors, requiring the AAV non-structural proteins, the AAV structural proteins, and a set of helper-virus gene products and cellular factors necessary for macromolecular synthesis [405]. Yield inconsistency from the BEV system due to passage-dependent loss of function in the baculovirus helper [400] and the labour intensive and time consuming nature of the rHSV system [514-516] made triple transfection of HEK293 T cells the most common method to produce rAAV.

The triple transfection method uses the AAV *cis*- and *trans*-plasmids (ITR-gene of interest-ITR), along with a helper plasmid (pXX6) providing the adenoviral gene products necessary for replication and packaging, and a plasmid that encodes the Rep and Cap genes of AAV [304, 517].

Following transient transfection of HEK 293 T cells, the nascent virus is generally purified by ultrahigh speed density gradient centrifugation that involves either CsCl or Iodixanol (Optiprep); the latter results in a high virus titre [498]. However, the ultrahigh speed density gradient centrifugation method is time consuming and labour intensive [518]. A simpler method of rAAV purification that does not require ultracentrifugation was described by Guo *et al*. 2012 [498]. Briefly, transfected cells were freeze-thawed to release the virus, the virus was precipitated using PEG/NaCl and cellular proteins were removed using chloroform [498].

Thus, the aim of this chapter was to synthesize rAAV-NS5B-2A-eGFP using triple transfection of HEK293 T cells followed by PEG/NaCl precipitation to purify the virus.

3.2 Aims

The main aim of this chapter was to prepare and purify rAAV encoding gt3a HCV NS5B

Specific aims of this chapter were to:

1. Prepare and purify rAAV-NS5B-2A-GFP
2. Determine the titre of the virus that can transduce 10-25% of mouse hepatocytes *in vivo*

3.3 Results

3.3.1 Prepare and purify rAAV-NS5B-2A-GFP

The production of rAAV-NS5B-2A-eGFP requires three plasmids; i) pAM2AA-NS5B-2A-eGFP (containing the genes of interest (NS5B-2A-eGFP) flanked by the ITRs of AAV-2), ii) p5E1VD2/8 (containing the *cap* gene from AAV-8 and the *rep*-gene from AAV-2) and iii) pXX6 (containing Ad genes E2a, E4Orf6, vaRNA).

3.3.1.1 Insertion of FMDV2A and gt3a HCV NS5B into pAM2AA-eGFP

The construction of pAM2AA-NS5B-2A-eGFP was generated by including a PCR product comprised of the FMDV 2A sequence (2A) immediately upstream of eGFP and is described below.

The genes for HCV gt3a NS5B and eGFP were inserted into pAM2AA (described in 2.2.1) to ensure that protein expression was driven by the hAAT promoter. To ensure expression of NS5B and eGFP as individual proteins the sequence which encodes the 2A protease was inserted between the genes that encode the two proteins.

The 55bp sequence that encodes 2A was added as an overhang to a forward primer that was specific to eGFP. PCR amplification of eGFP, from pAM2AA-eGFP, using this forward primer and a reverse primer specifically binding to eGFP resulted in 2A-eGFP. The vector was then digested with the restriction enzymes EcoRI and HindIII to remove eGFP and the resultant product was then treated with Antarctic phosphatase to avoid religation of the linearised DNA. The 2A-eGFP PCR product was ligated into pAM2AA as described in section 2.2.4 (Figure 3.1). Following transformation of SURE2 super-competent *E. coli,* random colonies were screened using forward and reverse primers that bind to the hAAT promoter and eGFP. Introduction of the 2A sequence was confirmed by sequencing. In order to insert NS5B, the sequence was PCR amplified using primers that contained NotI and HindIII restriction enzyme sites in the forward and reverse primers respectively. The amplified NS5B product and pAM2AA-2A-eGFP were then digested with NotI and HindIII. The insert was ligated to the linearised, Antarctic phosphatase-treated pAM2AA-2A-GFP (Figure 3.2).

All the PCR and digested products were analysed by 0.8-1% agarose gel electrophoresis to confirm the DNA amplicons and to confirm that digested products were of the correct size before successive purification (Figure 3.3).

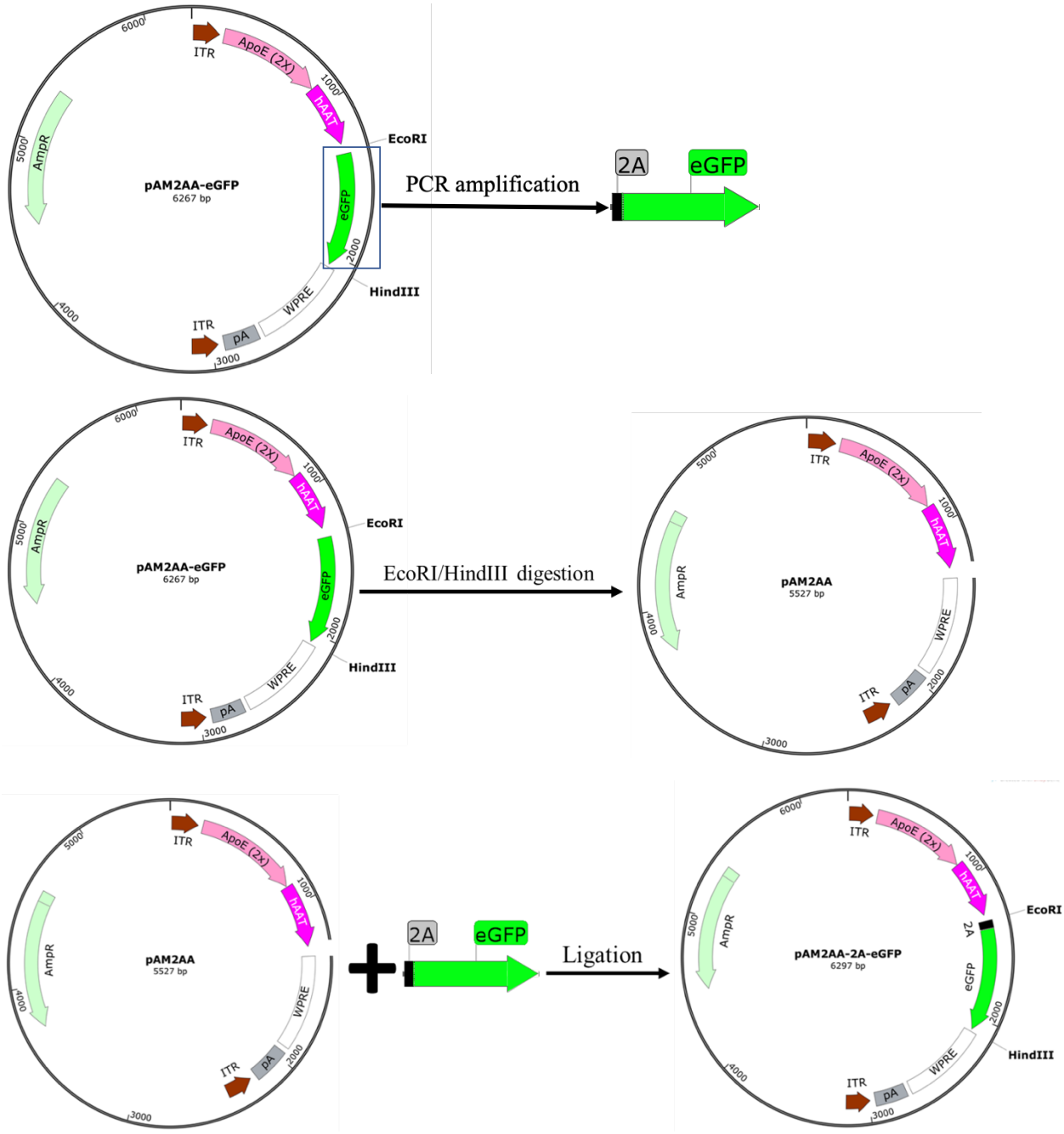

Figure 3.1: Introduction of the 2A sequence upstream of eGFP. Primers to amplify eGFP were designed by including an EcoRI and the 2A sequence overhang in the forward primer and a HindIII overhang in the reverse primer. PCR amplification using these primers resulted in 2A-eGFP. Both the PCR product and pAM2AA-eGFP were digested with EcoRI and HindIII restriction enzymes. The digested products were ligated overnight at 16°C in the presence of T4 ligase enzyme and SURE 2 *E. coli* cells were transformed with the ligation mix. Colonies were screened by colony PCR and confirmed by restriction enzyme digestion and sequencing.

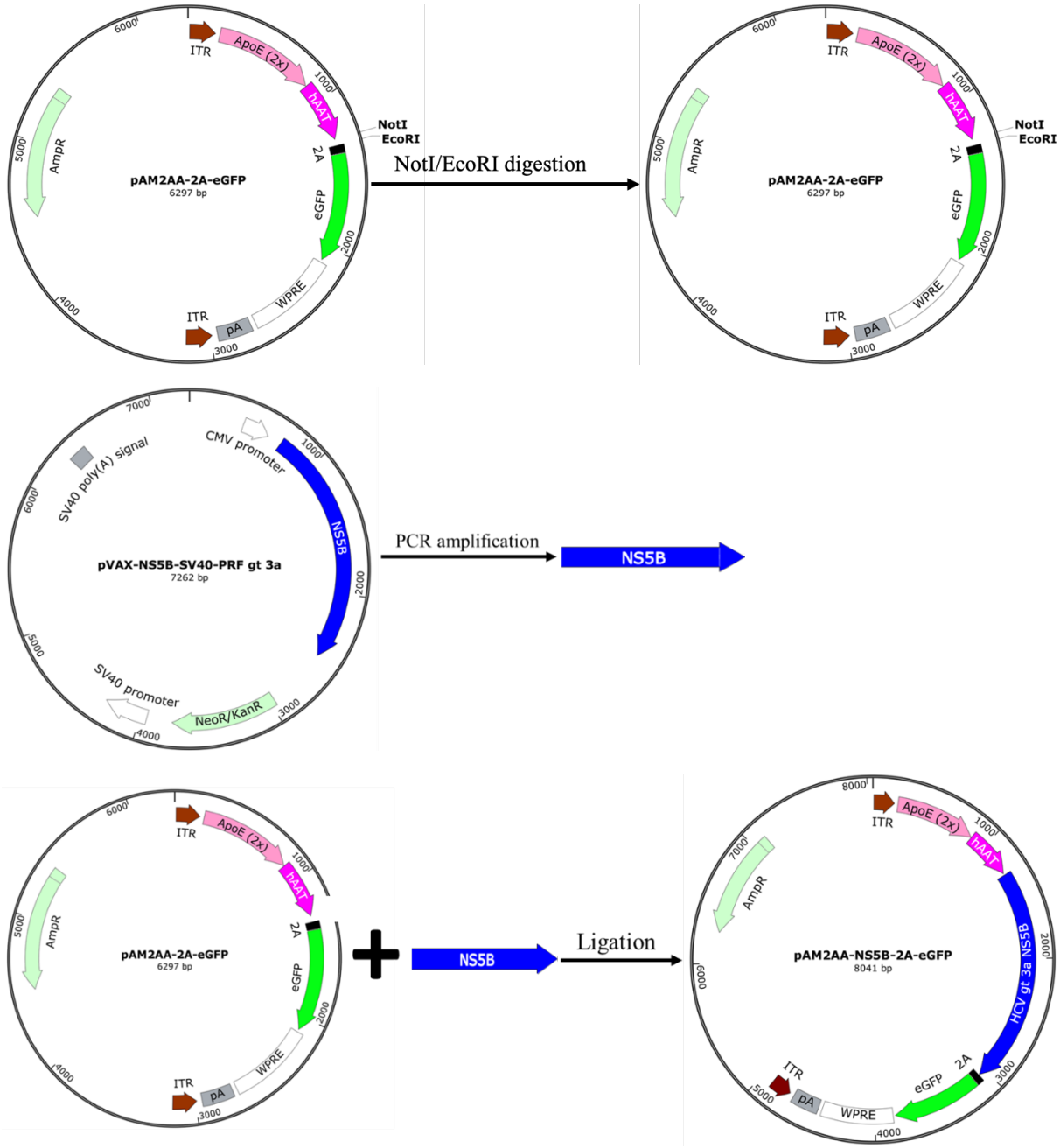

Figure 3.2: NS5B cloning in pAM2AA-2A-eGFP. Primers to amplify NS5B were designed by including NotI and EcoRI restriction enzyme sites in the forward and reverse primers, respectively. Both the PCR product and pAM2AA-2A-eGFP were digested with NotI and EcoRI enzymes. Ligation, transformation and screening of colonies were performed as described above in the legend to figure 3.1.

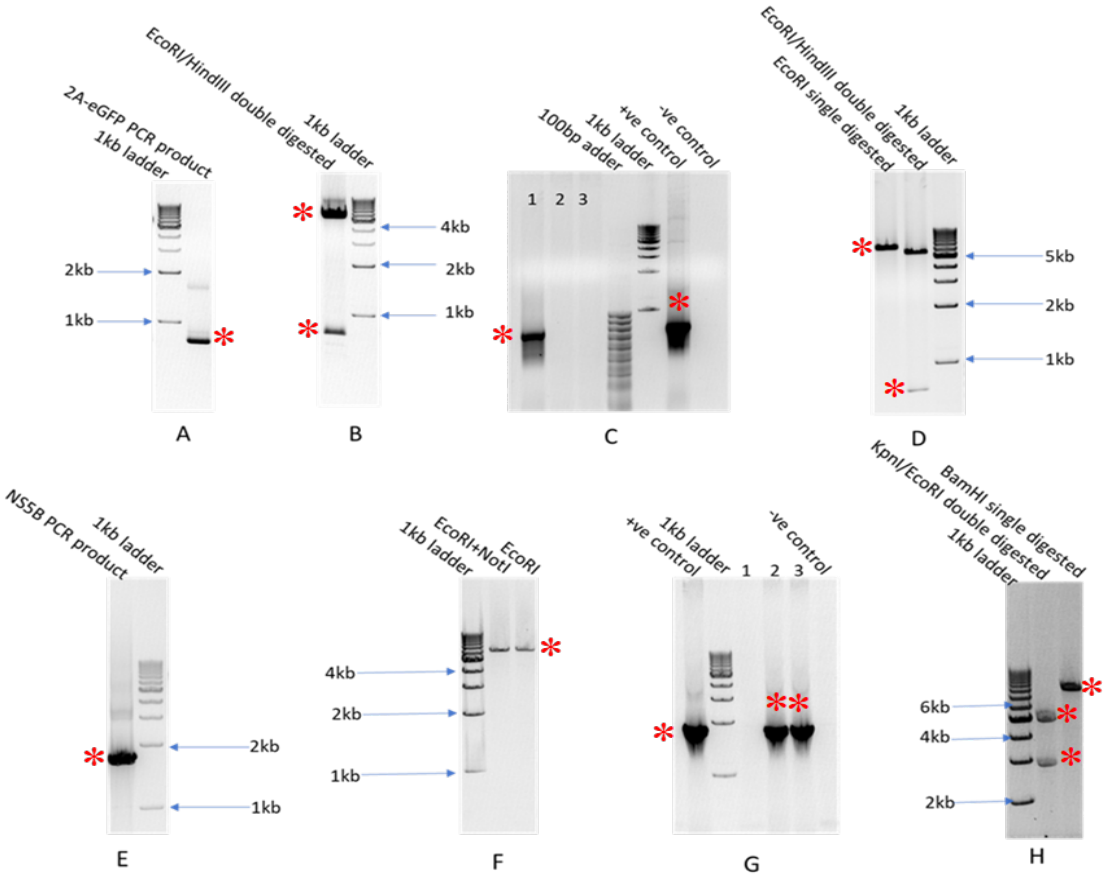

Figure 3.3: Gel photographs taken in the process of cloning NS5B-2A into the pAM2AA-GFP vector. A) PCR amplification of eGFP by including 2A sequence as a forward primer overhang. B) Digestion of pAM2AA-eGFP to remove eGFP. C) Random colonies, tracks 1, 2 & 3, were picked from agar plates and screened with colony PCR to detect positive clones. D) Confirmatory digestion of pAM2AA-2A-eGFP mini-prep. (EcoRI single digest = 6297bp; HindIII/EcoRI double digest = 5514bp + 783bp) E) PCR amplified product of HCV gt3a NS5B. F) Digestion of pAM2AA-2A-eGFP using Not I/EcoRI double digestion. G) Random colonies, tracks 1, 2 & 3, were picked from agar plates and screened by colony PCR to detect positive clone. H) Confirmatory digestion of pAM2AA-NS5B-2A-eGFP mini-prep (BamHI single digestion= 8041; KpnI /EcoRI double digestion = 2871bp +5170bp). (* indicates expected band sizes).

3.3.1.2 Protein expression from pAM2AA-NS5B-2A-eGFP

3.3.1.2.1 eGFP expression

The above sections reported the construction of pAM2AA-NS5B-2A-eGFP but it is necessary to ensure that the encoded proteins were expressed. Initially, the level of eGFP expression was assessed in HEK293 T cells transfected with pAM2AA-NS5B-2A-eGFP. The transfected cells were incubated for 48 hours and then examined by fluorescence microscopy. No background fluorescence was detected in cells that were left untransfected as a negative control. The intensity of eGFP expression was lower than that of the positive control pVAX-eGFP most likely attributed to the strong CMV promoter in pVAX as compared to hAAT in the pAM2AA vector. It has been shown that the alpha-1 antitrypsin promoter was able to result in transgene expression in 40% of the cells relative to the CMV promoter [519]. However, the experiment confirmed that hAAT was capable of directing expression of the inserted sequences (Figure 3.4) from the construct.

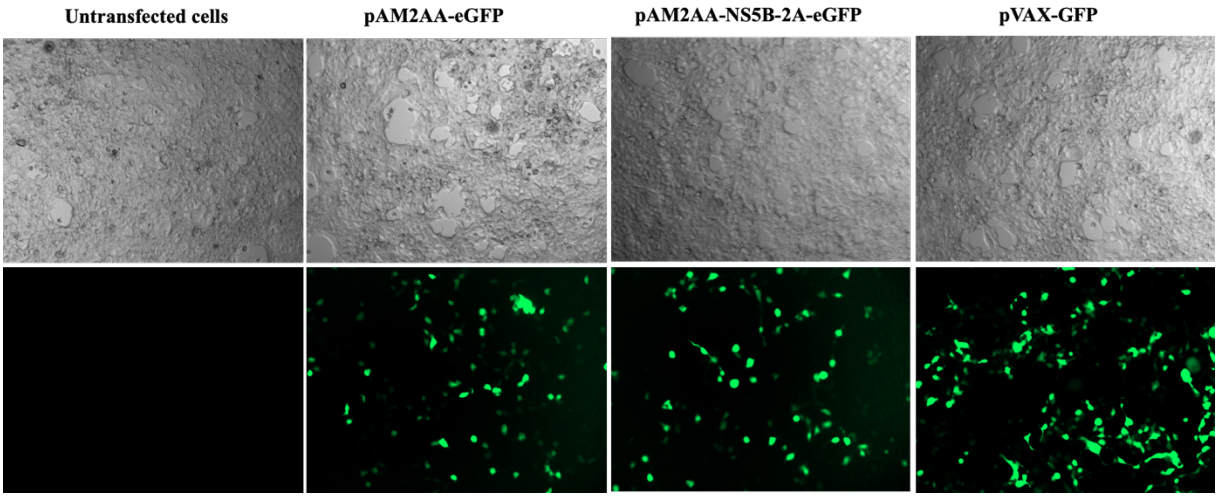

Figure 3.4: eGFP expression in HEK 293 T cells 48 hours post transfection with pAM2AA-eGFP. HEK 293 T cells were transfected with 200ηg of DNA using lipofectamine LTX plus reagent. Forty-eight hours post transfection the cells were examined for GFP expression. (Micrographs were taken using a ZEISS fluorescent microscope at 488ηm wavelength and 10x magnification).

3.3.1.2.2 NS5B expression

Although expression of eGFP from the monocistronic pAM2AA-NS5B-2A-eGFP plasmid suggests that NS5B would also be expressed, it was considered necessary to confirm expression of NS5B directly. This was examined by immunofluorescence staining of HEK 293 T cells following transfection with pAM2AA-NS5B-2A-GFP. Forty-eight hours post transfection the cells were fixed with 4% paraformaldehyde (PFA), permeabilised and stained with HCV positive human serum as described in Chapter 2, section 2.2.8. As shown in Figure 3.5, as a polyclonal serum was used and a protein was detected, this was most likely to represent NS5B in pAM2AA-NS5B-eGFP transfected cells (Figure 3.5 A) while expression was not observed in un-transfected cells (Figure 3.5 B). Moreover, NS5B expression correlated with eGFP expression as shown in the overlay (Figure 3.5 A).

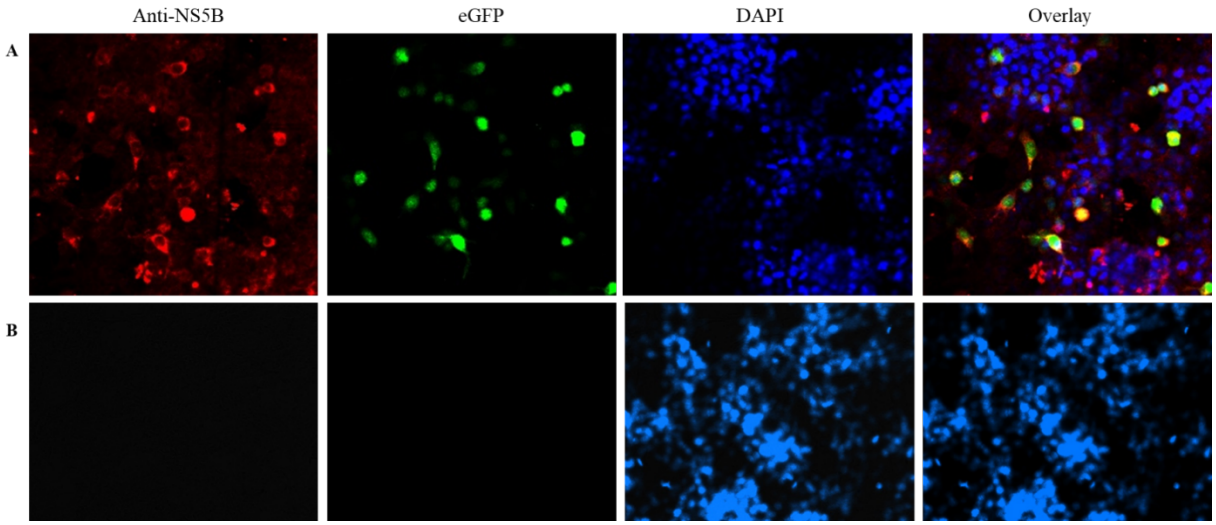

Figure 3.5: Immunofluorescence staining to detect NS5B expression from pAM2AA-NS5B-2A-eGFP. HEK293 T cells were transfected with pAM2AA-NS5B-2A-eGFP (A) or left un-transfected as a control (B). 48 hours post transfection, the cells were fixed, permeabilised and immunofluorescence was performed as described in Chapter 2, section 2.2.8. (Micrographs were taken using a ZEISS LSM 700 fluorescent microscope at 10x magnification).

3.3.1.3 Production of rAAV encoding HCV gt3a NS5B and eGFP

Transfection of HEK 293 T cells with the three plasmids, pAM2AA-NS5B-2A-eGFP, p5E1VD2/8 and pXX6, will result in the synthesis of rAAV-NS5B-2A-eGFP. The three plasmids were added at an equimolar ratio and mixed with PEI at a 3:1 ratio of PEI (1mg/ml) to total DNA as described in Chapter 2 section 2.2.9.3. The transfection efficiency was monitored by microscopic examination of eGFP expression (Figure 3.6). The transfected cells were incubated for 72 hours before virus harvest and purification as described in Chapter 2, section 2.2.9.4.

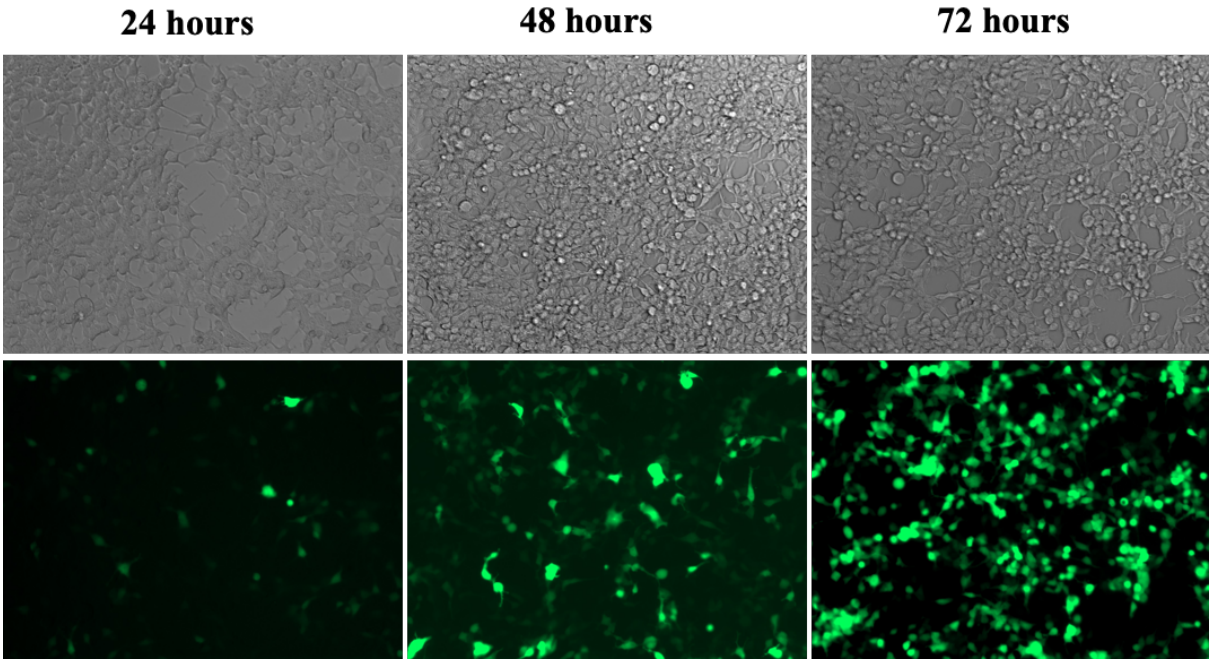

Figure 3.6: Monitoring eGFP expression following triple transfection. HEK293 T cells were transfected with the three plasmids using PEI to synthesise the rAAV-NS5B-2A-eGFP virus. Transfection was monitored using microscopic examination of eGFP expression at 24-, 48- and 72-hours post transfection. (Micrographs were taken using a ZEISS fluorescent microscope at 488ηm wavelength and 10x magnification).

3.3.1.4 rAAV characterization.

In purified rAAV stocks the dominant proteins that should be present are the three viral capsid proteins; VP1, VP2 and VP3 [306]. The molar ratio of VP1, VP2 and VP3 in the rAAV particle

is 1:1:10 and their molecular mass is 87, 72 and 62kDa, respectively [298]. SDS-PAGE is used to determine the capsid composition of the purified virus [306].

SDS-PAGE was performed as described in Chapter 2 section 2.2.9.5 using 5 µl of concentrated virus. As depicted in figure 3.7, the three VP of the capsid VP1, VP2, and VP3 were readily detected. The thick intense band with a molecular weight between 50 and 75kDa represents VP3 (Figure 3.7). These results were comparable those reported by Guo *et al*., who employed a similar purification technique [498]. Due to the high cost of anti-capsid antibodies and because subsequent *in vitro* studies (section 3.3.1.6) revealed expression of eGFP and NS5B (see below), western blotting of the virus capsid was not performed.

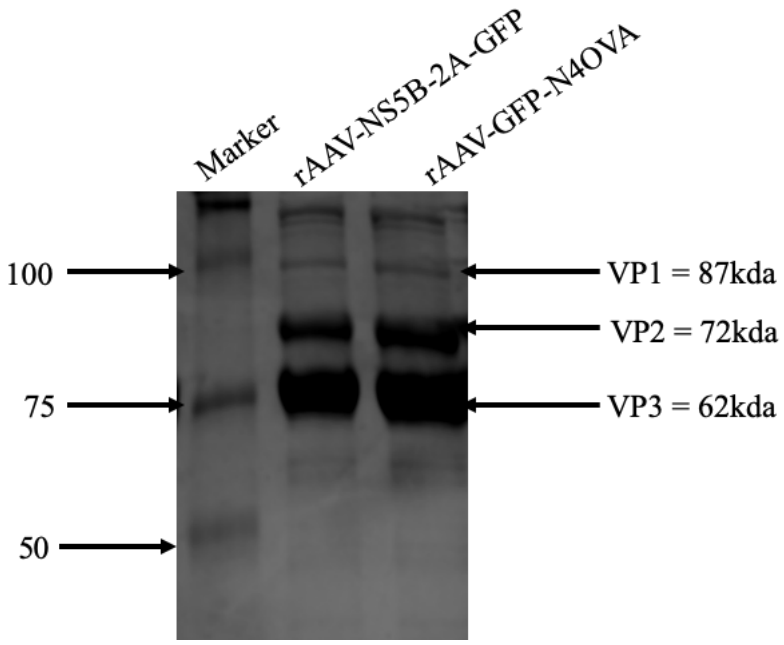

Figure 3.7: Coomassie blue stained SDS-PAGE of denatured rAAV. (rAAV-GFP-N4OVA, purified in the same manner, was used as a positive control (The pAM2AA-GFP-N4OVA plasmid used to synthesize rAAV-eGFP-N4OVA was a kind gift from David Bowen, Centenary Institute, University of Sydney)).

Once the viral capsid proteins were detected, it was necessary to determine that all the encoded genes were packaged. The purified virus was treated with DNase, the virus capsid was lysed to release the viral genome using phenol chloroform [520] and the extracted genome was used as a template for a PCR. The primers used for amplification encompassed the recombinant virus genome region from the hAAT promoter to the end of eGFP sequence (Figure 3.8 A). PCR was performed as described in chapter 2 (section 2.2.2.) and the products were analysed by 1% agarose gel electrophoresis to confirm the size of the amplicons. As a positive control, the PCR was performed using pAM2AA-NS5B-2A-eGFP plasmid DNA as a template. The results showed amplicons with expected band sizes that were similar between the PCR products from the virus genome and the plasmid DNA (Figure 3.8 B).

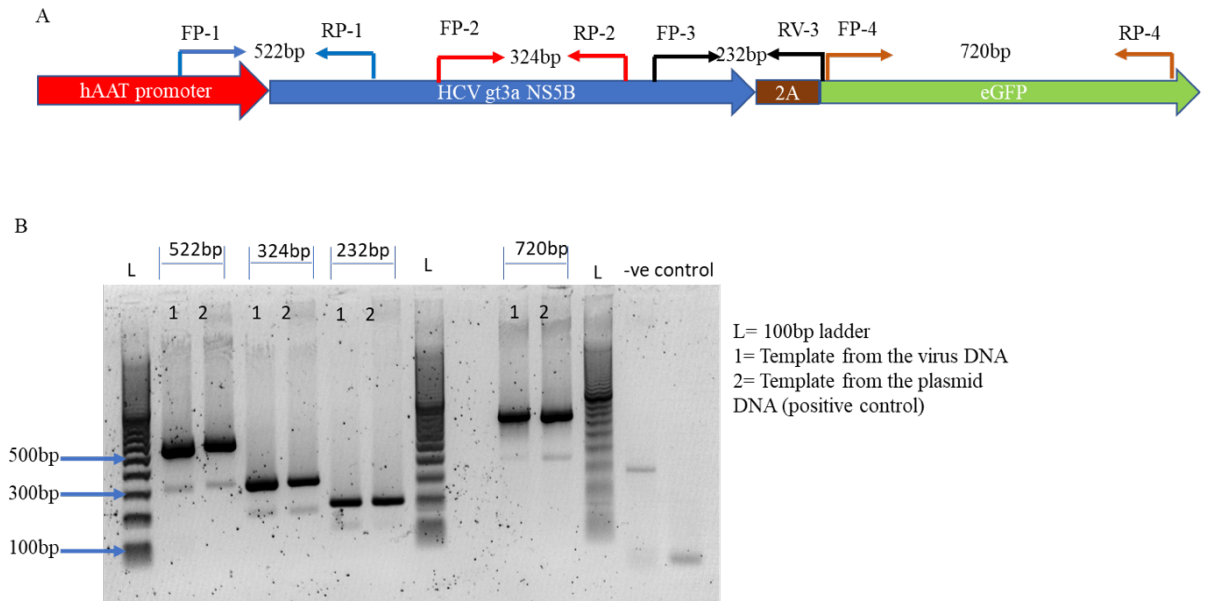

Figure 3.8: PCR amplification of NS5B-2A-eGFP sequences from DNA extracted from rAAV-NS5B-2A-eGFP. A) The location of primers used for the PCR. B) Analysis of the PCR products by 1% agarose gel electrophoresis.

3.3.1.5 Titration of rAAV-NS5B-2A-eGFP by quantitative PCR

The titre of rAAV-NS5B-2A-eGFP was determined using a commercial kit (AAV pro-titration kit for real time PCR V.2) as described in section 2.2.9.6. The viral genome was released from

purified virus as described above, diluted as necessary and used as a template for quantitative PCR. The PCR was performed using the conditions described in Section 2.2.9.6

The cycling melt curve and standard curve are shown in figure (Figure 3.9). The titre of the virus was determined based on the standard curve produced from the positive control provided in the kit. The positive control is a plasmid DNA that includes the AAV ITRs, adjusted to 2 x 10^7 copies/µl based on the value at OD_{260}. The plasmid was serially diluted, ranging from $2x10^2$ to $2x10^7$ copies/µl, to produce a standard curve for viral particle quantification. Based this standard curve, the average titre of virus obtained was 8.5 x 10^8 vgc/µl and the total yield from the transfection of 40 T-75 flasks was 2.5 x 10^{11} vgc.

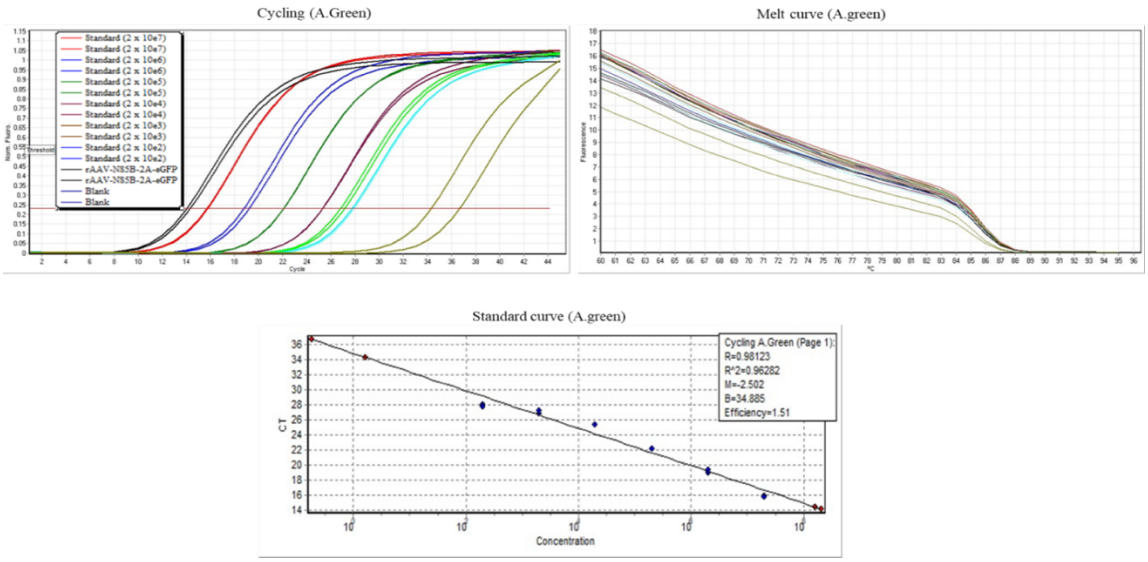

Figure 3.9: Representative images taken from the titration of rAAV-NS5B-2A-eGFP using quantitative PCR. DNAse treated, lysed virus was diluted using EASY dilution buffer (1:50) and 5µl of the diluted sample was used as a template for qPCR.

3.3.1.6 Transduction of HT1080 cells by rAAV-NS5B-2A-eGFP

The next logical step to assess successful construction of the virus was to check protein expression from the encoded genes. For this, HT1080 cells were transduced with rAAV-NS5B-2A-eGFP to examine expression of NS5B and eGFP. HT1080 cells are human fibrosarcoma cells that are

shown to be readily transduced by rAAV [521]. The cells were seeded at a density of 2.5 x10^4 cells/well in a 96 well cell culture plate and rAAV-NS5B-2A-eGFP was added to the cells at the multiplicity of infection (MOI) of 10^5. As a positive control for eGFP expression, cells were transduced with rAAV-eGFP-N4OVA at a similar MOI. eGFP expression was assessed by direct microscopic observation and flow cytometry analysis while immunofluorescence staining was used to detect NS5B expression.

Direct microscopic examination of transduced cells revealed expression of eGFP from the virus (Figure 3.10 A). Flow cytometry analysis showed only 3% and 12% of the cells transduced with rAAV-NS5B-2A-eGFP and rAAV-eGFP-N4OVA, respectively, were eGFP positive (Figure 3.10 B). Although the percentage of eGFP positive cells confirmed eGFP expression from rAAV-NS5B-2A-eGFP, it was difficult to detect NS5B expression using immunofluorescence staining most likely due to the low level of transduction. Hence, it was necessary to improve the level of transduction. To achieve this 5μM Hoechst 33342 (Invitrogen) was used as a transduction enhancer. It was reported that Hoechst 33342 enhances transduction of different cell lines by rAAV [501]. Accordingly, the level of transduction was improved from 3% to 17.8% in case of rAAV-NS5B-eGFP and from 12% to 28% in the case of rAAV-eGFP-N4OVA (Figure 3.10 B). Other studies reported greater than 600 GFP-positive cells per field when a similar MOI was used to transduce HT1080 cells in the presence of 10 μM Hoechst 33342 [502]. Others used a MOI of 10^4 to transduce HEK293 T cells, but fluorescent intensity of eGFP, not the frequency or percentage of transduced cells, was reported [522].

Using Hoechst 33342 as a transduction enhancer, expression of NS5B was assessed at two different stages. First using RT-PCR, transcription of the encoded genes was checked at the RNA level. RNA was extracted from the transduced cells using the RNeasy Mini-kit according to the manufacturer's instructions and cDNA was synthesised using the QuantiTect reverse transcription kit. This cDNA was used as a PCR template for RT-PCR and amplified using primer

pairs that bind specifically to the NS5B-2A-eGFP region. The primers (See Appendix IX for the list of primers) were designed in such way that the amplicon size was <400bp (Figure 3.11 A). A small amplicon was selected because the efficiency of amplification decreases as the amplicon size increases [523]. The housekeeping gene, GAPDH, was used as a control for reverse transcription.

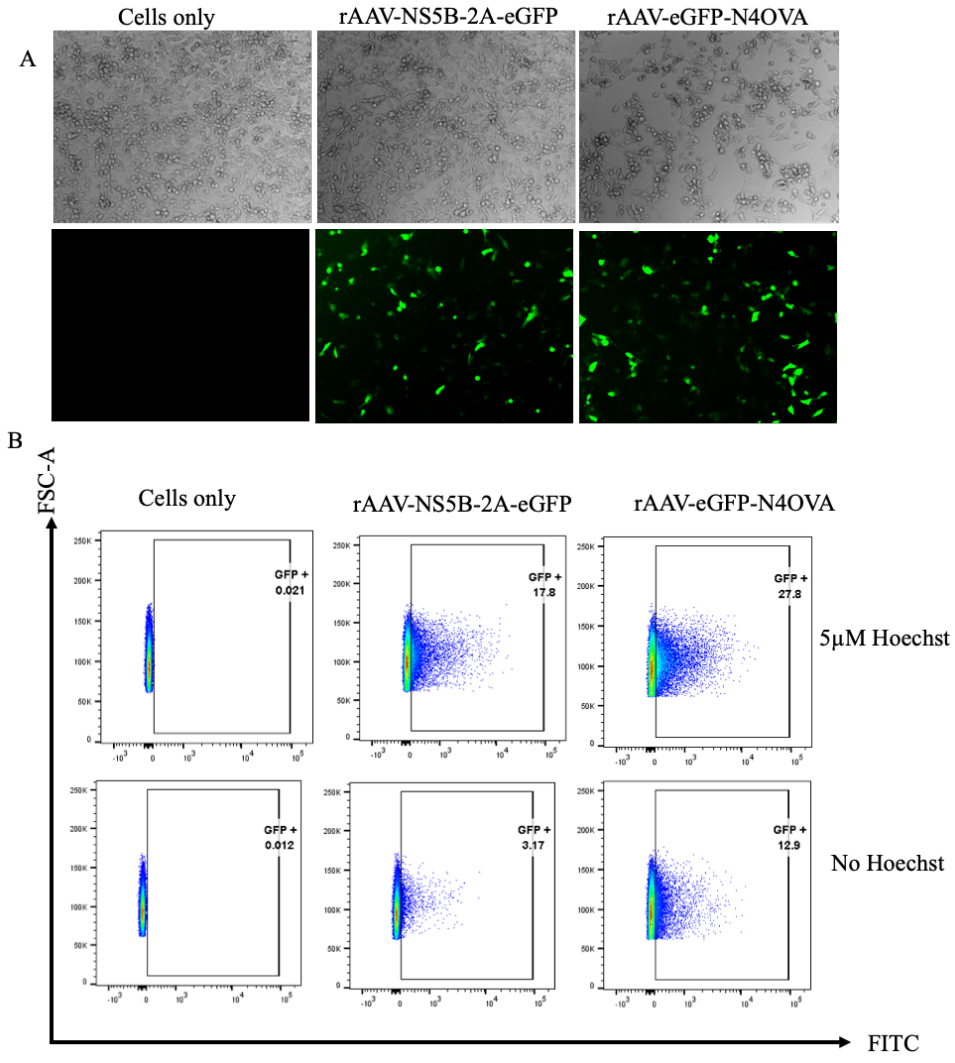

Figure 3.10: eGFP expression following transduction of HT1080 cells with rAAV-NS5B-2A-eGFP or rAAV-eGP-N4OVA. HT1080 cells were transduced with rAAV at a MOI of 10^5 in the presence of 5µM Hoechst 33342. Seventy-two hours post transduction representative images of eGFP expression were taken using a Zeiss microscope (A) and the percentage of cells expressing eGFP was determined using flow cytometry (B)

The RT-PCR was performed in a 3-step cycling program with initial denaturation at 95°C for 2 minutes, followed by 35 cycles at 95 °C for 5 seconds and fluorescent detection at 60 °C for 30 seconds. This showed that all the expected products were detected revealing that mRNA was transcribed from the virus genome (Figure 3.11 B).

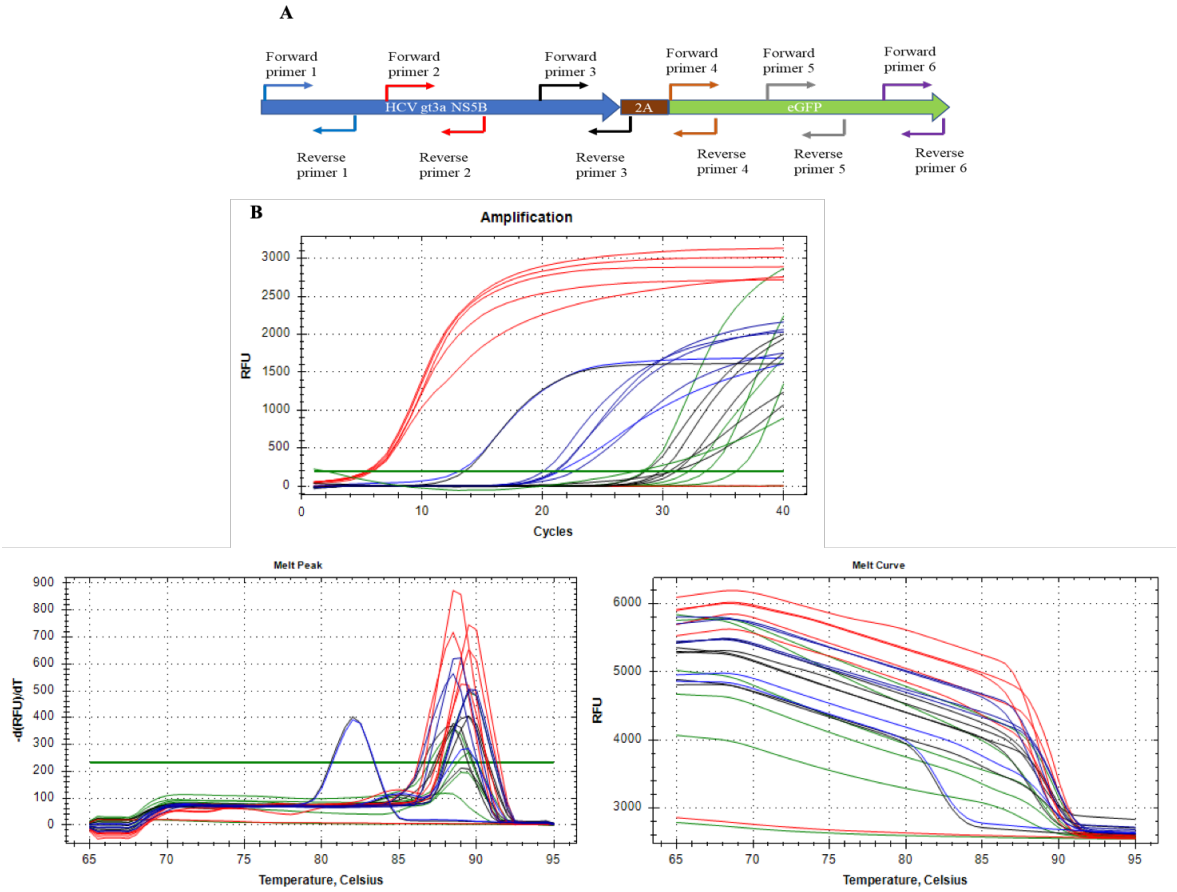

Figure 3.11: RT-PCR to detect NS5B and eGFP RNA in HT1080 cells transduced with rAAV-NS5B-2A-GFP. RNA was extracted from transduced cells and cDNA was synthesised which was then used as a template for RT-PCR. A) Primers designed to amplify cDNA fragments. B) RT-PCR showing amplification of segments of the cDNA using primers made in A.

Next NS5B expression was confirmed using immunofluorescence staining. HT1080 cells were transduced as described above and 72 hours post transduction, the cells were fixed and stained using HCV-positive human serum as a source for the primary antibody and goat anti-human

AlexaFluor-555 as a secondary antibody. Microscopic examination of stained cells revealed expression of NS5B and eGFP in rAAV-NS5B-2A-eGFP transduced cells (Figure 3.12 A). Although a few cells appeared to express NS5B but not eGFP, also reported by others [524], in general the two proteins were colocalised. In cells transfected with pVAX-GFP only GFP expression was observed (Figure 3.12 B) while un-transfected cells showed no expression of eGFP or NS5B (Figure 3.12 C) confirming that the NS5B expression observed in rAAV-NS5B-2A-eGFP transduced cells was specific (Figure 3.12 A).

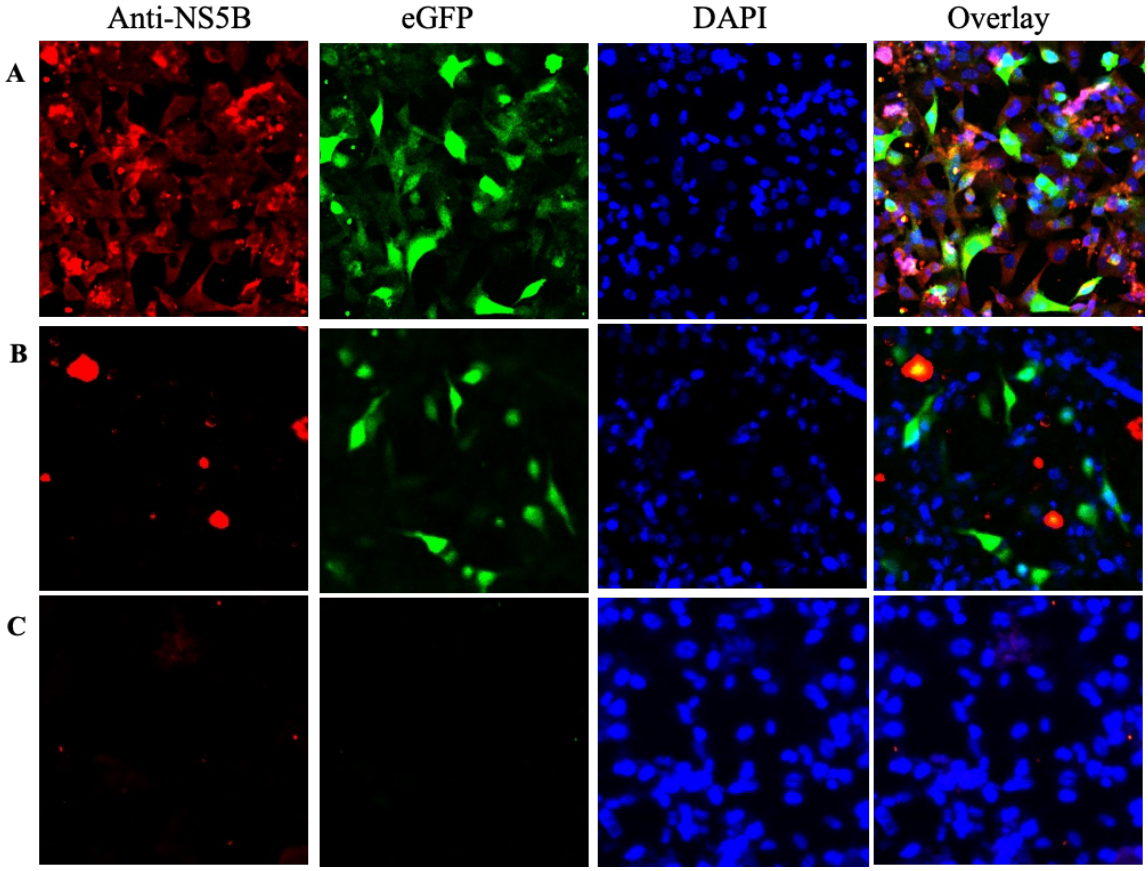

Figure 3.12: Immunofluorescence staining to detect NS5B expression from rAAV-NS5B-2A-eGFP. HT1080 cells were transduced with 10^5 vgc of rAAV-NS5B-2A-eGFP (A) or transfected with pVAX-GFP (B) or left un-transfected (C). Seventy-two hours immunofluorescence was performed as described in Chapter 2, section 2.2.8.

3.3.1.5 Transduction of mouse hepatocytes *in vivo* by rAAV-NS5B-2A-eGFP

A previous study showed that a dose of rAAV capable of transducing 5-10% of hepatocytes *in vivo* was highly immunogenic, but a dose which resulted in >25% of transduction of hepatocytes was tolerogenic [382]. To determine the dose of virus needed to transduce 10-25% of mouse hepatocytes, mice were injected IV with rAAV-NS5B-2A-eGFP or PBS in the case of the control mouse. Mice received different doses of the virus; $2x10^9$, $5x10^9$, $2x10^{10}$, $5x10^{10}$ or $2x10^{11}$ vgc. Seven days after injection, the mice were euthanised and liver samples were harvested. Hepatocytes were isolated according to the procedure described in section 2.3.5. The cells were stained by DAPI and analysed by flow cytometry to determine the percentage of GFP-expressing hepatocytes. From this analysis, a virus dose of $5x10^9$ vgc resulted in 10% transduction of mouse hepatocytes (Figure 3.13) and this dose was used for subsequent experiments. *In vivo* transduction and analysis of mouse hepatocytes was performed by Dr. Kieran English at the Centenary Institute, Sydney.

3.4 Discussion

The use of rAAV in gene therapy and to deliver vaccine antigens has been described previously [373, 525-527]. Therefore, the aim of this chapter was to synthesize rAAV-NS5B-2A-eGFP that can be used as a trapping agent for HCV-specific CD8 T cells in the liver, that are induced following vaccination with pVAX-NS5B-PRF.

The production of rAAV requires three plasmids; the plasmid that contains the gene of interest flanked between the ITRs, the plasmid that encodes the *rep* and *cap* genes and the helper plasmid that contains the adenoviral helper genes [497]. The first section of this chapter described the construction of the plasmid that encodes HCV gt3a NS5B and eGFP, pAM2AA-NS5B-2A-eGFP.

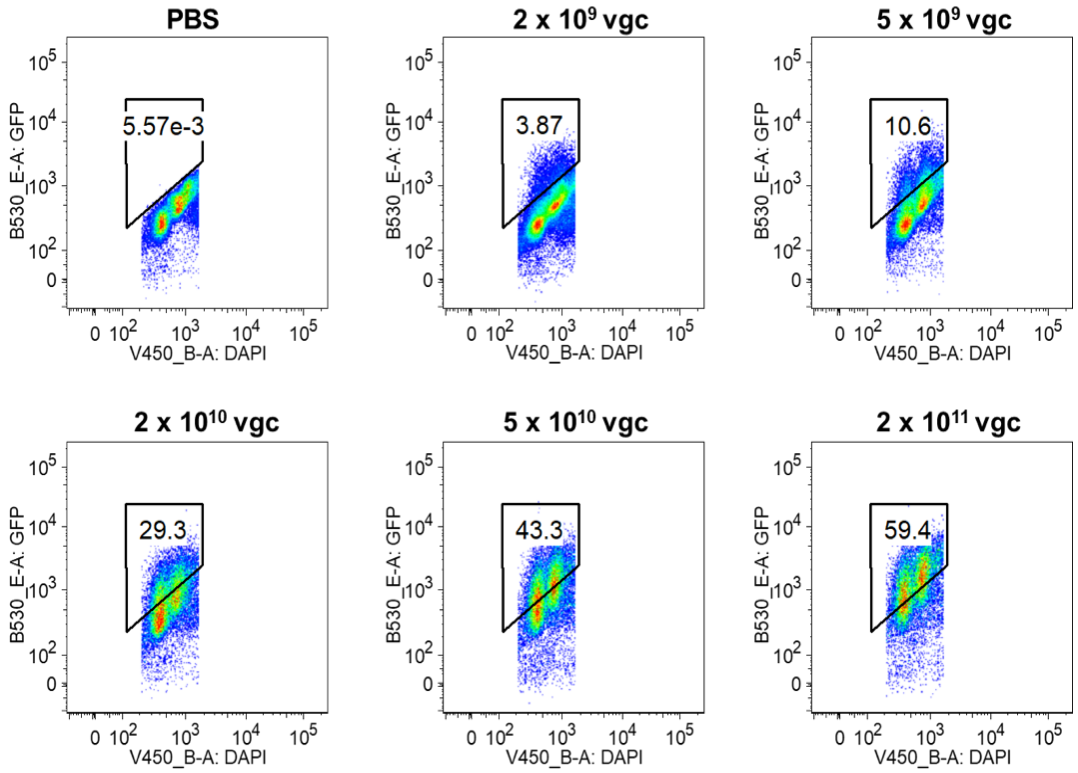

Figure 3.13: Analysis of eGFP expression in isolated mouse hepatocytes. The percentage of eGFP positive mouse hepatocytes was assessed seven days post injection with different doses of rAAV-NA5B-2A-eGFP. Eight weeks old male C57BL/6 mice were IV injected with different doses of rAAV-NS5B-2A-eGFP. Seven days later hepatocytes were harvested and eGFP expression was analysed by flow cytometry.

The pAM2AA vector was previously described and contains a liver specific, ApoE/hAAT enhancer/promoter [382, 528]. This restricts expression of the encoded genes to the liver [528]. Following successful cloning of NS5B and eGFP, these proteins need to be expressed as individual proteins from a single promoter. To achieve this the 2A protease was designed to cleave eGFP from NS5B [206, 529]. Expression of eGFP and NS5B from pAM2AA-NA5B-2A-eGFP was demonstrated following transfection of HEK293 T cells.

In the second section of this chapter, production of rAAV-NS5B-2A-eGFP was described. The virus construct was packaged in HEK 293 T cells with the help of the pXX6 plasmid and

pseudotyped to AAV type 8 capsid because this serotype was shown to increase transduction of hepatocytes [530, 531]. It has been reported that a lower proportion of hepatocytes are permissive to rAAV-2 and increasing the vector dose failed to show a linear relationship with the number of transduced cells and the level of transgene expression [532]. On the other hand, rAAV-8 showed a linear dose-response curve at a dose as high as $7.2x10^{12}$ vgc, making it the preferred serotype to transduce hepatocytes [530].

The ultra-high-speed density gradient centrifugation technique to purify rAAV is regarded as labour intensive and time consuming with significant amount of vector loss [518]. As a result, a simpler method of purification that avoids ultra-high-speed centrifugation was introduced by Guo *et al*., 2012 [498]. Using this technique $6.25x10^{8}$ vgc/ul of rAAV-NS5B-2A-eGFP was obtained as titrated by AAV-Pro titration kit (for real time PCR) Ver.2. The purified virus was also tested for its ability to transduce HT1080 cells *in vitro* and mouse hepatocytes *in vivo.*

In vitro transduction of HT1080 cells, at a MOI of 10^{5}, with the purified rAAV-NS5B-2A-eGFP virus resulted in approximately 18% GFP positive cells by flow cytometry. The use of DNA minor groove binding agents Hoechst 33258 and 33342 was reported to increase transgene expression from rAAV [501]. Similarly, in this experiment the use of 5uM Hoechst 33342 improved eGFP expression from 3% to 18% from rAAV-NS5B-2A-eGFP while it increased eGFP expression from rAAV-GFP-N4OVA from 13% to 28%. Although the effect of Hoechst is not clearly understood, it was suggested that the compound has a significant effect on the different stages of the cell cycle [501]. Although, the expression of eGFP can be considered as an indicator of NS5B expression because the expression of both proteins was driven by a single promoter and the 2A protease ensures cleavage of the two proteins as described elsewhere [206, 529], it was equally important to detect NS5B expression. Accordingly following transduction of HT1080 cells NS5B-specific mRNA was detected by RT-PCR and immunofluorescence staining confirmed expression of NS5B.

From a previous study it was indicated that the proportion of antigen-positive hepatocytes resulting from *in vivo* transduction with rAAV determines the fate of the $CD8^+$ T cell response in the liver [382]. According to this study, transduction of a high percentage (>25%) of hepatocytes will result in exhaustion of $CD8^+$ T cells [382]. Hence, rAAV-NS5B-2A-eGFP was titrated to determine the dose of virus required to transduce 10-25% of hepatocytes. From this experiment $5x10^9$ vgc of rAAV-NS5B-2A-eGFP was able to transduce 10.6% of mouse hepatocytes, *in vivo*, and this dose was selected as an immunologically functional virus dose for subsequent experiments.

3.5 Conclusion

The results in this chapter report cloning of HCV gt3a NS5B and eGFP under a liver specific promoter in a plasmid, pAM2AA-NS5B-2A-eGFP, that was later used to produce a rAAV that encodes these proteins. The data showed that rAAV-NS5B-2A-eGFP was able to transduce HT1080 cells *in vitro* and both eGFP and NS5B were detected in these cells. It was also shown that rAAV-NS5B-2A-eGFP was able to transduce mouse hepatocytes *in vivo*.

4 Chapter 4: *In vivo* T cell epitope mapping of gt3a HCV NS5B

4.1 Introduction

A recent study from our laboratory that compared CMI to NS3, NS4 and NS5B from gt1b and gt3a HCV in DNA-vaccinated BALB/c mice showed that the highest magnitude of T helper and $CD8^+$ killer T cell responses were directed against gt3a NS5B *in vivo* [288]. Thus, gt3a NS5B was chosen as a model antigen to optimise a vaccination strategy to elicit HCV-specific CMI in the liver.

Seminal studies that described the biological roles of $CD8^+$ T_{RM} cells stimulated adoptively transferred $CD8^+$ T cells that express a unique congenic marker on the cell surface compared to endogenous $CD8^+$ T cells found in recipient mice [455, 495]. In the context of vaccination, it is more physiological to analyse endogenous antigen-specific $CD8^+$ T cells and a convenient way to achieve this *ex vivo* is to use tetramers, which are essentially synthetic peptide-MHC-I monomers, joined by biotinylated streptavidin, conjugated to a fluorochrome [533, 534]. It is also important to analyse HCV-specific $CD4^+$ T helper cell responses as NS3-, NS4- and NS5-specific $CD4^+$ T cell responses also correlate with natural recovery from acute HCV infection [152]. However, a reliable method to develop successful tetramers to analyse antigen-specific polyclonal $CD4^+$ T cells that develop *in vivo* is not available. Thus, to identify the immunodominant T cell epitopes of gt3a NS5B *in vivo*, an in-house FTA technology was exploited. The FTA is the most versatile assay to measure the breadth, avidity, magnitude and epitope variant cross-reactivity of $CD8^+$ killer T cell and $CD4^+$ T_H cell responses *in vivo* in mice [503, 535]. This technology will also be used to analyse T cell responses in the spleen and the liver *in vivo* which is important given that T_{RM} cells, including those recovered from the liver, survive poorly in functional assays performed *in vitro* [433, 455].

This chapter describes the FTA-based mapping process of immunodominant T cell epitopes of gt3a NS5B in the liver and the spleen of BALB/c mice. In the FTA technology, $CD8^+$ T cell responses are measured by target cell (cells loaded with peptides representing the vaccine antigen) killing while $CD4^+$ T cell responses are measured by the upregulation of CD69 on FTA B ($B220^+$) cells [504, 535]. As noted in section 1.3.2.1, CD69 is associated with specific tissue residency, but CD69 is also recognized as a type II C-type lectin involved in lymphocyte migration and cytokine secretion [536] and is an early indicator of leucocyte activation [536, 537]. MHC-II-restricted antigen presentation by peptide-loaded B cells will result in an antigen-specific interaction with T_H cells. This interaction leads to activation and differentiation of the B cells resulting in high levels of expression of CD69, and this can be used to measure the $CD4^+$ T cell helper response resulting from vaccination [538, 539].

4.2 Aims

The aims of this chapter are to:

1. Map the immunodominant T cell epitopes of gt3a NS5B following vaccination of BALB/c mice with pVAX-NS5B-PRF
2. Synthesize and test a MHC-I tetramer ($H2\text{-}K^d$) in BALB/c mice based on the most immunodominant peptide mapped for $CD8^+$ killer T cell responses.

4.3 Results

4.3.1 Immunodominant peptides of HCV gt3a NS5B recognised by T cells

- Naive female BALB/c mice (7 mice per group) were immunised on two occasions at fortnightly intervals with 50 µg of pVAX-NS5B-PRF or pVAX-PRF using equimolar amounts of DNA. Thirteen days after the final DNA immunisation, the mice were challenged IV with autologous fluorescent, bar-coded splenocytes loaded with each of the NS5B peptides spanning $NS5B_{385\text{-}591}$ (pool 3 (P3) as described in the Methods chapter (2.2.10.1). $NS5B_{385\text{-}591}$ was chosen given the

published data from our laboratory which showed that this region contained the most immunodominant $CD8^+$ cytotoxic T cell epitopes [288]. The specific FTA matrix and the bar-coding scheme used in this chapter are shown in the diagram below (Figure 4.1). Fifteen hours post FTA challenge, the mice were euthanised and the FTA cells recovered from the spleen and the liver were analysed using flow cytometry (Figure 4.2). Each peptide was tested only once. However, peptides identified to contain CD8 and CD4 T cell epitopes were tested twice.

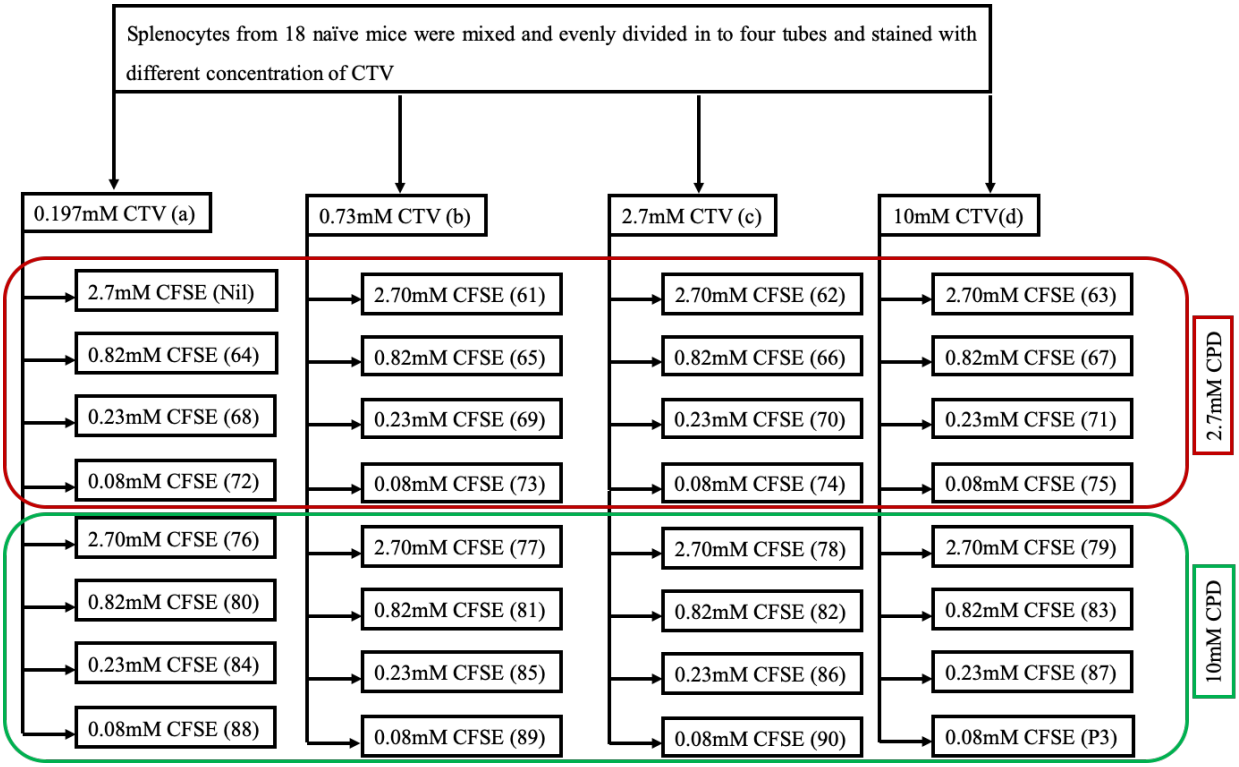

Figure 4.1: FTA setup for the identification of T cell epitopes in HCV gt3a NS5B P3. The numbers in brackets correspond to the individual peptides in P3 of HCV gt3a NS5B. Nil; these cells were not loaded with any peptide. P3: targets pulsed with the pooled peptides of gt3a NS5B.

Following flow cytometric analysis, the CTL response was measured based on the percentage of specific FTA lost (% specific killing) that was calculated according to the following formula described by Wijesundara *et al.*, [503].

$$\%specific\ killing = \frac{(\%\ of\ nil\ targets - \%\ of\ peptide\ pulsed\ target)}{\%\ of\ nil\ targets} X100$$

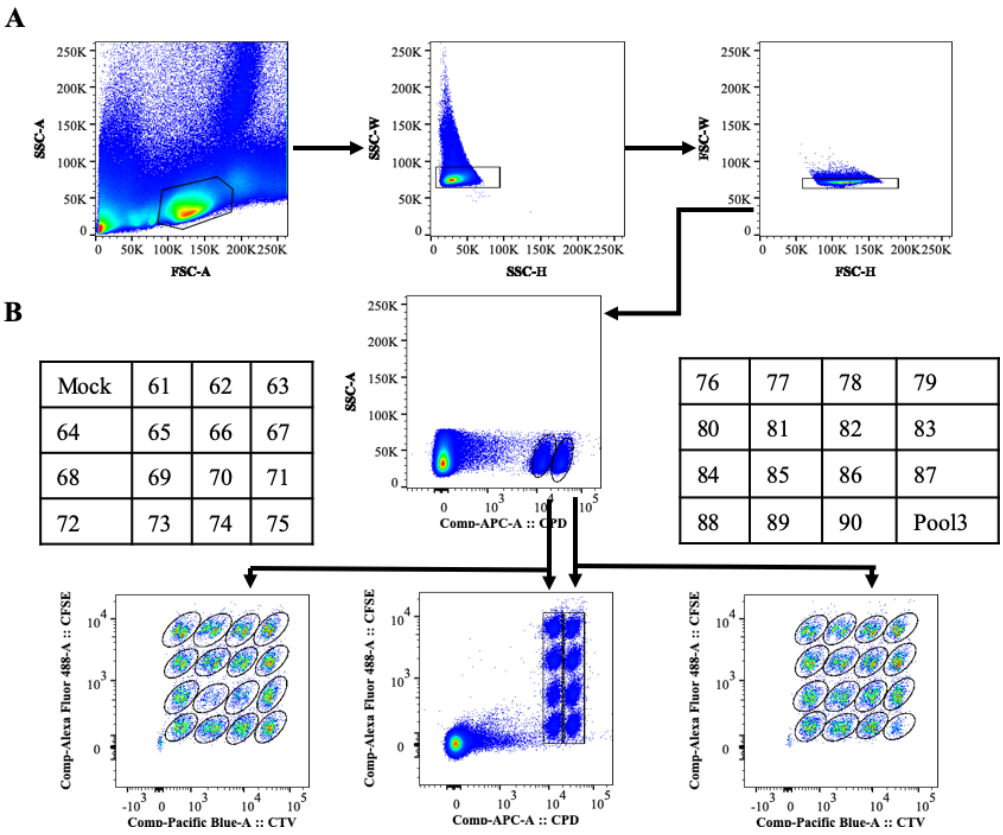

Figure 4.2: Representative plot of analysis of FTA cells recovered from the spleen of mice vaccinated with pVAX-NS5B-PRF. HCV gt3a NS5B-specific CTL responses were examined *in vivo* following vaccination of mice with pVAX-NS5B-PRF or pVAX-PRF. Female BALB/c mice (n = 7 per group) were vaccinated and 13 days after the final vaccination, $2x10^6$ peptide-loaded cells (for each target cell cluster) or mock target cells were transferred IV. Fifteen hours after FTA challenge, splenocytes and liver lymphocytes were harvested and analysed by flow cytometry to determine the surviving number of peptide-pulsed target cells relative to unstimulated target cells. (A) Gating strategy to discriminate lymphocytes. Lymphocytes were double discriminated using SSC-A/FSC-A followed by SSC-W/SSC-H and FSC-W/FSC-H before analysis of targets. B) Analysis of FTA cell death. All the peptide pulsed cell targets were gated and analysed for the percentage recovery relative to mock targets to determine the specific FTA cell loss. The cells gated using CFSE/CTV correspond to the table on the top which in turn is related to the scheme indicated in Figure 4.1.

The percentage loss of FTA target cells loaded with peptide 69 (P69; $NS5B_{442-459;}$ PLDFEMYGATYSVTPLDL) or peptide 70 (P70; $NS5B_{449-466;}$ GATYSVTPLDLPAIIERL) was comparable to the percentage loss of targets pulsed with P3 (Figure 4.3). The concentration of an individual peptide when used alone and its concentration when used in the pool was constant, *i.e.*, 10µg/ml. In the spleen, 84.5% and 65.1% of targets loaded with P69 and P70 were lost, respectively, while the corresponding percentage losses in the liver were 64.5% and 47.2% (Figure 4.3).

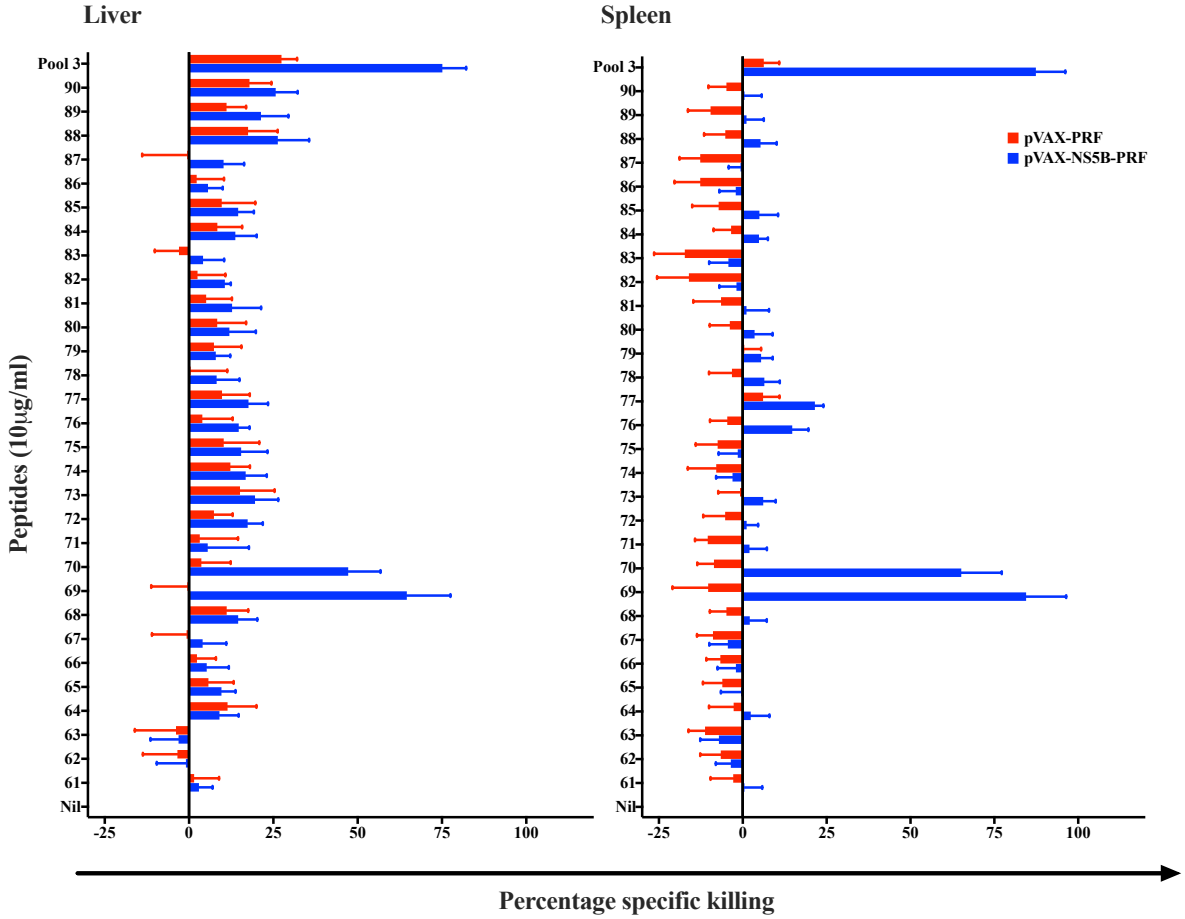

Figure 4.3: Specific loss of FTA cells pulsed with peptides in pool 3 of HCV g3a NS5B. FTA cells were loaded with 10µg/ml of either individual peptides in P3, the combined P3 or mock, and transferred to vaccinated mice (n= 7 mice per group). Fifteen hours after transfer spleen and liver were harvested and lymphocytes were isolated as described in Materials and Methods (section 2.3.6). Surviving peptide-loaded cells recovered from the liver and spleen were analysed by flow

cytometry and the specific loss of peptide FTA cells was calculated and plotted using Graph pad prism software.

Overall the *in vivo* T cell mapping study using the FTA assay revealed two immunogenic peptides, P69 and P70, that were likely to betargets of $CD8^+$ T cells.

Peptides in P3 were also analysed for the presence of $CD4^+$ T cell epitopes (Figure 4.4). Following the analysis of CD69 expression on recovered FTA B cells, the geometric mean fluorescent intensity (GMFI) of CD69 was determined. Expression of CD69 was calculated by subtracting the GMFI of CD69 in naive mice from that in the vaccinated mice [503]. Accordingly, peptide 77 (P77; $NS5B_{495-512}$) was identified as a target to increase expression of CD69 in the spleen, but not in the liver, of vaccinated mice. None of the remaining peptides was considered as a T_H cell immunodominant epitope as the GMFI of CD69 was not significantly higher in vaccinated mice compared with unvaccinated (mock) mice (Figure 4.4).

On the other hand, recently published data from our laboratory showed that pool 2 (P2: $NS5B_{197-395}$) contains immunodominant peptides that are targets for $CD4^+$ T cells [288]. As a result, NS5B peptides in P2 were assessed to determine any additional immunodominant peptides responsible for a helper T cell response. The results showed that a relatively higher GMFI of CD69 expression was observed in the spleen in FTA cells that were pulsed with peptide 36 (P36: $NS5B_{225-240}$) while responses in the liver were not significantly higher than the mock (Figure 4.5 A). From this study it was concluded that P36 was an immunodominant T_H cell epitope in the entire P2 of HCV gt3a NS5B. Overall, peptide 77 ($NS5B_{495-512}$; PPLRAWRHRARAVRAKLI) from P3 and P36 ($NS5B_{225-240;}$ DSTVTGQDIRVEEAVY) from P2 were identified to be immunodominant peptides for a $CD4^+$ T cell response.

To confirm the previously reported data on the absence of CTL epitopes in P2 of NS5B, the level of specific killing of FTA targets loaded with P2 peptides was analysed (Figure 4.5 B). The analysis showed that none of the peptides in P2 was a target of a CTL response (Figure 4.5 B).

Negative percentages following FTA analysis are indicative of no significant killing of peptide loaded target cells above that of the respective mock-pulsed target cells injected into animals. Similarly, negative GMFI results indicate the absence of a significant CD69 expression on FTA $B220^+$ target cells that were loaded with peptides as compared to mock-loaded target cells injected into animals.

4.3.2 Synthesis of MHC-I tetramer to characterize $CD8^+$ T cells

Tetramers have emerged as a key tool to determine the quantity and various phenotypic characteristics of antigen-specific $CD8^+$ T cells. They can be combined with other staining techniques to derive detailed information on antigen-specific T cells, such as activation, effector function, proliferation and apoptosis [534, 540, 541]. Tetramers are designed and synthesised from immunogenic peptides by selecting the most immunodominant sequences comprised of nine amino acids [534, 542, 543]. In this section, the selection of the nine amino acid sequence and the synthesis of the tetramer using MHC-I (H2-K^d in BALB/c mice) is described.

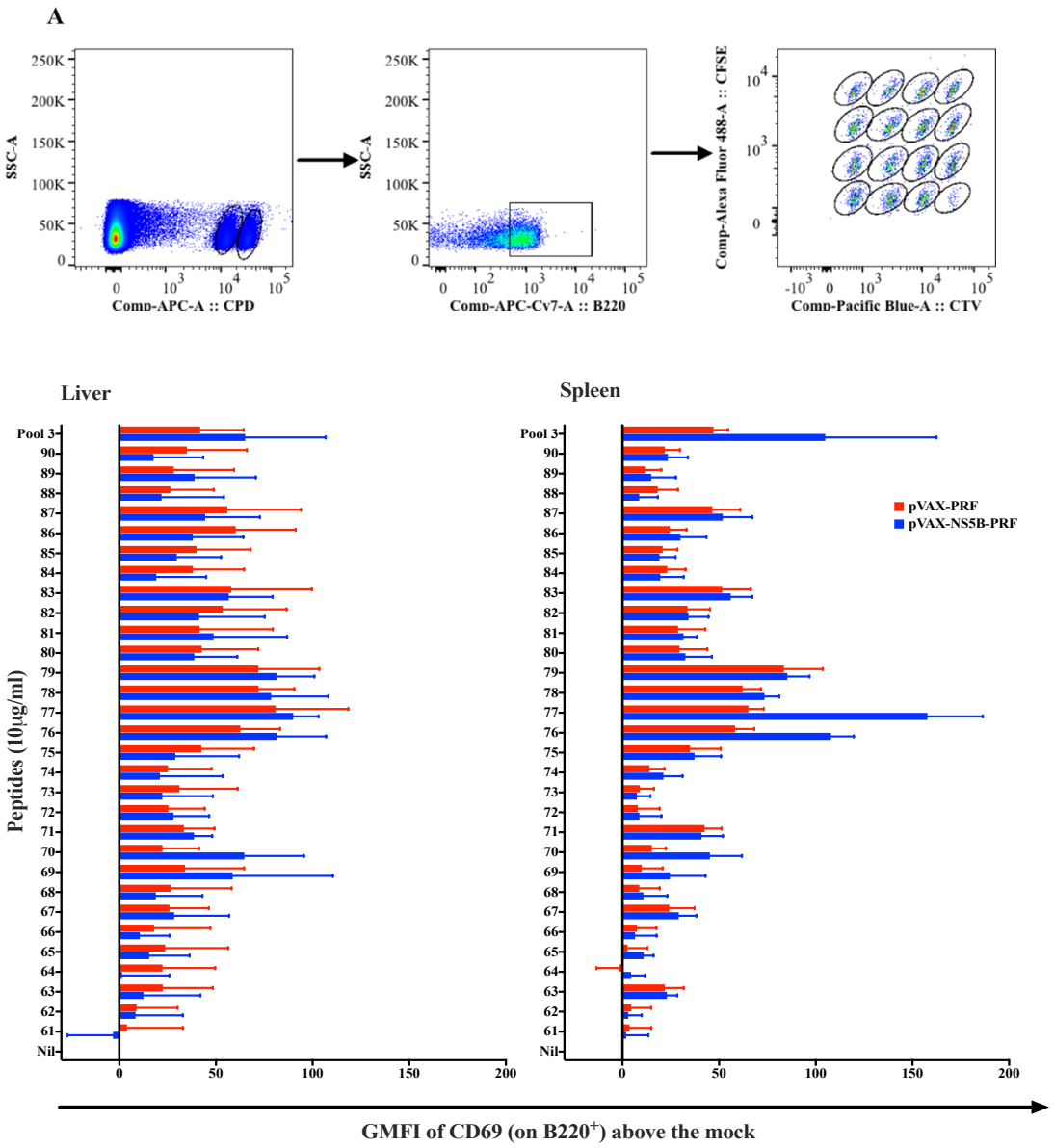

Figure 4.4: CD69 expression on B220$^+$ FTA cells. FTA cells were loaded with 10µg/ml of either individual peptides in P3, P3 or mock, and transferred to vaccinated mice. Fifteen hours later spleen and liver were harvested, and surviving lymphocytes were isolated and analysed by flow cytometry. The GMFI of CD69 expression on B220$^+$ cells was calculated using excel spread sheet and plotted using Graph pad prism software. A) Representative plot of gating strategy for FTA B220$^+$ cells. Lymphocytes were double discriminated as in Figure 4.2 followed by gating on B220$^+$ cells. B) GMFI of CD69 as plotted using Graph pad prism software.

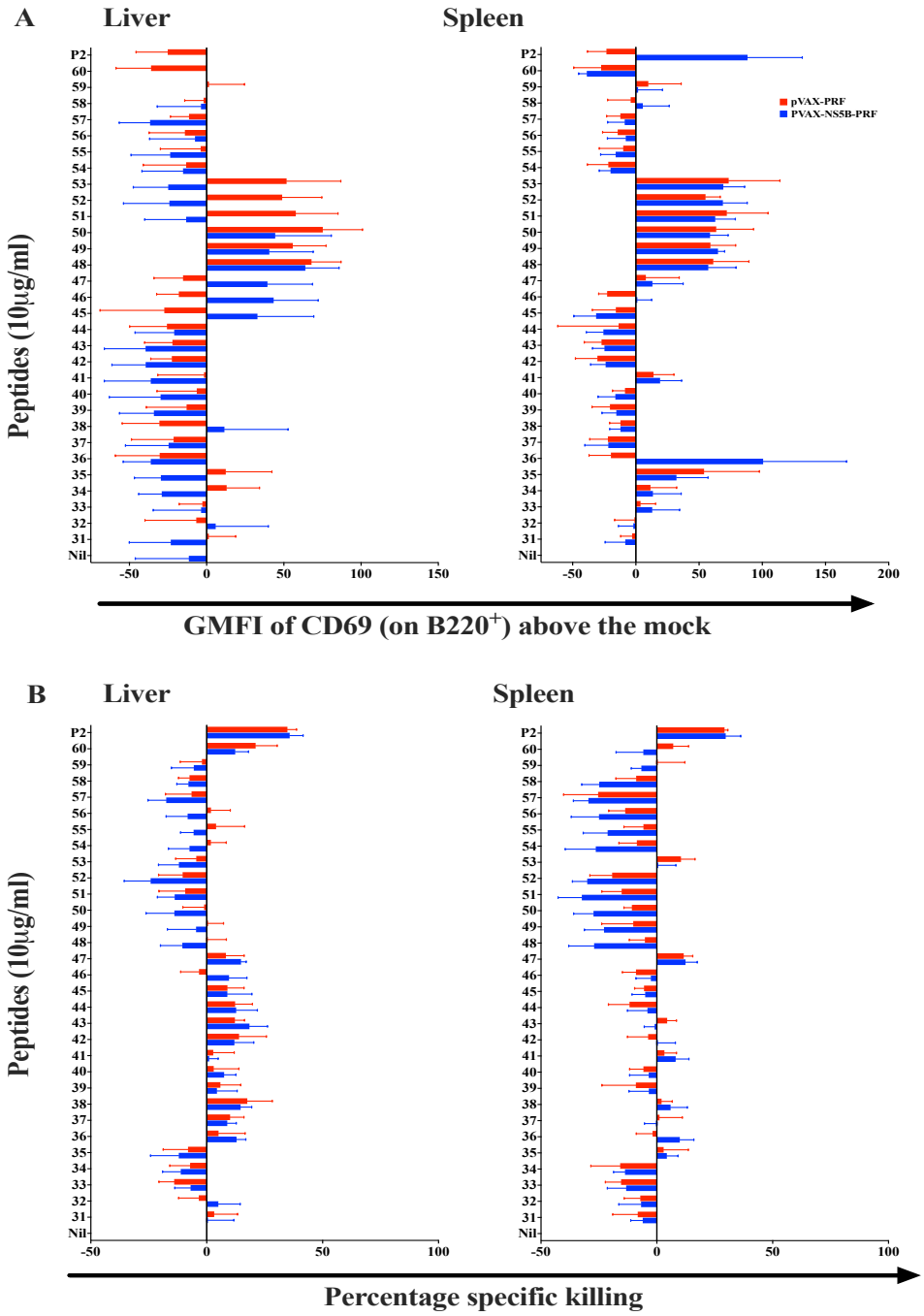

Figure 4.5: FTA analysis to identify immunodominant epitopes in P2 of HCV gt3a NS5B. FTA cells were recovered and analysed using flow cytometry and double discriminated as shown in Figure 4.2. CD69 expression on $B220^+$ FTA cells recovered from the liver and spleen were plotted as GMFI of CD69 (A). Similarly, the percentage loss of FTA cells was determined according to the formula described above and depicted (B).

The CTL immunodominant peptides, P69 and P70, identified from P3 of HCV gt3a NS5B were used as input to identify the most immunodominant nine amino acid sequence. Preston Leung from the Kirby Institute, University of New South Wales, used bioinformatics to predict the most immunogenic nine amino acid sequence. Based on the algorithm described in section 2.10.2, $NS5B_{451-459}$ (TYSVTPLDL), was identified as the most immunodominant region recognised by $CD8^+$ T cells. To confirm that this sequence is responsible for the observed CTL response, a peptide (immunodominant, ID) with this sequence was synthesised (China peptides, China) and loaded on to FTA target cells. FTA target cells were then transferred to vaccinated mice and the percentage killing response was determined (Figure 4.6). As depicted in the figure, the percentage loss of FTA target cells loaded with ID was similar to those in targets loaded with P69, P70 or P3. All the peptides as well as the ID peptide were used at 10µg/ml concentration. The level of the killing response was also similar in the spleen and in the liver.

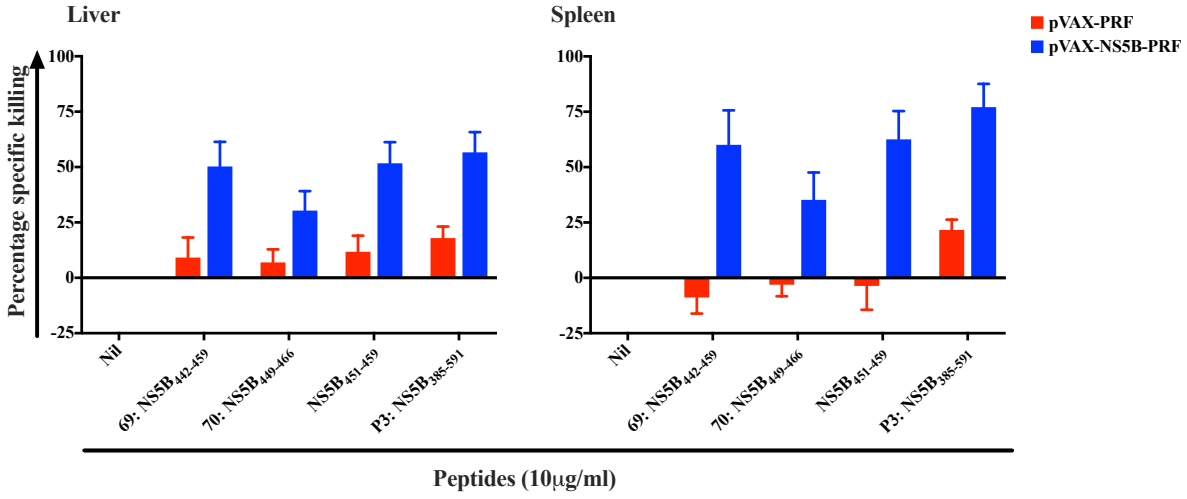

Figure 4.6: Percentage specific loss of peptide pulsed FTA cells. FTA cells were pulsed with P69 ($NS5B_{442-459}$), P70 ($NS5B_{449-466}$), $NS5B_{451-459}$ or P3 ($NS5B_{385-591}$) of NS5B. Peptide loaded FTA cells were transferred to vaccinated or unvaccinated mice (n= 7mice per group) and analysed 15 hours later as described above. The percentage specific killing response was assessed in the liver and spleen of mice.

The next step was to synthesise a MHC-class I binding tetramer based on the $NS5B_{451-459}$ peptide. The tetramer was synthesised based on the murine H2-K^d MHC-I allele and labelled with allophycocyanin (APC) at the ACRF Biomolecular Resource Facility, John Curtin School of Medical Research, Australian National University, Canberra. Before using this tetramer in large scale experiments, it was also tested in a pilot experiment in which mice (7 mice in each group) were vaccinated with two doses of 50 μg of either pVAX-NS5B-PRF or pVAX-PRF two weeks apart. Seven days after the second vaccination splenocytes were collected, stained with the tetramer and analysed by flow cytometry. Based on the results from this pilot experiment, the tetramer was able to specifically stain NS5B specific $CD8^+$ T cells. Accordingly, a significantly higher ($P < 0.0001$) number of tetramer positive NS5B specific $CD8^+$ T cells were identified in the pVAX-NS5B-PRF vaccinated mice (Figure 4.7).

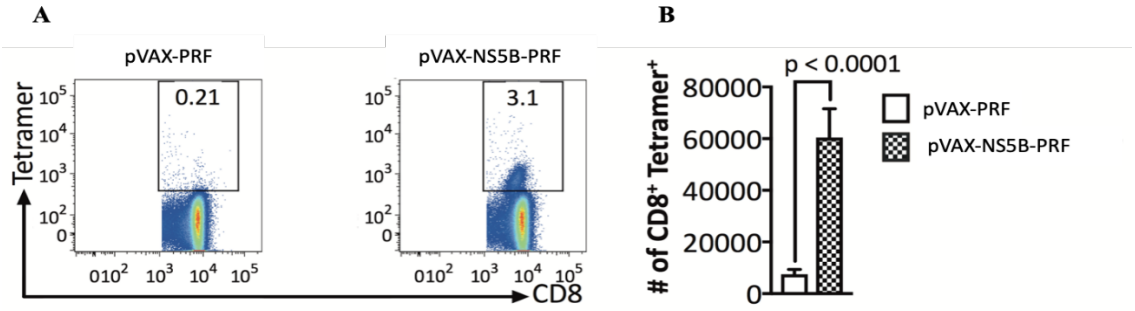

Figure 4.7: Tetramer analysis of NS5B specific $CD8^+$ T cells. Mice were vaccinated with pVAX-NS5B-PRF or pVAX-PRF and isolated splenocytes were stained with APC-$K^d$$NS5B_{451-459}$ for 45 minutes at room temperature. A) Representative plot of tetramer positive $CD8^+$ T cells. B) Comparison of the number of tetramer positive $CD8^+$ T cells between pVAX-NS5B-PRF and pVAX-PRF vaccinated groups (n= 7 per group).

4.4 Discussion

Quantitative parameters are important in understanding the dynamics of a T cell immune response following vaccination [533, 544]. The quantitative analysis of antigen-specific T cell responses has been significantly advanced by the development of MHC-peptide complexes [533]. While

tetramers provide valuable information regarding the number of antigen-specific cells, they fail to provide information about the functionality of these cells [534, 545] and consequently, different methods have been developed to address this limitation [544, 546-550]. *In vivo* CTL killing assays [544, 548, 550, 551] are used to measure the magnitude of the killing response, although, they cannot determine details such as functional avidity. *In vitro* assays like cytokine staining assays and ELISpot peptide dilution assays require *ex vivo* stimulation of host effector T cells which may result in changes in the functional avidity due to a preferential outgrowth of high avidity effector T cells [161]. On the other hand, the FTA technology can provide detailed measurement on multiple parameters of T cell responses in a single animal, *in vivo* [503, 504, 535]. Hence the main aim of this chapter was to determine the immunodominant epitopes of HCV gt3a NS5B using FTA technology and to develop a MHC-peptide tetramer for the analysis of NS5B-specific CTL.

Initially it was necessary to identify NS5B peptides recognised by $CD8^+$- and $CD4^+$- T cells. The mapping process basically involved the transfer of fluorescently labelled, peptide loaded naïve splenocytes to mice vaccinated with either pVAX-NS5B-PRF or pVAX-PRF as described in Chapter 2 section 2.2.10 [503, 504]. $CD8^+$ T cell epitopes were identified based on the specific killing or loss of FTA target cells. The efficiency of the killing response was based on the relative ratio of target cells recovered from vaccinated mice compared to the ratio in unvaccinated mice [535, 552]. From a previous report it was noted that pool 3 of NS5B was the immunodominant region that was targeted by $CD8^+$ T cells [288]. Accordingly, individual peptides from P3 were loaded onto FTA cells to identify the most immunodominant peptide. From flow cytometry analysis it was evident that the loss of FTA cells loaded with P3 was similar to the published data [288]. More specific analysis determined that P69 and P70 were the main targets for CTLs. Particularly, the loss of target cells pulsed with P69 was comparable to the loss of target cells pulsed with the entire P3 peptides both in the liver and the spleen of vaccinated mice. CTL killer

responses of cells pulsed with P69 is not higher than the killer responses of cells pulsed with P3, because the concentration of P69 in both situations was the same.

$CD4^+$ T cell-mediated B cell help was assessed based on the expression of CD69 on FTA $B220^+$ cells [504]. P77 from P3 resulted in a high level of CD69 expression on FTA B cells in the spleen but not in the liver. It is also known that target cells pulsed with P3, which also include FTA B cells, are killed by $CD8^+$ T cells, and this may cause low GMFI of CD69 from target cells due to the low number of cells recovered from vaccinated mice. In addition, from the previous report it was shown that target cells pulsed with NS5B P2 expressed a relatively higher level of GMFI of CD69 [288]. Hence, it was necessary to screen P2 of NS5B to identify peptides of $CD4^+$ T cell targets. Accordingly, target cells pulsed with P2 showed higher GMFI of CD69 and individual peptide analysis revealed that P36 resulted in a significantly higher level of CD69 expression. Peptides in P1 were not screened for the presence of T- cell epitopes because it was previously shown that FTA analysis of P1 loaded target cells were neither significantly lost nor express high level of CD69 [288]. The results obtained, for P2 and P3, in this chapter are also consistent with the previous report [288].

The second aspect of this chapter described the synthesis of an MHC-I tetramer complex that specifically binds to NS5B specific $CD8^+$ T cells. The peptide required for this process is a short amino acid sequence, usually 8-11 amino acids, representing a small portion of the entire antigen [553, 554]. Hence the identification of these immunologically-relevant regions of an antigen is important for the development of methods to monitor T cell responses [555].

The MHC-I-peptide complex was synthesised to track NS5B specific $CD8^+$ T cells and consequently immunodominant peptides recognised by CTL were used as input. P69 and P70 share an 11mer amino acid sequence from which nine amino acids of the sequence were used for the tetramer synthesis. The peptide prediction was performed using the immune epitope data base

(IEDB) analysis resource Consensus tool [556] which combines predictions from ANN aka NetMHC (4.0) [554, 557, 558], stabilised matrix method (SMM) [553] and Comblib [559]. Before the sequence was sent for tetramer synthesis, the peptide manufactured based on this sequence was tested in FTA analysis. Accordingly, the specific loss of FTA target cells loaded with the $NS5B_{451-459}$ peptide was comparable to the specific loss of FTA cells loaded with peptide 69 or pool 3. The tetramer was also tested in a pilot experiment for its specificity to NS5B specific $CD8^+$ T cells and the results showed insignificant non-specific staining from unvaccinated mice.

4.5 Conclusion

The results in this chapter reported the identification of T cell epitopes of gt3a HCV NS5B using FTA technology. From the analysis, two CTL peptides and two T helper cell peptides were identified. In addition, a nine amino acid sequence $NS5B_{451-459}$ peptide was also identified; a MHC-I tetramer, specific to NS5B-specific $CD8^+$ T cells, was synthesised based on this peptide and was shown to detect HCV-specific CTL.

5 Chapter 5: Prime/trap vaccination strategy to induce liver resident memory T cells against HCV

5.1 Introduction

Although circulating memory $CD8^+$ T cells, which comprise T_{CM} and T_{EM} subsets, have protective roles against pathogens, their ability to contain localised infections in tissues and non-lymphoid organs such as the liver is inferior compared to T_{RM} cells [428, 455]. One of the main reasons for this is the delay in generating a robust inflammatory response required to recruit substantial numbers of T_{CM} and T_{EM} cells from the circulation to infected tissues [411]. The presence of robust numbers of $CD8^+$ T_{RM} cells which reside in tissues for the lifespan of an individual obviates the requirement of a significant inflammatory response as these cells are well positioned to encounter and eliminate infected cells in tissues soon after infection occurs [560]. The ability of $CD8^+$ T_{RM} cells to rapidly control infections in tissues such as the skin, brain, eyes, reproductive tract, the gastrointestinal tract, liver and the lungs has been well established [485-489] making the induction of these cells for T cell based vaccines highly desirable.

Recent seminal studies have highlighted the importance of liver resident T cell responses in controlling and eliminating infections with hepatotropic pathogens [413, 455, 490, 561].

T_{RM} cells were established in the liver following vaccination of mice with radiation attenuated sporozoites of *Plasmodium berghei* ANKA (PbA). In an attempt to expand these cells in the liver, a prime-trap vaccination strategy was used [455]. The strategy involved priming of malaria specific $CD8^+$ T cells by using anti-Clec9 antibody-conjugated sporozoite antigen followed by IV vaccination of mice with rAAV encoding the vaccine antigen [455]. T_{RM} cells induced following this strategy provided sterilising immunity against *P. berghei* challenge [455]. In a human clinical trial, IV delivery of radiation-attenuated *Plasmodium falciparum* sporozoites (PfSPZ) had a cumulative protective efficacy of 55% against repetitive controlled human malaria infections and durable protection against infection was observed for as long as one year [471].

Analysis of immune correlates for protection of the PfSPZ vaccine in non-human primates revealed that protection was strongly correlated with an increased frequency of IFN-γ producing $CD8^+$ T cells in the liver compared with the blood (*i.e.* in circulation). In fact, the frequency of IFN-γ producing $CD8^+$ T was strikingly higher (100 fold) in the liver than in the blood [471].

These studies suggest that T_{RM} cells in the liver can be protective against hepatotropic pathogen infections and it is likely that these cells will also provide protection against HCV given that HCV, like *Plasmodium* species, infects hepatocytes. Furthermore, HCV infection appears to be mediated by one or a few variants, referred to as transmitted/founder (T/F) viruses, approximately 100 days before a pool of virus quasi-species emerges [562] making the rapid elimination of HCV extremely desirable. Hence, a vaccine that will induce CMI in the liver is expected to be of paramount importance to prevent the development of persistent virus infection. Thus, the prime/trap strategy as exploited by Ferndandez-Ruiz *et al* [455] described above will be adapted using cytolytic DNA (pVAX-NS5B-PRF) to prime HCV-specific T cells and rAAV-NS5B-2A-eGFP, constructed in Chapter 3, to trap the primed cells and encourage these cells to become resident in the liver. The following chapter describes the outcomes of this strategy.

5.2 Aims

1. Assess HCV-specific memory CMI responses following prime/trap vaccination *in vivo*
2. Evaluate whether prime/trap vaccination elicits HCV-specific $CD8^+$ T_{RM} cells

5.3 Results

5.3.1 Vaccination strategy

- The results presented in this chapter are derived from a prime/trap vaccination strategy performed as depicted in Figure 5.1. Female BALB/c mice were immunised twice ID with a 50 µg dose of pVAX-NS5B-PRF at fortnightly intervals. Two days after the first pVAX-NS5B-PRF vaccination, the mice were immunised IV with the rAAV-NS5B-2A-eGFP at a dose which results

in ~10% transduction of hepatocytes. Due to the complexity of the experiment in vivo titration of rAAV-NS5B-eGFP in mice was conducted only once.

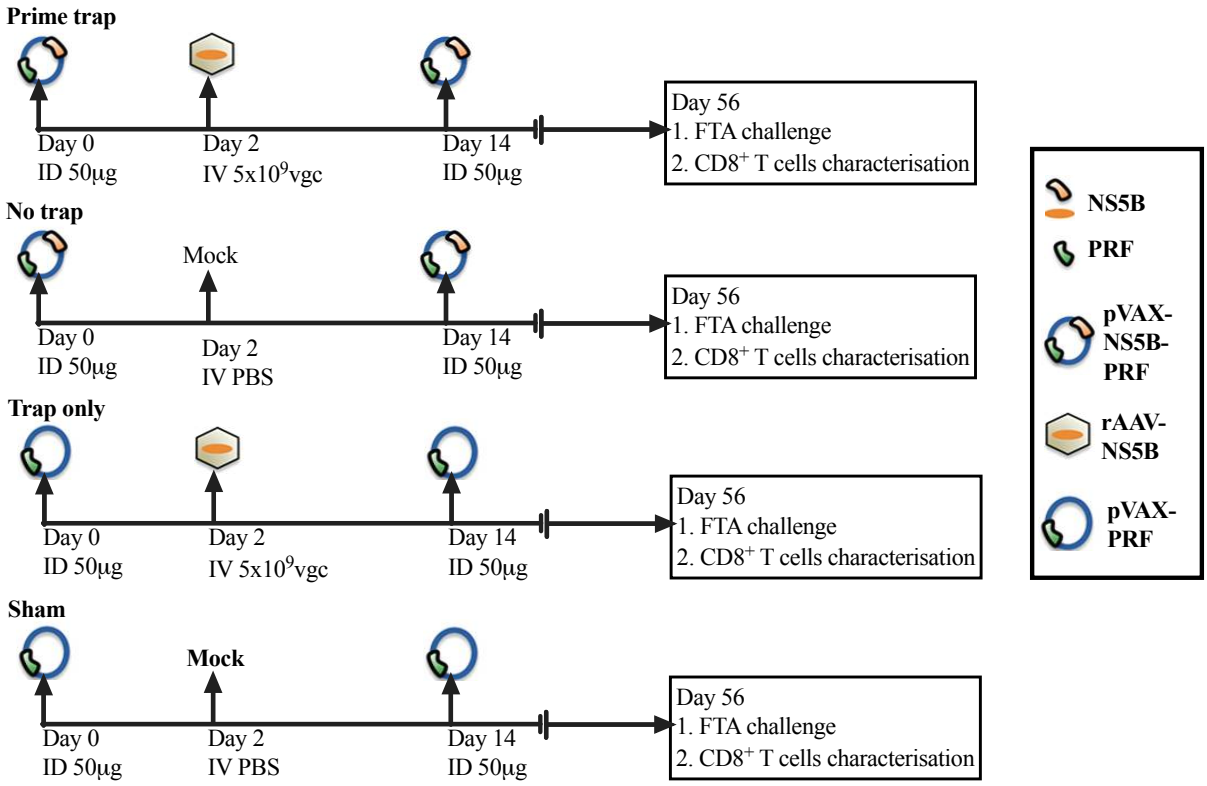

Figure 5.1: The vaccination schedule to test the ability of a prime/trap strategy to induce T_{RM} cells in the liver. Mice were vaccinated ID with two doses of 50 µg DNA (pVAX-NS5B-PRF or pVAX-PRF) fourteen days apart. Two days after the first DNA vaccination, mice received either rAAV-NS5B or PBS via the IV route. Forty-two days (*i.e.* 'Day 56' in the diagram) after the second DNA vaccination the mice were challenged with an FTA. In other experiments with the same vaccination groups and schedules, NS5B-specific $CD8^+$ were used characterised for their memory phenotype.

This vaccination schedule (Figure 5.1) was selected based on a previous prime/trap vaccination strategy for malaria [455], although the trapping agent was introduced two days after the first vaccination and a DNA boost was introduced 14 days after the first vaccination. The second DNA boost was introduced because it is known that rAAV can persist for up to 3 weeks [382]

which means introducing a second DNA vaccination will cause priming of new CD8 T cells which in-turn became T_{RM} cells due the persistent nature of rAAV. As described in Chapter 3, section 3.2.1.7, $5x10^9$ vgc of rAAV-NS5B resulted in transduction of 10.6% mouse hepatocytes and hence this dose was used as a trapping dose. Forty-two days after the final DNA vaccination, some of the mice were challenged with a FTA while others were analysed for the expression of tissue residency markers (CD69, CXCR3 and CD11a) using flow cytometry.

5.3.2 Functional assessment of *in vivo* cell mediated immune (CMI) response following prime/trap strategy

The FTA to assess CMI responses *in vivo* were prepared from naïve autologous splenocytes pulsed with either 10 μg/ml of NS5B P1, P2 or P3 peptides or titrated concentrations (0.001, 0.01, 1 or 10 μg/ml) of peptides 36, 77, 69 or the $NS5B_{451-459}$ peptide (Figure 5.2.).

FTA target cells loaded with the different peptide pools and recovered from vaccinated mice showed that the highest *in vivo* killer responses were directed against P3 of NS5B in all mice vaccinated with pVAX-NS5B-PRF and/or rAAV-NS5B-2A-eGFP (Figure 5.3) which is consistent with results reported previously by our group (13). The robust responses elicited by the trap only group authenticate the use of the rAAV and confirm that NS5B was expressed *in vivo*. Furthermore, prime/trap and trap only vaccinated mice exhibited the greatest CTL responses against targets loaded with each of the peptide pools (P1-P3) or P69 or $NS5B_{451-459}$ peptide (Figure 5.3). There were no differences in the NS5B-specific CTL responses observed between the prime/trap and trap only vaccinated groups. Both vaccination strategies resulted in > 95% killer response against P3 in the liver and the spleen. When compared to these two vaccination strategies, vaccination with no trap (two 50μg doses of DNA) resulted in significantly lower (P <0.01 both in the liver and spleen) killer responses against P3 (40% in the liver and 60% in the spleen) (Figure 5.3A).

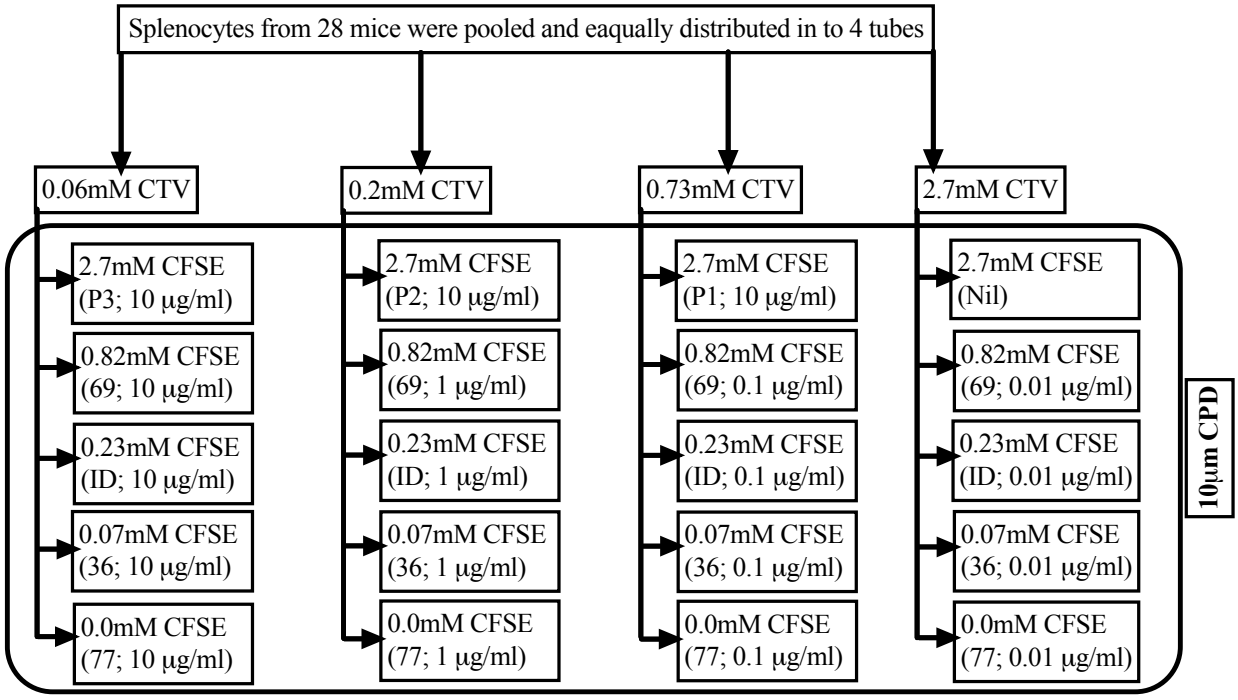

Figure 5.2: Preparation of FTA cells: Splenocytes from syngeneic naïve BALB/c mice were pooled and stained with different concentrations and combinations of CTV and CFSE as shown. Subsequently, the fluorescently bar-coded cells were pulsed with titrated (0, 0.01, 0.1, 1 and 10 μg/ml) concentrations of the indicated peptides or peptide pools. Following peptide loading, all target cells were labelled with 10 μM CPD to delineate the transferred cells from the endogenous population of cells found in FTA challenged mice.

One of the important advantages of the FTA technology is that it allows the analysis of the functional avidity or sensitivity of antigen-specific $CD8^+$ T cells *in vivo* [503] which was evaluated in this experiment using FTA target cells loaded with titrated concentrations of peptides 69 and $NS5B_{451-459}$. Accordingly, the prime/trap or trap only vaccinated mice showed higher avidity (sensitivity) killer responses compared to other groups as only mice in these groups elicited responses against targets loaded with the lowest concentration of peptide 69 {i.e. 0.1μg/ml (P = 0.003 relative to no trap group) and 0.01μg/ml (P = 0.017 relative to no trap

group)} (Figure 5.3B). The highest avidity response was detected against $NS5B_{451-459}$ peptide and the response showed no decline in targets loaded with 0.01 μg/ml.

Clinical data suggest that a robust correlate of recovery from acute HCV infection is the presence of $CD4^+$ T_H cells that could mobilise $CD8^+$ T cell responses [160]. Effector/memory $CD4^+$ T_H cells co-stimulate B ($B220^+$) cells presenting cognate antigens resulting in the up-regulation of CD69 on $B220^+$ cells [503]. Hence, although measuring T_H responses following vaccination is important to assess the effectiveness of a vaccine, the prime/trap strategy described in Fernandez-Ruiz *et al*. [455] did not assess the contribution of T_H cell responses as their strategy was primarily designed to elicit $CD8^+$ T_{RM} cells. To address this aspect of the response in the vaccinated mice (Figure 5.1) T_H cell responses were measured against the mapped immunodominant peptides 36 and 77 as well as P2 of NS5B.

Mice vaccinated using the prime/trap approach (P= 0.002 and P= 0.01) and mice vaccinated with the trap only (P= 0.009 and P=0.026) elicited the highest magnitude of $CD4^+$ T_H cell responses to P2 as compared to the no trap group. With respect to the immunodominant T_H epitopes, P36 and P77, significant differences in T_H cell responses were observed when the FTA cells were loaded with at least 1μg/ml peptide (Figure 5.4B). When FTA cells were loaded with 1μg/ml of P36 or P77, a significantly higher GMFI of CD69 was observed in the spleen of prime/trap (P<0.01) and trap only (P<0.01) vaccinated group as compared to the no trap group. However, in the liver FTA cells loaded with 1 μg/ml of either P36 or P77 did not result in a significant difference in the expression of CD69 between the trap only or the prime/trap vaccinated mice and the no trap vaccinated mice. When FTA cells were loaded with 10 μg/ml of P36 or P77 significant upregulation of CD69 was observed in the trap only vaccinated mice (P = 0.006) as compared to the no trap vaccinated mice. CD69 expression on FTA cells loaded with P3 was not assessed as almost all of these cells were killed by $CD8^+$ T cells.

Overall, FTA analysis revealed that prime/trap and trap only vaccination strategies induced superior intrahepatic and systemic CMI than the no trap vaccination strategy

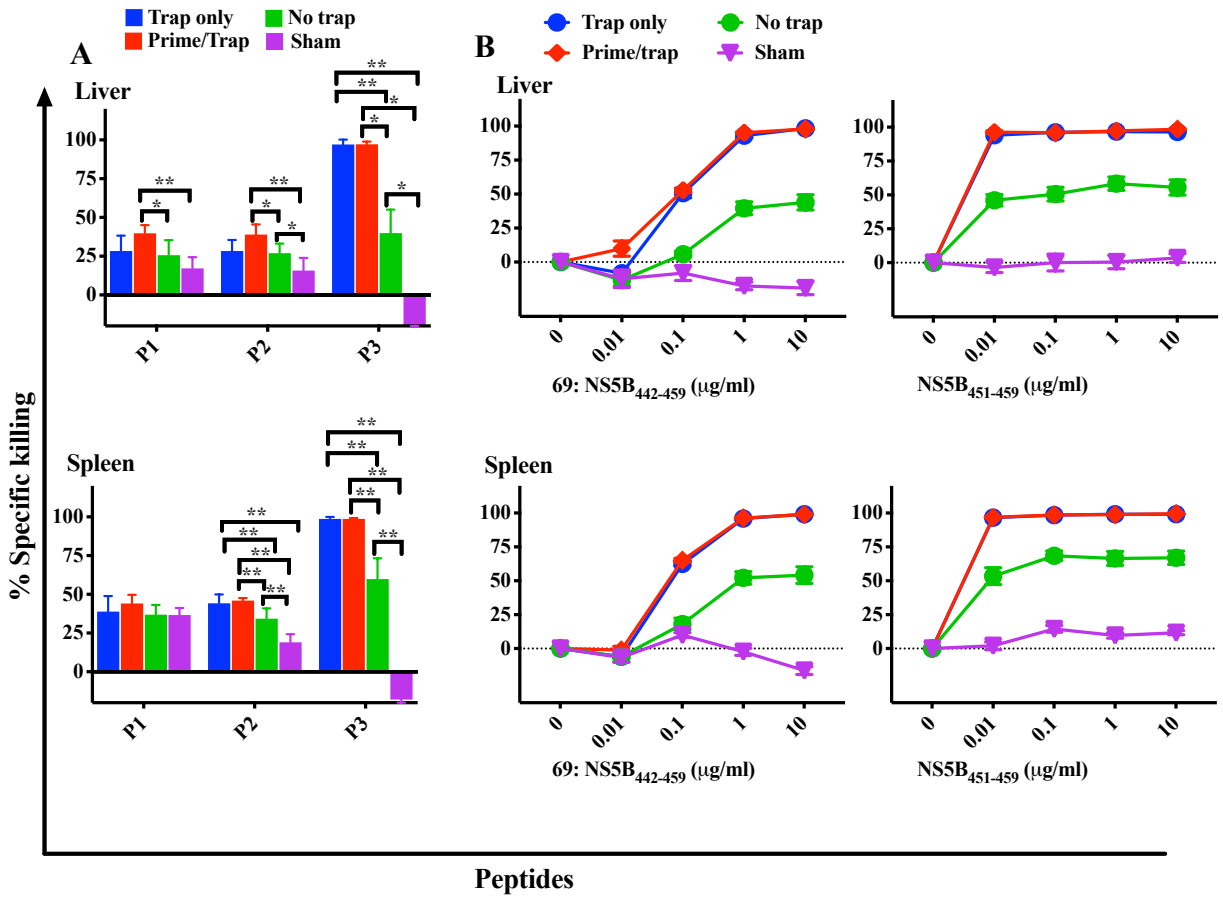

Figure 5.3: FTA analysis of *in vivo* NS5B specific CTL response following vaccination of mice. *In vivo* CTL responses were determined following vaccination of mice using a prime/trap, trap only or no trap (2x DNA only) vaccination regimen. The immune responses were examined 42 days after the final DNA vaccination using FTA technology. A) Bar graphs showing the means (n=7) and SEM of gt3a-specific CTL responses against target cells loaded with 10 µg/ml of NS5B P1, P2 or P3. B) P69 ($NS5B_{442-459}$) and $NS5B_{451-459}$ were titrated and loaded on to FTA cells to assess the avidity of induced CTLs. (**P* <0.05, ***P* <0.01).

5.3.3 The prime/trap vaccination strategy induces high frequency of intrahepatic NS5B specific $CD8^+$ T cells

The frequency of NS5B-specific $CD8^+$ T cells induced following prime/trap vaccination was analysed using the $K^dNS5B_{451-459}$ tetramer and flow cytometry. Double discriminated viable $K^dNS5B_{451-459}$ $tetramer^+$ $CD8^+$ cells were gated, and analysis of these cells revealed that the majority were found in the liver of mice vaccinated with the prime/trap or the trap only strategy (Figure 5.5A). The percentage and absolute number of NS5B-specific $CD8^+$ T cells were significantly higher in mice vaccinated with the prime/trap or trap only strategy compared with mice that were vaccinated with the no trap vaccination strategy which mainly induced systemic immunity.

The absolute number of $tetramer^+$ $CD8^+$ T cells (includes T_{CM}, T_{EM} and T_{RM} cells) in the liver of prime/trap and trap only vaccinated mice was ~8.7 times and ~38 times higher, respectively, than the cells in the no trap vaccinated mice (P= 0.009 and P = 0.004) (Figure 5.5B). However, a statistically significant difference in the number of systemic (spleen) NS5B specific $CD8^+$ T cells was not observed between these three vaccination strategies, although there was an increasing trend in the number of cells in those mice that received rAAV-NS5B-2A-eGFP (Figure 5.5B). It is likely that statistical significance would be achieved with greater numbers of vaccinated mice.

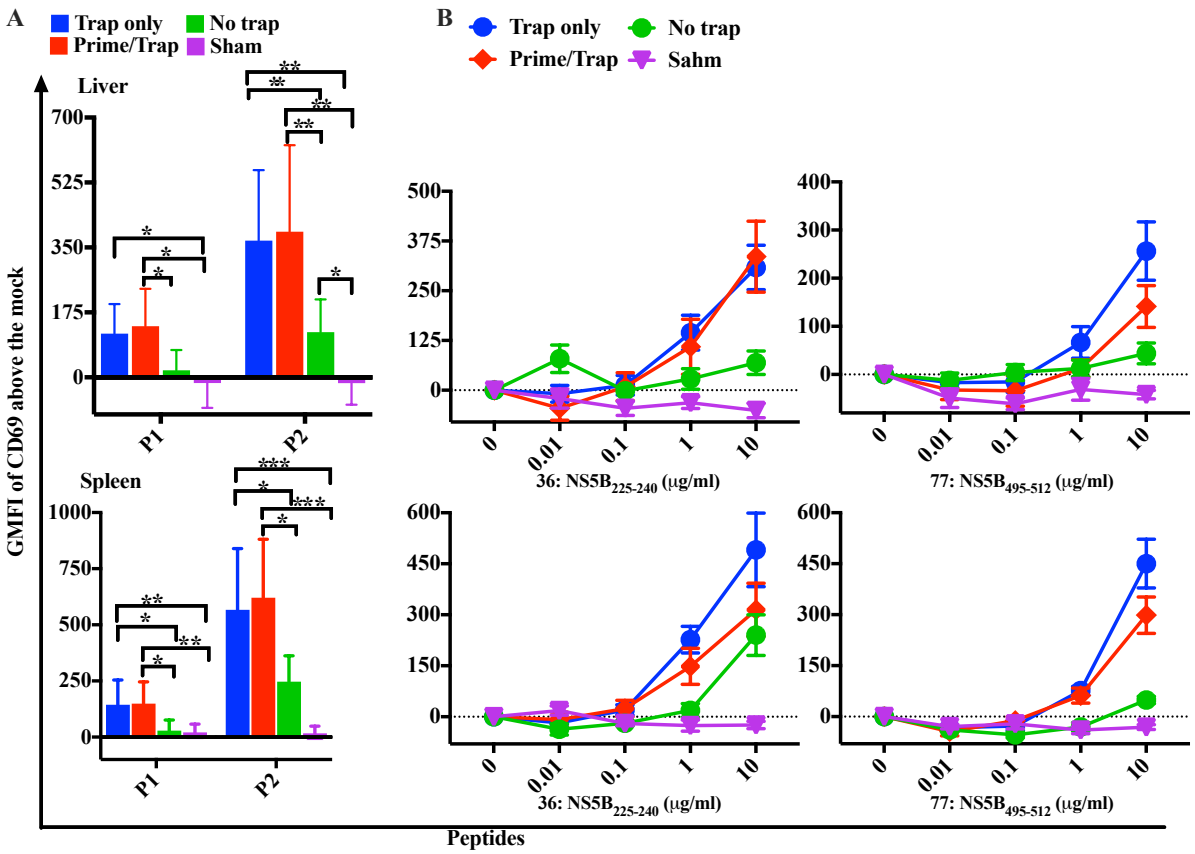

Figure 5.4: FTA analysis of *in vivo* NS5B-specific T_H cell responses. The *in vivo* T_H response was determined following vaccination of mice using a prime/trap, trap only or no trap vaccination regimen. A) Bar graphs showing the means (n=7) and SEM of GMFI of CD69 expression on FTA B cells pulsed with 10µg/ml of P1 or P2. B) FTA cells were pulsed with titrated concentrations of peptide 69 or 77 and the GMFI of CD69 was determined. (*P <0.05, **P <0.01).

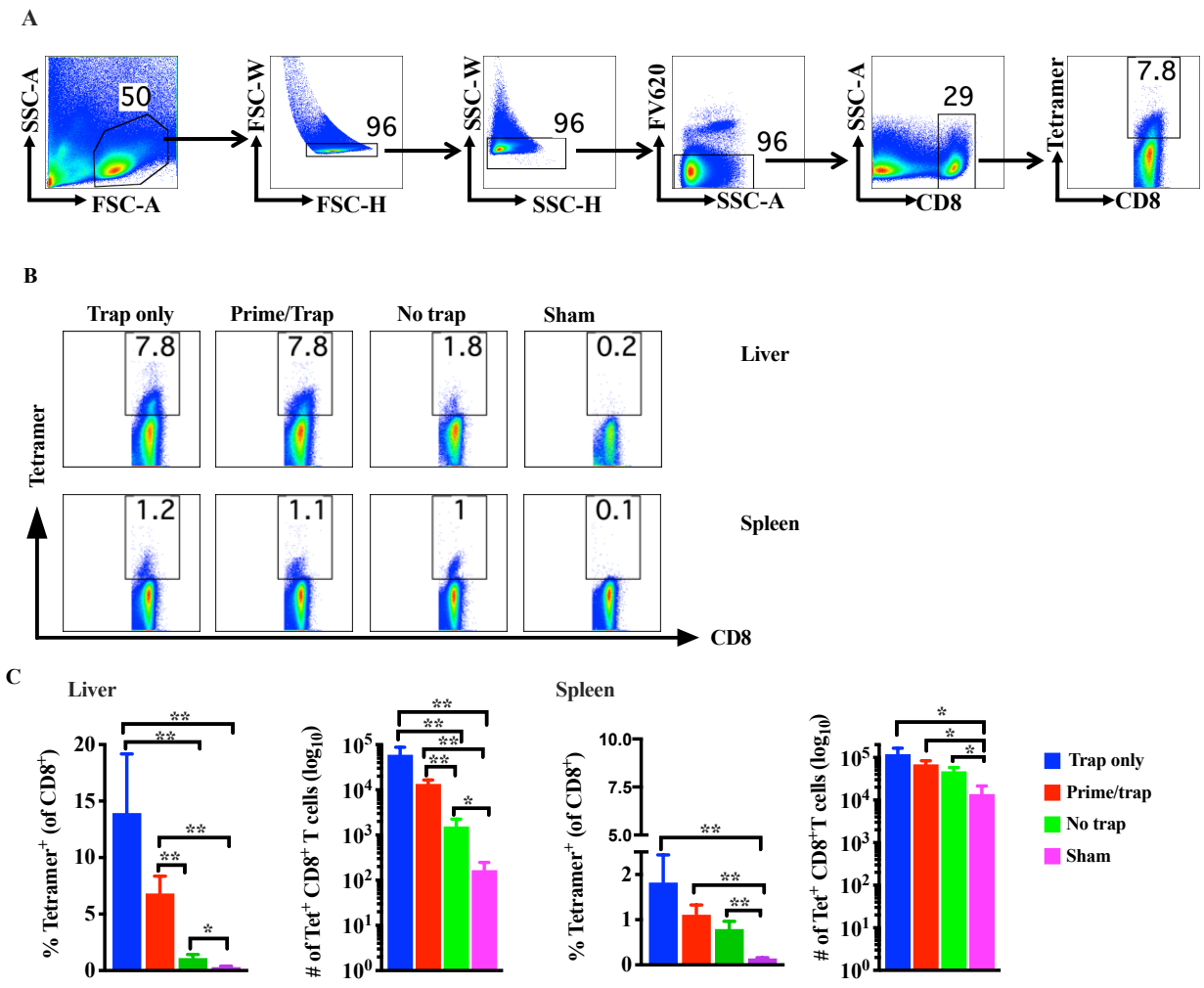

Figure 5.5: The frequency of NS5B specific CD8$^+$ T cells in the liver and spleen. A) Gating strategy to identify tetramer positive CD8$^+$ T cells. Lymphocytes were identified by sequential gating SSC-A/FCS-A followed by FSC-W/FSC-H and SSC-W/SSC-H. Dead cells were discriminated using FV620 staining and CD8$^+$ T cells were gated on live cells. Tetramer positive cells were gated on CD8$^+$ T cells. B) Representative dot plots showing the percentage (in gates) of $K^dNS5B_{451\text{-}459}$ tetramer$^+$CD8$^+$ T cells C) Percentage and absolute number of NS5B specific CD8$^+$ T cells in the liver and spleen of mice vaccinated with the different regimens (*P <0.05, **P <0.01).

In general, in mice vaccinated with the prime/trap or trap only strategy virtually all the CD8$^+$ T cells were NS5B specific suggesting that the introduction of rAAV-NS5B was crucial to elicit high numbers of liver-resident NS5B specific CD8$^+$ T cells.

5.3.4 The prime/trap vaccination strategy induces high frequency of NS5B-specific T_{RM} cells in the liver

The next logical step to characterise NS5B-specific $CD8^+$ T cells was to assess their phenotype for the expression of different markers specific to T_{RM} cells. Liver T_{RM} cells up-regulate CD69 and down-regulate CD62L [455]. Following sequential gating on $tetramer^+$ $CD8^+$ T cells, the cells were plotted based on CD69 and CD62L expression (Figure 5.6A). As depicted in the representative plot, the majority of the NS5B-specific $CD8^+$ T cells in the liver of mice vaccinated with either the prime/trap or trap only strategy were T_{RM} cells ($CD69^+CD62L^-$) (Figure 5.6 A). On the other hand, in mice vaccinated with the no trap vaccination regimen, the majority of the NS5B-specific $CD8^+$ T cells were T_{EM} cells (CD69-) that were mainly found in the spleen. The results also revealed that all mice vaccinated with prime/trap or trap only strategy showed a high percentage of NS5B-specific T_{RM} cells in the liver (Figure 5.6 B). The absolute number of NS5B specific $CD8^+$ T_{RM} cells was significantly higher in the liver of mice vaccinated with the prime/trap (P = 0.003) or trap only (P = 0.003) strategy as compared to the no trap vaccinated group (Figure 5.6C).

Liver $CD8^+$ T_{RM} cells are also known to express high levels of CD11a ($CD11a_{hi}$) and CXR3 [561]. Consequently, expression of CD11a and CXCR3 was also analysed by assessing the GMFI of these markers (Figure 5.7). Accordingly, statistically significant upregulation of CD11a was observed in NS5B-specific T_{RM} cells induced by the trap only- (P = 0.004 as compared to the sham control; P= 0.003 as compared to the no trap vaccination) or the prime/trap- vaccination regimen (P = 0.003 as compared to sham only control; P= 0.002 as compared to the no trap vaccination). There was no significant upregulation of CD11a by T_{RM} cells induced by the no trap vaccination as compared to the sham only control. When compared to the sham only control, CD11a was significantly upregulated by T_{EM} cells induced by- the trap only (P= 0.006) or the prime/trap (P= 0.004) or the no trap (P= 0.004) vaccinations. However, there was no difference

in the upregulation of CD11a by T_{CM} cells across the different vaccination groups (Figure 5.7 A). However, analysis of the CXCR3 data showed a high level of background in the sham control. The reason for this was unknown. Flow cytometric analysis showed that in the sham control group, only a small number of events were tetramer$^+$ CD8$^+$ in the liver (Figure 5.5B) while even fewer or no events represented NS5B-specific T_{EM}, T_{RM} and T_{CM} cells (Figure 5.6A). Hence the sham control was excluded during statistical comparisons. Nevertheless, CXCR3 was significantly upregulated by T_{RM} cells resulting from the trap only vaccination (P = 0.004) or prime/trap (P= 0.01) vaccination compared to the no trap vaccination. Differences were not observed in the expression of CXCR3 by T_{CM} or T_{EM} cells across the three vaccination groups (Figure 5.7 B).

Overall, the results suggest that the DNA prime/rAAV trap approach for HCV vaccination elicited CD8$^+$ T_{RM} cells in the liver and significantly improved the magnitude and/or quality of HCV-specific T cell responses *in vivo* compared to a DNA only vaccination regimen which mainly induced systemic immunity. Equally it was evident from this study that vaccination with rAAV-NS5B alone resulted in a similar level of immune response to the prime/trap vaccination strategy.

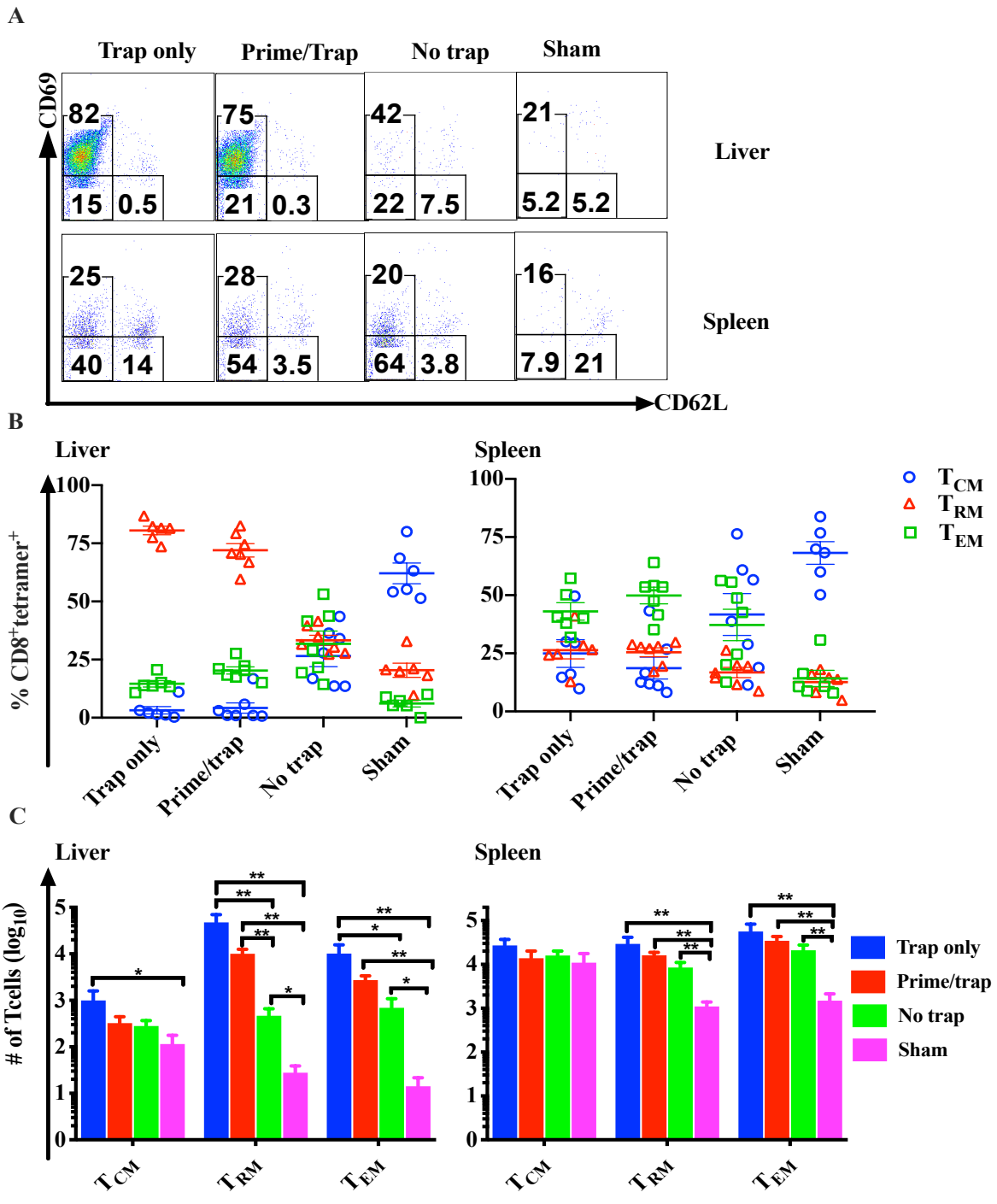

Figure 5.6: The frequency of the different subsets of memory CD8$^+$ T cells. A) Representative (n = 7/group) dot plots showing expression of CD69 and CD62L on gated K^{d}NS5B$_{451\text{-}459}$ tetramer$^+$ CD8$^+$ cells from panel A from Figure 5.5. B) The percentage of each memory T cell subset in individual mice. C) The absolute number of each of the CD8$^+$ memory T cell subsets across different vaccination strategies. (*P <0.05, **P <0.01).

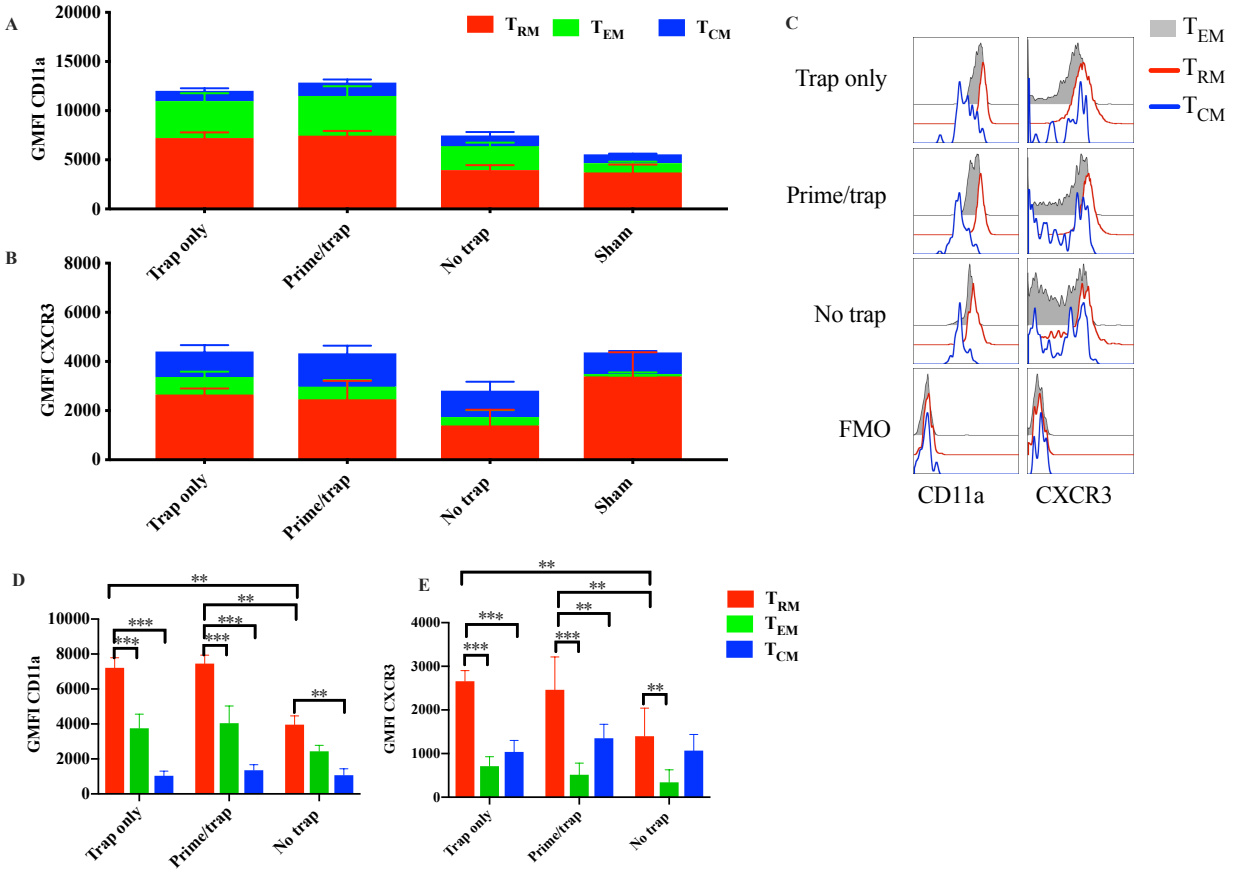

Figure 5.7: Expression of CD11a and CXCR3 on the different memory T cell subsets isolated from the liver of mice vaccinated with different strategies. GMFI of CD11a (A) and CXCR3 (B) expression on the different intrahepatic memory T cell subsets across the vaccination groups. Representative histogram plots (C) show the expression of CD11a or CXCR3 on NS5B-specific $CD8^+$ T_{CM}, T_{RM} and T_{EM} cells. Fluorescent minus one (FMO) plots represent the background staining for CD11a and CXCR3. The GMFI of CD11a (D) or CXCR3 (E) in each vaccine group were compared. Only comparisons between vaccinated groups that had a statistically significant difference are denoted as '** $p < 0.01$ and *** $p < 0.001$'.

5.3.5 Vaccination with rAAV-NS5B-2A-eGFP results in the persistence of NS5B-specific T_{RM} cells in the liver

From the results described above in section 5.2.2 and 5.2.3, it is clear that the no trap (pVAX-NS5B-PRF only) vaccination regimen was less effective than the regimens which included the rAAV-NS5B, particularly with regard to the induction of T_{RM} cells in the liver. This does not mean that the DNA vaccination is unable to induce NS5B-specific $CD8^+$ T cells as it is possible that NS5B specific $CD8^+$ T cells induced from the no trap vaccination strategy were established but not maintained over time. To test this hypothesis, mice were vaccinated as described above (Figure 5.1) but the $CD8^+$ T cell characterisation was performed 7 days after the last DNA vaccination. The results were then compared with the results from the 42 days post vaccination.

As depicted in Figure 5.8, significance differences were observed in the number of $CD8^+tet^+$ cells and T_{RM} cells in the liver of mice that did not receive the trapping agent. The results showed that the number of $CD8^+tet^+$ cells (includes T_{RM}-, T_{CM}- and T_{EM}-cells) detected 7 days after the final vaccination was significantly (P =0.01) higher than the number detected 42 days after the final vaccination. Similarly, the number of T_{RM} cells was significantly higher at day 7 post last vaccination than 42 days post last vaccination. These results suggest the no trap vaccination regimen is capable of inducing antigen (NS5B)- specific $CD8^+$ T cells in general and T_{RM} cells in particular. However, these cells were not persistently maintained as their number decreased significantly 42 days after the last vaccination. On the other hand, in mice groups that received the trapping agent the number of $CD8^+tet^+$ cells showed an increasing trend 42 days post final vaccination, although the difference was not significant. This is also true for the number of T_{RM} cells in these mice groups. This indicates that the trapping agent contributed to the maintenance of cells for longer period of time, for at least 42 days.

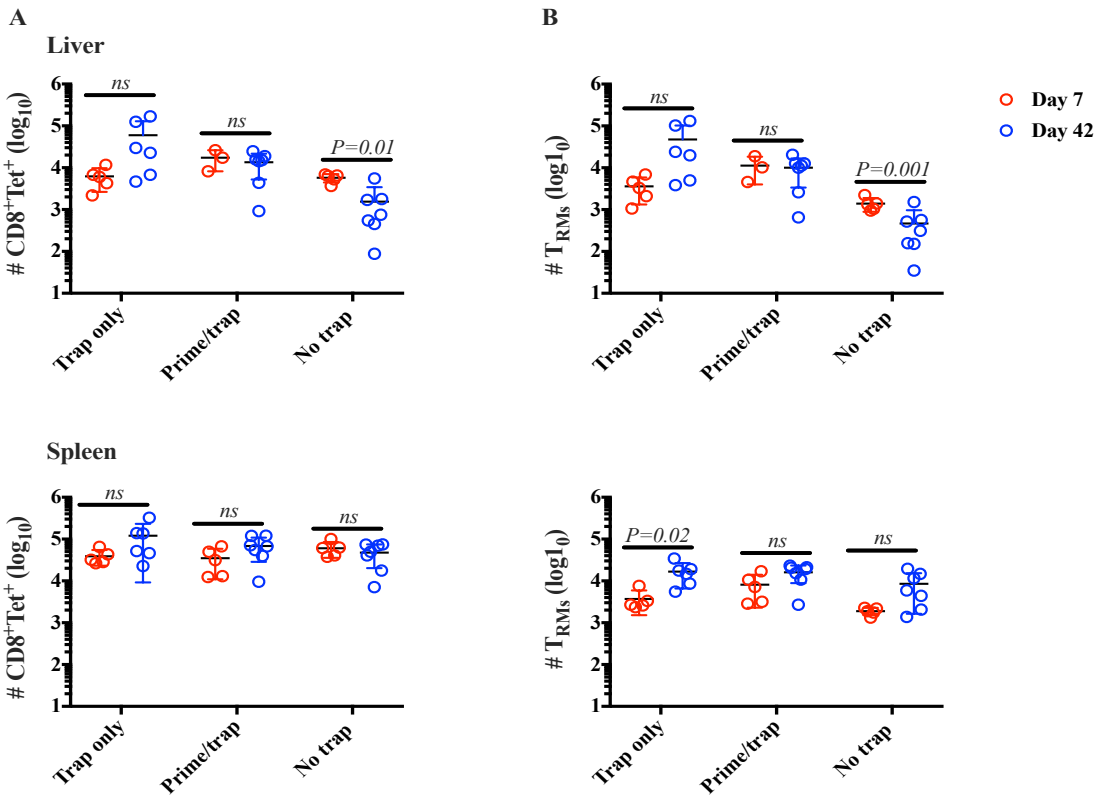

Figure 5.8. A comparison of the frequency of NS5B-specific CD8$^+$ T cells. Mice were vaccinated as described in Figure 5.1 and the results analysed 7 days after the second pNS5B-PRF vaccination were compared with the results from the 42 days post vaccination samples. A. Comparison of CD8$^+$ tetramer$^+$ T cells in the liver and spleen. B. Comparison of T_{RM} cells in the liver and spleen.

5.4 Discussion

In this chapter the use of a prime/trap vaccination strategy to induce HCV-specific liver T_{RM} cells was described. To achieve this a DNA vaccine encoding the cytolytic protein PRF, in addition to the HCV NS5B protein, was used to prime CD8$^+$ T cells. It is acknowledged that one of the limitations of DNA vaccines is their low immunogenicity and their inability to induce durable T cell immunity [563-565].

Consequently, to improve the immunogenicity of DNA vaccines, a cytolytic protein, PRF, was included in the DNA constructs and used to deliberately induce cell death [287, 288, 566-568].

Cytolytic DNA vaccines were proven to be more immunogenic than canonical DNA vaccines in mice [286, 288] and pigs [287]. These vaccines target cross-presenting dendritic cells and as a result induce increased proliferation of antigen-specific $CD8^+$ T cells [568].

Although local antigen deposition and antigen encounter is not essential to elicit $CD8^+$ T_{RM} cells in the skin, the female reproductive tract and the gastrointestinal tract, it is evident that this process leads to the formation of greatest densities of $CD8^+$ T_{RM} cells especially at sites such as the liver and the vagina [455, 474, 569]. Local antigen encounter/deposition also appears to be crucial to elicit $CD8^+$ T_{RM} cells in the liver even in humans [455, 471].

DNA vaccines can be delivered using ID and intramuscular routes in a homologous prime/boost manner without plausible anti-vector immunity and thus can be used as a vector to prime high numbers of circulating antigen-specific T cells which can then be recruited to the liver using vectors that efficiently transduce hepatocytes [455]. Considering the poor immunogenicity of DNA vaccines, it was hypothesised that the "prime/trap" vaccination strategy would be a feasible approach in exploiting DNA (as a priming agent) to elicit HCV specific T_{RM} cells in the liver. To test this hypothesis, pVAX-NS5B-PRF was used to prime HCV specific $CD8^+$ T cells and rAAV-NS5B-2A-eGFP used to trap the primed cells in the liver.

The first section of this chapter showed that the prime/trap and trap only vaccination regimens respectively resulted in superior hepatic and systemic immune responses. As revealed by the FTA challenge experiment, NS5B-specific CTL responses were observed in these groups of mice. Although, this challenge is not an authentic virus challenge model it can be used to assess the effectiveness of the vaccination strategy to induce NS5B-specific $CD8^+$ T cells. To this end, the observed *in vivo* CTL responses confirmed that the immune response induced by these two vaccination regimens was robust and induced high avidity T cells. A previous report showed that

mice which were vaccinated against malaria with the prime/trap vaccination strategy were protected from *P. berghei* infection [455].

Further analysis of the location of the NS5B-specific $CD8^+$ T cells was conducted using tetramer staining of cells isolated from the liver and spleen. Accordingly, a significantly higher proportion of NS5B specific $CD8^+$ T cells was localised in the liver of mice vaccinated with the prime/trap or trap only vaccination strategy. In contrast, the number of cells in the spleen was not significantly different between the groups. This indicates that a single dose of rAAV-NS5B-2A-eGFP was sufficient to attract high numbers of NS5B specific $CD8^+$ T cells into the liver. Similarly, a prime/pull vaccination strategy resulted in a high frequency of antigen specific $CD8^+$ T cells in the vagina while the frequency of systemic antigen-specific $CD8^+$ T cells in the spleen was not significantly changed [495].

Phenotypically, T_{RM} cells are $CD69^+CD62L^-$ cells [455, 461]. The results from this study also showed that NS5B-specific $CD8^+$ T_{RM} cells isolated from the liver of mice vaccinated with prime/trap or trap only vaccinations were $CD62L^-CD69^+$. Other markers of T_{RM} cells like CXCR3 and CD11a [433, 434] were also highly expressed by these cells. On the other hand, the phenotype of cells in mice vaccinated with the no trap strategy showed a higher frequency of T_{EM} cells and this was more pronounced in the spleen than the liver, confirming the results of a previous study [455].

The introduction of the trapping agent in the current vaccination strategy contributed to the high frequency of NS5B specific $CD8^+$ T cells in general and T_{RM} cells in particular in the liver of mice consistent with the fact that local antigen deposition is crucial to elicit $CD8^+$ T_{RM} cells in the liver [455, 471].

Studies in mice and humans suggest that IV immunisation is the most efficient route to facilitate local antigen encounter in the liver [382, 471, 570]. Imaging of live mice injected ID or IV with

P. berghei sporozoites suggested that the sporozoites were reproducibly detected in the liver only after IV injection, while the parasite load in the liver was 30-fold higher in the IV injected mice [570]. The same study also showed that IV compared to ID injection of irradiated sporozoites elicited a significantly higher proportion of $CD62L^-$ memory $CD8^+$ T cells and increased protection against live sporozoite challenge [570]. ID, SC and intramuscular immunisation of humans with radiation-attenuated *P. faliciparum* sporozoites (PfSPZ) also appeared to elicit suboptimal immunity and protection against malaria compared to IV vaccination [471, 571]. Analysis of vaccinated non-human primates suggest that the increased efficacy of IV PfSPZ vaccination in humans correlated strongly with the ability of this vaccine to elicit long lived liver-resident $CD8^+$ T cells [471, 571]. Furthermore, transduced hepatocytes have the capacity to present AAV-encoded antigens to $CD8_+$ T cells following IV vaccination with AAV [382] and analysis of liver biopsies from end stage hepatitis C patients suggest that HCV infection elicits $CD11_{hi}$ memory $CD8^+$ T cells [572]. Collectively these findings are consistent with our findings which showed that ID vaccination with pVAX-NS5B-PRF was less efficient in eliciting intrahepatic T cell immunity and $CD8^+$ T_{RM} cells compared to IV rAAV-NS5B vaccination.

5.5 Conclusion

In this chapter the contribution of a prime/trap or trap only vaccination strategy to induce a robust CMI against HCV is described. As a result of the rAAV-NS5B-2A-eGFP introduction to the liver, a high frequency of NS5B specific T_{RM} cells was observed in the liver. The efficacy of a DNA vaccine to develop a T cell-based vaccine against HCV will likely rely on its ability to elicit robust immune response in the liver. Considering the poor immunogenicity of DNA vaccines this seems difficult to achieve unless a strategy is designed to overcome this situation. In this regard the prime/trap vaccination strategy described in this chapter could be a potential strategy to elicit HCV specific T_{RM} cells in the liver that can act as a frontline defence against the virus.

6 Chapter 6: General Discussion

Vaccines are of great public health importance and the previous success of the smallpox and poliovirus vaccines suggest that vaccination is a cost-effective means to eliminate HCV infections worldwide [243].

A recent mathematical modelling study used empirical data to simulate HCV transmission amongst people who inject drugs and showed that an effective vaccine could reduce transmission rates by >90% during the first months of exposure in vaccinated individuals compared to naïve individuals [573]. An effective vaccine is considered essential to meet the WHO's Sustainable Development Goal of eliminating 90% of global hepatitis C incidence and viral hepatitis as a major public health threat by 2030 [574]. However, there is no licensed vaccine for HCV. The inability to reliably induce rare immune correlates of protection following vaccination and the lack of convenient animal models permissive to infection are significant issues that have contributed to this fact [252, 575]. After two decades of unsuccessful preclinical studies and Phase I HCV vaccine trials, the current lead candidate is an NIH-sponsored Phase IIb, placebo-controlled trial in high risk people who inject drugs utilising a prime-boost regimen of gt1 NS antigens delivered via ChAd and then modified vaccinia virus Ankara. However, this vaccine only induces systemic T cell immunity to gt1b antigens [284]. Assuming that the AAV alone is equally effective as the ChAd/MVA vaccine (although the efficacy of neither has been determined), then the AAV vaccine will be more cost effective.

The efficacy of any HCV vaccine based on CMI will be dependent on the speed of T cell migration to the liver and consequently a vaccine which elicits and maintains intrahepatic HCV-specific $CD8^+$ T_{RM} cells and $CD4^+$ T cell immunity has an intrinsic advantage as the immune cells are resident in the liver. Robust liver-resident $CD8^+$ T cell response elicited following vaccination were shown to be crucial for protection against controlled human malaria infection in humans [471] and *P.berghei* infection in mice [455].

Consequently, in this thesis, pre-clinical evaluation of a vaccination strategy to elicit intrahepatic HCV-specific $CD8^+$ T_{RM} cells is described for the first time. The strategy involved ID vaccination of mice with pVAX-NS5B-PRF followed by IV vaccination with rAAV-NS5B-2A-eGFP to improve $CD8^+$ killer T cell and $CD4^+$ helper T cell responses in vaccinated mice. A previous study exploiting AAV as a vector to elicit intrahepatic immunity used AAV encoding minitopes and TCR transgenic T cells to evaluate resident $CD8^+$ T cell response in adoptive transfer setting [455]. The study described in this thesis exploited vaccine vectors encoding codon-optimised gt3a full length NS5B protein and evaluated T cell immunity in a polyclonal repertoire in wild-type mice. Furthermore, the study described the use of a novel FTA assay to map immunodominant $CD4^+$ T helper cell and $CD8^+$ T cell epitopes of gt3a NS5B *in vivo* unlike previous studies which used *in vitro* peptide stimulation assays to map T cell epitopes. Poor survival of liver resident T cells, particularly $CD8^+$ T_{RM} cells, following *in vitro* peptide stimulation highlights the importance of exploiting the FTA assay. The *in vivo* epitope mapping analysis led to the development of a functional MHC-I tetramer and the identification of NS5B-specific $CD4^+$ T helper cell immunodominant peptides. The prime/trap vaccination strategy improved $CD8^+$ T killer cell and T_H cell responses in vaccinated mice as determined using tetramer and FTA challenge analysis. This was observed both in systemic (spleen) and intrahepatic T cell responses. However, the avidity and magnitude of systemic and intrahepatic T cell responses elicited were similar following trap only vaccination compared to the prime/trap vaccination.

6.1 AAV vector as a vaccine

Viral vectors are capable of inducing outstanding antibody responses and also elicit CTL that are crucial for control of intracellular pathogens [576]. The immune responses generated from viral vector vaccines are directed against the encoded heterologous antigen as well as the vector itself [577]. Thus, concerns associated with pre-existing immunity to-and the strong immunogenicity of- viral vectors are main barriers to the use of viral vectors in vaccine formulations [577]. Despite

these limitations, Adenovirus and pox virus based viral vector vaccines are the most widely investigated recombinant vaccines [506, 577-579].

The use of rAAV vectors has been explored since the first report by Manning *et al*. that documented the ability of intramuscular rAAV to induce a strong humoral and cellular responses against HSV type 1 glycoprotein B [580]. The overall absence of toxicity in rAAV-mediated gene therapy made AAV vectors attractive vectors in vaccine development [506]. rAAV vectors were evaluated in the development of vaccines for HIV [581, 582] and were able to reach to Phase I clinical trial [583]. Intranasal and intramuscular administration of rAAV encoding HIV env, tat and rev resulted in the production of high levels of HIV-specific antibodies [508]. Later oral administration of rAAV encoding HIV env was shown to induce local and systemic CMI and partially protected mice against rectal challenge with recombinant vaccinia virus encoding the HIV env [581]. A more advanced study in macaques investigated the efficacy of rAAV vectors encoding simian immunodeficiency (SIV) proteins [582]. This study demonstrated that a single vaccination induced robust T cell and antibody responses which were protective against low dose IV SIV challenge [582]. One phase I clinical trial revealed that rAAV-2 encoding HIV-gag, -protease and part of the reverse transcriptase was safe although it showed modest immunogenicity as only 16% of vaccinated individuals developed Gag-specific T cells [583]. Other reports also showed the progress made in the use of rAAV vectors in vaccine development against HPV [525, 584, 585] and influenza virus [511, 586], at least in animal models. More recently a rAAV vaccine was used to trap T cells in the liver of mice following priming of these cells in the spleen using a radiation attenuated sporozoite vaccine [455]. In this study radiation attenuated sporozoite vaccination was used to prime malaria-specific $CD8^+$ T cells in the spleen and rAAV encoding the vaccine antigen was used to trap primed cells in the liver. The immune response elicited by this vaccine was able to induce protective immunity against sporozoite challenge [455]. These studies suggested that rAAV vector vaccines can be used in vaccines development against HCV.

In this thesis, rAAV-NS5B-2A-eGFP was used to trap T cells in the liver, after these cells were primed by the cytolytic DNA vaccine, pVAX-NS5B-PRF. To ensure efficacy, it was necessary to confirm that gene expression was localized to the liver as antigen deposition leads to a higher number of T_{RM} cells [455, 474, 569]. This was achieved by two mechanisms *viz* the use of the liver specific hAAT promoter [519] and the use of AAV capsid, AAV 8, that is known to transduce mouse hepatocytes [530, 531, 587]. It is estimated that 7-20% of hepatocytes will be HCV infected during persistent HCV infection [588]. It has also been shown that a CTL response was maintained when less than 25% of hepatocytes were antigen positive following vaccination [382]. Using eGFP expression to quantitate antigen-expressing hepatocytes, 5 x 10^9 vgc of rAAV-NS5B-2A-eGFP was able to transduce 10.6% of hepatocytes and this dose was used in the vaccination strategy. Previously it was reported that 5x10^{10} or 1x 10^{11} vgc of rAAV encoding eGFP and/or mOVA transduced 100% of hepatocytes *in vivo* [381, 382, 528]. When the dose was lowered to 5x10^8 vgc small proportion of hepatocytes were transduced although the percentage of antigen-expressing hepatocytes was not indicated [382]. The level of eGFP expression described in this thesis is lower than the previous reports and this may be due to the larger size of the gene inserted in the current study. It is known that rAAV encoding larger inserts has lower level of transduction [317, 385, 386].

The main limitation of AAV 8-mediated gene transfer for either gene therapy or vaccination is the requirement of a relatively higher vector dose due to its low capacity to transduce human hepatocytes [587, 589]. Hence, apart from using a tissue-specific promoter to localize antigen expression, selection of an effective AAV serotype that can transduce the target tissue is necessary. Capsid engineering has been proposed as a strategy to improve the clinical efficacy of AAV-based vectors by making the viral capsid unrecognized by the immune system [371]. Paulk *et al*., reported rAAV with a bioengineered capsid that showed improved levels of transduction in mice xenografted with human liver [590]. According to this report, the new variants (NP40 and

NP59) significantly reduced the seroreactivity profile as compared to AAV 8 [590]. Although ensuring scalable production of rAAV based on synthetic peptides and understanding the prevalence of anti-capsid antibodies in the general population are important steps in the use of synthetic peptides, the achievements suggest that AAV-based vaccines represent a potential strategy for the development of vaccines for HCV.

6.2 T cell epitope mapping

Vaccine development requires measurement and understanding of the adaptive immune response induced following vaccination. The analysis of the $CD8^+$ T cell response is of particular interest in vaccine development for viral infections [535, 591]. T cell functional analysis using methods like the ^{51}Cr-release assay [592] has several drawbacks including its reliance on cell lines that can take up ^{51}Cr, high spontaneous release of ^{51}Cr from cells over time, its semiquantitative nature, inter-assay variability, the requirement to restimulate CTLs prior to the assay, its biohazardous nature and its inability to directly assess cell killing *in vivo* [535]. On the other hand, ELISpot assays are only surrogate markers as they do not directly measure cytotoxic activity [591]. Flow cytometry-based techniques to detect target cell death by CTL activity are emerging methods of CTL immune responses [593-596]. Continuous improvement of the flow cytometry methods led to the development of the FTA technology, a technique that is used to measure CMI *in vivo* [535, 552]. FTA technology can be considered the most useful, not only because it is performed *in vivo,* but also because it has the capacity to assess killing of multiple targets presenting different concentrations and different types of peptide epitopes, which is required to assess functional avidity of $CD8^+$ T cells [503]. The assay can also provide information on $CD4^+$T cell responses [503, 504].

In this thesis the FTA technology was used to identify immunodominant peptides of the vaccine antigen, HCV NS5B, from an array of 90 peptides following vaccination of mice with pVAX-

NS5B-PRF. From the analysis two CTL immunodominant peptides and two T_H immunodominant peptides were identified (Chapter 4). CTL immunodominant peptides were found in P3 and T_H cell immunodominant peptides were identified from P2 and P3. Whether these peptides will be responsible for immune response in humans will be an area of further exploration. According to the human clinical trial reports based on the human Ad/ChAd and ChAd/MVA vaccination, that encoded NS3-NS4A-NS4B-NS5A-NS5B from HCV gt 1B, it was described that NS3 was the immunodominant peptide pool from the NS proteins encoded in the vaccine [283, 284, 597, 598]. Peptide tracking was done in smaller peptide pools, rather than individual peptides, and this also confirmed that the immunodominant region was located in NS3 [283]. Based on these observations it is difficult to make direct comparison to the vaccination described in this thesis as the genotype tested here is HCV gt3a where we identified NS5B as an immunodominant peptide that contained $CD8^+$ T cell epitopes. Moreover, there were no reports that analysed individual peptides of HCV NS proteins for immunodominance in human clinical trial. Hence, it will not be conclusive to state that NS5B will be "immunogenic" or "not immunogenic" in humans.

Quantitative analysis and phenotyping of antigen-specific T cells is advanced by the development of fluorochrome-conjugated peptide-MHC multimers [599-601]. Hence, to further characterize and quantitate $CD8^+$ T cells, antigen-specific $CD8^+$ T cells were first discriminated using peptide MHC-I tetramer staining. In order to synthesize the tetramer, the CTL immunodominant peptides identified previously were used as an input. Tetramer design for MHC-II restricted T cells is complex due to the weaker affinity TCR on $CD4^+$ T cells [602-604]. As a result, a MHC-II tetramer was not used in the study described in Chapter 5.

6.3 Prime/trap vaccination strategy to induce robust CMI in the liver

DNA vaccines are simple to design, cheap to manufacture and, due to their stability, they do not require cold chain for storage and transportation [285, 605-608]. DNA vaccines are non-viable which avoids the chance of reversion to a disease-causing agent [609]. Furthermore, DNA

vaccines do not induce vector-mediated immune responses which is an advantage if multiple doses of an antigen are desirable [610]. These qualities made DNA-based vaccines attractive vaccine delivery candidates.

DNA vaccines encoding HPV E6 and E7 resulted in histological regression and/or eliminated persistent HPV infection and HPV-related cervical lesions [611, 612]. More recently, a DNA vaccine was developed that induced protective NAb to Zika virus (ZIKV) in mice [613] and rhesus macaques [565] which have also led to the development of safe and immunogenic ZIKV DNA vaccines in humans [614, 615].

However, DNA vaccines are unable to induce long-term immune responses following a single or a few vaccinations [565]. To overcome their poor immunogenicity, DNA vaccines have been modified to allow improved uptake of the vaccine antigen by DC by conjugation with anti-Clec9A and anti-DEC2015 antibodies to target DC surface receptors [455, 616, 617]. However, this strategy required the use of additional adjuvants [566]. As a result, more recently DNA vaccines that encode the cytolytic protein, PRF, were developed [287, 566-568, 618]. These vaccines were developed to achieve cell death-induced innate immune activation to enhance antigen uptake by DC and hence improve the immunogenicity of vaccines [619, 620]. Following necrotic cell death intracellular factors will be released and act as DAMPs that are capable of signaling DC [566, 621]. The addition of PRF as a genetically encoded adjuvant within a DNA vaccine has been shown to increase immune response to HCV-NS3 [287], HCV-NS3, 4 and 5 [286] and HIV gag [567].

The recent emergence of DNA vaccines in eliciting protective immunity in humans and higher animal models warrants further examination as to how DNA vaccines can be harnessed in vaccination regimens to target HCV. However, DNA vaccines are not optimized to elicit localised

immunity in the liver suggesting a requirement for further refinements of DNA-based vaccination regimens in order to elicit lifelong protection against HCV.

The concept of priming circulating antigen-specific T cells and trapping activated cells in different organs like the liver [455] and vaginal epithelial cells [474, 495] has been tested and induced protective immune responses. Given the poor transfection efficiency and immunogenicity of DNA when delivered into the liver, this strategy appears to be a more feasible approach in exploiting DNA (as a priming agent) to elicit HCV-specific T_{RM} cells in the liver.

The work described in Chapter 5 of this thesis aimed to develop a strategy to induce localised CMI against HCV in the liver. The CMI response after vaccination using the prime/trap vaccination strategy (Chapter 5, section 5.3.1) was assessed in mice. The strategy involved vaccination of mice with two 50μg doses of pVAX-NS5B-PRF 14 days apart. Two days after the first vaccination the mice received rAAV-NS5B-2A-eGFP IV and the immune response was measured 42 days after the final DNA vaccination (Chapter 5 section 5.3.2), to ensure that memory as opposed to acute responses were measured.

Ideally, the assessment of T cell responses is best performed *in vivo* with no manipulation of T cells to avoid changes in functional parameters [552]. To achieve this FTA was used to assess CMI responses resulted from prime/trap vaccination strategy. This technology is particularly important for the *in vivo* analysis of T_{RM} cells as these cells survive poorly in functionality assays performed *in vitro* [433, 455].

FTA analysis showed that the prime/trap vaccination strategy induced significantly higher CTL and T_H cell immune responses. The induced CTL were also of high avidity as they were able to recognise FTA cells loaded with 0.01μg/ml peptide. Previously it has been shown that, in mice vaccinated with a cocktail of DNA vaccines encoding gt1b NS5B and gt3a NS5B, the CTL killer response was higher against FTA cells loaded with P3 of gt3a NS5B [288]. Although the avidity

of CTL cells induced following this vaccination not reported, the overall killer response against FTA cells loaded with P3 was similar to that reported in this thesis. In the prime/trap vaccination strategy described by Fernandez-Ruiz *et al.*, although the trapping agent, rAAV-NVY, alone was able to induce high numbers of T_{RM} cells in the liver, protection from sporozoite challenge was achieved only when T_{RM} cells were generated after the prime/trap vaccination rather than the rAAV-NVY alone [455]. In contrast, the result described in this thesis showed that vaccination with rAAV-NS5B-2A-eGFP alone was able to induce significantly higher number of T_{RM} cells and these cells showed higher percentage killer response towards peptide-loaded FTA cells as compared to the no trap vaccination. The use of a rAAV-based vaccine on its own against HCV represents a potential area of investigation for future studies.

Phenotypic characterisation of HCV antigen-specific $CD8^+$ T cells, described in section 5.3.4, revealed that cells isolated from the liver of mice that received the trapping agent expressed high levels of CD69, CXCR3 and CD11a which are described as residency markers [433, 434, 440]. The frequency of T_{RM} cells was also higher in mice that received the rAAV-NS5B-2A-eGFP compared with mice that did not receive the trapping agent. Although the necessity of local antigen deposition to elicit $CD8^+$ T_{RM} cells is controversial, it is believed that antigen deposition led to a high frequency of these cells in the liver and vagina [455, 471, 474, 569]. In the results described in this thesis, antigen deposition from rAAV-NS5B-2A-eGFP contributed to the high frequency and persistence of T_{RM} cells. Comparison of the frequency of T_{RM} cells 7 days and 42 days after the second DNA vaccination showed longer maintenance of T_{RM} cells in mice that received rAAV-NS5B-2A-eGFP suggesting its role in the persistence of these cells.

Overall, rDNA and rAAV based vaccination strategies that can be exploited to elicit systemic and intrahepatic HCV-specific T cell immunity which have ramifications for the design of effective vaccines against hepatotropic pathogens such as malaria, HBV and HCV were evaluated. This

study also highlights the importance of exploiting hepatotropic vaccine vectors to elicit robust and durable intrahepatic cytotoxic $CD8^+$ T cell immunity and T_H cell responses against HCV *in vivo*. Specifically, it appears that AAV alone will represent the most efficient approach.

6.4 Future studies

The results described in this thesis support further testing of the prime/trap vaccination strategy both in small and large animal models. The results from future studies will be crucial for further evaluation of the vaccination strategy in human clinical trials.

6.4.1 Simplifying the prime/trap vaccination strategy

The vaccination strategy described in this thesis involved a three-stage vaccination approach. Such multiple encounters coupled with the IV route used to deliver rAAV-NS5B-2A-eGFP may be an obstacle to translate this vaccination approach to the clinic. However, IV vaccine delivery was used in a recent malaria vaccine clinical trials and was reported as painless by the volunteers [471, 622]. The results described in this thesis also suggest that a single IV rAAV-NS5B injection is more immunogenic than two dose ID DNA vaccination. Although it has been described that the IV route is more effective route, as compared to ID or SC routes, for antigen deposition in the liver [382, 471, 570] the procedure is still complex as compared to other vaccines delivery routes. Hence, comparing the IV route ID or SC routes may be a way forward to develop the simplest possible strategy for rAAV delivery.

6.4.2 T_{RM} depletion studies

Although the FTA challenge studies showed strong CMI responses and a high frequency of T_{RM} cells following prime/trap vaccination strategy, the immune response was not evaluated in the absence of T_{RM} cells. A previous study used anti-CXCR3 to deplete T_{RM} cells in the liver [455], however the results in this thesis showed that this marker was also expressed by other subsets of memory T cells. Hence it was difficult to perform depletion studies. Hence, future studies should consider the identification of specific biomarkers for the establishment T_{RM} cells in the liver. On

the other hand, it was reported that T_{RM} cells attract T_{EM} cells in different organs [623]. However, the relationship between T_{RM} cells and T_{EM} cells was not investigated and the role of T_{EM} cells during FTA challenge was not assessed. Thus, it will be important for future studies to demonstrate these immunological interactions. In the transgenic mouse model study, it was reported that T_{RM} cells in the liver associated with liver sinusoids [455]. However, it is not determined if this is also true for wild type mice in the context of HCV. Hence it will be important to investigate the location of these cells in the liver.

6.4.3 Generating a universal HCV vaccine

The induction of broad CMI that can protect against heterologous HCV strains to cover a range of HCV genotypes is important for the development of a universal vaccine against HCV [161, 288]. Equally, an effective HCV should ideally induce NAb, because passive transfer of these antibodies showed protection from heterologous virus in mice and chimpanzees [624-626]. Therefore, a vaccine covering viral heterogeneity able to induce a strong NAb response and a vigorous multi-specific broad CMI may be necessary to overcome viral immune escape.

The proof of concept study described in this thesis needs further exploration for the development of a universal HCV vaccine based on the prime/trap vaccination. One of the main hurdles to achieve is the low cargo capacity of AAV [384] that will require the use of multiple viral vectors to accommodate multiple HCV genes from multiple genotypes [627, 628]. Although insufficient to allow packaging of full-length genomes, minimising the size of regulatory elements may provide additional space to accommodate transgenes. To this end promoters like CMV can be shortened from ~600bp to 173bp [629] while the 300bp SV40 poly A sequence can be replaced by a 32bp-long polyadenylation of soluble neurophilin 1 without significant reduction in gene expression [630]. Moreover, the rAAV used in this study encodes eGFP to allow easy analysis of transduction efficacy. Complete removal of eGFP or changing eGFP to a smaller size, like iLOV [631], should be considered. Together these amendments may allow the insertion of another HCV

gene or if this is not possible this will still provide an advantage as it will minimize the genome size and improve the transduction efficacy.

6.4.4 HCV challenge model to test efficacy of prime/trap vaccination strategy

The protective efficacy of a vaccination strategy is best evaluated using authentic virus challenge. Chimpanzees, considered the optimal animal model to test HCV vaccine efficacy, are endangered and their use is subject to stringent ethical considerations limiting the use of these animals in preclinical studies of candidate vaccines [5, 188, 192]. Hence, developing alternative small and large animal models is necessary to test HCV vaccines before human clinical trials. As far as large animal models are considered, pigs are very similar to humans in terms of anatomy, genetics and physiology with > 80% similarity in the immune system [632]. Pigs were used to test immunogenicity of a candidate HCV vaccine [287]. Hence these animals can be alternative large animal model to test the immunogenicity of the prime/trap vaccination strategy.

The immunocompetent transgenic mouse models that support HCV infection would be helpful to evaluate the protective efficacy of prime/trap vaccination strategy [207, 633]. The GB Virus B (GBV-B) has been shown to infect marmosets and results in HCV-like disease [634]. A HCV/GBV-B chimera, containing HCV structural genes, developed by Li *et al*., was able to induce persistent infection in marmosets which suggests the potential of these animal models to test vaccine efficacy [635]. Another HCV/GBV-B chimera containing the HCV NS2-4A genes was also capable of infecting marmosets resulting in persistent viremia with typical viral hepatitis including histopathological changes in the liver tissue [636]. Both chimeras would be useful to test the protective efficacy of the prime/trap or trap only strategy in a non-human primate, prior to future human clinical trials.

6.4.5 Conclusion

The use of DNA in the development of T cell-based HCV vaccine will likely rely on its ability to be exploited in a regimen that can elicit robust immunity in the liver. In this regard, with further

studies, the prime/trap or trap only vaccination strategy described in this thesis should be considered for the development of vaccination strategies to elicit immune responses, localised in the liver, against HCV.

7 Appendices

7.1 Appendix I: Table of Chemicals and reagents

Chemical/Reagent	Manufacturer
2-mercaptoethanol	Sigma-Aldrich
30% acrylamide/Bis solution	BioRad
Absolute ethanol	Sigma-Aldrich
Acetic acid	ThermoFisher Scientific
Agar	AMRESCO
Agarose	AMRESCO
Albumin (bovine)	Sigma-Aldrich
Ammonium chloride	Sigma-Aldrich
Ammonium persulfate	Sigma-Aldrich
Ampicillin	Sigma-Aldrich
Boric acid	Sigma-Aldrich
Bromophenol blue	Sigma-Aldrich
Calcium chloride	Sigma-Aldrich
Chloroform	Sigma-Aldrich
DAPI (4’6-Diamindino-2-Phenylindole, Dihydrochloride)	ThermoFisher Scientific
DMEM	ThermoFisher Scientific
DMSO	Sigma-Aldrich
EDTA	Sigma-Aldrich
Foetal calf serum (0.1um filtered)	ThermoFisher Scientific
GenElute	Life Technologies
Glucose	Sigma-Aldrich

Glycerol	Sigma-Aldrich
Glycine	Sigma-Aldrich
HEPES	Life Technologies
Hydrogen chloride	Sigma-Aldrich
Hydrogen chloride	Sigma-Aldrich
Imidazole	Sigma-Aldrich
Isopropanol	Sigma-Aldrich
Kanamycin	Sigma-Aldrich
Lipofectamine® LTX with Plus™ Reagent	Thermofisher Scientific
Magnesium chloride	VWR International
Magnesium sulphate	VWR International
Manganese chloride	Sigma-Aldrich
MOPS	Sigma-Aldrich
Non-fat dried milk	Black and Gold
optiMEM	Life Technologies (Gibco)
Penicillin/streptomycin	Life Technologies (Gibco)
Phosphate-buffered saline	Life Technologies
Polyethylene glycol (PEG)	Sigma-Aldrich
Polyethyleneimine (PEI)	Sigma-Aldrich
Potassium acetate	ACE chemical company
Potassium bicarbonate	Sigma-Aldrich
Potassium chloride	Thermofisher Scientific
Potassium hydroxide	Thermofisher Scientific
RPMI 1640	Life Technologies

Sodium acetate	AMRESCO
Sodium azide	Sigma-Aldrich
Sodium Chloride	ChemSupply
Sodium dihydrogen phosphate	Thermofisher Scientific
Sodium Dodecyl Sulphate	Sigma-Aldrich
Sodium hydroxide	Sigma-Aldrich
Sodium pyruvate	Life Technologies
TEMED	Sigma-Aldrich
Triton-X	BioRad
Trizma-base	Sigma-Aldrich
Trizol	Life Technologies
Trizol	Life Technologies
Trypsin	Life Technologies (Gibco)
Tryptone	Becton Dickinson and Company
Yeast extract	Becton, Dickinson and Company

7.2 Appendix II: Table of equipment

Equipment	Manufacturer
Platform shaker	Heidolph Instruments
Heat block	BioRad Digital dry bath
Bacterial shaker	Ratek Orbital mixer incubator
Bacterial spectrophotometer	BioRad Smartspec 3000
Small table-top centrifuge	Sigma 1-15PK
Large table-top centrifuge	Eppendorf centrifuge 5810R
Large centrifuge	Beckman T2-21M/E centrifuge
Bacterial incubator	Labmaster Anax Division
Cell culture incubator	SANYO CO_2 incubator
Real-time PCR cycler	Corbett Rotor-Gene 3000
Western blot imager	FujiFilm LAS-4000
Flow cytometer	BD Biosciences FACScanto
Fluorescence microscope	Zeiss AxioLab inverted Microscope
Agarose gel imager	BioRad Gel DocXR system

7.3 Appendix III: Table of Kits

Kit	Manufacturer
Pierce™ BCA protein Assay Kit	ThermoFisher Scientific
PreLink® Quick gel Extraction and PCR purification Combo kit	Life Technologies
PureLink® Quick plasmid Miniprep kit	Life Technologies
KAPA high fidelity PCR kit	KAPA biosystems
KAPA Taq PCR kit	KAPA biosystems
AAVpro® Titration kit for Real time PCR	Takara Bio Inc

7.4 Appendix IV: Bacterial Growth media

Media/solution	Components
Luria-Broth (LB)	10 g Tryptone, 10 g NaCl, 5 g yest extract, adjust to 1 L MQ H_2O
LB agar	10 g Tryptone, 10 g NaCl, 5 g yest extract, 15 g agar, adjust to 1 L MQ H_2O
TfbI solution	30 mM KAc, 100 mM KCl, 10 mM CaCl2, 50 mM MnCl2, 15% glycerol, water. Adjust the pH to 5.8 with acetic acid
TfbII solution	10 mM MOPS, 10 mM KCl, 75 mM CaCl2, 15% glycerol, water. Adjust the pH to 6.5 with kOH
Psi-a media	6 g yeast extract, 24 g tryptone, 6 g MgSO4 adjust the pH to 7.6 with KOH (final volume 1.2 L)
Psi-b agar	Add 2.8 g of Agar to 200 ml of Psi-a media
SOC Media	20 g tryptone, 5 g yeast extract, 0.58 g NaCl, 0.19 g KCl, 2.03 g MgCl2, 2.46 g MgSO4, 3.6 g glucose (Final volume 1 L using MQ H20)

7.5 Appendix V: Media for mammalian cell culture growth and media for lymphocyte isolation

Medium	Components
Supplemented DMEM	500 ml DMEM, 50 ml FCS, 5 ml pen/strep
R-10	RPMI-1640, 10% FCS, 25 mM HEPES, 1 mM Sodium Pyruvate, 1x 2ME, 1% Pen/Strep
R-5	RPMI-1640, 5% FCS, 25 mM HEPES, 1 mM Sodium Pyruvate, 1x 2ME, 1% Pen/Strep
Supplemented HBSS	HBSS, 3% FCS, 1% Pen/Strep
Isotonic percoll	90% percoll, 10% supplemented HBSS

7.6 Appendix VI: List of labelling dyes and antibodies

Labelling dye or antibody	Manufacturer
CTV	Eugene
CFSE	Life Technologies
CDP	eBioscience
Fixable viability dye (FV620)	BD Bioscience
Anti-CD44 (FITC)	Biolegened
Anti-CD11a (BV510)	DB Bioscience
Anti-CXCR3(BV421	BD Bioscience
Anti-CD69 (PE-Cy7)	BD Bioscience
Anti-CD62L (PE)	BD Bioscience
Anti-CD8 (AF780)	eBioscience
NS5B tetramer-APC	Biomolecular Research Facility, the Jhon Curtin School of Medical Research, Canberra
Alex-fluor 555 goat anti-human IgG	Invitrogen

7.7 Appendix VII: SDS-PAGE buffers

Solution	Components
Running gel buffer	40 mM Tris, 185 mM Glycine, 0.1% SDS
Resolving gel buffer	2 M Tris HCl pH8.8, 10% SDS, 30% Acrylamide
Stacking gel buffer	2 M Tris HCl pH6.8, 10% SDS, 30% Acrylamide
5 x SDS loading buffer	100 mM Tris HCl pH6.8, 2% SDS, 2 ml 10% glycerol, 5% β-mercaptoethanol, 1 μg/ml bromophenol blue
Running buffer	6.25 ml Tris pH8, 6.25 ml Tris pH8.8, 10 ml 10% SDS, 14.4 g glycine, to 1000 ml MQ H_2O

7.8 Appendix VIII: Primers used for cloning, sequencing and RT-PCR

Gene	Primer name	Primer sequence (5' to 3') (Lower case= restriction enzyme, Upper case only= overhang, italic = kozak sequence, Bold= start codon, Bold & Italic= stop codon, underlined= region of homology to the gene of interest)	Restriction site
eGFP	2A-eGFP forward	AAAgaattcAACTTCGACCTGCTGAAGCTGGCC GGCGACGTGGAGAGCAACCCCGGCCCC**ATG** GTG AGC AAG GGC GAG GAG CTG	EcoRI
	eGFP reverse	TTTaagctt ***TTA***CTTGTACAGCTCGTCCATGCCGAG	HindIII
HCV gt3a NS5B	NS5B forward	AAAgcggccgc *GCCACC***ATG**TCTATGTCGTACTCTTGGAC	NotI
	Ns5B reverse	TTTgaattcTCACCGAGCTGGCAGGAGAAAGAT G	EcoRI
hAAT	hAAT sequencing primer	GATCCCAGCCAGTGGACTTAGCC	
HCV gt3a NS5B	RT-PCR forward 1	AAAGCGGCCGCGCCACC**ATG**TCTATGTCGT ACTCTTGGAC	

	RT-PCR reverse 1	CACGCT GCGGAT CTG GTTGATGGCTC	
	RT-PCR forward 1	GAGCCG CTTGGGAGACTGCCAG	
	RT-PCR reverse 2	GTCTCCAAGCCCGCAGTGGAGGAC	
	RT-PCR forward 3	GCCTGCTAGAGAATTCAACTTCGACCTG	
	RT-PCR reverse 3	GGGCAGCTTGCCGGTGGTGCA	
eGFP	RT-PCR forward 4	ATGGTGAGCAAGGGCGAGGAGCTG	
	RT-PCR reverse 4	CTCGAACTTCACCTCGGCGCGG	
	RT-PCR forward 5	CATCCTGGGGCACAAGCTGGAGTAC	
	RT-PCR reverse 5	TTACTTGTACAGCTCGTCCATGCCGAG	

8 References

1. Kim, C.W. and K.M. Chang, *Hepatitis C virus: virology and life cycle.* Clin Mol Hepatol, 2013. **19**(1): p. 17-25.
2. Messina, J.P., et al., *Global distribution and prevalence of hepatitis C virus genotypes.* Hepatology, 2015. **61**(1): p. 77-87.
3. Suzuki, T., et al., *Hepatitis C viral life cycle.* Adv Drug Deliv Rev, 2007. **59**(12): p. 1200-12.
4. Racanelli, V. and B. Rehermann, *Hepatitis C virus infection: when silence is deception.* Trends Immunol, 2003. **24**(8): p. 456-64.
5. Catanese, M.T. and M. Dorner, *Advances in experimental systems to study hepatitis C virus in vitro and in vivo.* Virology, 2015. **479-480**: p. 221-233.
6. Soriano, V., B. Young, and N. Reau, *Report from the International Conference on Viral Hepatitis - 2017.* AIDS Rev, 2018. **20**(1): p. 58-70.
7. WHO, *Global Hepatitis Report 2017. Geneva: World Health Organisation.* 2017.
8. Calvaruso, V., S. Petta, and A. Craxi, *Is global elimination of HCV realistic?* Liver Int, 2018. **38 Suppl 1**: p. 40-46.
9. Sievert, W., et al., *Enhanced antiviral treatment efficacy and uptake in preventing the rising burden of hepatitis C-related liver disease and costs in Australia.* J Gastroenterol Hepatol, 2014. **29 Suppl 1**: p. 1-9.
10. Holmes, J., A. Thompson, and S. Bell, *Hepatitis C--an update.* Aust Fam Physician, 2013. **42**(7): p. 452-6.
11. Hainsworth, S.W., et al., *Hepatitis C virus notification rates in Australia are highest in socioeconomically disadvantaged areas.* PLOS ONE, 2018. **13**(6): p. e0198336.

12. Borgia, S.M., et al., *Identification of a Novel Hepatitis C Virus Genotype From Punjab, India: Expanding Classification of Hepatitis C Virus Into 8 Genotypes.* J Infect Dis, 2018. **218**(11): p. 1722-1729.

13. Smith, D.B., et al., *Expanded classification of hepatitis C virus into 7 genotypes and 67 subtypes: updated criteria and genotype assignment web resource.* Hepatology, 2014. **59**(1): p. 318-27.

14. Murphy, D.G., et al., *Hepatitis C virus genotype 7, a new genotype originating from central Africa.* J Clin Microbiol, 2015. **53**(3): p. 967-72.

15. Westbrook, R.H. and G. Dusheiko, *Natural history of hepatitis C.* J Hepatol, 2014. **61**(1 Suppl): p. S58-68.

16. McHutchison, J.G., *Hepatitis C advances in antiviral therapy: what is accepted treatment now?* J Gastroenterol Hepatol, 2002. **17**(4): p. 431-41.

17. Hullegie, S.J., et al., *Current knowledge and future perspectives on acute hepatitis C infection.* Clin Microbiol Infect, 2015. **21**(8): p. 797 e9-797 e17.

18. Kamal, S.M., et al., *Host and viral determinants of the outcome of exposure to HCV infection genotype 4: a large longitudinal study.* Am J Gastroenterol, 2014. **109**(2): p. 199-211.

19. Kumar, V., et al., *Genome-wide association study identifies a susceptibility locus for HCV-induced hepatocellular carcinoma.* Nat Genet, 2011. **43**(5): p. 455-8.

20. Tanaka, Y., et al., *Genome-wide association of IL28B with response to pegylated interferon-alpha and ribavirin therapy for chronic hepatitis C.* Nat Genet, 2009. **41**(10): p. 1105-9.

21. Gauthiez, E., et al., *A systematic review and meta-analysis of HCV clearance.* Liver Int, 2017. **37**(10): p. 1431-1445.

22. Yan, Z. and Y. Wang, *Viral and host factors associated with outcomes of hepatitis C virus infection (Review).* Mol Med Rep, 2017. **15**(5): p. 2909-2924.

23. Pudi, R., et al., *Hepatitis C virus internal ribosome entry site-mediated translation is stimulated by specific interaction of independent regions of human La autoantigen.* J Biol Chem, 2003. **278**(14): p. 12231-40.

24. Scheel, T.K. and C.M. Rice, *Understanding the hepatitis C virus life cycle paves the way for highly effective therapies.* Nat Med, 2013. **19**(7): p. 837-49.

25. Shimakami, T., et al., *Stabilization of hepatitis C virus RNA by an Ago2-miR-122 complex.* Proc Natl Acad Sci U S A, 2012. **109**(3): p. 941-6.

26. Jangra, R.K., M. Yi, and S.M. Lemon, *Regulation of hepatitis C virus translation and infectious virus production by the microRNA miR-122.* J Virol, 2010. **84**(13): p. 6615-25.

27. Jopling, C.L., et al., *Modulation of Hepatitis C Virus RNA Abundance by a Liver-Specific MicroRNA.* Science, 2005. **309**(5740): p. 1577.

28. Lyu, J., et al., *Roles of lipoprotein receptors in the entry of hepatitis C virus.* World J Hepatol, 2015. **7**(24): p. 2535-42.

29. Barth, H., et al., *Cellular binding of hepatitis C virus envelope glycoprotein E2 requires cell surface heparan sulfate.* J Biol Chem, 2003. **278**(42): p. 41003-12.

30. Jiang, J., et al., *Hepatitis C virus attachment mediated by apolipoprotein E binding to cell surface heparan sulfate.* J Virol, 2012. **86**(13): p. 7256-67.

31. Aizawa, Y., et al., *Chronic hepatitis C virus infection and lipoprotein metabolism.* World J Gastroenterol, 2015. **21**(36): p. 10299-313.

32. Xu, Y., et al., *Characterization of hepatitis C virus interaction with heparan sulfate proteoglycans.* J Virol, 2015. **89**(7): p. 3846-58.

33. Owen, D.M., et al., *Apolipoprotein E on hepatitis C virion facilitates infection through interaction with low-density lipoprotein receptor.* Virology, 2009. **394**(1): p. 99-108.

34. Molina, S., et al., *The low-density lipoprotein receptor plays a role in the infection of primary human hepatocytes by hepatitis C virus.* J Hepatol, 2007. **46**(3): p. 411-9.

35. Lindenbach, B.D. and C.M. Rice, *The ins and outs of hepatitis C virus entry and assembly.* Nat Rev Microbiol, 2013. **11**(10): p. 688-700.

36. Zhu, Y.Z., et al., *How hepatitis C virus invades hepatocytes: the mystery of viral entry.* World J Gastroenterol, 2014. **20**(13): p. 3457-67.

37. Zona, L., et al., *CD81-receptor associations--impact for hepatitis C virus entry and antiviral therapies.* Viruses, 2014. **6**(2): p. 875-92.

38. Feneant, L., S. Levy, and L. Cocquerel, *CD81 and hepatitis C virus (HCV) infection.* Viruses, 2014. **6**(2): p. 535-72.

39. Zhang, J., et al., *CD81 is required for hepatitis C virus glycoprotein-mediated viral infection.* J Virol, 2004. **78**(3): p. 1448-55.

40. Catanese, M.T., et al., *Role of scavenger receptor class B type I in hepatitis C virus entry: kinetics and molecular determinants.* J Virol, 2010. **84**(1): p. 34-43.

41. Scarselli, E., et al., *The human scavenger receptor class B type I is a novel candidate receptor for the hepatitis C virus.* Embo j, 2002. **21**(19): p. 5017-25.

42. Zeisel, M.B., et al., *Scavenger receptor class B type I is a key host factor for hepatitis C virus infection required for an entry step closely linked to CD81.* Hepatology, 2007. **46**(6): p. 1722-31.

43. Ploss, A., et al., *Human occludin is a hepatitis C virus entry factor required for infection of mouse cells.* Nature, 2009. **457**(7231): p. 882-6.

44. Evans, M.J., et al., *Claudin-1 is a hepatitis C virus co-receptor required for a late step in entry.* Nature, 2007. **446**(7137): p. 801-5.

45. Sainz, B., Jr., et al., *Identification of the Niemann-Pick C1-like 1 cholesterol absorption receptor as a new hepatitis C virus entry factor.* Nat Med, 2012. **18**(2): p. 281-5.

46. Dubuisson, J. and F.L. Cosset, *Virology and cell biology of the hepatitis C virus life cycle--an update.* J Hepatol, 2014. **61**(1 Suppl): p. S3-S13.

47. Paul, D., V. Madan, and R. Bartenschlager, *Hepatitis C Virus RNA Replication and Assembly: Living on the Fat of the Land.* Cell Host & Microbe, 2014. **16**(5): p. 569-579.

48. El-Hage, N. and G. Luo, *Replication of hepatitis C virus RNA occurs in a membrane-bound replication complex containing nonstructural viral proteins and RNA.* J Gen Virol, 2003. **84**(Pt 10): p. 2761-9.

49. Bartenschlager, R., F.L. Cosset, and V. Lohmann, *Hepatitis C virus replication cycle.* J Hepatol, 2010. **53**(3): p. 583-5.

50. Gastaminza, P., S.B. Kapadia, and F.V. Chisari, *Differential Biophysical Properties of Infectious Intracellular and Secreted Hepatitis C Virus Particles.* Journal of Virology, 2006. **80**(22): p. 11074.

51. Gastaminza, P., et al., *Cellular determinants of hepatitis C virus assembly, maturation, degradation, and secretion.* J Virol, 2008. **82**(5): p. 2120-9.

52. Moradpour, D., F. Penin, and C.M. Rice, *Replication of hepatitis C virus.* Nat Rev Microbiol, 2007. **5**(6): p. 453-63.

53. Oehler, V., et al., *Structural analysis of hepatitis C virus core-E1 signal peptide and requirements for cleavage of the genotype 3a signal sequence by signal peptide peptidase.* J Virol, 2012. **86**(15): p. 7818-28.

54. Zimmermann, M., et al., *Hepatitis C virus core protein impairs in vitro priming of specific T cell responses by dendritic cells and hepatocytes.* J Hepatol, 2008. **48**(1): p. 51-60.

55. Lin, W., et al., *Hepatitis C virus core protein blocks interferon signaling by interaction with the STAT1 SH2 domain.* J Virol, 2006. **80**(18): p. 9226-35.

56. von Hahn, T., et al., *Hepatitis C virus continuously escapes from neutralizing antibody and T-cell responses during chronic infection in vivo.* Gastroenterology, 2007. **132**(2): p. 667-78.

57. Vieyres, G., et al., *Characterization of the envelope glycoproteins associated with infectious hepatitis C virus.* J Virol, 2010. **84**(19): p. 10159-68.

58. Scheel, T.K.H. and C.M. Rice, *Understanding the hepatitis C virus life cycle paves the way for highly effective therapies.* Nature medicine, 2013. **19**(7): p. 837-849.

59. Sievert, W., *Management issues in chronic viral hepatitis: hepatitis C.* J Gastroenterol Hepatol, 2002. **17**(4): p. 415-22.

60. Chang, M., et al., *Dynamics of hepatitis C virus replication in human liver.* The American journal of pathology, 2003. **163**(2): p. 433-444.

61. Bartenschlager, R. and V. Lohmann, *Replication of hepatitis C virus.* J Gen Virol, 2000. **81**(Pt 7): p. 1631-48.

62. Hajarizadeh, B., J. Grebely, and G.J. Dore, *Epidemiology and natural history of HCV infection.* Nat Rev Gastroenterol Hepatol, 2013. **10**(9): p. 553-62.

63. Hajarizadeh, B., et al., *Dynamics of HCV RNA levels during acute hepatitis C virus infection.* J Med Virol, 2014. **86**(10): p. 1722-9.

64. Hajarizadeh, B., et al., *Patterns of Hepatitis C Virus RNA Levels during Acute Infection: The InC3 Study.* PLOS ONE, 2015. **10**(4): p. e0122232.

65. Freeman, A.J., et al., *Immunopathogenesis of hepatitis C virus infection.* Immunol Cell Biol, 2001. **79**(6): p. 515-36.

66. Caruntu, F.A. and L. Benea, *Acute hepatitis C virus infection: Diagnosis, pathogenesis, treatment.* J Gastrointestin Liver Dis, 2006. **15**(3): p. 249-56.

67. Steinmann, E. and T. Pietschmann, *Hepatitis C virus p7-a viroporin crucial for virus assembly and an emerging target for antiviral therapy.* Viruses, 2010. **2**(9): p. 2078-95.

68. Nieva, J.L., V. Madan, and L. Carrasco, *Viroporins: structure and biological functions.* Nature Reviews Microbiology, 2012. **10**: p. 563.

69. Wozniak, A.L., et al., *Intracellular proton conductance of the hepatitis C virus p7 protein and its contribution to infectious virus production.* PLoS Pathog, 2010. **6**(9): p. e1001087.

70. Popescu, C.I., et al., *NS2 Protein of Hepatitis C Virus Interacts with Structural and Non-Structural Proteins towards Virus Assembly.* PLoS Pathog, 2011. **7**(2): p. e1001278.

71. Kaukinen, P., et al., *Hepatitis C virus NS2 protease inhibits host cell antiviral response by inhibiting IKKε and TBK1 functions.* Journal of Medical Virology, 2013. **85**(1): p. 71-82.

72. Boukadida, C., et al., *NS2 proteases from hepatitis C virus and related hepaciviruses share composite active sites and previously unrecognized intrinsic proteolytic activities.* PLOS Pathogens, 2018. **14**(2): p. e1006863.

73. Moradpour, D. and F. Penin, *Hepatitis C virus proteins: from structure to function.* Curr Top Microbiol Immunol, 2013. **369**: p. 113-42.

74. Schregel, V., et al., *Hepatitis C virus NS2 is a protease stimulated by cofactor domains in NS3.* Proc Natl Acad Sci U S A, 2009. **106**(13): p. 5342-5347.

75. Ferreon, J.C., et al., *Molecular Determinants of TRIF Proteolysis Mediated by the Hepatitis C Virus NS3/4A Protease.* Journal of Biological Chemistry, 2005. **280**(21): p. 20483-20492.

76. Bellecave, P., et al., *Cleavage of mitochondrial antiviral signaling protein in the liver of patients with chronic hepatitis C correlates with a reduced activation of the endogenous interferon system.* Hepatology, 2010. **51**(4): p. 1127-1136.

77. Sklan, E.H. and J.S. Glenn, *HCV NS4B: From Obscurity to Central Stage*, in *Hepatitis C Viruses: Genomes and Molecular Biology*, S.L. Tan, Editor. 2006, Horizon Bioscience: Norfolk (UK). p. 245-266.

78. Nitta, S., et al., *Hepatitis C virus NS4B protein targets STING and abrogates RIG-I–mediated type I interferon-dependent innate immunity.* Hepatology, 2013. **57**(1): p. 46-58.

79. Tanji, Y., et al., *Phosphorylation of hepatitis C virus-encoded nonstructural protein NS5A.* J. Virol, 1995. **69**(7): p. 3980-86.

80. Fridell, R.A., et al., *Distinct functions of NS5A in hepatitis C virus RNA replication uncovered by studies with the NS5A inhibitor BMS-790052.* J Virol, 2011. **85**(14): p. 7312-20.

81. Abe, T., et al., *Hepatitis C Virus Nonstructural Protein 5A Modulates the Toll-Like Receptor-MyD88-Dependent Signaling Pathway in Macrophage Cell Lines.* J. Virol, 2007. **81**(17): p. 8953-66.

82. Ranjith-Kumar, C.T. and C.C. Kao, *Biochemical Activities of the HCV NS5B RNA-Dependent RNA Polymerase*, in *Hepatitis C Viruses: Genomes and Molecular Biology*, S.L. Tan, Editor. 2006, Horizon Bioscience: Norfolk (UK). p. 293-310.

83. Le Guillou-Guillemette, H., et al., *Genetic diversity of the hepatitis C virus: Impact and issues in the antiviral therapy.* World Journal of Gastroenterology : WJG, 2007. **13**(17): p. 2416-2426.

84. Toshikuni, N., T. Arisawa, and M. Tsutsumi, *Hepatitis C-related liver cirrhosis - strategies for the prevention of hepatic decompensation, hepatocarcinogenesis, and mortality.* World J Gastroenterol, 2014. **20**(11): p. 2876-87.

85. Tsochatzis, E.A., J. Bosch, and A.K. Burroughs, *Liver cirrhosis.* Lancet, 2014. **383**(9930): p. 1749-61.

86. Nguyen, D.L. and K.Q. Hu, *Clinical Monitoring of Chronic Hepatitis C Based on its Natural History and Therapy.* N Am J Med Sci (Boston), 2014. **7**(1): p. 21-27.

87. Michielsen, P.P., S.M. Francque, and J.L. van Dongen, *Viral hepatitis and hepatocellular carcinoma.* World J Surg Oncol, 2005. **3**: p. 27-44.

88. Fassio, E., *Hepatitis C and hepatocellular carcinoma.* Ann Hepatol, 2010. **9 Suppl**: p. 119-22.

89. Heim, M.H. and R. Thimme, *Innate and adaptive immune responses in HCV infections.* J Hepatol, 2014. **61**(1 Suppl): p. S14-25.

90. Buonaguro, L., et al., *Innate immunity and hepatitis C virus infection: a microarray's view.* Infect Agent Cancer, 2012. **7**(1): p. 7-19.

91. Yang, D.R. and H.Z. Zhu, *Hepatitis C virus and antiviral innate immunity: Who wins at tug-of-war?* World J Gastroenterol, 2015. **21**(13): p. 3786-3800.

92. Saito, T. and M. Gale, Jr., *Regulation of innate immunity against hepatitis C virus infection.* Hepatol Res, 2008. **38**(2): p. 115-22.

93. Garg, A.D., et al., *Immunogenic cell death, DAMPs and anticancer therapeutics: an emerging amalgamation.* Biochim Biophys Acta, 2010. **1805**(1): p. 53-71.

94. Meurs, E.F. and A. Breiman, *The interferon inducing pathways and the hepatitis C virus.* World J Gastroenterol, 2007. **13**(17): p. 2446-54.

95. Reikine, S., J.B. Nguyen, and Y. Modis, *Pattern Recognition and Signaling Mechanisms of RIG-I and MDA5.* Front Immunol, 2014. **5**: p. 342.

96. Berke, I.C., Y. Li, and Y. Modis, *Structural basis of innate immune recognition of viral RNA.* Cell Microbiol, 2013. **15**(3): p. 386-94.

97. Saito, T., et al., *Innate immunity induced by composition-dependent RIG-I recognition of hepatitis C virus RNA.* Nature, 2008. **454**(7203): p. 523-7.

98. Heim, M.H., *Innate immunity and HCV.* J Hepatol, 2013. **58**(3): p. 564-74.

99. Kato, H., et al., *Length-dependent recognition of double-stranded ribonucleic acids by retinoic acid–inducible gene-I and melanoma differentiation–associated gene 5.* J. Exp. Med., 2008. **205**(7): p. 1601-10.

100. Horner, S.M. and M. Gale, Jr., *Regulation of hepatic innate immunity by hepatitis C virus.* Nat Med, 2013. **19**(7): p. 879-88.

101. Kim, Y.K., J.S. Shin, and M.H. Nahm, *NOD-Like Receptors in Infection, Immunity, and Diseases.* Yonsei Med J, 2016. **57**(1): p. 5-14.

102. Kawai, T. and S. Akira, *The roles of TLRs, RLRs and NLRs in pathogen recognition.* Int Immunol, 2009. **21**(4): p. 317-37.

103. Jensen, S. and A.R. Thomsen, *Sensing of RNA viruses: a review of innate immune receptors involved in recognizing RNA virus invasion.* J Virol, 2012. **86**(6): p. 2900-10.

104. Wang, Y., et al., *Retinoic acid inducible gene-I (RIG-I) signaling of hepatic stellate cells inhibits hepatitis C virus replication in hepatocytes.* Innate Immun, 2013. **19**(2): p. 193-202.

105. Du, X., et al., *Hepatitis C virus replicative double-stranded RNA is a potent interferon inducer that triggers interferon production through MDA5.* J Gen Virol, 2016. **97**(11): p. 2868-2882.

106. Cao, X., et al., *MDA5 plays a critical role in interferon response during hepatitis C virus infection.* J Hepatol, 2015. **62**(4): p. 771-8.

107. Bender, S., et al., *Activation of Type I and III Interferon Response by Mitochondrial and Peroxisomal MAVS and Inhibition by Hepatitis C Virus.* PLoS Pathog, 2015. **11**(11): p. e1005264.

108. Loo, Y.M. and M. Gale, Jr., *Immune signaling by RIG-I-like receptors.* Immunity, 2011. **34**(5): p. 680-92.

109. Howell, J., et al., *Toll-like receptors in hepatitis C infection: implications for pathogenesis and treatment.* J Gastroenterol Hepatol, 2013. **28**(5): p. 766-76.

110. Zhang, Y.L., et al., *Hepatitis C virus single-stranded RNA induces innate immunity via Toll-like receptor 7.* J Hepatol, 2009. **51**(1): p. 29-38.

111. Machida, K., et al., *Hepatitis C virus induces toll-like receptor 4 expression, leading to enhanced production of beta interferon and interleukin-6.* J Virol, 2006. **80**(2): p. 866-74.

112. Broering, R., et al., *Toll-like receptor-stimulated non-parenchymal liver cells can regulate hepatitis C virus replication.* J Hepatol, 2008. **48**(6): p. 914-22.

113. Vegna, S., et al., *NOD1 Participates in the Innate Immune Response Triggered by Hepatitis C Virus Polymerase.* J.Virol., 2016. **90**(13): p. 6022-35.

114. Negash, A.A., et al., *IL-1β Production through the NLRP3 Inflammasome by Hepatic Macrophages Links Hepatitis C Virus Infection with Liver Inflammation and Disease.* PLOS Pathogens, 2013. **9**(4): p. e1003330.

115. Ahlenstiel, G., *The natural killer cell response to HCV infection.* Immune Netw, 2013. **13**(5): p. 168-76.

116. Li, Y., et al., *Natural killer cells inhibit hepatitis C virus expression.* J Leukoc Biol, 2004. **76**(6): p. 1171-9.

117. Larkin, J., et al., *Cytokine-activated natural killer cells exert direct killing of hepatoma cells harboring hepatitis C virus replicons.* J Interferon Cytokine Res, 2006. **26**(12): p. 854-65.

118. Rivero-Juarez, A., et al., *Natural killer KIR3DS1 is closely associated with HCV viral clearance and sustained virological response in HIV/HCV patients.* PLoS One, 2013. **8**(4): p. e61992.

119. Pelletier, S., et al., *Increased degranulation of natural killer cells during acute HCV correlates with the magnitude of virus-specific T cell responses.* J Hepatol, 2010. **53**(5): p. 805-16.

120. Gale, M., Jr. and E.M. Foy, *Evasion of intracellular host defence by hepatitis C virus.* Nature, 2005. **436**(7053): p. 939-45.

121. Ghorbani, M., et al., *Comparison of antibody- and cell-mediated immune responses after intramuscular hepatitis C immunizations of BALB/c mice.* Viral Immunol, 2005. **18**(4): p. 637-48.

122. Foy, E., et al., *Regulation of interferon regulatory factor-3 by the hepatitis C virus serine protease.* Science, 2003. **300**(5622): p. 1145-8.

123. Ahlen, G., et al., *In vivo clearance of hepatitis C virus nonstructural 3/4A-expressing hepatocytes by DNA vaccine-primed cytotoxic T lymphocytes.* J Infect Dis, 2005. **192**(12): p. 2112-6.

124. Ding, Q., et al., *Hepatitis C virus NS4B blocks the interaction of STING and TBK1 to evade host innate immunity.* J Hepatol, 2013. **59**(1): p. 52-8.

125. Nitta, S., et al., *Hepatitis C virus NS4B protein targets STING and abrogates RIG-I-mediated type I interferon-dependent innate immunity.* Hepatology, 2013. **57**(1): p. 46-58.

126. Horner, S.M. and M. Gale, Jr., *Intracellular innate immune cascades and interferon defenses that control hepatitis C virus.* J Interferon Cytokine Res, 2009. **29**(9): p. 489-98.

127. Garaigorta, U. and F.V. Chisari, *Hepatitis C virus blocks interferon effector function by inducing protein kinase R phosphorylation.* Cell Host Microbe, 2009. **6**(6): p. 513-22.

128. Basu, A., et al., *Hepatitis C virus core protein modulates the interferon-induced transacting factors of Jak/Stat signaling pathway but does not affect the activation of downstream IRF-1 or 561 gene.* Virology, 2001. **288**(2): p. 379-90.

129. Tseng, C.T. and G.R. Klimpel, *Binding of the hepatitis C virus envelope protein E2 to CD81 inhibits natural killer cell functions.* J Exp Med, 2002. **195**(1): p. 43-9.

130. Crotta, S., et al., *Inhibition of natural killer cells through engagement of CD81 by the major hepatitis C virus envelope protein.* J Exp Med, 2002. **195**(1): p. 35-41.

131. Yoon, J.C., et al., *Natural killer cell function is intact after direct exposure to infectious hepatitis C virions.* Hepatology, 2009. **49**(1): p. 12-21.

132. Larrubia, J.R., et al., *Adaptive immune response during hepatitis C virus infection.* World J Gastroenterol, 2014. **20**(13): p. 3418-30.

133. Zeisel, M.B., F.L. Cosset, and T.F. Baumert, *Host neutralizing responses and pathogenesis of hepatitis C virus infection.* Hepatology, 2008. **48**(1): p. 299-307.

134. Brenndorfer, E.D. and M. Sallberg, *Hepatitis C virus-mediated modulation of cellular immunity.* Arch Immunol Ther Exp (Warsz), 2012. **60**(5): p. 315-29.

135. Cashman, S.B., B.D. Marsden, and L.B. Dustin, *The Humoral Immune Response to HCV: Understanding is Key to Vaccine Development.* Front Immunol, 2014. **5**: p. 550-60.

136. Osburn, W.O., et al., *Clearance of hepatitis C infection is associated with the early appearance of broad neutralizing antibody responses.* Hepatology, 2014. **59**(6): p. 2140-51.

137. Pestka, J.M., et al., *Rapid induction of virus-neutralizing antibodies and viral clearance in a single-source outbreak of hepatitis C.* Proc Natl Acad Sci U S A, 2007. **104**(14): p. 6025-30.

138. Zhang, P., et al., *Depletion of interfering antibodies in chronic hepatitis C patients and vaccinated chimpanzees reveals broad cross-genotype neutralizing activity.* Proc Natl Acad Sci U S A, 2009. **106**(18): p. 7537-41.

139. Feray, C., et al., *Incidence of hepatitis C in patients receiving different preparations of hepatitis B immunoglobulins after liver transplantation.* Ann Intern Med, 1998. **128**(10): p. 810-6.

140. Tarr, A.W., et al., *Naturally occurring antibodies that recognize linear epitopes in the amino terminus of the hepatitis C virus E2 protein confer noninterfering, additive neutralization.* J Virol, 2012. **86**(5): p. 2739-49.

141. Keck, Z., et al., *Cooperativity in virus neutralization by human monoclonal antibodies to two adjacent regions located at the amino terminus of hepatitis C virus E2 glycoprotein.* J Virol, 2013. **87**(1): p. 37-51.

142. Ball, J.K., A.W. Tarr, and J.A. McKeating, *The past, present and future of neutralizing antibodies for hepatitis C virus.* Antiviral Research, 2014. **105**(100): p. 100-111.

143. Simmonds, P., *Genetic diversity and evolution of hepatitis C virus--15 years on.* J Gen Virol, 2004. **85**(Pt 11): p. 3173-88.

144. Dowd, K.A., et al., *Selection pressure from neutralizing antibodies drives sequence evolution during acute infection with hepatitis C virus.* Gastroenterology, 2009. **136**(7): p. 2377-86.

145. Timpe, J.M., et al., *Hepatitis C virus cell-cell transmission in hepatoma cells in the presence of neutralizing antibodies.* Hepatology, 2008. **47**(1): p. 17-24.

146. Thimme, R., et al., *Viral and immunological determinants of hepatitis C virus clearance, persistence, and disease.* Proc Natl Acad Sci U S A, 2002. **99**(24): p. 15661-8.

147. Houghton, M., *Prospects for prophylactic and therapeutic vaccines against the hepatitis C viruses.* Immunol Rev, 2011. **239**(1): p. 99-108.

148. Shoukry, N.H., et al., *Memory CD8+ T cells are required for protection from persistent hepatitis C virus infection.* J Exp Med, 2003. **197**(12): p. 1645-55.

149. Grakoui, A., et al., *HCV persistence and immune evasion in the absence of memory T cell help.* Science, 2003. **302**(5645): p. 659-62.

150. Shin, E.-C., et al., *Virus-induced type I IFN stimulates generation of immunoproteasomes at the site of infection.* Journal of Clinical Investigation, 2006. **116**(11): p. 3006-3014.

151. Diepolder, H.M., et al., *Possible mechanism involving T-lymphocyte response to non-structural protein 3 in viral clearance in acute hepatitis C virus infection.* Lancet, 1995. **346**(8981): p. 1006-7.

152. Urbani, S., et al., *Outcome of acute hepatitis C is related to virus-specific CD4 function and maturation of antiviral memory CD8 responses.* Hepatology, 2006. **44**(1): p. 126-39.

153. Missale, G., et al., *Different clinical behaviors of acute hepatitis C virus infection are associated with different vigor of the anti-viral cell-mediated immune response.* J Clin Invest, 1996. **98**(3): p. 706-14.

154. Rehermann, B., *Hepatitis C virus versus innate and adaptive immune responses: a tale of coevolution and coexistence.* J Clin Invest, 2009. **119**(7): p. 1745-54.

155. Kurktschiev, P.D., et al., *Dysfunctional CD8+ T cells in hepatitis B and C are characterized by a lack of antigen-specific T-bet induction.* J Exp Med, 2014. **211**(10): p. 2047-59.

156. Szabo, S.J., et al., *A novel transcription factor, T-bet, directs Th1 lineage commitment.* Cell, 2000. **100**(6): p. 655-69.

157. Sullivan, B.M., et al., *Antigen-driven effector CD8 T cell function regulated by T-bet.* Proc Natl Acad Sci U S A, 2003. **100**(26): p. 15818-23.

158. Lechner, F., et al., *Analysis of successful immune responses in persons infected with hepatitis C virus.* J Exp Med, 2000. **191**(9): p. 1499-512.

159. Lechner, F., et al., *CD8+ T lymphocyte responses are induced during acute hepatitis C virus infection but are not sustained.* Eur J Immunol, 2000. **30**(9): p. 2479-87.

160. Smyk-Pearson, S., et al., *Spontaneous recovery in acute human hepatitis C virus infection: functional T-cell thresholds and relative importance of CD4 help.* J Virol, 2008. **82**(4): p. 1827-37.

161. Yerly, D., et al., *Increased cytotoxic T-lymphocyte epitope variant cross-recognition and functional avidity are associated with hepatitis C virus clearance.* J Virol, 2008. **82**(6): p. 3147-53.

162. Boonstra, A., et al., *Experimental models for hepatitis C viral infection.* Hepatology, 2009. **50**(5): p. 1646-55.

163. Ashfaq, U.A., et al., *In-vitro model systems to study Hepatitis C Virus.* Genet Vaccines Ther, 2011. **9**: p. 7-12.

164. Lazaro, C.A., et al., *Hepatitis C virus replication in transfected and serum-infected cultured human fetal hepatocytes.* Am J Pathol, 2007. **170**(2): p. 478-89.

165. Banaudha, K., et al., *Primary hepatocyte culture supports hepatitis C virus replication: a model for infection-associated hepatocarcinogenesis.* Hepatology, 2010. **51**(6): p. 1922-32.

166. Lohmann, V., et al., *Replication of subgenomic hepatitis C virus RNAs in a hepatoma cell line.* Science, 1999. **285**(5424): p. 110-3.

167. Abe, K., et al., *Cell culture-adaptive NS3 mutations required for the robust replication of genome-length hepatitis C virus RNA.* Virus Res, 2007. **125**(1): p. 88-97.

168. Zhang, X., *Direct anti-HCV agents.* Acta Pharm Sin B, 2016. **6**(1): p. 26-31.

169. Bartenschlager, R., *Hepatitis C virus replicons: potential role for drug development.* Nat Rev Drug Discov, 2002. **1**(11): p. 911-6.

170. Kato, T., et al., *Efficient replication of the genotype 2a hepatitis C virus subgenomic replicon.* Gastroenterology, 2003. **125**(6): p. 1808-17.

171. Kato, T., et al., *Sequence analysis of hepatitis C virus isolated from a fulminant hepatitis patient.* J Med Virol, 2001. **64**(3): p. 334-9.

172. Wakita, T., et al., *Production of infectious hepatitis C virus in tissue culture from a cloned viral genome.* Nat Med, 2005. **11**(7): p. 791-6.

173. Lindenbach, B.D., et al., *Cell culture-grown hepatitis C virus is infectious in vivo and can be recultured in vitro.* Proc Natl Acad Sci U S A, 2006. **103**(10): p. 3805-9.

174. Lindenbach, B.D., et al., *Complete replication of hepatitis C virus in cell culture.* Science, 2005. **309**(5734): p. 623-6.

175. Zhong, J., et al., *Robust hepatitis C virus infection in vitro.* Proc Natl Acad Sci U S A, 2005. **102**(26): p. 9294-9.

176. Ghasemi, F., et al., *Design, Construction and Evaluation of 1a/JFH1 HCV Chimera by Replacing the Intergenotypic Variable Region.* Hepatitis monthly, 2016. **16**(10): p. e38261-e38261.

177. McClure, C.P., et al., *Flexible and rapid construction of viral chimeras applied to hepatitis C virus.* J Gen Virol, 2016. **97**(9): p. 2187-93.

178. Bartosch, B., J. Dubuisson, and F.L. Cosset, *Infectious hepatitis C virus pseudo-particles containing functional E1-E2 envelope protein complexes.* J Exp Med, 2003. **197**(5): p. 633-42.

179. Hsu, M., et al., *Hepatitis C virus glycoproteins mediate pH-dependent cell entry of pseudotyped retroviral particles.* Proc Natl Acad Sci U S A, 2003. **100**(12): p. 7271-6.

180. Bukh, J., *Animal models for the study of hepatitis C virus infection and related liver disease.* Gastroenterology, 2012. **142**(6): p. 1279-1287.e3.

181. Choo, Q.L., et al., *Isolation of a cDNA clone derived from a blood-borne non-A, non-B viral hepatitis genome.* Science, 1989. **244**(4902): p. 359-62.

182. MacArthur, K.L., C.H. Wu, and G.Y. Wu, *Animal models for the study of hepatitis C virus infection and replication.* World J Gastroenterol, 2012. **18**(23): p. 2909-13.

183. Major, M.E., et al., *Previously infected and recovered chimpanzees exhibit rapid responses that control hepatitis C virus replication upon rechallenge.* J Virol, 2002. **76**(13): p. 6586-95.

184. Nascimbeni, M., et al., *Kinetics of CD4+ and CD8+ memory T-cell responses during hepatitis C virus rechallenge of previously recovered chimpanzees.* J Virol, 2003. **77**(8): p. 4781-93.

185. Dahari, H., S.M. Feinstone, and M.E. Major, *Meta-analysis of hepatitis C virus vaccine efficacy in chimpanzees indicates an importance for structural proteins.* Gastroenterology, 2010. **139**(3): p. 965-74.

186. Chen, C.M., et al., *Activity of a potent hepatitis C virus polymerase inhibitor in the chimpanzee model.* Antimicrob Agents Chemother, 2007. **51**(12): p. 4290-6.

187. Carroll, S.S., et al., *Robust antiviral efficacy upon administration of a nucleoside analog to hepatitis C virus-infected chimpanzees.* Antimicrob Agents Chemother, 2009. **53**(3): p. 926-34.

188. Akari, H., et al., *Non-human primate surrogate model of hepatitis C virus infection.* Microbiol Immunol, 2009. **53**(1): p. 53-7.

189. Zhao, X., et al., *Primary hepatocytes of Tupaia belangeri as a potential model for hepatitis C virus infection.* J Clin Invest, 2002. **109**(2): p. 221-32.

190. Xu, X., et al., *Efficient infection of tree shrew (Tupaia belangeri) with hepatitis C virus grown in cell culture or from patient plasma.* J Gen Virol, 2007. **88**(Pt 9): p. 2504-12.

191. Amako, Y., et al., *Pathogenesis of hepatitis C virus infection in Tupaia belangeri.* J Virol, 2010. **84**(1): p. 303-11.

192. Billerbeck, E., et al., *Animal models for hepatitis C.* Curr Top Microbiol Immunol, 2013. **369**: p. 49-86.

193. Tsukiyama-Kohara, K. and M. Kohara, *Tupaia belangeri as an experimental animal model for viral infection.* Exp Anim, 2014. **63**(4): p. 367-74.

194. von Schaewen, M. and A. Ploss, *Murine models of hepatitis C: what can we look forward to?* Antiviral Res, 2014. **104**: p. 15-22.

195. Mercer, D.F., et al., *Hepatitis C virus replication in mice with chimeric human livers.* Nat Med, 2001. **7**(8): p. 927-33.

196. Heckel, J.L., et al., *Neonatal bleeding in transgenic mice expressing urokinase-type plasminogen activator.* Cell, 1990. **62**(3): p. 447-56.

197. Ilan, E., et al., *The hepatitis C virus (HCV)-Trimera mouse: a model for evaluation of agents against HCV.* J Infect Dis, 2002. **185**(2): p. 153-61.

198. Flisiak, R., et al., *The cyclophilin inhibitor Debio 025 combined with PEG IFNalpha2a significantly reduces viral load in treatment-naive hepatitis C patients.* Hepatology, 2009. **49**(5): p. 1460-8.

199. Bissig, K.D., et al., *Human liver chimeric mice provide a model for hepatitis B and C virus infection and treatment.* J Clin Invest, 2010. **120**(3): p. 924-30.

200. Yu, W., et al., *Immunocompetent mouse models to evaluate intrahepatic T cell responses to HCV vaccines.* Hum Vaccin Immunother, 2014. **10**(12): p. 3576-8.

201. Brass, V., H.E. Blum, and D. Moradpour, *Of mice and men: a small animal model of hepatitis C virus replication.* Hepatology, 2002. **35**(3): p. 722-4.

202. Wu, G.Y., et al., *A novel immunocompetent rat model of HCV infection and hepatitis.* Gastroenterology, 2005. **128**(5): p. 1416-23.

203. Washburn, M.L., et al., *A humanized mouse model to study hepatitis C virus infection, immune response, and liver disease.* Gastroenterology, 2011. **140**(4): p. 1334-44.

204. Dorner, M., et al., *A genetically humanized mouse model for hepatitis C virus infection.* Nature, 2011. **474**(7350): p. 208-11.

205. Dorner, M., et al., *Completion of the entire hepatitis C virus life cycle in genetically humanized mice.* Nature, 2013. **501**(7466): p. 237-41.

206. Yu, W., et al., *A novel challenge model to evaluate the efficacy of hepatitis C virus vaccines in mice.* Vaccine, 2014. **32**(27): p. 3409-16.

207. Chen, J., et al., *Persistent hepatitis C virus infections and hepatopathological manifestations in immune-competent humanized mice.* Cell Res, 2014. **24**(9): p. 1050-66.

208. Hsu, Y.C., C.Y. Wu, and J.T. Lin, *Hepatitis C Virus Infection, Antiviral Therapy, and Risk of Hepatocellular Carcinoma.* Semin Oncol, 2015. **42**(2): p. 329-338.

209. Ghany, M.G., et al., *An update on treatment of genotype 1 chronic hepatitis C virus infection: 2011 practice guideline by the American Association for the Study of Liver Diseases.* Hepatology, 2011. **54**(4): p. 1433-44.

210. Zhang, B., et al., *Re-treatment of patients with chronic hepatitis C virus genotype 4 infection with pegylated interferon and ribavirin: a meta-analysis.* BMJ Open Gastroenterol, 2015. **2**(1): p. e000057.

211. Stahmeyer, J.T., et al., *Costs and outcomes of treating chronic hepatitis C patients in routine care - results from a nationwide multicenter trial.* J Viral Hepat, 2015. **23**: p. 105-115.

212. Schneider, M.D. and C. Sarrazin, *Antiviral therapy of hepatitis C in 2014: do we need resistance testing?* Antiviral Res, 2014. **105**: p. 64-71.

213. Dhingra, A., S. Kapoor, and S.A. Alqahtani, *Recent advances in the treatment of hepatitis C.* Discov Med, 2014. **18**(99): p. 203-8.

214. Majumdar, A., M.T. Kitson, and S.K. Roberts, *Treatment of hepatitis C in patients with cirrhosis: remaining challenges for direct-acting antiviral therapy.* Drugs, 2015. **75**(8): p. 823-34.

215. Kjellin, M., et al., *The effect of the first-generation HCV-protease inhibitors boceprevir and telaprevir and the relation to baseline NS3 resistance mutations in genotype 1: experience from a small Swedish cohort.* Upsala journal of medical sciences, 2018. **123**(1): p. 50-56.

216. Gomes, L.O., et al., *Hepatitis C in Brazil: lessons learned with boceprevir and telaprevir.* Revista do Instituto de Medicina Tropical de Sao Paulo, 2018. **60**: p. e29-e29.

217. Wang, G.P., et al., *Prevalence and impact of baseline resistance-associated substitutions on the efficacy of ledipasvir/sofosbuvir or simeprevir/sofosbuvir against GT1 HCV infection.* Sci Rep, 2018. **8**(1): p. 3199-3213.

218. Keating, G.M., *Elbasvir/Grazoprevir: First Global Approval.* Drugs, 2016. **76**(5): p. 617-24.

219. Sulejmani, N. and S.-M. Jafri, *Grazoprevir/elbasvir for the treatment of adults with chronic hepatitis C: a short review on the clinical evidence and place in therapy.* Hepatic medicine : evidence and research, 2018. **10**: p. 33-42.

220. Xu, F., et al., *Synthesis of Grazoprevir, a Potent NS3/4a Protease Inhibitor for the Treatment of Hepatitis C Virus.* Organic Letters, 2018. **20**(22): p. 7261-7265.

221. Gao, M., et al., *Chemical genetics strategy identifies an HCV NS5A inhibitor with a potent clinical effect.* Nature, 2010. **465**: p. 96.

222. Pawlotsky, J.M., *NS5A inhibitors in the treatment of hepatitis C.* J Hepatol, 2013. **59**(2): p. 375-82.

223. Sharafi, H. and S.M. Alavian, *Hepatitis C resistance to NS5A inhibitors: Is it going to be a problem?* World J Hepatol, 2018. **10**(9): p. 543-548.

224. Smith, M.A., R.E. Regal, and R.A. Mohammad, *Daclatasvir: A NS5A Replication Complex Inhibitor for Hepatitis C Infection.* Annals of Pharmacotherapy, 2015. **50**(1): p. 39-46.

225. Childs, K., et al., *Directly acting antivirals for hepatitis C virus arrive in HIV/hepatitis C virus co-infected patients: from 'mind the gap' to 'where's the gap?'.* Aids, 2016. **30**(7): p. 975-89.

226. Cheng, G., et al., *In Vitro Antiviral Activity and Resistance Profile Characterization of the Hepatitis C Virus NS5A Inhibitor Ledipasvir.* Antimicrobial agents and chemotherapy, 2016. **60**(3): p. 1847-1853.

227. Liu, R., et al., *Susceptibilities of genotype 1a, 1b, and 3 hepatitis C virus variants to the NS5A inhibitor elbasvir.* Antimicrobial agents and chemotherapy, 2015. **59**(11): p. 6922-6929.

228. Feld, J.J., et al., *Sofosbuvir and Velpatasvir for HCV Genotype 1, 2, 4, 5, and 6 Infection.* New England Journal of Medicine, 2015. **373**(27): p. 2599-2607.

229. Kwo, P.Y., et al., *Glecaprevir and pibrentasvir yield high response rates in patients with HCV genotype 1–6 without cirrhosis.* Journal of Hepatology, 2017. **67**(2): p. 263-271.

230. Zeuzem, S., et al., *Glecaprevir–Pibrentasvir for 8 or 12 Weeks in HCV Genotype 1 or 3 Infection.* New England Journal of Medicine, 2018. **378**(4): p. 354-369.

231. Mantry, P.S. and L. Pathak, *Dasabuvir (ABT333) for the treatment of chronic HCV genotype I: a new face of cure, an expert review.* Expert Rev Anti Infect Ther, 2016. **14**(2): p. 157-65.

232. Tamori, A., M. Enomoto, and N. Kawada, *Recent Advances in Antiviral Therapy for Chronic Hepatitis C.* Mediators Inflamm, 2016. **2016**: p. 6841628.

233. Eltahla, A.A., et al., *Inhibitors of the Hepatitis C Virus Polymerase; Mode of Action and Resistance.* Viruses, 2015. **7**(10): p. 5206-24.

234. Kattakuzhy, S., R. Levy, and S. Kottilil, *Sofosbuvir for treatment of chronic hepatitis C.* Hepatol Int, 2015. **9**(2): p. 161-73.

235. Burstow, N.J., et al., *Hepatitis C treatment: where are we now?* International journal of general medicine, 2017. **10**: p. 39-52.

236. Mantry, P.S. and L. Pathak, *Dasabuvir (ABT333) for the treatment of chronic HCV genotype I: a new face of cure, an expert review.* Expert Review of Anti-infective Therapy, 2016. **14**(2): p. 157-165.

237. Pawlotsky, J.-M., et al., *EASL Recommendations on Treatment of Hepatitis C 2018.* Journal of Hepatology, 2018. **69**(2): p. 461-511.

238. Halfon, P. and C. Sarrazin, *Future treatment of chronic hepatitis C with direct acting antivirals: is resistance important?* Liver Int, 2012. **32 Suppl 1**: p. 79-87.

239. Bickerstaff, C., *The cost-effectiveness of novel direct acting antiviral agent therapies for the treatment of chronic hepatitis C.* Expert Rev Pharmacoecon Outcomes Res, 2015. **15**(5): p. 787-800.

240. Iyengar, S., et al., *Prices, Costs, and Affordability of New Medicines for Hepatitis C in 30 Countries: An Economic Analysis.* PLoS Med, 2016. **13**(5): p. e1002032.

241. Hurley, R., *Slashed cost of hepatitis C drugs spurs drive to eliminate the disease.* BMJ, 2018. **361**: p. k1679.

242. Latimer, B., et al., *Strong HCV NS3/4a, NS4b, NS5a, NS5b-specific cellular immune responses induced in Rhesus macaques by a novel HCV genotype 1a/1b consensus DNA vaccine.* Hum Vaccin Immunother, 2014. **10**(8): p. 2357-65.

243. Zingaretti, C., R. De Francesco, and S. Abrignani, *Why is it so difficult to develop a hepatitis C virus preventive vaccine?* Clin Microbiol Infect, 2014. **20 Suppl 5**: p. 103-9.

244. Jakobsen, J.C., et al., *Do direct acting antivirals cure chronic hepatitis C?* BMJ, 2018. **361**: p. K1382.

245. Radkowski, M., et al., *Persistence of hepatitis C virus in patients successfully treated for chronic hepatitis C.* Hepatology, 2005. **41**(1): p. 106-14.

246. Hara, K., et al., *Sequence Analysis of Hepatitis C Virus From Patients With Relapse After a Sustained Virological Response: Relapse or Reinfection?* The Journal of Infectious Diseases, 2014. **209**(1): p. 38-45.

247. Swadling, L., P. Klenerman, and E. Barnes, *Ever closer to a prophylactic vaccine for HCV.* Expert Opin Biol Ther, 2013. **13**(8): p. 1109-24.

248. Amanna, I.J. and M.K. Slifka, *Wanted, dead or alive: new viral vaccines.* Antiviral Res, 2009. **84**(2): p. 119-30.

249. Lauring, A.S., J.O. Jones, and R. Andino, *Rationalizing the development of live attenuated virus vaccines.* Nat Biotechnol, 2010. **28**(6): p. 573-9.

250. Minor, P.D., *Live attenuated vaccines: Historical successes and current challenges.* Virology, 2015. **479**: p. 379-392.

251. Bull, J.J., *Evolutionary reversion of live viral vaccines: Can genetic engineering subdue it?* Virus Evol, 2015. **1**(1): p. vev005.

252. Liang, T.J., *Current progress in development of hepatitis C virus vaccines.* Nat Med, 2013. **19**(7): p. 869-78.

253. Hajj Hussein, I., et al., *Vaccines Through Centuries: Major Cornerstones of Global Health.* Front Public Health, 2015. **3**: p. 269-85.

254. Sanders, B., M. Koldijk, and H. Schuitemaker, *Inactivated Viral Vaccines*, in *Vaccine Analysis: Strategies, Principles, and Control*, B.K. Nunnally, V.E. Turula, and R.D. Sitrin, Editors. 2015, Springer Berlin Heidelberg: Berlin, Heidelberg. p. 45-80.

255. Huang, D.B., J.J. Wu, and S.K. Tyring, *A review of licensed viral vaccines, some of their safety concerns, and the advances in the development of investigational viral vaccines.* J Infect, 2004. **49**(3): p. 179-209.

256. Akazawa, D., et al., *Neutralizing antibodies induced by cell culture-derived hepatitis C virus protect against infection in mice.* Gastroenterology, 2013. **145**(2): p. 447-55.e1-4.

257. Man John Law, L., et al., *Progress towards a hepatitis C virus vaccine.* Emerg Microbes Infect, 2013. **2**(11): p. e79.

258. Houghton, M., J.L. Law, and D.L. Tyrrell, *An Inactivated Hepatitis C Virus Vaccine on the Horizon?* Gastroenterology, 2013. **145**(2): p. 285-288.

259. Hansson, M., P.A. Nygren, and S. Stahl, *Design and production of recombinant subunit vaccines.* Biotechnol Appl Biochem, 2000. **32 (Pt 2)**: p. 95-107.

260. Moyle, P.M. and I. Toth, *Modern subunit vaccines: development, components, and research opportunities.* ChemMedChem, 2013. **8**(3): p. 360-76.

261. Cox, R.J., K.A. Brokstad, and P. Ogra, *Influenza virus: immunity and vaccination strategies. Comparison of the immune response to inactivated and live, attenuated influenza vaccines.* Scand J Immunol, 2004. **59**(1): p. 1-15.

262. Meireles, L.C., R.T. Marinho, and P. Van Damme, *Three decades of hepatitis B control with vaccination.* World journal of hepatology, 2015. **7**(18): p. 2127-2132.

263. Li, D., et al., *Altered Glycosylation Patterns Increase Immunogenicity of a Subunit Hepatitis C Virus Vaccine, Inducing Neutralizing Antibodies Which Confer Protection in Mice.* J Virol, 2016. **90**(23): p. 10486-10498.

264. Li, D., et al., *Immunization With a Subunit Hepatitis C Virus Vaccine Elicits Pan-Genotypic Neutralizing Antibodies and Intrahepatic T-Cell Responses in Nonhuman Primates.* The Journal of infectious diseases, 2017. **215**(12): p. 1824-1831.

265. Mohsen, M.O., et al., *Major findings and recent advances in virus-like particle (VLP)-based vaccines.* Semin Immunol, 2017. **34**: p. 123-132.

266. Chroboczek, J., I. Szurgot, and E. Szolajska, *Virus-like particles as vaccine.* Acta Biochim Pol, 2014. **61**(3): p. 531-9.

267. Garrone, P., et al., *A prime-boost strategy using virus-like particles pseudotyped for HCV proteins triggers broadly neutralizing antibodies in macaques.* Sci Transl Med, 2011. **3**(94): p. 94ra71.

268. Christiansen, D., et al., *Antibody Responses to a Quadrivalent Hepatitis C Viral-Like Particle Vaccine Adjuvanted with Toll-Like Receptor 2 Agonists.* Viral Immunol, 2018. **31**(4): p. 338-343.

269. Christiansen, D., et al., *Immunological responses following administration of a genotype 1a/1b/2/3a quadrivalent HCV VLP vaccine.* Scientific Reports, 2018. **8**(1): p. 6483-96.

270. Stamataki, Z., et al., *Hepatitis C virus envelope glycoprotein immunization of rodents elicits cross-reactive neutralizing antibodies.* Vaccine, 2007. **25**(45): p. 7773-84.

271. Youn, J.W., et al., *Sustained E2 antibody response correlates with reduced peak viremia after hepatitis C virus infection in the chimpanzee.* Hepatology, 2005. **42**(6): p. 1429-36.

272. Rollier, C., et al., *Control of heterologous hepatitis C virus infection in chimpanzees is associated with the quality of vaccine-induced peripheral T-helper immune response.* J Virol, 2004. **78**(1): p. 187-96.

273. Meunier, J.C., et al., *Isolation and characterization of broadly neutralizing human monoclonal antibodies to the e1 glycoprotein of hepatitis C virus.* J Virol, 2008. **82**(2): p. 966-73.

274. Verstrepen, B.E., et al., *Clearance of genotype 1b hepatitis C virus in chimpanzees in the presence of vaccine-induced E1-neutralizing antibodies.* J Infect Dis, 2011. **204**(6): p. 837-44.

275. Choo, Q.L., et al., *Vaccination of chimpanzees against infection by the hepatitis C virus.* Proc Natl Acad Sci U S A, 1994. **91**(4): p. 1294-8.

276. Meunier, J.-C., et al., *Vaccine-Induced Cross-Genotype Reactive Neutralizing Antibodies Against Hepatitis C Virus.* The Journal of Infectious Diseases, 2011. **204**(8): p. 1186-1190.

277. Esumi, M., et al., *Experimental vaccine activities of recombinant E1 and E2 glycoproteins and hypervariable region 1 peptides of hepatitis C virus in chimpanzees.* Archives of Virology, 1999. **144**(5): p. 973-980.

278. Forns, X., et al., *Vaccination of chimpanzees with plasmid DNA encoding the hepatitis C virus (HCV) envelope E2 protein modified the infection after challenge with homologous monoclonal HCV.* Hepatology, 2000. **32**(3): p. 618-25.

279. Law, J.L., et al., *A hepatitis C virus (HCV) vaccine comprising envelope glycoproteins gpE1/gpE2 derived from a single isolate elicits broad cross-genotype neutralizing antibodies in humans.* PLoS One, 2013. **8**(3): p. e59776.

280. Frey, S.E., et al., *Safety and immunogenicity of HCV E1E2 vaccine adjuvanted with MF59 administered to healthy adults.* Vaccine, 2010. **28**(38): p. 6367-73.

281. Leroux-Roels, G., et al., *A candidate vaccine based on the hepatitis C E1 protein: tolerability and immunogenicity in healthy volunteers.* Vaccine, 2004. **22**(23-24): p. 3080-6.

282. Firbas, C., et al., *Immunogenicity and safety of a novel therapeutic hepatitis C virus (HCV) peptide vaccine: a randomized, placebo controlled trial for dose optimization in 128 healthy subjects.* Vaccine, 2006. **24**(20): p. 4343-53.

283. Barnes, E., et al., *Novel adenovirus-based vaccines induce broad and sustained T cell responses to HCV in man.* Sci Transl Med, 2012. **4**(115): p. 115ra1.

284. Swadling, L., et al., *A human vaccine strategy based on chimpanzee adenoviral and MVA vectors that primes, boosts, and sustains functional HCV-specific T cell memory.* Sci Transl Med, 2014. **6**(261): p. 261ra153.

285. Flingai, S., et al., *Synthetic DNA vaccines: improved vaccine potency by electroporation and co-delivered genetic adjuvants.* Front Immunol, 2013. **4**: p. 354-64.

286. Gummow, J., et al., *A Multiantigenic DNA Vaccine That Induces Broad Hepatitis C Virus-Specific T-Cell Responses in Mice.* J Virol, 2015. **89**(15): p. 7991-8002.

287. Grubor-Bauk, B., et al., *Intradermal delivery of DNA encoding HCV NS3 and perforin elicits robust cell-mediated immunity in mice and pigs.* Gene Ther, 2016. **23**(1): p. 26-37.

288. Wijesundara, D.K., et al., *Induction of Genotype Cross-Reactive, Hepatitis C Virus-Specific, Cell-Mediated Immunity in DNA-Vaccinated Mice.* J Virol, 2018. **92**(8): p. e02133-17.

289. Gorzin, Z., et al., *Immunogenicity evaluation of a DNA vaccine expressing the hepatitis C virus non-structural protein 2 gene in C57BL/6 mice.* Iran Biomed J, 2014. **18**(1): p. 1-7.

290. Ahlen, G., et al., *Long-term functional duration of immune responses to HCV NS3/4A induced by DNA vaccination.* Gene Ther, 2014. **21**(8): p. 739-50.

291. Holmstrom, F., et al., *A synthetic codon-optimized hepatitis C virus nonstructural 5A DNA vaccine primes polyfunctional CD8+ T cell responses in wild-type and NS5A-transgenic mice.* J Immunol, 2013. **190**(3): p. 1113-24.

292. Weiland, O., et al., *Therapeutic DNA vaccination using in vivo electroporation followed by standard of care therapy in patients with genotype 1 chronic hepatitis C.* Mol Ther, 2013. **21**(9): p. 1796-805.

293. Habersetzer, F., et al., *A poxvirus vaccine is safe, induces T-cell responses, and decreases viral load in patients with chronic hepatitis C.* Gastroenterology, 2011. **141**(3): p. 890-899.

294. Alvarez-Lajonchere, L., et al., *Immunogenicity of CIGB-230, a therapeutic DNA vaccine preparation, in HCV-chronically infected individuals in a Phase I clinical trial.* J Viral Hepat, 2009. **16**(3): p. 156-67.

295. Duenas-Carrera, S., et al., *Enhancement of the immune response generated against hepatitis C virus envelope proteins after DNA vaccination with polyprotein-encoding plasmids.* Biotechnol Appl Biochem, 2002. **35**(Pt 3): p. 205-12.

296. Feinstone, S.M., D.J. Hu, and M.E. Major, *Prospects for prophylactic and therapeutic vaccines against hepatitis C virus.* Clin Infect Dis, 2012. **55 Suppl 1**: p. S25-32.

297. Atchison, R.W., B.C. Casto, and W.M. Hammon, *Adenovirus-Associated Defective Virus Particles.* Science, 1965. **149**(3685): p. 754-6.

298. Goncalves, M.A., *Adeno-associated virus: from defective virus to effective vector.* Virol J, 2005. **2**: p. 43-60.

299. Weitzman, M.D. and R.M. Linden, *Adeno-associated virus biology.* Methods Mol Biol, 2011. **807**: p. 1-23.

300. Samulski, R.J. and N. Muzyczka, *AAV-Mediated Gene Therapy for Research and Therapeutic Purposes.* Annual Review of Virology, 2014. **1**(1): p. 427-451.

301. Schultz, B.R. and J.S. Chamberlain, *Recombinant adeno-associated virus transduction and integration.* Mol Ther, 2008. **16**(7): p. 1189-99.

302. Wu, Z., A. Asokan, and R.J. Samulski, *Adeno-associated virus serotypes: vector toolkit for human gene therapy.* Mol Ther, 2006. **14**(3): p. 316-27.

303. Bartel, M.A., J.R. Weinstein, and D.V. Schaffer, *Directed evolution of novel adeno-associated viruses for therapeutic gene delivery.* Gene Ther, 2012. **19**(6): p. 694-700.

304. Salganik, M., M.L. Hirsch, and R.J. Samulski, *Adeno-associated Virus as a Mammalian DNA Vector.* Microbiol Spectr, 2015. **3**(4).

305. Kotterman, M.A. and D.V. Schaffer, *Engineering adeno-associated viruses for clinical gene therapy.* Nat Rev Genet, 2014. **15**(7): p. 445-51.

306. Ayuso, E., F. Mingozzi, and F. Bosch, *Production, purification and characterization of adeno-associated vectors.* Curr Gene Ther, 2010. **10**(6): p. 423-36.

307. Van Vliet, K.M., et al., *The role of the adeno-associated virus capsid in gene transfer.* Methods Mol Biol, 2008. **437**: p. 51-91.

308. Trempe, J.P. and B.J. Carter, *Alternate mRNA splicing is required for synthesis of adeno-associated virus VP1 capsid protein.* Journal of Virology, 1988. **62**(9): p. 3356-3363.

309. Becerra, S.P., et al., *Synthesis of adeno-associated virus structural proteins requires both alternative mRNA splicing and alternative initiations from a single transcript.* Journal of Virology, 1988. **62**(8): p. 2745-2754.

310. Balakrishnan, B. and G.R. Jayandharan, *Basic biology of adeno-associated virus (AAV) vectors used in gene therapy.* Curr Gene Ther, 2014. **14**(2): p. 86-100.

311. Nam, H.-J., et al., *Structure of Adeno-Associated Virus Serotype 8, a Gene Therapy Vector.* Journal of Virology, 2007. **81**(22): p. 12260.

312. Grimm, D., et al., *Liver transduction with recombinant adeno-associated virus is primarily restricted by capsid serotype not vector genotype.* J Virol, 2006. **80**(1): p. 426-39.

313. Johnson, J.S., et al., *Mutagenesis of adeno-associated virus type 2 capsid protein VP1 uncovers new roles for basic amino acids in trafficking and cell-specific transduction.* J Virol, 2010. **84**(17): p. 8888-902.

314. Ruffing, M., H. Zentgraf, and J.A. Kleinschmidt, *Assembly of viruslike particles by recombinant structural proteins of adeno-associated virus type 2 in insect cells.* J Virol, 1992. **66**(12): p. 6922-30.

315. Steinbach, S., et al., *Assembly of adeno-associated virus type 2 capsids in vitro.* J Gen Virol, 1997. **78 (Pt 6)**: p. 1453-62.

316. Warrington, K.H., Jr., et al., *Adeno-associated virus type 2 VP2 capsid protein is nonessential and can tolerate large peptide insertions at its N terminus.* J Virol, 2004. **78**(12): p. 6595-609.

317. Grieger, J.C. and R.J. Samulski, *Packaging capacity of adeno-associated virus serotypes: impact of larger genomes on infectivity and postentry steps.* J Virol, 2005. **79**(15): p. 9933-44.

318. Brister, J.R. and N. Muzyczka, *Mechanism of Rep-mediated adeno-associated virus origin nicking.* J Virol, 2000. **74**(17): p. 7762-71.

319. Young, S.M., Jr., et al., *Roles of adeno-associated virus Rep protein and human chromosome 19 in site-specific recombination.* J Virol, 2000. **74**(9): p. 3953-66.

320. King, J.A., et al., *DNA helicase-mediated packaging of adeno-associated virus type 2 genomes into preformed capsids.* Embo j, 2001. **20**(12): p. 3282-91.

321. Zaiss, A.K., et al., *Hepatocyte Heparan Sulfate Is Required for Adeno-Associated Virus 2 but Dispensable for Adenovirus 5 Liver Transduction In Vivo.* J Virol, 2015. **90**(1): p. 412-20.

322. Kashiwakura, Y., et al., *Hepatocyte growth factor receptor is a coreceptor for adeno-associated virus type 2 infection.* J Virol, 2005. **79**(1): p. 609-14.

323. Sanlioglu, S., et al., *Endocytosis and nuclear trafficking of adeno-associated virus type 2 are controlled by rac1 and phosphatidylinositol-3 kinase activation.* J Virol, 2000. **74**(19): p. 9184-96.

324. Summerford, C., J.S. Bartlett, and R.J. Samulski, *AlphaVbeta5 integrin: a co-receptor for adeno-associated virus type 2 infection.* Nat Med, 1999. **5**(1): p. 78-82.

325. Akache, B., et al., *The 37/67-kilodalton laminin receptor is a receptor for adeno-associated virus serotypes 8, 2, 3, and 9.* Journal of virology, 2006. **80**(19): p. 9831-9836.

326. Raupp, C., et al., *The Threefold Protrusions of Adeno-Associated Virus Type 8 Are Involved in Cell Surface Targeting as Well as Postattachment Processing.* J Virol, 2012. **86**(17): p. 9396-9408.

327. Kaludov, N., et al., *Adeno-associated virus serotype 4 (AAV4) and AAV5 both require sialic acid binding for hemagglutination and efficient transduction but differ in sialic acid linkage specificity.* J Virol, 2001. **75**(15): p. 6884-93.

328. Seiler, M.P., et al., *Adeno-associated virus types 5 and 6 use distinct receptors for cell entry.* Hum Gene Ther, 2006. **17**(1): p. 10-19.

329. Wu, Z., et al., *Alpha2,3 and alpha2,6 N-linked sialic acids facilitate efficient binding and transduction by adeno-associated virus types 1 and 6.* J Virol, 2006. **80**(18): p. 9093-103.

330. Pillay, S., et al., *An essential receptor for adeno-associated virus infection.* Nature, 2016. **530**(7588): p. 108-12.

331. Pillay, S., et al., *AAV serotypes have distinctive interactions with domains of the cellular receptor AAVR.* J virol, 2017. **91**(18): p. e00391-17.

332. Xiao, P.J. and R.J. Samulski, *Cytoplasmic trafficking, endosomal escape, and perinuclear accumulation of adeno-associated virus type 2 particles are facilitated by microtubule network.* J Virol, 2012. **86**(19): p. 10462-73.

333. Nicolson, S.C. and R.J. Samulski, *Recombinant adeno-associated virus utilizes host cell nuclear import machinery to enter the nucleus.* J Virol, 2014. **88**(8): p. 4132-44.

334. Duan, D., et al., *Dynamin is required for recombinant adeno-associated virus type 2 infection.* J Virol, 1999. **73**(12): p. 10371-6.

335. Stoneham, C.A., M. Hollinshead, and A. Hajitou, *Clathrin-mediated endocytosis and subsequent endo-lysosomal trafficking of adeno-associated virus/phage.* J Biol Chem, 2012. **287**(43): p. 35849-59.

336. Ferrari, F.K., et al., *Second-strand synthesis is a rate-limiting step for efficient transduction by recombinant adeno-associated virus vectors.* J Virol, 1996. **70**(5): p. 3227-34.

337. Malik, A.K., et al., *Kinetics of recombinant adeno-associated virus-mediated gene transfer.* J virol, 2000. **74**(8): p. 3555-3565.

338. Hansen, J., et al., *Impaired intracellular trafficking of adeno-associated virus type 2 vectors limits efficient transduction of murine fibroblasts.* J Virol, 2000. **74**(2): p. 992-6.

339. Ding, W., et al., *Intracellular trafficking of adeno-associated viral vectors.* Gene Ther, 2005. **12**(11): p. 873-80.

340. Douar, A.M., et al., *Intracellular trafficking of adeno-associated virus vectors: routing to the late endosomal compartment and proteasome degradation.* J Virol, 2001. **75**(4): p. 1824-33.

341. Miller, S.G., L. Carnell, and H.H. Moore, *Post-Golgi membrane traffic: brefeldin A inhibits export from distal Golgi compartments to the cell surface but not recycling.* J Cell Biol, 1992. **118**(2): p. 267-83.

342. Hansen, J., K. Qing, and A. Srivastava, *Adeno-associated virus type 2-mediated gene transfer: altered endocytic processing enhances transduction efficiency in murine fibroblasts.* J Virol, 2001. **75**(9): p. 4080-90.

343. Tullis, G.E. and T. Shenk, *Efficient Replication of Adeno-Associated Virus Type 2 Vectors: a cis-Acting Element outside of the Terminal Repeats and a Minimal Size.* Journal of Virology, 2000. **74**(24): p. 11511.

344. Henckaerts, E. and R.M. Linden, *Adeno-associated virus: a key to the human genome?* Future Virol, 2010. **5**(5): p. 555-574.

345. Fraefel, C., et al., *Spatial and Temporal Organization of Adeno-Associated Virus DNA Replication in Live Cells.* Journal of Virology, 2003. **78**(1): p. 389-398.

346. Sonntag, F., K. Schmidt, and J.A. Kleinschmidt, *A viral assembly factor promotes AAV2 capsid formation in the nucleolus.* Proc Natl Acad Sci U S A, 2010. **107**(22): p. 10220-5.

347. Earley, L.F., et al., *Identification and characterization of nuclear and nucleolar localization signals in the adeno-associated virus serotype 2 assembly-activating protein.* J Virol, 2015. **89**(6): p. 3038-48.

348. Chang, L.S., Y. Shi, and T. Shenk, *Adeno-associated virus P5 promoter contains an adenovirus E1A-inducible element and a binding site for the major late transcription factor.* J Virol, 1989. **63**(8): p. 3479-88.

349. Horer, M., et al., *Mutational analysis of adeno-associated virus Rep protein-mediated inhibition of heterologous and homologous promoters.* J Virol, 1995. **69**(9): p. 5485-96.

350. Ward, P., et al., *Role of the adenovirus DNA-binding protein in in vitro adeno-associated virus DNA replication.* J Virol, 1998. **72**(1): p. 420-7.

351. Weindler, F.W. and R. Heilbronn, *A subset of herpes simplex virus replication genes provides helper functions for productive adeno-associated virus replication.* J Virol, 1991. **65**(5): p. 2476-83.

352. Slanina, H., et al., *Role of the herpes simplex virus helicase-primase complex during adeno-associated virus DNA replication.* J Virol, 2006. **80**(11): p. 5241-50.

353. Ni, T.H., et al., *Cellular proteins required for adeno-associated virus DNA replication in the absence of adenovirus coinfection.* J Virol, 1998. **72**(4): p. 2777-87.

354. Ni, T.H., et al., *In vitro replication of adeno-associated virus DNA.* Journal of virology, 1994. **68**(2): p. 1128-1138.

355. Nash, K., et al., *Purification of host cell enzymes involved in adeno-associated virus DNA replication.* J Virol, 2007. **81**(11): p. 5777-87.

356. Nash, K., W. Chen, and N. Muzyczka, *Complete in vitro reconstitution of adeno-associated virus DNA replication requires the minichromosome maintenance complex proteins.* J Virol, 2008. **82**(3): p. 1458-64.

357. Monahan, P.E. and R.J. Samulski, *Adeno-associated virus vectors for gene therapy: more pros than cons?* Mol Med Today, 2000. **6**(11): p. 433-40.

358. Henckaerts, E., et al., *Site-specific integration of adeno-associated virus involves partial duplication of the target locus.* Proc Natl Acad Sci U S A, 2009. **106**(18): p. 7571-6.

359. Giraud, C., E. Winocour, and K.I. Berns, *Site-specific integration by adeno-associated virus is directed by a cellular DNA sequence.* Proc Natl Acad Sci U S A, 1994. **91**(21): p. 10039-43.

360. Weitzman, M.D., et al., *Adeno-associated virus (AAV) Rep proteins mediate complex formation between AAV DNA and its integration site in human DNA.* Proc Natl Acad Sci U S A, 1994. **91**(13): p. 5808-12.

361. Linden, R.M., E. Winocour, and K.I. Berns, *The recombination signals for adeno-associated virus site-specific integration.* Proc Natl Acad Sci U S A, 1996. **93**(15): p. 7966-72.

362. Xu, Z.X., et al., *A 16-bp RBE element mediated Rep-dependent site-specific integration in AAVS1 transgenic mice for expression of hFIX.* Gene Ther, 2009. **16**(5): p. 589-95.

363. Feng, D., et al., *A 16bp Rep binding element is sufficient for mediating Rep-dependent integration into AAVS1.* J Mol Biol, 2006. **358**(1): p. 38-45.

364. Li, C., et al., *Neutralizing antibodies against adeno-associated virus examined prospectively in pediatric patients with hemophilia.* Gene Ther, 2012. **19**(3): p. 288-94.

365. Calcedo, R., et al., *Adeno-associated virus antibody profiles in newborns, children, and adolescents.* Clin Vaccine Immunol, 2011. **18**(9): p. 1586-8.

366. Calcedo, R., et al., *Worldwide epidemiology of neutralizing antibodies to adeno-associated viruses.* J Infect Dis, 2009. **199**(3): p. 381-90.

367. Ling, C., et al., *Prevalence of neutralizing antibodies against liver-tropic adeno-associated virus serotype vectors in 100 healthy Chinese and its potential relation to body constitutions.* J Integr Med, 2015. **13**(5): p. 341-6.

368. Greenberg, B., et al., *Prevalence of AAV1 neutralizing antibodies and consequences for a clinical trial of gene transfer for advanced heart failure.* Gene Ther, 2016. **23**(3): p. 313-9.

369. Liu, Q., et al., *Neutralizing antibodies against AAV2, AAV5 and AAV8 in healthy and HIV-1-infected subjects in China: implications for gene therapy using AAV vectors.* Gene Ther, 2014. **21**(8): p. 732-8.

370. Vasileva, A. and R. Jessberger, *Precise hit: adeno-associated virus in gene targeting.* Nat Rev Microbiol, 2005. **3**(11): p. 837-47.

371. Sen, D., *Improving clinical efficacy of adeno associated vectors by rational capsid bioengineering.* J Biomed Sci, 2014. **21**(1): p. 103.

372. Coura Rdos, S. and N.B. Nardi, *The state of the art of adeno-associated virus-based vectors in gene therapy.* Virol J, 2007. **4**: p. 99-106.

373. Flotte, T.R., et al., *Phase 2 clinical trial of a recombinant adeno-associated viral vector expressing alpha1-antitrypsin: interim results.* Hum Gene Ther, 2011. **22**(10): p. 1239-47.

374. Blits, B., et al., *Adeno-associated viral vector (AAV)-mediated gene transfer in the red nucleus of the adult rat brain: comparative analysis of the transduction properties of seven AAV serotypes and lentiviral vectors.* J Neurosci Methods, 2010. **185**(2): p. 257-63.

375. Towne, C., et al., *Recombinant adeno-associated virus serotype 6 (rAAV2/6)-mediated gene transfer to nociceptive neurons through different routes of delivery.* Mol Pain, 2009. **5**: p. 52.

376. Jung, S.C., et al., *Protective effect of recombinant adeno-associated virus 2/8-mediated gene therapy from the maternal hyperphenylalaninemia in offsprings of a mouse model of phenylketonuria.* J Korean Med Sci, 2008. **23**(5): p. 877-83.

377. Nienhuis, A.W., A.C. Nathwani, and A.M. Davidoff, *Gene Therapy for Hemophilia.* Mol Ther, 2017. **25**(5): p. 1163-1167.

378. Kay, M.A., et al., *Evidence for gene transfer and expression of factor IX in haemophilia B patients treated with an AAV vector.* Nat Genet, 2000. **24**(3): p. 257-61.

379. Nathwani, A.C., et al., *Long-Term Safety and Efficacy of Factor IX Gene Therapy in Hemophilia B.* New England Journal of Medicine, 2014. **371**(21): p. 1994-2004.

380. McIntosh, J., et al., *Therapeutic levels of FVIII following a single peripheral vein administration of rAAV vector encoding a novel human factor VIII variant.* Blood, 2013. **121**(17): p. 3335-44.

381. Tay, S.S., et al., *Intrahepatic activation of naive CD4+ T cells by liver-resident phagocytic cells.* J Immunol, 2014. **193**(5): p. 2087-95.

382. Tay, S.S., et al., *Antigen expression level threshold tunes the fate of CD8 T cells during primary hepatic immune responses.* Proc Natl Acad Sci U S A, 2014. **111**(25): p. E2540-9.

383. Dion, S., et al., *Adeno-associated virus-mediated gene transfer leads to persistent hepatitis B virus replication in mice expressing HLA-A2 and HLA-DR1 molecules.* J Virol, 2013. **87**(10): p. 5554-63.

384. Wu, J., et al., *Self-complementary recombinant adeno-associated viral vectors: packaging capacity and the role of rep proteins in vector purity.* Hum Gene Ther, 2007. **18**(2): p. 171-82.

385. Allocca, M., et al., *Serotype-dependent packaging of large genes in adeno-associated viral vectors results in effective gene delivery in mice.* J Clin Invest, 2008. **118**(5): p. 1955-64.

386. Wu, Z., H. Yang, and P. Colosi, *Effect of genome size on AAV vector packaging.* Mol Ther, 2010. **18**(1): p. 80-6.

387. McCarty, D.M., *Self-complementary AAV vectors; advances and applications.* Mol Ther, 2008. **16**(10): p. 1648-56.

388. McCarty, D.M., P.E. Monahan, and R.J. Samulski, *Self-complementary recombinant adeno-associated virus (scAAV) vectors promote efficient transduction independently of DNA synthesis.* Gene Ther, 2001. **8**(16): p. 1248-54.

389. Natkunarajah, M., et al., *Assessment of ocular transduction using single-stranded and self-complementary recombinant adeno-associated virus serotype 2/8.* Gene Ther, 2008. **15**(6): p. 463-7.

390. Gruenert, A.K., et al., *Self-Complementary Adeno-Associated Virus Vectors Improve Transduction Efficiency of Corneal Endothelial Cells.* PLoS One, 2016. **11**(3): p. e0152589.

391. Maina, N., et al., *Recombinant self-complementary adeno-associated virus serotype vector-mediated hematopoietic stem cell transduction and lineage-restricted, long-term transgene expression in a murine serial bone marrow transplantation model.* Hum Gene Ther, 2008. **19**(4): p. 376-83.

392. Fu, H., et al., *Self-complementary adeno-associated virus serotype 2 vector: global distribution and broad dispersion of AAV-mediated transgene expression in mouse brain.* Mol Ther, 2003. **8**(6): p. 911-7.

393. McCarty, D.M., et al., *Adeno-associated virus terminal repeat (TR) mutant generates self-complementary vectors to overcome the rate-limiting step to transduction in vivo.* Gene Ther, 2003. **10**(26): p. 2112-8.

394. Raj, D., A.M. Davidoff, and A.C. Nathwani, *Self-complementary adeno-associated viral vectors for gene therapy of hemophilia B: progress and challenges.* Expert Rev Hematol, 2011. **4**(5): p. 539-49.

395. Grimm, D., et al., *Novel tools for production and purification of recombinant adenoassociated virus vectors.* Hum Gene Ther, 1998. **9**(18): p. 2745-60.

396. Matsushita, T., et al., *Adeno-associated virus vectors can be efficiently produced without helper virus.* Gene Ther, 1998. **5**(7): p. 938-45.

397. Xiao, X., J. Li, and R.J. Samulski, *Production of high-titer recombinant adeno-associated virus vectors in the absence of helper adenovirus.* J Virol, 1998. **72**(3): p. 2224-32.

398. Smith, R.H., J.R. Levy, and R.M. Kotin, *A simplified baculovirus-AAV expression vector system coupled with one-step affinity purification yields high-titer rAAV stocks from insect cells.* Mol Ther, 2009. **17**(11): p. 1888-96.

399. Mietzsch, M., et al., *OneBac: platform for scalable and high-titer production of adeno-associated virus serotype 1-12 vectors for gene therapy.* Hum Gene Ther, 2014. **25**(3): p. 212-22.

400. Kohlbrenner, E., et al., *Successful production of pseudotyped rAAV vectors using a modified baculovirus expression system.* Mol Ther, 2005. **12**(6): p. 1217-25.

401. Liu, X.L., K.R. Clark, and P.R. Johnson, *Production of recombinant adeno-associated virus vectors using a packaging cell line and a hybrid recombinant adenovirus.* Gene Ther, 1999. **6**(2): p. 293-9.

402. Feudner, E., et al., *Optimization of recombinant adeno-associated virus production using an herpes simplex virus amplicon system.* J Virol Methods, 2001. **96**(2): p. 97-105.

403. Qiao, C., et al., *Feasibility of generating adeno-associated virus packaging cell lines containing inducible adenovirus helper genes.* J Virol, 2002. **76**(4): p. 1904-13.

404. Grimm, D., M.A. Kay, and J.A. Kleinschmidt, *Helper virus-free, optically controllable, and two-plasmid-based production of adeno-associated virus vectors of serotypes 1 to 6.* Mol Ther, 2003. **7**(6): p. 839-50.

405. Kotin, R.M., *Large-scale recombinant adeno-associated virus production.* Hum Mol Genet, 2011. **20**(R1): p. R2-6.

406. Zhang, X., et al., *High-titer recombinant adeno-associated virus production from replicating amplicons and herpes vectors deleted for glycoprotein H.* Hum Gene Ther, 1999. **10**(15): p. 2527-37.

407. Burova, E. and E. Ioffe, *Chromatographic purification of recombinant adenoviral and adeno-associated viral vectors: methods and implications.* Gene Ther, 2005. **12 Suppl 1**: p. S5-17.

408. Clark, K.R., *Recent advances in recombinant adeno-associated virus vector production.* Kidney Int, 2002. **61**(1 Suppl): p. S9-15.

409. Gao, G., et al., *Purification of recombinant adeno-associated virus vectors by column chromatography and its performance in vivo.* Hum Gene Ther, 2000. **11**(15): p. 2079-91.

410. Potter, M., et al., *A simplified purification protocol for recombinant adeno-associated virus vectors.* Molecular Therapy — Methods & Clinical Development, 2014. **1**: p. 14034.

411. Gebhardt, T. and L.K. Mackay, *Local immunity by tissue-resident CD8(+) memory T cells.* Front Immunol, 2012. **3**: p. 340-52.

412. Ariotti, S., J.B. Haanen, and T.N. Schumacher, *Behavior and function of tissue-resident memory T cells.* Adv Immunol, 2012. **114**: p. 203-16.

413. Steinert, E.M., et al., *Quantifying Memory CD8 T Cells Reveals Regionalization of Immunosurveillance.* Cell, 2015. **161**(4): p. 737-49.

414. Sallusto, F., et al., *Two subsets of memory T lymphocytes with distinct homing potentials and effector functions.* Nature, 1999. **401**(6754): p. 708-12.

415. Sallusto, F., J. Geginat, and A. Lanzavecchia, *Central memory and effector memory T cell subsets: function, generation, and maintenance.* Annu Rev Immunol, 2004. **22**: p. 745-63.

416. Lanzavecchia, A. and F. Sallusto, *Dynamics of T lymphocyte responses: intermediates, effectors, and memory cells.* Science, 2000. **290**(5489): p. 92-7.

417. Lanzavecchia, A. and F. Sallusto, *Understanding the generation and function of memory T cell subsets.* Curr Opin Immunol, 2005. **17**(3): p. 326-32.

418. Hammarlund, E., et al., *Duration of antiviral immunity after smallpox vaccination.* Nat Med, 2003. **9**(9): p. 1131-7.

419. Murali-Krishna, K., et al., *Persistence of Memory CD8 T Cells in MHC Class I-Deficient Mice.* Science, 1999. **286**(5443): p. 1377.

420. Leignadier, J., et al., *Memory T-lymphocyte survival does not require T-cell receptor expression.* Proceedings of the National Academy of Sciences, 2008. **105**(51): p. 20440.

421. Weninger, W., N. Manjunath, and U.H. von Andrian, *Migration and differentiation of CD8+ T cells.* Immunol Rev, 2002. **186**: p. 221-33.

422. Opferman, J.T., B.T. Ober, and P.G. Ashton-Rickardt, *Linear differentiation of cytotoxic effectors into memory T lymphocytes.* Science, 1999. **283**(5408): p. 1745-8.

423. Wherry, E.J., et al., *Lineage relationship and protective immunity of memory CD8 T cell subsets.* Nat Immunol, 2003. **4**(3): p. 225-34.

424. Bouneaud, C., et al., *Lineage relationships, homeostasis, and recall capacities of central- and effector-memory CD8 T cells in vivo.* J Exp Med, 2005. **201**(4): p. 579-90.

425. Manjunath, N., et al., *Effector differentiation is not prerequisite for generation of memory cytotoxic T lymphocytes.* The Journal of Clinical Investigation, 2001. **108**(6): p. 871-878.

426. Masopust, D. and J.M. Schenkel, *The integration of T cell migration, differentiation and function.* Nat Rev Immunol, 2013. **13**(5): p. 309-20.

427. Bingaman, A.W., et al., *Novel phenotypes and migratory properties distinguish memory CD4 T cell subsets in lymphoid and lung tissue.* Eur J Immunol, 2005. **35**(11): p. 3173-86.

428. Woodland, D.L. and J.E. Kohlmeier, *Migration, maintenance and recall of memory T cells in peripheral tissues.* Nat Rev Immunol, 2009. **9**(3): p. 153-61.

429. Hogan, R.J., et al., *Activated antigen-specific CD8+ T cells persist in the lungs following recovery from respiratory virus infections.* J Immunol, 2001. **166**(3): p. 1813-22.

430. Koelle, D.M., et al., *Expression of cutaneous lymphocyte-associated antigen by CD8(+) T cells specific for a skin-tropic virus.* The Journal of Clinical Investigation, 2002. **110**(4): p. 537-548.

431. Wiley, J.A., et al., *Antigen-Specific CD8+T Cells Persist in the Upper Respiratory Tract Following Influenza Virus Infection.* J Immunol, 2001. **167**(6): p. 3293-3299.

432. Masopust, D., et al., *Preferential localization of effector memory cells in nonlymphoid tissue.* Science, 2001. **291**(5512): p. 2413-7.

433. Rosato, P.C., L.K. Beura, and D. Masopust, *Tissue resident memory T cells and viral immunity.* Curr Opin Virol, 2017. **22**: p. 44-50.

434. Shin, H., *Formation and function of tissue-resident memory T cells during viral infection.* Curr Opin Virol, 2017. **28**: p. 61-67.

435. Mackay, L.K., et al., *Long-lived epithelial immunity by tissue-resident memory T (TRM) cells in the absence of persisting local antigen presentation.* Proc Natl Acad Sci U S A, 2012. **109**(18): p. 7037-42.

436. Gebhardt, T., et al., *Peripheral tissue surveillance and residency by memory T cells.* Trends in Immunology, 2013. **34**(1): p. 27-32.

437. Mackay, L.K. and A. Kallies, *Transcriptional Regulation of Tissue-Resident Lymphocytes.* Trends Immunol, 2017. **38**(2): p. 94-103.

438. Bergsbaken, T. and M.J. Bevan, *Proinflammatory microenvironments within the intestine regulate the differentiation of tissue-resident CD8(+) T cells responding to infection.* Nat Immunol, 2015. **16**(4): p. 406-14.

439. Beura, L.K., et al., *T Cells in Nonlymphoid Tissues Give Rise to Lymph-Node-Resident Memory T Cells.* Immunity, 2018. **48**(2): p. 327-338.e5.

440. Cheuk, S., et al., *CD49a Expression Defines Tissue-Resident CD8+ T Cells Poised for Cytotoxic Function in Human Skin.* Immunity, 2017. **46**(2): p. 287-300.

441. Frost, E.L., et al., *Cutting Edge: Resident Memory CD8 T Cells Express High-Affinity TCRs.* J Immunol, 2015. **195**(8): p. 3520-4.

442. Conese, M., et al., *The Fountain of Youth: A Tale of Parabiosis, Stem Cells, and Rejuvenation.* Open Med, 2017. **12**: p. 376-383.

443. Shin, H. and A. Iwasaki, *Tissue-resident memory T cells.* Immunol Rev, 2013. **255**(1): p. 165-81.

444. Gebhardt, T., et al., *Memory T cells in nonlymphoid tissue that provide enhanced local immunity during infection with herpes simplex virus.* Nature Immunology, 2009. **10**: p. 524-530.

445. Jiang, X., et al., *Skin infection generates non-migratory memory CD8+ T(RM) cells providing global skin immunity.* Nature, 2012. **483**(7388): p. 227-31.

446. Gebhardt, T., et al., *Different patterns of peripheral migration by memory CD4+ and CD8+ T cells.* Nature, 2011. **477**(7363): p. 216-9.

447. Wakim, L.M., A. Woodward-Davis, and M.J. Bevan, *Memory T cells persisting within the brain after local infection show functional adaptations to their tissue of residence.* Proceedings of the National Academy of Sciences, 2010. **107**(42): p. 17872-17879.

448. Masopust, D., et al., *Dynamic T cell migration program provides resident memory within intestinal epithelium.* J Exp Med, 2010. **207**(3): p. 553-64.

449. Hofmann, M. and H. Pircher, *E-cadherin promotes accumulation of a unique memory CD8 T-cell population in murine salivary glands.* Proc Natl Acad Sci U S A, 2011. **108**(40): p. 16741-6.

450. Lee, Y.T., et al., *Environmental and antigen receptor-derived signals support sustained surveillance of the lungs by pathogen-specific cytotoxic T lymphocytes.* J Virol, 2011. **85**(9): p. 4085-94.

451. Takamura, S., et al., *The route of priming influences the ability of respiratory virus-specific memory CD8+ T cells to be activated by residual antigen.* J Exp Med, 2010. **207**(6): p. 1153-60.

452. Piet, B., et al., *CD8(+) T cells with an intraepithelial phenotype upregulate cytotoxic function upon influenza infection in human lung.* J Clin Invest, 2011. **121**(6): p. 2254-63.

453. Mueller, S.N., et al., *Memory T cell subsets, migration patterns, and tissue residence.* Annu Rev Immunol, 2013. **31**: p. 137-61.

454. Masopust, D. and J.M. Schenkel, *The integration of T cell migration, differentiation and function.* Nature Reviews Immunology, 2013. **13**: p. 309.

455. Fernandez-Ruiz, D., et al., *Liver-Resident Memory CD8(+) T Cells Form a Front-Line Defense against Malaria Liver-Stage Infection.* Immunity, 2016. **45**(4): p. 889-902.

456. Casey, K.A., et al., *Antigen-independent differentiation and maintenance of effector-like resident memory T cells in tissues.* J Immunol, 2012. **188**(10): p. 4866-75.

457. Mackay, L.K. and T. Gebhardt, *Tissue-resident memory T cells: local guards of the thymus.* Eur J Immunol, 2013. **43**(9): p. 2259-62.

458. Lee, E.F., et al., *The functional differences between pro-survival and pro-apoptotic B cell lymphoma 2 (Bcl-2) proteins depend on structural differences in their Bcl-2 homology 3 (BH3) domains.* J Biol Chem, 2014. **289**(52): p. 36001-17.

459. Sheridan, B.S., et al., *Oral infection drives a distinct population of intestinal resident memory CD8(+) T cells with enhanced protective function.* Immunity, 2014. **40**(5): p. 747-57.

460. Schenkel, J.M., K.A. Fraser, and D. Masopust, *Cutting edge: resident memory CD8 T cells occupy frontline niches in secondary lymphoid organs.* J Immunol, 2014. **192**(7): p. 2961-4.

461. Schenkel, J.M. and D. Masopust, *Tissue-resident memory T cells.* Immunity, 2014. **41**(6): p. 886-97.

462. Cyster, J.G. and S.R. Schwab, *Sphingosine-1-phosphate and lymphocyte egress from lymphoid organs.* Annu Rev Immunol, 2012. **30**: p. 69-94.

463. Mackay, L.K., et al., *The developmental pathway for CD103+ CD8+ tissue-resident memory T cells of skin.* Nat Immunol, 2013. **14**(12): p. 1294-301.

464. Skon, C.N., et al., *Transcriptional downregulation of S1pr1 is required for the establishment of resident memory CD8+ T cells.* Nat Immunol, 2013. **14**(12): p. 1285-93.

465. Kaech, S.M. and W. Cui, *Transcriptional control of effector and memory CD8+ T cell differentiation.* Nat Rev Immunol, 2012. **12**(11): p. 749-61.

466. Mackay, Laura K., et al., *T-box Transcription Factors Combine with the Cytokines TGF-β and IL-15 to Control Tissue-Resident Memory T Cell Fate.* Immunity, 2015. **43**(6): p. 1101-1111.

467. Zaid, A., et al., *Persistence of skin-resident memory T cells within an epidermal niche.* Proc Natl Acad Sci U S A, 2014. **111**(14): p. 5307-12.

468. Graham, J.B., A. Da Costa, and J.M. Lund, *Regulatory T cells shape the resident memory T cell response to virus infection in the tissues.* J Immunol, 2014. **192**(2): p. 683-90.

469. Laidlaw, Brian J., et al., *CD4+ T Cell Help Guides Formation of CD103+ Lung-Resident Memory CD8+ T Cells during Influenza Viral Infection.* Immunity, 2014. **41**(4): p. 633-645.

470. Steinfelder, S., et al., *Intestinal helminth infection induces highly functional resident memory CD4(+) T cells in mice.* Eur J Immunol, 2017. **47**(2): p. 353-363.

471. Ishizuka, A.S., et al., *Protection against malaria at 1 year and immune correlates following PfSPZ vaccination.* Nat Med, 2016. **22**(6): p. 614-23.

472. Perdomo, C., et al., *Mucosal BCG Vaccination Induces Protective Lung-Resident Memory T Cell Populations against Tuberculosis.* MBio, 2016. **7**(6): p. e01686-16.

473. Hamann, A., et al., *Role of alpha 4-integrins in lymphocyte homing to mucosal tissues in vivo.* J Immunol, 1994. **152**(7): p. 3282-93.

474. Cuburu, N., et al., *Intravaginal immunization with HPV vectors induces tissue-resident CD8+ T cell responses.* J Clin Invest, 2012. **122**(12): p. 4606-20.

475. Srivastava, R., et al., *CXCL17 Chemokine-Dependent Mobilization of CXCR8+ CD8+ Effector Memory and Tissue-Resident Memory T Cells in the Vaginal Mucosa Is Associated with Protection against Genital Herpes.* J Immunol, 2018. **200**(8): p. 2915-2926.

476. Wu, T., et al., *Lung-resident memory CD8 T cells (TRM) are indispensable for optimal cross-protection against pulmonary virus infection.* J Leukoc Biol, 2014. **95**(2): p. 215-24.

477. Platt, L., et al., *Prevalence and burden of HCV co-infection in people living with HIV: a global systematic review and meta-analysis.* The Lancet Infectious Diseases, 2016. **16**(7): p. 797-808.

478. WHO, *Global action plan on HIV drug resistance 2017–2021. Geneva: World Health Organization.* 2017.

479. Pontesilli, O., et al., *Longitudinal analysis of human immunodeficiency virus type 1-specific cytotoxic T lymphocyte responses: a predominant gag-specific response is associated with nonprogressive infection.* J Infect Dis, 1998. **178**(4): p. 1008-18.

480. Saez-Cirion, A., et al., *HIV controllers exhibit potent CD8 T cell capacity to suppress HIV infection ex vivo and peculiar cytotoxic T lymphocyte activation phenotype.* Proc Natl Acad Sci U S A, 2007. **104**(16): p. 6776-81.

481. Hansen, S.G., et al., *Profound early control of highly pathogenic SIV by an effector memory T-cell vaccine.* Nature, 2011. **473**(7348): p. 523-7.

482. Borducchi, E.N., et al., *Ad26/MVA therapeutic vaccination with TLR7 stimulation in SIV-infected rhesus monkeys.* Nature, 2016. **540**(7632): p. 284-287.

483. Baumert, T.F., et al., *A prophylactic hepatitis C virus vaccine: a distant peak still worth climbing.* J Hepatol, 2014. **61**(1 Suppl): p. S34-44.

484. Bailey, J.R., et al., *Broadly neutralizing antibodies with few somatic mutations and hepatitis C virus clearance.* JCI Insight, 2017. **2**(9).

485. Shin, H., et al., *CD301b+ dendritic cells stimulate tissue-resident memory CD8+ T cells to protect against genital HSV-2.* Nat Commun, 2016. **7**: p. 13346.

486. Steinbach, K., et al., *Brain-resident memory T cells represent an autonomous cytotoxic barrier to viral infection.* J Exp Med, 2016. **213**(8): p. 1571-87.

487. Oja, A.E., et al., *Trigger-happy resident memory CD4+T cells inhabit the human lungs.* Mucosal Immunol, 2017. **11**(3): p. 654-667.

488. Srivastava, R., et al., *CXCL10/CXCR3-Dependent Mobilization of Herpes Simplex Virus-Specific CD8+ TEM and CD8+ TRM Cells within Infected Tissues Allows Efficient Protection against Recurrent Herpesvirus Infection and Disease.* J Virol, 2017. **91**(14): p. e00278-17.

489. Muschaweckh, A., et al., *Antigen-dependent competition shapes the local repertoire of tissue-resident memory CD8+ T cells.* J Exp Med, 2016. **213**(13): p. 3075-3086.

490. Pallett, L.J., et al., *IL-2(high) tissue-resident T cells in the human liver: Sentinels for hepatotropic infection.* J Exp Med, 2017. **214**(6): p. 1567-1580.

491. Tan, H.X., et al., *Induction of vaginal-resident HIV-specific CD8 T cells with mucosal prime-boost immunization.* Mucosal Immunol, 2018. **11**(3): p. 994-1007.

492. Zaric, M., et al., *Long-lived tissue resident HIV-1 specific memory CD8(+) T cells are generated by skin immunization with live virus vectored microneedle arrays.* J Control Release, 2017. **268**: p. 166-175.

493. Kiniry, B.E., et al., *Detection of HIV-1-specific gastrointestinal tissue resident CD8+ T-cells in chronic infection.* Mucosal Immunol, 2018. **11**(3): p. 909-920.

494. Tan, H.X., et al., *Recombinant influenza virus expressing HIV-1 p24 capsid protein induces mucosal HIV-specific CD8 T-cell responses.* Vaccine, 2016. **34**(9): p. 1172-9.

495. Shin, H. and A. Iwasaki, *A vaccine strategy that protects against genital herpes by establishing local memory T cells.* Nature, 2012. **491**(7424): p. 463-7.

496. Nakanishi, Y., et al., *CD8+ T lymphocyte mobilization to virus-infected tissue requires CD4+ T-cell help.* Nature, 2009. **462**(7272): p. 510-3.

497. Huang, X., et al., *AAV2 production with optimized N/P ratio and PEI-mediated transfection results in low toxicity and high titer for in vitro and in vivo applications.* J Virol Methods, 2013. **193**(2): p. 270-7.

498. Guo, P., et al., *Rapid and simplified purification of recombinant adeno-associated virus.* J Virol Methods, 2012. **183**(2): p. 139-46.

499. Wu, X., et al., *A novel method for purification of recombinant adenoassociated virus vectors on a large scale.* Chinese Science Bulletin, 2001. **46**(6): p. 485-488.

500. Kohlbrenner, E., et al., *Quantification of AAV particle titers by infrared fluorescence scanning of coomassie-stained sodium dodecyl sulfate-polyacrylamide gels.* Hum Gene Ther Methods, 2012. **23**(3): p. 198-203.

501. Li, L., L. Yang, and R.M. Kotin, *The DNA minor groove binding agents Hoechst 33258 and 33342 enhance recombinant adeno-associated virus (rAAV) transgene expression.* J Gene Med, 2005. **7**(4): p. 420-31.

502. Dickey, D.D., et al., *Hoechst increases adeno-associated virus-mediated transgene expression in airway epithelia by inducing the cytomegalovirus promoter.* J Gene Med, 2012. **14**(6): p. 366-73.

503. Wijesundara, D.K., et al., *Use of an in vivo FTA assay to assess the magnitude, functional avidity and epitope variant cross-reactivity of T cell responses following HIV-1 recombinant poxvirus vaccination.* PLoS One, 2014. **9**(8): p. e105366.

504. Quah, B.J., et al., *Fluorescent target array T helper assay: a multiplex flow cytometry assay to measure antigen-specific CD4+ T cell-mediated B cell help in vivo.* J Immunol Methods, 2013. **387**(1-2): p. 181-90.

505. Aponte-Ubillus, J.J., et al., *Molecular design for recombinant adeno-associated virus (rAAV) vector production.* Appl Microbiol Biotechnol, 2018. **102**(3): p. 1045-1054.

506. Nieto, K. and A. Salvetti, *AAV Vectors Vaccines Against Infectious Diseases.* Frontiers in Immunology, 2014. **5**: p. 5.

507. Xin, K.-Q., et al., *Induction of Robust Immune Responses against Human Immunodeficiency Virus Is Supported by the Inherent Tropism of Adeno-Associated Virus Type 5 for Dendritic Cells.* Journal of Virology, 2006. **80**(24): p. 11899.

508. Xin, K.-Q., et al., *A Novel Recombinant Adeno-Associated Virus Vaccine Induces a Long-Term Humoral Immune Response to Human Immunodeficiency Virus.* Human Gene Therapy, 2001. **12**(9): p. 1047-1061.

509. Nieto, K., et al., *Combined prophylactic and therapeutic intranasal vaccination against human papillomavirus type-16 using different adeno-associated virus serotype vectors.* Antivir Ther, 2009. **14**(8): p. 1125-37.

510. Liu, D.W., et al., *Co-vaccination with adeno-associated virus vectors encoding human papillomavirus 16 L1 proteins and adenovirus encoding murine GM-CSF can elicit strong and prolonged neutralizing antibody.* Int J Cancer, 2005. **113**(1): p. 93-100.

511. Sipo, I., et al., *Vaccine protection against lethal homologous and heterologous challenge using recombinant AAV vectors expressing codon-optimized genes from pandemic swine origin influenza virus (SOIV).* Vaccine, 2011. **29**(8): p. 1690-1699.

512. Logan, G.J., et al., *AAV vectors encoding malarial antigens stimulate antigen-specific immunity but do not protect from parasite infection.* Vaccine, 2007. **25**(6): p. 1014-1022.

513. Grieger, J.C. and R.J. Samulski, *Adeno-associated virus vectorology, manufacturing, and clinical applications.* Methods Enzymol, 2012. **507**: p. 229-54.

514. Kang, W., et al., *An efficient rHSV-based complementation system for the production of multiple rAAV vector serotypes.* Gene Ther, 2009. **16**(2): p. 229-39.

515. Thomas, D.L., et al., *Scalable Recombinant Adeno-Associated Virus Production Using Recombinant Herpes Simplex Virus Type 1 Coinfection of Suspension-Adapted Mammalian Cells.* Human Gene Therapy, 2009. **20**(8): p. 861-870.

516. Ye, G.J., et al., *Herpes simplex virus clearance during purification of a recombinant adeno-associated virus serotype 1 vector.* Hum Gene Ther Clin Dev, 2014. **25**(4): p. 212-7.

517. Mueller, C., et al., *Production and discovery of novel recombinant adeno-associated viral vectors.* Curr Protoc Microbiol, 2012. **Chapter 14**: p. Unit14D.1.

518. Guo, P., et al., *A simplified purification method for AAV variant by polyethylene glycol aqueous two-phase partitioning.* Bioengineered, 2013. **4**(2): p. 103-6.

519. Kramer, M.G., et al., *In vitro and in vivo comparative study of chimeric liver-specific promoters.* Molecular Therapy, 2003. **7**(3): p. 375-385.

520. Espy, M.J., et al., *Comparison of three methods for extraction of viral nucleic acids from blood cultures.* J Clin Microbiol, 1995. **33**(1): p. 41-4.

521. Sugano, E., et al., *Establishment of effective methods for transducing genes into iris pigment epithelial cells by using adeno-associated virus type 2.* Invest Ophthalmol Vis Sci, 2005. **46**(9): p. 3341-8.

522. Lock, M., et al., *Rapid, simple, and versatile manufacturing of recombinant adeno-associated viral vectors at scale.* Hum Gene Ther, 2010. **21**(10): p. 1259-71.

523. Duchâteau, H., L. Duvigneaud, and C. Speth, *Instruments à la disposition des pouvoirs publics pour encourager une meilleure mobilité des Belges : focus sur le péage urbain et recherche de l'optimum.* Reflets et perspectives de la vie économique, 2017. **LVI**(2): p. 75-88.

524. Furler, S., et al., *Recombinant AAV vectors containing the foot and mouth disease virus 2A sequence confer efficient bicistronic gene expression in cultured cells and rat substantia nigra neurons.* Gene Therapy, 2001. **8**: p. 864.

525. Kuck, D., et al., *Intranasal Vaccination with Recombinant Adeno-Associated Virus Type 5 against Human Papillomavirus Type 16 L1.* Journal of Virology, 2006. **80**(6): p. 2621-2630.

526. Malecki, M., et al., *Recombinant adeno-associated viruses (rAAV2) facilitate the intraperitoneal gene delivery to cancer cells.* Oncol Lett, 2010. **1**(1): p. 177-180.

527. Li, X., et al., *Novel AAV-based genetic vaccines encoding truncated dengue virus envelope proteins elicit humoral immune responses in mice.* Microbes Infect, 2012. **14**(11): p. 1000-7.

528. Cunningham, S.C., et al., *Gene delivery to the juvenile mouse liver using AAV2/8 vectors.* Mol Ther, 2008. **16**(6): p. 1081-8.

529. Mattion, N.M., et al., *Foot-and-mouth disease virus 2A protease mediates cleavage in attenuated Sabin 3 poliovirus vectors engineered for delivery of foreign antigens.* J Virol, 1996. **70**(11): p. 8124-7.

530. Nakai, H., et al., *Unrestricted hepatocyte transduction with adeno-associated virus serotype 8 vectors in mice.* J Virol, 2005. **79**(1): p. 214-24.

531. Conlon, T.J., et al., *Efficient Hepatic Delivery and Expression from a Recombinant Adeno-associated Virus 8 Pseudotyped α1-Antitrypsin Vector.* Molecular Therapy, 2005. **12**(5): p. 867-875.

532. Nakai, H., et al., *A limited number of transducible hepatocytes restricts a wide-range linear vector dose response in recombinant adeno-associated virus-mediated liver transduction.* Journal of virology, 2002. **76**(22): p. 11343-11349.

533. Altman, J.D., et al., *Phenotypic analysis of antigen-specific T lymphocytes.* Science, 1996. **274**(5284): p. 94-6.

534. Sims, S., C. Willberg, and P. Klenerman, *MHC-peptide tetramers for the analysis of antigen-specific T cells.* Expert Rev Vaccines, 2010. **9**(7): p. 765-74.

535. Quah, B.J., et al., *Fluorescent target array killing assay: a multiplex cytotoxic T-cell assay to measure detailed T-cell antigen specificity and avidity in vivo.* Cytometry A, 2012. **81**(8): p. 679-90.

536. Vazquez, B.N., et al., *CD69 gene is differentially regulated in T and B cells by evolutionarily conserved promoter-distal elements.* J Immunol, 2009. **183**(10): p. 6513-21.

537. Radulovic, K., et al., *The Early Activation Marker CD69 Regulates the Expression of Chemokines and CD4 T Cell Accumulation in Intestine.* PLOS ONE, 2013. **8**(6): p. e65413.

538. Zhu, J., H. Yamane, and W.E. Paul, *Differentiation of effector CD4 T cell populations (*).* Annu Rev Immunol, 2010. **28**: p. 445-89.

539. Fazilleau, N., et al., *Follicular helper T cells: lineage and location.* Immunity, 2009. **30**(3): p. 324-35.

540. Mealey, R.H., et al., *Early detection of dominant Env-specific and subdominant Gag-specific CD8+ lymphocytes in equine infectious anemia virus-infected horses using major histocompatibility complex class I/peptide tetrameric complexes.* Virology, 2005. **339**(1): p. 110-26.

541. Leisner, C., et al., *One-Pot, Mix-and-Read Peptide-MHC Tetramers.* PLoS ONE, 2008. **3**(2): p. e1678.

542. Oyarzun, P., et al., *A bioinformatics tool for epitope-based vaccine design that accounts for human ethnic diversity: Application to emerging infectious diseases.* Vaccine, 2015. **33**(10): p. 1267-1273.

543. Newell, E.W., *Higher Throughput Methods of Identifying T Cell Epitopes for Studying Outcomes of Altered Antigen Processing and Presentation.* Frontiers in Immunology, 2013. **4**: p. 430.

544. Barchet, W., et al., *Direct quantitation of rapid elimination of viral antigen-positive lymphocytes by antiviral CD8(+) T cells in vivo.* Eur J Immunol, 2000. **30**(5): p. 1356-63.

545. Murali-Krishna, K., et al., *Counting antigen-specific CD8 T cells: a reevaluation of bystander activation during viral infection.* Immunity, 1998. **8**(2): p. 177-87.

546. Fischer, K., R. Andreesen, and A. Mackensen, *An improved flow cytometric assay for the determination of cytotoxic T lymphocyte activity.* J Immunol Methods, 2002. **259**(1-2): p. 159-69.

547. Quah, B.J., H.S. Warren, and C.R. Parish, *Monitoring lymphocyte proliferation in vitro and in vivo with the intracellular fluorescent dye carboxyfluorescein diacetate succinimidyl ester.* Nat Protoc, 2007. **2**(9): p. 2049-56.

548. Regoes, R.R., et al., *Estimation of the rate of killing by cytotoxic T lymphocytes in vivo.* Proceedings of the National Academy of Sciences of the United States of America, 2007. **104**(5): p. 1599-1603.

549. Durward, M., J. Harms, and G. Splitter, *Antigen specific killing assay using CFSE labeled target cells.* J Vis Exp, 2010(45).

550. Yates, A., et al., *Revisiting Estimates of CTL Killing Rates In Vivo.* PLOS ONE, 2007. **2**(12): p. e1301.

551. Oehen, S., et al., *A simple method for evaluating the rejection of grafted spleen cells by flow cytometry and tracing adoptively transferred cells by light microscopy.* J Immunol Methods, 1997. **207**(1): p. 33-42.

552. Quah, B.J., et al., *The use of fluorescent target arrays for assessment of T cell responses in vivo.* J Vis Exp, 2014(88): p. e51627.

553. Peters, B. and A. Sette, *Generating quantitative models describing the sequence specificity of biological processes with the stabilized matrix method.* BMC Bioinformatics, 2005. **6**: p. 132.

554. Andreatta, M. and M. Nielsen, *Gapped sequence alignment using artificial neural networks: application to the MHC class I system.* Bioinformatics, 2016. **32**(4): p. 511-7.

555. Schirle, M., T. Weinschenk, and S. Stevanovic, *Combining computer algorithms with experimental approaches permits the rapid and accurate identification of T cell epitopes from defined antigens.* J Immunol Methods, 2001. **257**(1-2): p. 1-16.

556. Kim, Y., et al., *Immune epitope database analysis resource.* Nucleic Acids Res, 2012. **40**(Web Server issue): p. W525-30.

557. Nielsen, M., et al., *Reliable prediction of T-cell epitopes using neural networks with novel sequence representations.* Protein Sci, 2003. **12**(5): p. 1007-17.

558. Lundegaard, C., et al., *NetMHC-3.0: accurate web accessible predictions of human, mouse and monkey MHC class I affinities for peptides of length 8-11.* Nucleic Acids Res, 2008. **36**(Web Server issue): p. W509-12.

559. Sidney, J., et al., *Quantitative peptide binding motifs for 19 human and mouse MHC class I molecules derived using positional scanning combinatorial peptide libraries.* Immunome Res, 2008. **4**: p. 2.

560. Park, S.L., et al., *Local proliferation maintains a stable pool of tissue-resident memory T cells after antiviral recall responses.* Nature Immunology, 2018. **19**(2): p. 183-191.

561. McNamara, H.A., et al., *Up-regulation of LFA-1 allows liver-resident memory T cells to patrol and remain in the hepatic sinusoids.* Sci Immunol, 2017. **2**(9).

562. Bull, R.A., et al., *Sequential Bottlenecks Drive Viral Evolution in Early Acute Hepatitis C Virus Infection.* PLOS Pathogens, 2011. **7**(9): p. e1002243.

563. Kutzler, M.A. and D.B. Weiner, *DNA vaccines: ready for prime time?* Nature reviews. Genetics, 2008. **9**(10): p. 776-788.

564. Casimiro, D.R., et al., *Comparative immunogenicity in rhesus monkeys of DNA plasmid, recombinant vaccinia virus, and replication-defective adenovirus vectors expressing a human immunodeficiency virus type 1 gag gene.* J Virol, 2003. **77**(11): p. 6305-13.

565. Abbink, P., et al., *Durability and correlates of vaccine protection against Zika virus in rhesus monkeys.* Sci Transl Med, 2017. **9**(420): p. eaao4163.

566. Gargett, T., et al., *Induction of antigen-positive cell death by the expression of perforin, but not DTa, from a DNA vaccine enhances the immune response.* Immunol Cell Biol, 2014. **92**(4): p. 359-67.

567. Gargett, T., et al., *Increase in DNA vaccine efficacy by virosome delivery and co-expression of a cytolytic protein.* Clin Transl Immunology, 2014. **3**(6): p. e18.

568. Wijesundara, D.K., et al., *Cytolytic DNA vaccine encoding lytic perforin augments the maturation of- and antigen presentation by- dendritic cells in a time-dependent manner.* Sci Rep, 2017. **7**(1): p. 8530.

569. Davies, B., et al., *Cutting Edge: Tissue-Resident Memory T Cells Generated by Multiple Immunizations or Localized Deposition Provide Enhanced Immunity.* J Immunol, 2017. **198**(6): p. 2233-2237.

570. Gola, A., et al., *Prime and target immunization protects against liver-stage malaria in mice.* Sci Transl Med, 2018. **10**(460).

571. Epstein, J.E., et al., *Live attenuated malaria vaccine designed to protect through hepatic CD8(+) T cell immunity.* Science, 2011. **334**(6055): p. 475-80.

572. Heydtmann, M., et al., *Detailed analysis of intrahepatic CD8 T cells in the normal and hepatitis C-infected liver reveals differences in specific populations of memory cells with distinct homing phenotypes.* J Immunol, 2006. **177**(1): p. 729-38.

573. Major, M., et al., *Modeling of patient virus titers suggests that availability of a vaccine could reduce hepatitis C virus transmission among injecting drug users.* Science Translational Medicine, 2018. **10**(449): p. eaao4496.

574. WHO, *Global Health Sector Strategy on Viral Hepatitis 2016–2021; Towards Ending Viral Hepatitis.* 2016.

575. Haigwood, N.L., *Update on animal models for HIV research.* Eur J Immunol, 2009. **39**(8): p. 1994-9.

576. Rollier, C.S., et al., *Viral vectors as vaccine platforms: deployment in sight.* Curr Opin Immunol, 2011. **23**(3): p. 377-82.

577. Liu, M.A., *Immunologic basis of vaccine vectors.* Immunity, 2010. **33**(4): p. 504-15.

578. Rollier, C.S., A.V.S. Hill, and A. Reyes-Sandoval, *Influence of adenovirus and MVA vaccines on the breadth and hierarchy of T cell responses.* Vaccine, 2016. **34**(38): p. 4470-4474.

579. Ramezanpour, B., et al., *Vector-based genetically modified vaccines: Exploiting Jenner's legacy.* Vaccine, 2016. **34**(50): p. 6436-6448.

580. Manning, W.C., et al., *Genetic immunization with adeno-associated virus vectors expressing herpes simplex virus type 2 glycoproteins B and D.* J Virol, 1997. **71**(10): p. 7960-2.

581. Xin, K.Q., et al., *Oral administration of recombinant adeno-associated virus elicits human immunodeficiency virus-specific immune responses.* Hum Gene Ther, 2002. **13**(13): p. 1571-81.

582. Johnson, P.R., et al., *Vector-mediated gene transfer engenders long-lived neutralizing activity and protection against SIV infection in monkeys.* Nat Med, 2009. **15**(8): p. 901-6.

583. Mehendale, S., et al., *A phase 1 study to evaluate the safety and immunogenicity of a recombinant HIV type 1 subtype C adeno-associated virus vaccine.* AIDS Res Hum Retroviruses, 2008. **24**(6): p. 873-80.

584. Zhou, L., et al., *Long-term protection against human papillomavirus e7-positive tumor by a single vaccination of adeno-associated virus vectors encoding a fusion protein of inactivated e7 of human papillomavirus 16/18 and heat shock protein 70.* Hum Gene Ther, 2010. **21**(1): p. 109-19.

585. Nieto, K., et al., *Intranasal vaccination with AAV5 and 9 vectors against human papillomavirus type 16 in rhesus macaques.* Hum Gene Ther, 2012. **23**(7): p. 733-41.

586. Limberis, M.P., et al., *Intranasal antibody gene transfer in mice and ferrets elicits broad protection against pandemic influenza.* Sci Transl Med, 2013. **5**(187): p. 187ra72.

587. Vercauteren, K., et al., *Superior In vivo Transduction of Human Hepatocytes Using Engineered AAV3 Capsid.* Mol Ther, 2016.

588. Liang, Y., et al., *Visualizing hepatitis C virus infections in human liver by two-photon microscopy.* Gastroenterology, 2009. **137**(4): p. 1448-58.

589. Nietupski, J.B., et al., *Systemic administration of AAV8-alpha-galactosidase A induces humoral tolerance in nonhuman primates despite low hepatic expression.* Mol Ther, 2011. **19**(11): p. 1999-2011.

590. Paulk, N.K., et al., *Bioengineered AAV Capsids with Combined High Human Liver Transduction In Vivo and Unique Humoral Seroreactivity.* Mol Ther, 2018. **26**(1): p. 289-303.

591. Zaritskaya, L., et al., *New flow cytometric assays for monitoring cell-mediated cytotoxicity.* Expert Rev Vaccines, 2010. **9**(6): p. 601-16.

592. Brunner, K.T., et al., *Quantitative assay of the lytic action of immune lymphoid cells on 51-Cr-labelled allogeneic target cells in vitro; inhibition by isoantibody and by drugs.* Immunology, 1968. **14**(2): p. 181-196.

593. Flieger, D., et al., *A novel non-radioactive cellular cytotoxicity test based on the differential assessment of living and killed target and effector cells.* J Immunol Methods, 1995. **180**(1): p. 1-13.

594. Karawajew, L., et al., *A flow cytometric long-term cytotoxicity assay.* J Immunol Methods, 1994. **177**(1-2): p. 119-30.

595. Popescu, I., et al., *Phenotypic and functional characterization of cytotoxic T lymphocytes by flow cytometry.* Methods Mol Biol, 2014. **1186**: p. 21-47.

596. Noto, A., P. Ngauv, and L. Trautmann, *Cell-based flow cytometry assay to measure cytotoxic activity.* Journal of visualized experiments : JoVE, 2013(82): p. e51105-e51105.

597. Kelly, C., et al., *Cross-reactivity of hepatitis C virus specific vaccine-induced T cells at immunodominant epitopes.* Eur J Immunol, 2015. **45**(1): p. 309-16.

598. Folgori, A., et al., *A T-cell HCV vaccine eliciting effective immunity against heterologous virus challenge in chimpanzees.* Nat Med, 2006. **12**(2): p. 190-7.

599. Wooldridge, L., et al., *Tricks with tetramers: how to get the most from multimeric peptide-MHC.* Immunology, 2009. **126**(2): p. 147-64.

600. Laugel, B., et al., *Different T cell receptor affinity thresholds and CD8 coreceptor dependence govern cytotoxic T lymphocyte activation and tetramer binding properties.* J Biol Chem, 2007. **282**(33): p. 23799-810.

601. Dolton, G., et al., *More tricks with tetramers: a practical guide to staining T cells with peptide–MHC multimers.* Immunology, 2015. **146**(1): p. 11-22.

602. Cole, D.K., et al., *Human TCR-binding affinity is governed by MHC class restriction.* J Immunol, 2007. **178**(9): p. 5727-34.

603. Crawford, F., et al., *Detection of antigen-specific T cells with multivalent soluble class II MHC covalent peptide complexes.* Immunity, 1998. **8**(6): p. 675-82.

604. Wooldridge, L., et al., *Interaction between the CD8 coreceptor and major histocompatibility complex class I stabilizes T cell receptor-antigen complexes at the cell surface.* J Biol Chem, 2005. **280**(30): p. 27491-501.

605. Manoj, S., L.A. Babiuk, and S. van Drunen Littel-van den Hurk, *Approaches to enhance the efficacy of DNA vaccines.* Crit Rev Clin Lab Sci, 2004. **41**(1): p. 1-39.

606. Belakova, J., et al., *DNA vaccines: are they still just a powerful tool for the future?* Arch Immunol Ther Exp (Warsz), 2007. **55**(6): p. 387-98.

607. Kowalczyk, D.W. and H.C. Ertl, *Immune responses to DNA vaccines.* Cell Mol Life Sci, 1999. **55**(5): p. 751-70.

608. Jorritsma, S.H.T., et al., *Delivery methods to increase cellular uptake and immunogenicity of DNA vaccines.* Vaccine, 2016. **34**(46): p. 5488-5494.

609. Ferraro, B., et al., *Clinical applications of DNA vaccines: current progress.* Clin Infect Dis, 2011. **53**(3): p. 296-302.

610. Frahm, N., et al., *Human adenovirus-specific T cells modulate HIV-specific T cell responses to an Ad5-vectored HIV-1 vaccine.* J Clin Invest, 2012. **122**(1): p. 359-67.

611. Kim, K.S., et al., *Current status of human papillomavirus vaccines.* Clin Exp Vaccine Res, 2014. **3**(2): p. 168-75.

612. Trimble, C.L., et al., *Safety, efficacy, and immunogenicity of VGX-3100, a therapeutic synthetic DNA vaccine targeting human papillomavirus 16 and 18 E6 and E7 proteins for cervical intraepithelial neoplasia 2/3: a randomised, double-blind, placebo-controlled phase 2b trial.* The Lancet, 2015. **386**(10008): p. 2078-2088.

613. Larocca, R.A., et al., *Vaccine protection against Zika virus from Brazil.* Nature, 2016. **536**(7617): p. 474-8.

614. Tebas, P., et al., *Safety and Immunogenicity of an Anti-Zika Virus DNA Vaccine - Preliminary Report.* N Engl J Med, 2017.

615. Gaudinski, M.R., et al., *Safety, tolerability, and immunogenicity of two Zika virus DNA vaccine candidates in healthy adults: randomised, open-label, phase 1 clinical trials.* The Lancet, 2018. **391**(10120): p. 552-562.

616. Nchinda, G., et al., *Dendritic cell targeted HIV gag protein vaccine provides help to a DNA vaccine including mobilization of protective CD8(+) T cells.* Proceedings of the National Academy of Sciences of the United States of America, 2010. **107**(9): p. 4281-4286.

617. Idoyaga, J., et al., *Comparable T helper 1 (Th1) and CD8 T-cell immunity by targeting HIV gag p24 to CD8 dendritic cells within antibodies to Langerin, DEC205, and Clec9A.* Proc Natl Acad Sci U S A, 2011. **108**(6): p. 2384-9.

618. Wijesundara, D.K., et al., *Induction of Genotype Cross-Reactive, Hepatitis C Virus-Specific, Cell-Mediated Immunity in DNA-Vaccinated Mice.* J Virol, 2018. **92**(8).

619. Barry, M. and R.C. Bleackley, *Cytotoxic T lymphocytes: all roads lead to death.* Nat Rev Immunol, 2002. **2**(6): p. 401-9.

620. Racanelli, V., et al., *Dendritic cells transfected with cytopathic self-replicating RNA induce crosspriming of CD8+ T cells and antiviral immunity.* Immunity, 2004. **20**(1): p. 47-58.

621. Garrod, T., et al., *Encoded novel forms of HSP70 or a cytolytic protein increase DNA vaccine potency.* Hum Vaccin Immunother, 2014. **10**(9): p. 2679-83.

622. Jongo, S.A., et al., *Safety, Immunogenicity, and Protective Efficacy against Controlled Human Malaria Infection of Plasmodium falciparum Sporozoite Vaccine in Tanzanian Adults.* The American journal of tropical medicine and hygiene, 2018. **99**(2): p. 338-349.

623. Schenkel, J.M., et al., *Sensing and alarm function of resident memory CD8(+) T cells.* Nat Immunol, 2013. **14**(5): p. 509-13.

624. Giang, E., et al., *Human broadly neutralizing antibodies to the envelope glycoprotein complex of hepatitis C virus.* Proc Natl Acad Sci U S A, 2012. **109**(16): p. 6205-10.

625. Law, M., et al., *Broadly neutralizing antibodies protect against hepatitis C virus quasispecies challenge.* Nature Medicine, 2007. **14**: p. 25.

626. Morin, T.J., et al., *Human Monoclonal Antibody HCV1 Effectively Prevents and Treats HCV Infection in Chimpanzees.* PLOS Pathogens, 2012. **8**(8): p. e1002895.

627. Halbert, C.L., J.M. Allen, and A.D. Miller, *Efficient mouse airway transduction following recombination between AAV vectors carrying parts of a larger gene.* Nat Biotechnol, 2002. **20**(7): p. 697-701.

628. Odom, G.L., et al., *Gene therapy of mdx mice with large truncated dystrophins generated by recombination using rAAV6.* Mol Ther, 2011. **19**(1): p. 36-45.

629. Ostedgaard, L.S., et al., *A shortened adeno-associated virus expression cassette for CFTR gene transfer to cystic fibrosis airway epithelia.* Proc Natl Acad Sci U S A, 2005. **102**(8): p. 2952-7.

630. McFarland, T.J., et al., *Evaluation of a novel short polyadenylation signal as an alternative to the SV40 polyadenylation signal.* Plasmid, 2006. **56**(1): p. 62-7.

631. Christie, J.M., et al., *Structural tuning of the fluorescent protein iLOV for improved photostability.* J Biol Chem, 2012. **287**(26): p. 22295-304.

632. Meurens, F., et al., *The pig: a model for human infectious diseases.* Trends Microbiol, 2012. **20**(1): p. 50-7.

633. Ding, Q., et al., *Mice Expressing Minimally Humanized CD81 and Occludin Genes Support Hepatitis C Virus Uptake In Vivo.* J Virol, 2017. **91**(4).

634. Iwasaki, Y., et al., *Long-Term Persistent GBV-B Infection and Development of a Chronic and Progressive Hepatitis C-Like Disease in Marmosets.* Front Microbiol, 2011. **2**: p. 240.

635. Li, T., et al., *Infection of common marmosets with hepatitis C virus/GB virus-B chimeras.* Hepatology, 2014. **59**(3): p. 789-802.

636. Zhu, S., et al., *Infection of Common Marmosets with GB Virus B Chimeric Virus Encoding the Major Nonstructural Proteins NS2 to NS4A of Hepatitis C Virus.* J Virol, 2016. **90**(18): p. 8198-211.